UNIVERZITET U BEOGRADU

BIOLOŠKI FAKULTET

Milorad M. Dragić

ULOGA PURINSKOG SIGNALNOG SISTEMA U PROCESIMA NEURODEGENERACIJE I NEUROINFLAMACIJE IZAZVANIH TRIMETIL-KALAJEM U HIPOKAMPUSU ŽENKI PACOVA

DOKTORSKA DISERTACIJA

Beograd, 2021.

UNIVERSITY OF BELGRADE

FACULTY OF BIOLOGY

Milorad M. Dragić

THE ROLE OF PURINERGIC SIGNALING SYSTEM IN TRIMETHYLTIN-INDUCED NEURODEGENERATION AND NEUROINFLAMMATION OF HIPPOCAMPUS OF FEMALE RATS

DOCTORAL DISSERTAION

Belgrade, 2021.

MENTORI I ČLANOVI KOMISIJE

Mentori:

1. dr Ivana Grković, viši naučni saradnik, Univerzitet u Beogradu, Institut za nuklearne nauke „Vinča“ – Institut od nacionalnog značaja za Republiku Srbiju

2. prof. dr Nadežda Nedeljković, redovni profesor, Univerzitet u Beogradu, Biološki fakultet

Članovi komisije:

1. prof. dr Tihomir V. Ilić, redovni profesor, Univerzitet odbrane, Medicinski fakultet Vojnomedicinske akademije

2. prof. dr Danijela Laketa, vanredni profesor, Univerzitet u Beogradu, Biološki fakultet

3. dr Nataša Mitrović, naučni saradnik, Univerzitet u Beogradu, Institut za nuklearne nauke „Vinča“ – Institut od nacionalnog značaja za Republiku Srbiju

ZAHVALNICA

Ova doktorska disertacija urađena je u Laboratoriji za molekularnu biologiju i endokrinologiju Instituta za nuklearne nauke Vinča – Institut od nacionalnog značaja i u Laboratoriji za neurobiologiju Biološkog fakulteta Univerziteta u Beogradu, u okviru projekta finansiranog od strane Ministarstva prosvete, nauke i tehnološkog razvoja Republike Srbije: „Ćelijska i molekulska osnova neuroinflamacije: potencijalna ciljna mesta za translacionu medicinu i terapiju“ (III41014, 2011-2019) kao i teme: Ćelijska i molekulska osnova neurodegeneracije i neuroprotekcije, pod rukovodstvom dr Ivane Grković (2020- u toku, Program 2, Životna sredina i zdravlje, INN Vinča).

Najveću zahvalnost dugujem svojoj mentorki dr Ivani Grković koja je bila uz mene za svaki naučni i nenaučni korak tokom izrade ove doktorske disertacije, na prenetom znanju, iskustvu i svim savetima koji su me oblikovali naučno i životno na ovom neverovatnom putovanju.

Posebnu zahvalnost dugujem i mentorki prof. dr Nadeždi Nedeljković koja me je svojim savetima i podrškom u svakom trenutku usmeravala i na naučnom i na nastavnom putu, i i dalje to čini. Hvala na svim diskusijama o životu i nauci, na podsticajima i kritikama koji su suštinski doprineli oblikovanju mog profesionalnog razvoja.

Želeo da se zahvalim dr Nataši Mitrović pored koje sam napravio prve laboratorijske korake, naučio prve metode i obradio prve rezultate. Hvala na ukazanom poverenju. Hvala na studioznom čitanju disertacije i svim komentarima koji su unapredili ovaj doktorat.

Veliko hvala prof. dr Danijeli Laketi na izdvojenom vremenu, trudu i pomoći prilikom pisanja i čitanja ove disertacije kao i na komentarima koji su doprineli kvalitetu teksta.

Hvala prof. dr Tihomiru V. Iliću na pažljivom čitanju teksta i komentarima koji su uobličili disertaciju i značajno unapredili njen kvalitet.

Želeo bih da se posebno zahvalim koleginicama Marini Zarić, Emiliji Glavonić i Katarini Milićević, za sve diskusije, i za trenutke kada je bilo lako ali i kada nije. Hvala Vam na podršci.

Hvala koleginicama iz laboratorije Mariji Adžić, Milici Zeljković, Sanji Dacić, Anđeli Stekić, Katarini Mihajlović, Ivani Guševac Stojanović, Jeleni Martinović koje su uvek bile podrška i pored kojih je rad uvek bio zabavan, a ponekad i smešan.

Hvala mojoj porodici na podršci, onima koji su tu i onima kojih više nema.

Mojoj baki i mom deki

ULOGA PURINSKOG SIGNALNOG SISTEMA U PROCESIMA NEURODEGENERACIJE I NEUROINFLAMACIJE IZAZVANIH TRIMETIL-KALAJEM U HIPOKAMPUSU ŽENKI PACOVA

Neurodegeneracija je proces koji se odlikuje progresivnim gubitkom nervnog tkiva, posebno nervnih ćelija, nervnih nastavaka i mijelina, koji se uočava kod velikog broja neuroloških bolesti, a za koji do danas nije razvijena adekvatna terapija, niti su u brojnim bolestima otkriveni uzroci. S obzirom na to da neurodegeneracija podrazumeva oštećenje tkiva, ona je nužno praćena neuroinflamatornom aktivacijom mikroglije i astrocita, što može doprineti progresiji inicijalne patologije. Predmet istraživanja ove doktorske disertacije bio je ispitivanje promena komponenti purinske signalizacije u hipokampusu ženki pacova u modelu neurodegeneracije i neuroinflamacije izazvane trimetil kalajem (TMK). TMK je neurotoksin koji dovodi do selektivne smrti neurona limbičkog sistema, naročito u hipokampusu, što rezultuje histopatološkim i bihejvioralnim promenama koje verno reprodukuju neke od glavnih karakteristika mnogih neurodegenerativnih bolesti. Prvi set rezultata dobijenih u okviru ove disertacije pokazuje da tokom prve tri nedelje nakon delovanja TMT javlja progresivno umiranje nervnih ćelija, što je praćeno snažnom i specifičnom aktivacijom astrocita i mikroglije. Aktivirani astrociti u hipokamusu ispoljavaju morfološku i funkcionalnu dihotomiju, tako što astrociti CA1 regiona hipokampusa pokazuju odlike hipertrofiranih ćelija, dok astrociti hilarnog regiona pokazuju odlike atrofije. Aktivirane mikroglijske ćelije pojačanao eksprimiraju početni enzim purinske kaskade, NTPDaza1/CD39, dok mikroglijske ćelije ameobidnog oblika, na mestima aktivne neurodegeneracije, pojačano eksprimiraju završni enzim purinske kaskade, eN/CD73. Reaktivni astrociti pojačano eksprimiraju A_1R, $A_{2A}R$ i $P2Y_1R$ receptore kao i C3, iNOS, NF-kB, koji ukazuju na njihov proinflamacijski karakter. U mikroglijskim ćelijama, povećana ekspresija purinskih receptora $P2Y_{12}R$, $P2Y_6R$ i $P2X_4R$ na genskom nivou, ukazuje na migratorni fenotip aktivirane mikroglije tokom rane faze neurodegeneracije, dok je povećana proteinska ekspresija $P2X_7R$ verovato povezana sa fagocitozom ameboidne mikroglije. Pojačana ekspresija navedenih komponenti purinske transmisije na mikrogliji (NTPDaze1/CD39, eN/CD73 kao i $P2X_7R$) i astrocitima (A_1R, $A_{2A}R$, $P2Y_1R$) u neurodegeneraciji i neuroinflamaciji izazvanoj TMK, kao i smanjena ekspresija A_1R, $P2Y_{12}R$, ukazuju na ulogu purinske signalizacije u neurodegeneraciji i neuroinflamaciji.

KLJUČNE REČI: Neurodegeneracija, trimetil-kalaj, purinska signalizacija, neuroinflamacija, hipokampus, NTPDaza1/CD39, eN/CD73, astrociti, mikroglija

NAUČNA OBLAST: Biologija

UŽA NAUČNA OBLAST: Neurobiologija

THE ROLE OF PURINERGIC SIGNALING SYSTEM IN TRIMETHYLTIN-INDUCED NEURODEGENERATION AND NEUROINFLAMMATION OF HIPPOCAMPUS OF FEMALE RATS

Neurodegeneration reffers to a progressive loss of neuronal tissue, specifically nerve cells, nerve endings and myelin sheet, and it is common for many neurological disorders. There is no known effective drug or therapeutic approach for virtually all neurodegenerative diseases and cause for many of them has not been discovered yet. Neurodegenerative disorders are often accompanied by neuroinflammatory activation of microglia and astrocytes which can further contribute to pathology progression. The main goal of this dissertation was to examine changes in the main components of purinergic signaling in trimethyltin-induced (TMT) neurodegeneration and neurofinflammation of hippocampus of female rats. TMT is a potent neurotoxin which causes selective neuronal death of lymbic system, especially hippocampus which results in histopathological and behavioral changes resulting in some of the main common characteristics of neurodegenerative disorders. First set of the results of this doctoral dissertation shows that the first three weeks after TMT intoxication are accompanied by extensive neuronal death in CA sectors of hippocampus, followed by reactive astro- and microgliosis. Reactive astrocytes in hippocampus showed morphological and functional dichotomy. Astrocytes of CA1 region were characterized by hypetrhophic morphology while astrocytes od hilar region had atrophy-like morphology. Activated microglial cells showed increased expression of NTPDase1/CD39, while ameboid microglia in the site of active neurodegeneration showed eN/CD73. Reactive astrocytes showed increase expression of A_1R, $A_{2A}R$ i $P2Y_1R$ and C3, iNOS, NF-kB, which points to their proinflammatory phenotype. Increased gene expression of $P2Y_{12}R$, $P2Y_6R$ i $P2X_4R$ points toward migratory phenotype of microglia during early phase of neurodegeneration, while late expression of $P2X_7R$ is probably related to phagocitic properties of amoeboid microglial cells. Increased expression of microglial (NTPDase1/CD39, eN/CD73 and $P2X_7R$) and astrocytic (A_1R, $A_{2A}R$, $P2Y_1R$) purinergic compontents in TMT-induced neurodegeneration and neuroinflammation as well as loss of homeostatic A_1R, $P2Y_{12}R$ receptors in neurons definitely points to an active role of purinergic signaling in neurodegenerative process.

KEY WORDS: Neurodegeneration,trimethyltin, purinergic signaling, neuroinflammation, hippocampus, NTPDase1/CD39, eN/CD73, astrocytes, microglia

RESEARCH AREA: Biology

RESEARCH FIELD: Neurobiology

SKRAĆENICE

AC – Adenil ciklaza
AD – Alchajmerova bolest
ALS – Amiotrofična lateralna skleroza
Arg-1 – Arginaza 1
ATP – Adenozin-5' –trifosfat
cAMP – ciklični adenozin-5'-monofosfat
CNS – Centralni nervni sistem
CNT – Koncentrativni transporter za adenozin
DAMP – (*engl. Danger associated molecular pattern*) Molekulski obrasci povezani sa oštećenjem
ENT – Ekvilibrativni transporter za adenozin
GFAP – Glijski kiseli fibrilarni protein
GPI – Glikozilfosfatidilinozitol
IGF-1 – Insulinski faktor rasta 1
IL-1β – Interleukin 1β
IL-4 – Interleukin 4
IL-6 – Interleukin 6
IL-10 – Interleukin 10
NEST - Nestin
NO – Azot-monoksid
PD – Parkinsonova bolest
Pi – Neorganski fosfat
PPi – Neorganski pirofosfat
TGF-β – Transformišući faktor rasta β
TMK – Trimetil-kalaj
TNF-α – Faktor nekroze tumora α
VIM - Vimentin

SADRŽAJ

I UVOD 1

1. Neurodegeneracija 1

2. Neuroinflamacija 1

2.1. Uloga mikroglije 2

2.2. Uloga astrocita 3

3. Neurodegeneracija i neuroinflamacija izazvane trimetil-kalajem 5

3.1. Trimetil-kalaj (TMK) 5

3.2. Mehanizam neurotoksičnog delovanja TMK 6

3.3. Aktivacija mikroglije i astrocita u neuroinflamaciji izazvanoj primenomTMK 7

4. Purinska signalizacija 7

4.1. Purini kao signalni molekul 8

4.2. Purinski receptori 8

4.3. Ektonukleotidaze 10

4.3.1. Ekto-nukleozid 5'- trifosfat difosfohidrolaze (NTPDaze) 10

4.3.3. Ekto-5'-nukleotidaza (CD73, eN) 12

4.3.4. Alkalna fosfataza 13

4.4. Uloga purinske signalizacija u fiziološkim i patološkim uslovima 14

II CILJ ISTRAŽIVANJA 16

III RADOVI PROIZAŠLI IZ DOKTORSKE DISERTACIJE 17

IV DISKUSIJA 62

1. Trimetil-kalaj izaziva promene ponašanja pacova koje su praćene progresivnim gubitkom piramidnih neurona CA1-CA3 regiona hipokapusa 62

2. Neurodegeneracija izazvana trimetil-kalajem praćena je aktivacijom glijskih ćelija 63

3. Neurodegeneracija izazvana trimetil-kalajem dovodi do promena aktivnosti i ekspresiji NTPDaze 1 i eN 66

4. Neurodegeneracija izazvana trimetil-kalajem uzrokuje promene ekspresije P2 i P1 receptora 68

5. Neurodegeneracija izazvana trimetil-kalajem uzrokuje inflamatornu aktivaciju glijskih ćelija 69

6. Neurodegeneracija izazvana trimetil-kalajem dovodi do ekspresije specifičnog repertoara purinskih receptora na glijskim ćelijama 70

V ZAKLJUČCI 73

VI LITERATURA 75

VII PRILOZI 93

I UVOD

1. Neurodegeneracija

Neurodegenerativne bolesti odlikuju se dugotrajnim i progresivnim propadanjem neurona u centralnom nervnom sistemu (CNS), što se manifestuje narušavanjem ili gubitkom neuroloških funkcija. Ove bolesti predstavljaju jedan od vodećih uzroka smrtnosti u razvijenim državama sveta, pogotovo među starijom populacijom. Neurodegenerativne promene mogu nastati akutno, kao rezultat niza bolesti nervnog sistema, obuhvatajući raspon od mehaničkih povreda i ishemijske bolesti mozga sve do psihijatrijskih oboljenja. Trenutno je u svetu registrovano oko 50 miliona obolelih od neurodegenerativnih bolesti, od kojih je najveći broj sa Alchajmerovom bolešću (AD), a predviđa se da će taj broj dostići 131 milion do 2050. godine (Arvanitakis et al., 2019). Iako u osnovi heterogene, svim neurodegenerativnim bolestima zajednički je gubitak neurona i degeneracija nervnih vlakana, što je najčešće praćeno reaktivnom gliozom i neuroinflamacijom (Erkkinen et al., 2018).

Neurodegenerativne bolesti mogu se kategorisati prema primarnim kliničkim manifestacijama (na primer, demencije, bolest motornog neurona, parkinsonizam), anatomske i regionalne distribucije neurodegenerativnih promena (frontotemporalne degeneracije, spinocerebelarne degeneracije, ekstrapiramidalni poremećaji) ili na osnovu patoloških promena na molekulskom nivou (amiloidoze, taupatije, α-sinukleinopatije) (Dugger and Dickson, 2017). Etiopatogeneza neurodegenerativnih bolesti je veoma kompleksna, a glavni uzročnici koji dovode do nastanka bolesti još uvek nisu poznati. Genetička predispozicija i izlaganje sredinskim faktorima, najčešće toksinima, značajno doprinose nastanku/razvoju neurodegeneracije (Cannon and Greenamyre, 2011). Među spoljašnjim faktorima, ustanovljena je jasna veza između akumulacije toksičnih metala - aluminijuma, olova, gvožđa, kadmijuma i kalaja - i neurodegenerativnih bolesti pogotovo AD, PD i ALS (Zatta et al., 2003; Mitra et al., 2014a). Kao važni sredinski faktori još se navode neuhranjenost, duvanski dim i drugi tipovi toksičnih zagađenja hrane i vode (Mitra et al., 2014b). Jedna od čestih manifestacija i verovatnih uzroka umiranja neurona u neurodegenerativnim bolestima je pojava “patoloških” proteina sa izmenjenom kvaternernom strukturom i fizičko-hemijskim svojstvima, koji se talože u mozgu (Godeau et al., 2021). Ovakvi proteinski agregati, koji u svom središtu neretko sadrže jone teških i prelaznih metala (Maynard et al., 2005), postaju nesolubilni i nedostupni normalnoj razgradnji, pa time i “toksični” za nervne ćelije.

2. Neuroinflamacija

Propadanje neurona i degeneracija nervnih vlakana, bilo da je uslovljena povredom, toksinima ili infekcijom od strane patogena, praćeno je neuroinflamacijskim procesom. Neuroinflamacija je zapaljenski odgovor tkiva CNS, posredovan signalnim faktorima, citokinima, hemokinima, reaktivnim vrstama kiseonika i azota i sekundarnim glasnicima (DiSabato et al., 2016). Glavni izvori ovih medijatora su mikroglija i astrociti, ali ove faktore oslobađaju i druge glijske ćelije, kao i neuroni. Fiziološki smisao inflamatornog odgovora je kontrola i ograničavanje povrede ili infekcije, kao i pospešivanje reparacije tkiva, pa kao takav, akutan neuroinflamacijski odgovor ima pozitivan uticaj na ishod ovakvih stanja. U neurodegenerativnim bolestima koje se odlikuju kontinualnim odumiranjem neurona, i neuroinflamacija postaje hronična, između ostalog i zbog toga što glijske ćelije gube

sposobnost autoregulacije oslobađanja proinflamacijskih faktora, pa u tom slučaju neuroinflamacijski proces postaje još jedan uzročni faktor napredovanja patologije (Howcroft et al., 2013).

2.1. Uloga mikroglije

Mikroglijske ćelije su mijeloidne ćelije CNS koje vode poreklo od progenitorskih ćelija žumancetne kese. Ove ćelije naseljavaju nervno tkivo rano tokom razvića CNS, a pre zatvaranja krvno-moždane barijere (Arnò et al., 2014). Odlikuju se izrazito heterogenom morfologijom i u fiziološkim i u patološkim uslovima, koja se kreće od razgranate preko štapolike do okruglaste/ameboidne (Lawson et al., 1990). U fiziološkim uslovima mikroglija je ravnomerno raspoređena u tkivu, poseduje razgranat fenotip i svoju homeostatsku ulogu ostvaruje kroz tri funkcije. Prva se odnosi na detektovanje homeostatskog stanja tkivnog parenhima CNS posredstvom „*senzozoma*“, skupa membranskih receptora koji čine transkripcioni „*potpis*“ mirujuće mikroglije (Hickman et al., 2013). Druga uloga se odnosi na homeostatsku ulogu mikroglije u regulaciji neurogeneze (Diaz-Aparicio et al., 2020), gustine sinapsi i plastičnosti (Ji et al., 2013; Nguyen et al., 2020), prevenciji lokalne ekscitotoksičnosti (Nosi et al., 2021) i u homeostazi mijelina (Zhan et al., 2014; Hickman et al., 2018). Treća, posebno naglašena u patofiziološkim uslovima, ogleda se u sposobnosti razgranate mikroglije da reaguje na štetne stimuluse, poput molekulskih obrazaca povezanih sa patogenima (*engl. pathogen-associated molecular paterns - PAMP)* i molekulskih obrazaca povezanih sa oštećenjem (*engl. damage-associated molecular patterns – DAMP*) (Kwon and Koh, 2020). Sve navedene aktivnosti regulisane su interkacijama koje mikroglija, posredstvom svojih membranskih receptora, ostvaruje sa komponentama vanćelijskog matriksa, kao i sa solubilnnim faktorima i/ili membranskim proteinima poreklom od drugih ćelija (Nguyen et al., 2020). U patološkim uslovima, pojavom molekulskih obrazaca opasnosti i citokina, mikroglija se aktivira u jednom od dva pravca, čija su krajnja stanja označena kao M1 i M2 aktivirana mikroglija. M1 podrazumeva ‘’neurotoksičnu’’ aktivaciju ćelija, koja svojim delovanjem doprinosi daljem oštećenju tkiva, dok M2 fenotip ispoljava neuroprotektivni efekat na tkivo (Mills et al., 2000). U patološkim uslovima mikroglija započinje produkciju proinflamacijskih citokina, poput faktora nekroze tumora-α (TNF-α), interleukina-1β (IL-1β), interleukina 6 (IL-6), kao i brojnih hemokina, uključujući CCL2, CCL5, CXCL1 (Glass et al., 2010; Norden et al., 2016; Hickman et al., 2018). Proinflamacijski citokini, povećana količina vanćelijskog adenozin-5' trifosfata (ATP), kao i prisustvo molekulskih obrazaca opasnosti izaziva transformaciju mikroglije iz mirujućeg u inflamacijski fenotip M1, koji se odlikuje oslobađanjem velike količine IL-6, IL-1β, TNF-α, pojačanom produkcijom azot-(II) oksida (NO) i oslobađanjem nekoliko serin-, cistein- i metaloproteaza, što štetno utiče na integritet zahvaćenog tkiva (Glass et al., 2010). Sa druge strane, citokini poput interleukina 4 (IL-4), interleukina 10 (IL-10), interleukina 13 (IL-13) i transformišućeg faktora rasta β (TGF- β), deo su molekulskog „potpisa“ mikroglije sa antiinflamacijskim fenotipom M2. Osim navedenih anti-inflamacijskih citokina, M2 mikroglija oslobađa/eksprimira faktore poput arginaze 1 (Arg-1), Ym1, FIZZ1, CD206 i insulinu-sličan faktor rasta 1 (IGF-1) (Glass et al., 2010; Tang and Le, 2016; Liddelow and Barres, 2017). Faktori M2 mikroglije povezani su sa neuroprotekcijom i oporavkom tkiva (Slika 1) (Tang and Le, 2016). Pomenuta M1/M2 kategorizacija predstavlja dva krajnja stanja ukupnog spektra aktivacije mikroglije, između kojih postoji čitav niz prelaznih stupnjeva.

Novije transkriptomske studije u modelima neurodegeneracije ukazuju da reaktivna mikroglija istovremeno eksprimira gene koji odlikuju oba krajnja stanja (Colonna and Butovsky, 2017), pa i da postoje fenotipovi koji su specifični za patologiju (engl. disease-associated microglia) (Glass et al., 2010). Uprkos zastupljenosti u literaturi, potreban je oprez prilikom korišćenja pojednostavljenje M1/M2 klasifikacije (Ransohoff, 2016; Nosi et al., 2021).

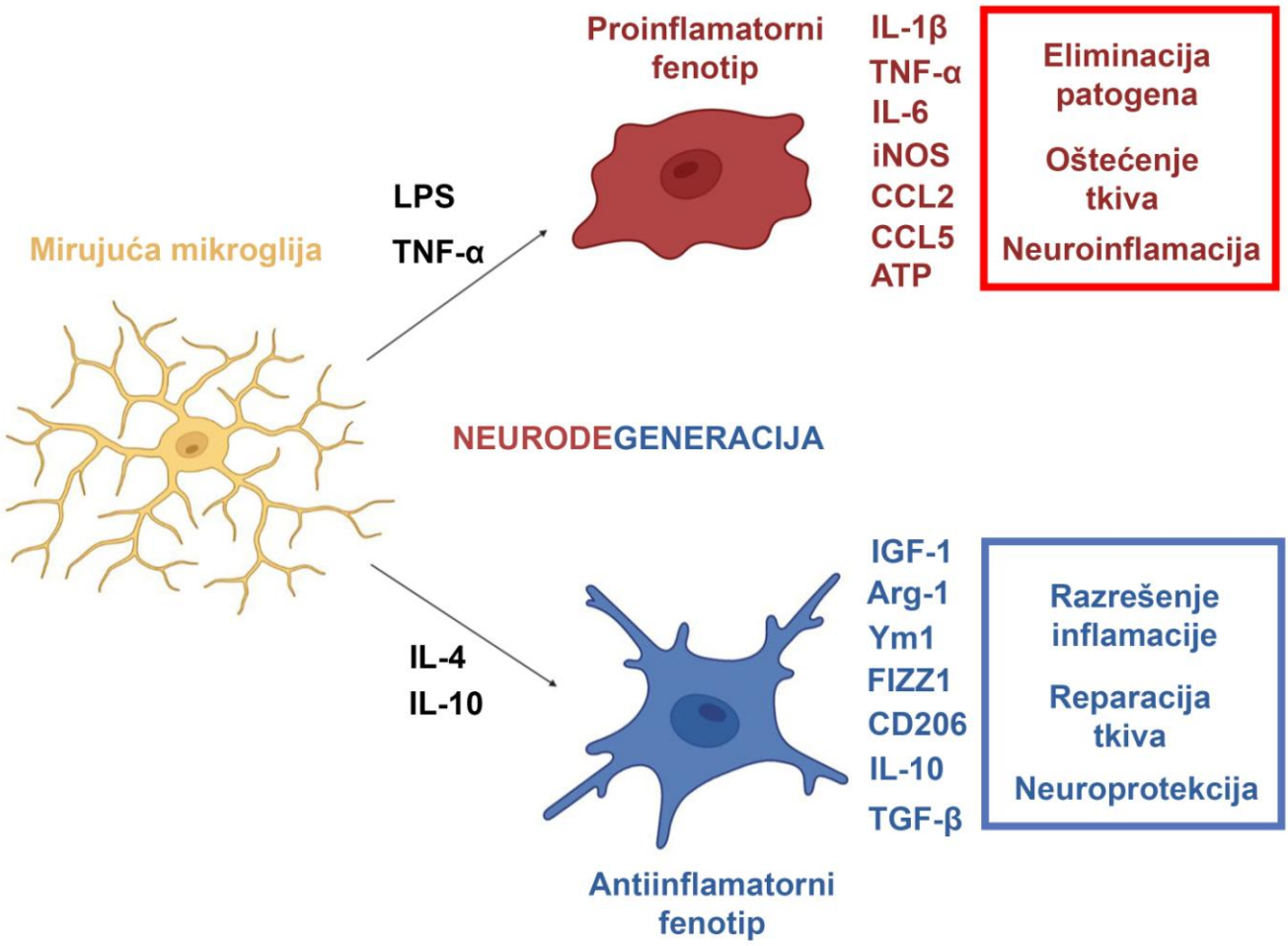

Slika 1. Shematski prikaz aktivacije i polarizacije mikrogliije u uslovima neurodegeneracije

2.2. Uloga astrocita

Astrociti su najzastupljenije glijske ćelije ključne u održavanju ukupne homeostaze CNS (Sofroniew and Vinters, 2010). Astrociti obavljaju brojne uloge u fiziološkim i patološkim uslovima, među kojima su održavanje integriteta krvno-moždane barijere, jonske i vodene homeostaze, sinaptičke aktivnosti, regulacija protoka krvi kroz vaskularni sistem mozga, kontrola sekrecije faktora rasta, uklanjanje ćelijskog debrisa i formiranje glijskog ožiljka (Sofroniew, 2009; Sofroniew and Vinters, 2010; Colombo and Farina, 2016; Oksanen et al., 2019).

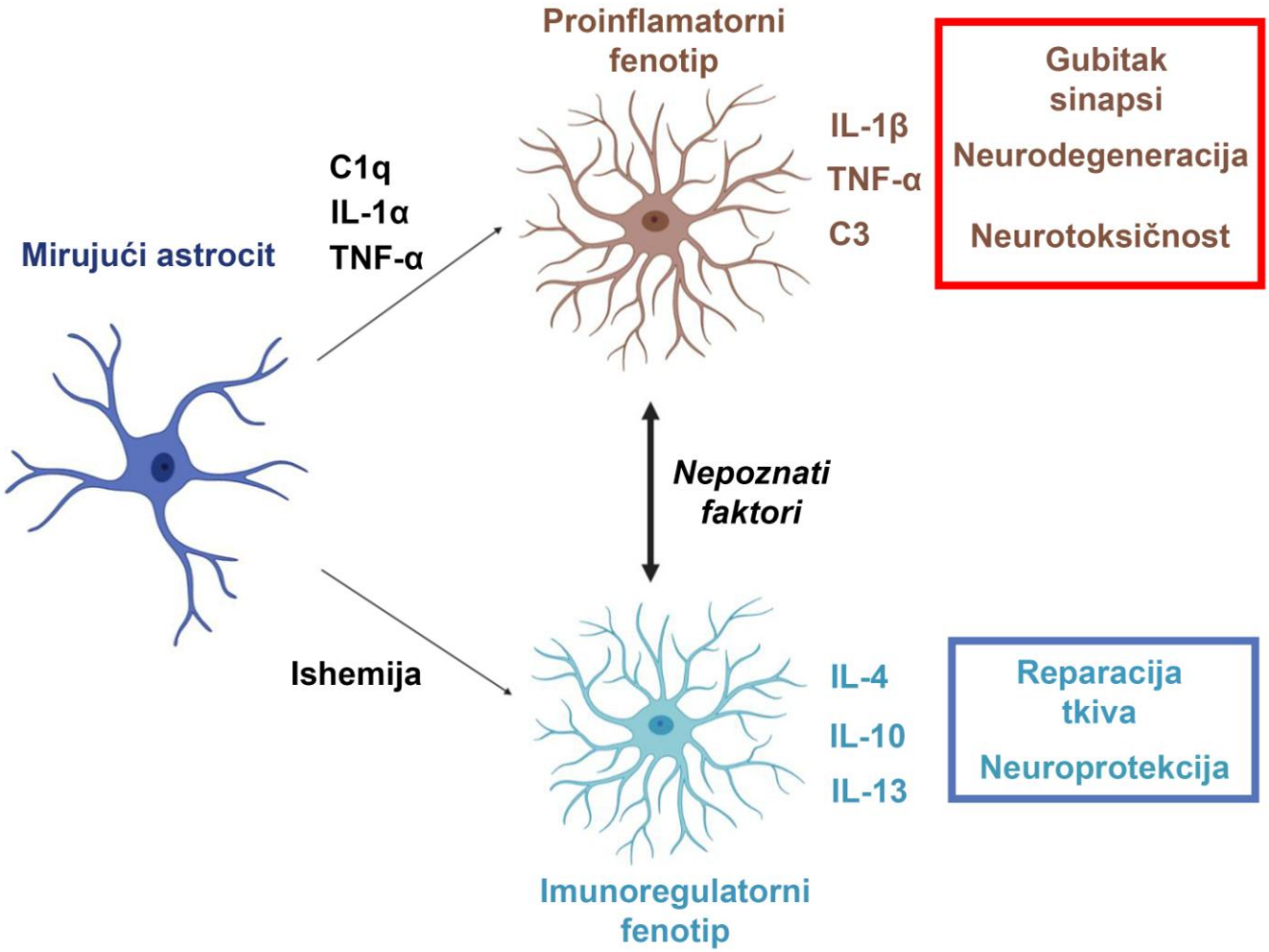

Slika 2. Shematski prikaz aktivacije i polarizacije astrocita u uslovima neurodegeneracije

Astrociti pokazuju veliku regionalnu heterogenost, kako morfološku, tako i u pogledu specifičnih uloga u mikrookruženju u kojem se nalaze (Matias et al., 2019). Novije studije ukazuju na postojanje pet subpopulacija astrocita, od kojih svaka eksprimira specifični „*molekulski potpis*“, a koji se mogu naći u istim regionima mozga u različitim odnosima. Ove populacije su otkrivene u mirisnoj kvržici, moždanoj kori, talamusu, malom mozgu, moždanom stablu i kičmenoj moždini glodara (John Lin et al., 2017). Tradicionalna klasifikacija podrazumeva podelu astrocita na protoplazmatske, koji okupiraju sivu masu, i fibrozne koji se nalaze u beloj masi. U fiziološkim uslovima protoplazmatski astrociti imaju striktnu *domensku* organizaciju, koja podrazumeva da svaki astrocit okupira njemu svojstvenu zapreminu tkiva CNS i da se ne preklapa sa domenima susednih astrocita (Bushong et al., 2002; Ogata and Kosaka, 2002). Kao odgovor na narušenu homeostazu CNS, kakva se viđa pri povredama mozga i kičmene moždine kao i u neurodegenerativnim bolestima, astrociti prolaze kroz proces transformacije koji obuhvata ćelijske, molekulske i funkcionalne promene koje se zajednički označavaju imenom *reaktivna astroglioza* (Colombo and Farina, 2016; Escartin et

al., 2021) (Slika 2). Istraživanja su pokazala da tokom neuroinflamacijskih procesa deo protoplazmatskih astrocita zadobija sposobnost proliferacije, te su stoga definisane dve reaktivne subpopulacije astrocita – *proliferativna i neproliferativna* (Sofroniew, 2020; Escartin et al., 2021). Astrociti koji pripadaju neproliferativnoj populaciji zadržavaju svoju domensku organizaciju, dok proliferativni astrociti migriraju ka mestu povrede, okružuju ga i izoluju, formirajući tako *glijski ožiljak* (Wanner et al., 2013). Po analogiji sa ćelijama mikroglije, i astrociti mogu imati proinflamacijski (A1 fenotip) ili imunoregulatorni fenotip (A2 fenotip) (Kwon and Koh, 2020). Reaktivni astrociti sa proinflamacijskim fenotipom pojačano eksprimiraju proteine komplementa (C3), IL-1β, TNF-α, pojačano proizvode reaktivne vrste kiseonika i azota, poput NO, što doprinosi pojačanju neuroinflamacije (Glass et al., 2010; Liddelow and Barres, 2017). Astrociti sa protektivnim fenotipom pojačano eksprimiraju neurotrofne faktore i antiinflamacijske citokine, poput IL-4, IL-13, IL-10, što im daje osobine neuroprotektivnih astrocita (Slika 2) (Oksanen et al., 2019). Nakon identifikacije i podele astrocita na A1 i A2 subpopulacije, po uzoru na već postojeću klasifikaciju reaktivne mikroglije, nameće se sličan zaključak a to je da ovakva podela predstavlja pojednostavljenu dihotomiju koja je samo krajnja tačka čitavog spektra stanja tj. statusa, od kojih astrociti mogu zauzeti bilo koji na ovom kontinuumu (Oksanen et al., 2019; Escartin et al., 2021).

3. Neurodegeneracija i neuroinflamacija izazvane trimetil-kalajem

3.1. Trimetil-kalaj (TMK)

Organska jedinjenja kalaja (IV), zavisno od broja kovalentnih C-Sn veza u molekulu, kojih može biti od jedan do četiri, odnosno, broja za njih vezanih alkilnih i arilnih grupa, klasifikuju se na mono-, di-, tri- i tetraorganokalajna jednjenja (Costa et al., 2006). Organokalajna jedinjenja imaju široku primenu u industriji, kao toplotni stabilizatori u procesu proizvodnje polivinil hlorida i gume, i u poljoprivredi, kao biocidi (Piver, 1973; Florea and Büsselberg, 2006). Tokom nekoliko decenija od kada su u upotrebi, zabeležena su sporadična trovanja ovim jedinjenjima, uglavnom usled akcidentalnog izlaganja radnika u postrojenjima koja koriste ova jedinjenja. Osobe izložene organokalajnim jedinjenjima razvijaju simptome koji ukazuju na oštećenje limbičkog sistema, a uključuju akutno konfuzno stanje i nesanicu, prostornu dezorijentaciju i kognitivne poremećaje, koji mogu biti prisutni godinama nakon izlaganja (Feldman et al., 1993). Upravo je zbog toksičnih svojstava ograničena upotreba organokalajnih jedinjenja, mada ona i dalje predstavljaju značajne zagađivače životne sredine (Tang et al., 2010). Neka od ovih jedinjenja pronašla su primenu u naučnim istraživanjima, najviše zbog selektivnosti delovanja u specifičnim regionima mozga.

Trimetil-kalaj (C_3H_9ClSn, TMK) je organsko jedinjenje koje nastaje kao intermedijerni produkt sinteze drugih organskih jedinjena kalaja, često korišćeno u industriji kao stabilizator sinteze plastike i u poljoprivredi kao insekticid (Lee et al., 2016). TMK je “našao” svoje mesto u istraživanjima neurodegeneracije i neuroinflamacije zahvaljujući neurotoksičnosti i selektivnom delovanju na strukture limbičkog sistema, naročito na hipokampus (Geloso et al., 2011). Trovanje eksperimentalnih životinja TMK dovodi do pojave simptoma koji su zabeleženi kod ljudi izloženih ovom toksinu, a koji uključuju epileptične napade, hiperaktivnost, samopovređivanje, agresivnost kao i poremećaj učenja i pamćenja (Geloso et

al., 2011; Lee et al., 2016). Neurodegeneracija izazvana TMK kod eksperimentalnih životinja pokazuje suštinske patofiziološke karakteristike svih neurodegenerativnih bolesti, pa stoga ona predstavlja koristan eksperimentalni model za izučavanje neurodegeneracije i neuroinflamacije praćene kognitivnim deficitiom i sklerozom hipokampusa. Obrazac neurodegeneracije unekoliko se razlikuje kod miševa i pacova, a varira i u zavisnosti od soja, doze, nosača, načina administracije, i starosti životinja (Balaban et al., 1988; O'Callaghan et al., 1989; Harry and Lefebvre d'Hellencourt, 2003; Geloso et al., 2011). Kod miševa, TMK izaziva akutne lezije u granularnom sloju zubate vijuge (lat. *gyrus dentatus*) (Geloso et al., 2011). Kod pacova se razvijaju znatno ekstenzivnije lezije, koje se uočavaju dva dana nakon intoksikacije, i progresivno se razvijaju tokom tri nedelje, a u najvećoj meri zahvataju CA1 i CA3/hilarni region (Brock and O'Callaghan, 1987; Balaban et al., 1988; Whittington et al., 1989). Razlika u osetljivosti i efektima kod miševa i pacova pripisuje se razlikama afiniteta hemoglobina ka TMK, koji je veći kod pacova, što uzrokuje brže i lakše oslobađanje toksina i dugotrajniji karakter neurodegeneracije kod pacova (Chang et al., 1983). Osim neurodegeneracije, TMK dovodi do pojave histopatoloških markera AD, kako u humanoj populaciji, tako i u životinjskim modelima AD, poput amiloidnog prekursornog proteina, presenilina-1 i amiloida beta (Nilsberth et al., 2002). Rezultujuće kognitivne promene i promene ponašanja izazvane TMK (Kang et al., 2016; Park et al., 2019) upućuju na to da ovaj eksperimentalni model može da bude koristan životinjski model za izučavanje Alchajmerove bolesti.

3.2. Mehanizam neurotoksičnog delovanja TMK

Jednokratna primena TMK kod glodara najčešće dovodi do prostorno i vremenski specifične masivne smrti neurona u međupovezanim strukturama limbičkog sistema, posebno u entorinalnoj kori (*lat. cortex entorhinalis*), piriformnoj kori (*lat. cortex piriformis*), mirisnoj kvržici (lat. *bulbus olfactorius*), bademastim jedrima (lat. *nuclei amygdaloides*), i naročito, u hipokampalnoj formaciji (Balaban et al., 1988). Brojna istraživanja pokazuju da je prevladavajući tip ćelijske smrti neurona izazvan primenom TMK – kontrolisana ćelijska smrt tipa apoptoze (Andersson et al., 1997; Kane et al., 1998; Kassed et al., 2002, 2004; Jenkins and Barone, 2004; Shuto et al., 2009a, 2009b). Iako citotoksični mehanizam delovanja TMK nije u potpunosti rasvetljen (Cook et al., 1984), značajan pomak je načinjen otkrićem proteina stanina (Krady et al., 1990; Toggas et al., 1992), visoko konzerviranog proteina u membrani mitohondrija i endoplazmatskog retikuluma. Pokazalo se da se nakon ulaska u ćelije, TMK vezuje za stanin, što dovodi do narušavanja integriteta mitohondrijske membrane (Dejneka et al., 1997; Billingsley et al., 2006), oslobađanja unutarćelijskih depoa jona Ca^{2+} (Zhang et al., 2006; Wang et al., 2008) i generisanja reaktivnih vrsta kiseonika (Geloso et al., 2011). Na značajnu ulogu deregulacije unutarćelijskog Ca^{2+} u apoptozi izazvanoj TMK ukazuju podaci nekoliko studija *in vivo* i *in vitro* o većem preživljavanju hipokampalnih neurona koji su bogato snabdeveni kalcijum-vezujućim proteinima, parvalbuminom i kalretininom (Geloso et al., 1996, 1997; Florea et al., 2005a, 2005b; Piacentini et al., 2008).

Osim što narušava unutarćelijsku homeostazu Ca^{2+} i izaziva oksidativni stres, TMK izaziva ekscitotoksičnost posredovanu glutamatom (Geloso et al., 2011). Pretpostavlja se da svi navedeni događaji dovode do aktivacije ushodnih protein-kinaza (JNK, protein-kinaze C), aktivacije transkripcionih faktora (NF-κB), proteina uključenih u odgovor na stres i gena ranog odgovora, što rezultuje kaskadom koja se završava apoptozom. Narušavanje integriteta mitohondrijske membrane dovodi do oslobađanja unutarćelijskih depoa jona Ca^{2+},

generisanja reaktivnih vrsta kiseonika, što sve doprinosi ćelijskoj smrti (Zhang et al., 2006; Wang et al., 2008). Kao i u drugim patološkim situacijama povezanim sa smrću neurona, neurodegeneracija izazvana TMK izaziva specifičan proces aktivacije mikroglije i astrocita.

3.3. Aktivacija mikroglije i astrocita u neuroinflamaciji izazvanoj primenomTMK

Neurodegeneracija izazvana TMK praćena je aktivacijom mikroglije i astrocita u regionima mozga pogođenim ćelijskom smrću, posebno u hipokampusu (Geloso et al., 2011). Histohemijske analize ukazale su da smrt hipokampalnih neurona prati burna aktivacija astrocita koja dostiže maksimum između treće i pete nedelje od intoksikacije (Brock and O'Callaghan, 1987). Nakon toga, ova reakcija slabi, mada se histološki može detektovati i šest meseci nakon intoksikacije, što je ujedno i najkasnija vremenska tačka koja je izučavana u ovom modelu (Koczyk and Oderfeld-Nowak, 2000). Aktivirani astrociti pojačano eksprimiraju glavne markere reaktivne glioze – glijski kiseli fibrilarni protein (*engl. glial acidic fibrilarly protein* - *GFAP*) i S100B, a neke subpopulacije reaktivnih astrocita prolazno eksprimiraju intermedijarne filamente vimentin i nestin (Andersson et al., 1997; Geloso et al., 2004). Pored astrocita, primećena je aktivacija mikroglije, koja okružuje regione sa aktivnom neurodegeneracijom, naročito piramidne neurone CA1 i CA3 regiona (Koczyk and Oderfeld-Nowak, 2000). Aktivacija mikroglije, slično astrocitima, primećuje se u prvim danima nakon davanja TMK i detektuje se i šest meseci nakon intoksikacije (Koczyk and Oderfeld-Nowak, 2000). Aktivacija glijskih ćelija praćena je pojačanim oslobađanjem citokina, iako izvor ovih proinflamacijskih faktora nije utvrđen. Osim što deluje na neurone, čija ćelijska smrt inicira neuroinflamaciju, novije *in vitro* studije ukazuju da TMK ostvaruje direktan uticaj na astrocite (Aschner and Aschner, 1992), bez čijeg prisustva nije moguća aktivacija mikroglije (Röhl and Sievers, 2005; Röhl et al., 2009).

Nezavisno od mehanizam oštećenja i aktivacije glijskih ćelija, jedan od univerzalnih događaja u uslovima oštećenja nervnog tkiva jeste pojačano oslobađanje ATP, koji deluje kao molekulski signal opasnosti DAMP. Oslobođeni ATP deluje na membranske purinoceptore, nakon čega se degraduje katalitičkom aktivnošću enzima ektoenukleotidaza, koji zajedno čine osnovne komponente sistema purinske signalizacije.

4. Purinska signalizacija

Ubrzo nakon otkrića da adeninski nukleotidi i njegovi derivati mogu imati ulogu i signalnih molekula, Geoffrey Burnstock na osnovu svojih i pređašnjih istraživanja postavlja hipotezu da ATP može obavljati ulogu neurotransmitera i predlaže termin *purinska signalizacija* (Burnstock, 1972). Danas je poznato da ćelije poseduju dve klase receptora koji vezuju purinske nukleotide i nukleozide, te da postoje enzimi koji kontrolišu vanćelijsku koncentraciju purina (Robson et al., 2006). Nukleotidi oslobođeni u vanćelijski prostor modulišu/regulišu brojne tkivne funkcije uključujući razviće, sekreciju drugih molekula, inflamacijski i imunski odgovor, cirkulaciju telesnih tečnosti i mnoge druge (Robson et al., 2006). Nakon oslobađanja nukleotida u vanćelijsku sredinu i njihovog delovanja na odgovarajuće receptore, ćelija ne može da preuzme nukleotide, zbog naelektrisanja i veličine. Stoga se na površini svih ćelija CNS (ali i svih drugih tkiva) nalaze enzimi ektonukleotidaze, koji sekvencijalno razgrađuju nukleotide do nukleozida i time regulišu njihovu dostupnost i posredno aktivaciju odgovorajućih receptora (Zimmermann et al., 2012).

4.1. Purini kao signalni molekul

U svim tipovima ćelija ATP je izvor energije za ćelijske procese i donor fosfatne grupe u reakcijama fosforilacije. Osim toga u CNS, neuroni, mikroglija, oligodendrociti, endotelne ćelije i posebno astrociti koriste ATP kao signalni molekul koji se oslobađa u vanćelijsku sredinu na regulisan način (Abbracchio et al., 2009). ATP koji se oslobađa zavisno od neuronske aktivnosti ima ulogu kotransmitera, dok ATP poreklom iz astrocita ima ulogu gliotransmitera i neuromodulatora (Fiebich et al., 2014). ATP se u vanćelijski prostor oslobađa na kontrolisan način, putem vezikula, transportera ili jonskih kanala. ATP se oslobađa egzocitozom, u sastavu vezikula sa neurotransmiterom (Franke and Illes, 2006). ATP se iz glijskih ćelija transportuje olakšanom difuzijom, putem transportera ili jonskih kanala. Transmembranski transport ATP odvija se posredstvom kanala paneksina, i koneksina (Suadicani et al., 2006). S obzirom na to da je u fiziološkim uslovima količina ATP u vanćelijskoj sredini regulisana kontrolisanim oslobađanjem ATP i njegovom razgradnjom posredstvom ektinukleotidaza, nivo ATP se održava u nanomolskom opsegu (Lazarowski et al., 2003). U tom opsegu koncentracija, ATP aktivira visoko-afinitetne P2 receptore, i to prevashodno $P2X_{1-6}R$ i $P2Y_2R$ (Burnstock 2018). Fina ravnoteža između oslobađanja i razgradnje ATP može biti narušena u patološkim stanjima. Metabolički kompromitovani i/ili oštećeni neuroni i aktivirane glijske ćelije oslobađaju znatne količine ATP i drugih nukleotida u vanćelijsku sredinu (Fiebich et al., 2014). U takvim uslovima nivo vanćelijskog ATP dostiže mikromolske koncentracije i deluje kao DAMP molekul, aktivirajući P2 receptore niskog afiniteta, prevashodno $P2X_7R$, (Gourine et al., 2007). Specifičnost purinske signalizacije je činjenica da i proizvodi enzimske razgradnje ATP, imaju ulogu signalnih molekula. Adenozin-difosfat (ADP) deluje na set P2YR receptora, i to $P2Y_1R$, $P2Y_6R$, $P2Y_{12}R$ i $P2Y_{13}R$, dok nukleozid adenozin aktivira P1 receptore.

4.2. Purinski receptori

Purinski receptori čine familiju membranskih receptora, široko eksprimiranu u svim tkivima, uključujući i CNS (Burnstock, 2014). Čine je dve velike podfamilije – P1 receptori, koji vezuju nukleozide i P2 receptori, koji se aktiviraju u prisustvu nukleotida. P1 grupa obuhvata četiri podtipa adenozinskih receptora spregnutih sa proteinom G - A_1R, $A_{2A}R$, $A_{2B}R$ i A_3R receptori, od kojih su prva da sa visokim afinitetom dok su druga dva sa niskim afinitetom. A_1R i A_3R su spregnuti sa G_i proteinom koji inhibira adenil-ciklazu (AC), što dovodi do smanjene produkcije i unutarćelijske koncentracije cikličnog AMP (cAMP). $A_{2A}R$ i $A_{2B}R$ su spregnuti sa proteinom G_s, koji stimiliše AC i dovodi do povećanje unutarćelijske koncentracije cAMP (Boison et al., 2010). Signalizacija posredovana ATP odvija se posredstvom P2 receptora (Oliveira-Giacomelli et al., 2018), koji se eksprimiraju u gotovo svim tkivima i učestvuju u regulaciji različtiih procesa u fiziološkim i patološkim stanjima (Agostinho et al., 2020). P2 podfamilija obuhvata dve klase receptora, P2X i P2Y (Oliveira-Giacomelli et al., 2018). P2XR broji sedam članova jonotropnih receptora ($P2X_{1-7}R$), koji posreduju u brzim odgovorima ćelije na ATP i njegove derivate (Jarvis and Khakh, 2009; Saul et al., 2013). Drugu potklasu P2Y receptora čine metabotropni receptori ($P2Y_{1-14}R$), koji selektivno odgovaraju na prisustvo ATP, ADP UTP, UDP i UDP-glukoze. Detaljniji pregled P1 i P2 receptora dat je u Tabeli 1.

Tabela 1. Karakteristike P1 i P2 receptora (*modifikovano iz Burnstock 2018*)

Receptor	Distribucija u CNS	Agonista	Mehanizam delovanja
A_1R	Mozak i kičmena moždina	Adenozin	G_i/G_o ↓cAMP
$A_{2A}R$	Bazalne ganglije	Adenozin	G_s ↑cAMP
$A_{2B}R$	Glijske ćelije	Adenozin	G_s ↑cAMP
A_3R	Glijske ćelije	Adenozin	G_i/G_o, G_q/G_{11} ↓cAMP
$P2X_1R$	Mali mozak i kičmena moždina	ATP	$[Ca^{2+}]_i$ i $[Na^+]_i$ ↑
$P2X_2R$	Senzorne ganglije	ATP	$[Ca^{2+}]_i$ ↑
$P2X_3R$	Senzorni neuroni i simpatičke ganglije	ATP	$[Ca^{2+}]_i$ i $[Na^+]_i$ ↑
$P2X_4R$	Mikroglija	ATP	$[Ca^{2+}]_i$ ↑
$P2X_5R$	Kičmena moždina	ATP	$[Ca^{2+}]_i$ ↑
$P2X_6R$	Motoneuroni kičmene moždine	ATP	$[Ca^{2+}]_i$ ↑
$P2X_7R$	Mikroglija, astrociti, neuroni	ATP	$[Ca^{2+}]_i$ i $[Na^+]_i$ ↑
$P2Y_1R$	Astrociti, neuroni	ADP	G_q/G_{11} ; Aktivacija PLC-β
$P2Y_2R$	Mikroglija	UTP	G_q/G_{11} ; Aktivacija PLC-β
$P2Y_4R$	Neuroni, astrociti	UTP > ATP	G_q/G_{11} ; Aktivacija PLC-β
$P2Y_6R$	Aktivirana mikroglija	UDP > UTP > ATP	G_q/G_{11} ; Aktivacija PLC-β
$P2Y_{11}R$	Neuroni	ATP	G_q/G_{11} i G_s; Aktivacija PLC-β
$P2Y_{12}R$	Mikroglija	ADP >> ATP	$G_{αI}$; Inhibicija AC
$P2Y_{13}R$	Mikroglija	ADP > ATP	G_i/G_o
$P2Y_{14}R$	Oligodendrociti	UDP > UDP-glukoza	G_q/G_{11}; Inhibicija AC

4.3. Ektonukleotidaze

Nukleotidi oslobođeni u vanćelijsku sredinu, zbog svoje veličine i naelektrisanja, teško se transportuju kroz ćelijsku membranu. Problem viška nukleotida u vanćelijskom prostoru rešava se enzimskom razgradnjom nukleotida, posredstvom enzima čije je katalitičko mesto okrenuto ka vanćelijskoj sredini - ektonukleotidaza (Zimmermann et al., 2012). Konačni proizvod razlaganja ATP pod dejstvom ektonukleotidaza je nukleozid adenozin, koji se vraća u ćelije i uključuje u spasonosni put purina. Transport adenozina u ćelija odvija se posredstvom dvosmernih ekvilibrativnih (ENT) i/ili jednosmernih koncentrativnih (CNT) transportera (Frenguelli, 2019).

Ektonukleotidaze su ektoenzimi, čija je osnovna uloga hidroliza γ-, β- i α-fosfodiestarske veze nukleotida u vanćelijskoj sredini (Zimmermann, 2008). U zavisnosti od fosfatne grupe koju hidrolizuju, ektonukleotidaze mogu biti trinukleotid-, dinukleotid ili mononukleoitid fosfataze kao i nukleozid polifosfataze pri čemu nastaju nukleozid difosfati, nukleozid monofosfati, nukleozidi , fosfati (P_i) i pirofosfati (PP_i). Glavna uloga svih ektonukleotidaza jeste kontrola dostupnosti liganada za dve velike klase receptora – P2 i P1 klasu, ali i regulacija nivoa vanćelijskih nukleotida (Kukulski et al., 2011; Zimmermann et al., 2012).

Identifikovane su četiri grupe ektonukleotidaza (Slika 3):

1) Ekto-nukleozid 5'- trifosfat difosfohidrolaze (NTPD-aze);

2) Ekto-nukleotid pirofosfateze/fosfodiesteraze (NPP);

3) Ekto-5'–nukleotidaza (eN, CD73);

4) Alkalne fosfataze (AP).

4.3.1. Ekto-nukleozid 5'- trifosfat difosfohidrolaze (NTPDaze)

Ekto-nukleozid 5'- trifosfat difosfohidrolaze (NTPDaze) su enzimi koji hidrolizuju razgradnju γ- i β-fosfatne grupe ATP, u prisustvu milimolarnih koncentracija Mg^{2+} ili Ca^{2+} u fiziološkom opsegu pH vrednosti (Robson et al., 2006; Yegutkin, 2008). Identifikovano je osam različitih NTPD-aza kod sisara. Četiri su tipični ektoenzimi (NTPDaza1, 2, 3 i 8), NTPDaza 4 i 7 su takođe membranski enzimi ali smešteni unutar ćelije u membranama organela, dok se NTPDaze 5 i 6 predominantno sekretuju u vanćelijsku sredinu (Robson et al., 2006; Knowles, 2011). Kristalografske i molekulske analize pokazale su da su NTPDaza 1, 2, 3 i 8 glikoproteini slične strukture, sačinjene od blizu 500 aminokiselina od kojih je oko 40 % zajedničko za sva četiri ektoenzima, molekulske mase između 70 – 80 kDa (Zimmermann et al., 2012). Takođe, ovi enzimi dele i važne strukturne i funkcionalne domene, uključujući i pet visoko konzerviranih aminokiselinskih sekvenci koji se nazivaju *apirazni domeni* (*engl. apyrase-conserved regions, APR*). Apirazni domeni su glavna odlika čitave familije enzima i mogu se naći čak i u enzimima kvasca, što ukazuje na njihovu evolutivnu konzerviranost (Handa and Guidotti, 1996; Schulte am Esch et al., 1999; Smith and Kirley, 1999). NTPDaze se eksprimiraju u gotovo svim tkivima, ali imaju jasno definisanu ćelijsku distribuciju. U CNS se dominantno eksprimiraju NTPDaze 1, 2 i 3 gde pokazuju veliku heterogenost u pogledu regionalne i ćelijske distribucije (Braun et al., 2000; Belcher et al.,

2006; Robson et al., 2006; Langer et al., 2008; Kiss et al., 2009; Grković et al., 2016, 2019a, 2019b).

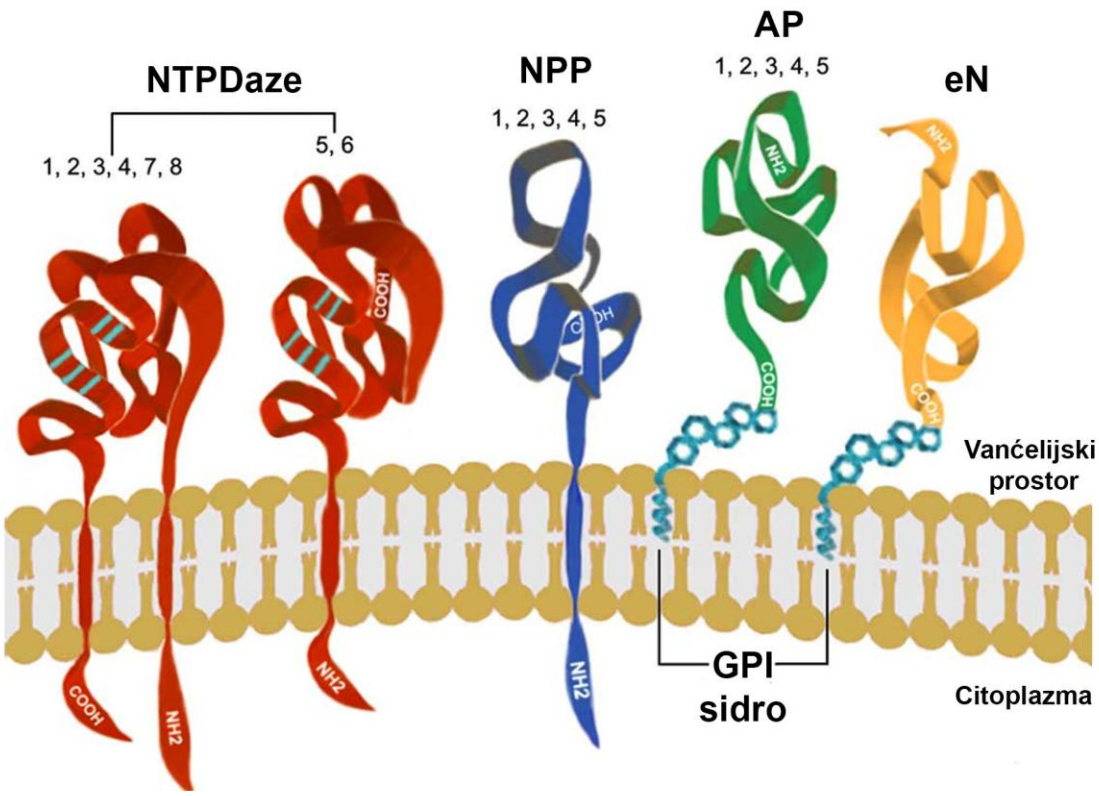

Slika 3. Podela i tipovi ektonukleotidaza (*Modifikovano iz Zimmermann et al 2012*)

NTPDaza 1 je jedna od najbolje proučenih ektonukleotidaza. Ovaj ektoenzim predstavlja marker aktivacije limfocita zbog čega i nosi alternativni naziv CD39 (*engl. cluster of differntiation 39*). Pokazano je da se NTPDaza1 eksprimira na ćelijama prirodnim ubicama (*engl. Natural killer cells*) ćelijama, monocitima, dendritskim ćelijama i u različitim subpopulacijama reaktivnih T limfocita (Zimmermann et al., 2012). Ekspresija NTPDaze 1 na imunskim ćelijama doprinosi regulaciji purinske signalizacije u homeostatskim i inflamacijskim uslovima što ukazuje na njenu značajnu ulogu u ćelijskom imunskom odgovoru (Takenaka et al., 2016). U CNS ovaj enzim ima ograničenu distribuciju na endotelne ćelije kapilara i ćelije mikroglije (Braun et al., 2000), ali je njegovo prisustvo pokazano i u sinapsama (Grković et al., 2019a). NTPDaza 1 pokazuje različit afinitet prema adeninskim i uridinskim nukelotidima, pa će tako ATP i ADP biti podjednako efikasno hidrolizovani zbog gotovo jednakog afiniteta ovog ezima za ATP i ADP, dok u slučaju UTP i UDP, NTPDaza 1 pokazuje veći afinitet prema UTP. Gotovo sav ATP koji se nađe u vanćelijskoj sredini NTPDaza 1 hidrolizuje direktno do AMP, uz vrlo male količine slobodnog ADP, te tako reguliše stepen aktivacije P2Y receptora (Kukulski et al., 2005; Robson et al., 2006).Jedna od najvažnijih uloga NTPDaze 1 u mozgu i kičmenoj moždini jeste regulacija hemotaksije mikroglije u homeostatskim i patološkim uslovima (Matyash et al., 2017; Jakovljevic et al., 2019). Pored katalitičke uloge, pokazano je da ovaj enzim može učestvovati i u ćelijskoj adheziji (Wu et al., 2006).

NTPDaza 2 je široko rasprostranjena ektonukleozidaza u CNS, sa dominantnom ekspresijom na astrocitima mozga i kičmene moždine (Wink et al 2006). Zbog svoje sličnosti sa NTPDazom 1, ovaj enzim se označava još i kao CD39L1 (*engl. cluster of differentiation 39 like 1*). Pored ekspresije na astrocitima, pokazano je da je NTPDaza 2 visoko eksprimira u regionima gde se odvija neurogeneza kako tokom embrionalnog razviča mozga tako i u adultnom mozgu, poput subgranularne zone hipokampusa (Braun et al 2003). Za razliku od NTPDaze 1, NTPDaza 2 pokazuje veći afinitet prema ATP molekulu, pri čemu dolazi do hidrolize akumulira značajne količine ADP, koji se potom postepeno hidrolizuje do AMP (Robson et al 2006). Ovakav hidrolitički mehanizam naglašava ulogu NTPDaze 2 u regulaciji nukleozid tri- i difosfata kao liganada za P2 receptore (Sèvigny et al 2002). Novija literatura ukazuje i na značaj ovog enzima u neurodegenerativnim i neuroinflamamtornim bolestima poput multiple skleroze (Jakovljević et al 2017).

NTPDaza 3 je ektonukleotidaza sa veoma ograničenom distribucijom u CNS. Njena ekspresija je ograničena na subpopulacije neurona u međumozgu, talamusu i hipotalamusu ali i u produženoj i kičmenoj moždini (Belcher et al 2006; Bjelobala et al 2010; Grkovic et al 2016). Neuroni koji eksprimiraju NTPDazu 3 takođe eksprimiraju hipokretin/oreksin-A, što ukazuje na njenu potencijalnu ulogu u regulaciji ishrane, budnosti i spavanja (Belcher et al 2006). NTPDaza 3 pokazuje preferencije i prema ATP i ADP, ali u manjoj meri od NTPDaze 1, što takođe dovodi do prolazne akumulacije ADP u vanćelijskoj sredini (Vorhoff et al 2005). S obzirom da je ona dominantna ektonukleotidaza eksprimirana na neuronima u ovim regionima, pretpostavlja se da ima značajnu ulogu u regulaciji aktivacije/deaktivacije P2 receptora.

4.3.2. Ekto-nukleotid pirofosfateze/fosfodiesteraze (NPP)

Ekto-nukleotid pirofosfateze/fosfodiesteraze su grupa od tri ektoenzima (NPP1-3) koji se eksprimiraju u gotovo svim tkivima i uključene su u regulaciju purinske signalizacije, recikliranje nukleotida, regulaciju vanćelijskih nivoa pirofosfata, regulaciju pokretljivosti kao i regulaciju ekto-kinaza (Goding et al., 2003). NPP1-3 se klasifikuju kao alkalne ekto-nukleotid pirofosfateze/fosfodiesteraze I i katalizuju hidrolizu pirofosfata i fosfodiestarskih veza u dvostepenom procesu uz pomoć dvovalentnih katjona koji su neophodni za katalitičku funkciju (Gijsbers et al., 2001). NPP1 je funkcionani dimer od dve identične subjedinice, vrši hidrolizu ATP ili do ADP ili direktno do AMP a pokazano je da se eksprimira na nervnim ćelijama (Bjelobaba et al., 2006). NPP2, iako pripada ovoj grupi eznima, predstavlja autokrini faktor motilnosti i označava se još i kao autotaksin i široko je eksprimiran u mozgu sisara (Lee et al., 1996). NPP3 je prvobitno identifikovan kao površinski glikoproteinski antigen RB13-6 od 130 kDa i njegova ekspresija pronađena je specifično u prekursorima glijskih ćelija (Blass-Kampmann et al., 1997). Pored njihove uloge u regulaciji hidrolize vanćelijskih nukleotida u fiziološkim uslovima, pokazano je i da NPP imaju ulogu u određenim patofiziološkim stanjima ali do sada uloga NPP u neurodegenerativnim bolestima nije ispitana (Goding et al., 2003).

4.3.3. Ekto-5'-nukleotidaza (CD73, eN)

Ekto-5'-nukleotidaza je tipičan ektoenzim, dominantno eksprimiran na površini limfocita te se alternativno označava još i kao CD73 (*engl. CD73, cluster of differentiation 73*). Ovaj ektoenzim za svoju hidrolitičku aktivnost zahteva jone Zn^{2+} i njegova glavna funkcija je defosforilacija AMP do adenozina, iako pored purinskih može da hidrolizuje i pirimidinske

nukleotide (DePierre and Karnovsky, 1974; Pilz et al., 1982). Funkcionalni molekul se sastoji od dve identične subjedinice povezane nekovaletnim vezama, dok se za ćelijsku membranu vezuje preko glikozil-fosfatidilinozitol (GPI) sidra (Ogata et al., 1990). Takođe, funkcionalni molekul eN je glikoprotein, a sam proces glikozilacije je neophodan za pravilno savijanje i ugradnju u ćelijsku membranu (Sträter, 2006). Iako, pored eN, tkivno-nespecifična alkalna fosfataza takođe hidrolizuje AMP do adenozina (Sebastián-Serrano et al., 2015), gotovo 90 % ukupnog adenozina u CNS potiče od hidrolitičke aktivnosti eN, te je stoga ovaj enzim u fokusu mnogih farmakoloških studija kao meta potencijalne blokade (Gessi et al., 2011). I pored široke zastupljenosti u gotovo svim regionima mozga i kičmene moždine, eN pokazuje veliku heterogenost u pogledu nivoa ekspresije u različitim regionima mozga. Pokazano je da eN ima nisku ekspresiju/aktivnost u kori velikog mozga, veću u strukturama limbičkog sistema, dok je najveći nivo ovog enzima prisutan u bazalnim ganglijama, malom mozgu i senzornim relejnim jedrima talamusa (Nedeljkovic et al., 2006; Bjelobaba et al., 2007, 2009; Langer et al., 2008; Kovács et al., 2013). Na ćelijskom nivou, eN je uglavnom lokalizovana na glijskim ćelijama, astrocitima (Adzic and Nedeljkovic, 2018) i mikrogliji, ali i na ependimskim ćelijama, ćelijama horoidnog pleksusa kao i endotelnim ćelijama moždane vaskulature (Bjelobaba et al., 2007; Langer et al., 2008; Bjelobaba et al., 2009; Dragić et al., 2021b). Takođe, ovaj enzim eksprimira se i na telima neurona i nervnim završecima (Schoen and Kreutzberg, 1994; Grkovic et al., 2014). S obzirom da je osnovna uloga eN proizvodnja adenozina koji je glavni ligand P1 receptora, ovaj enzim predstavlja glavnu kontrolnu tačku regulacije dostupnosti liganada za četiri receptora P1 klase, kako u homeostatskim tako i u patofiziološkim uslovima (Nedeljković., 2019). eN predstavlja glavni izvor adenozina koji pored neuromodulatorne ima i imunomodulatornu ulogu, te je ovaj enzim u fokusu istraživanja neuroinflamacije. Brojna neuroinflamatorna stanja praćena su značajnim povećanjem genske i proteinske ekspresije ovog proteina (Zamanian., et al 2012; Nedeljković 2019). Pokazano je da se genska i proteinska ekspresija eN menja u uslovima ishemije (Braun et al 1998), epilepsije (Bonan., et al 2000), povrede kičmene moždine (Xu et al., 2013) ali i u modelima multiple sklerote (Lavrnja., et al 2015, Dragić., et al 2021b) kao i u neuroinflamacijskim uslovima *in vitro* (Brisevac., et al 2015).

4.3.4. Alkalna fosfataza

Alkalne fosfataze (AP) su široko rasprostranjeni ektoenzimi koji katalizuju defosforilaciju i transfosforilaciju različitih ne-bioloških i bioloških supstrata uključujući i proteine (Millán, 2006). U okviru AP postoje četiri izoenzima koje kodiraju četiri homologa gena (Buchet et al., 2013). Dok placentalna, intestinalna i germinativna alkalna fosfataza imaju tkivno-specifičnu distribuciju, četvrta AP, tkivno-nespecifična alkalna fosfataza (TNAP) eksprimira se u gotovo svim tkivima, a najviše u koštanom tkivu, bubrezima i jedina je AP u CNS (Sebastián-Serrano et al., 2015). TNAP je homodimer prikačen za citoplazmu pomoću dva GPI sidra. Svaki homodimer sadrži dva jona Zn^{2+} i jedan jon Mg^{2+} kao i jon fosfatata koji su neophodni za njegovu katalitičku aktivnost. Glavna uloga ovog enzima je u procesu razvića CNS a novija literatura ukazuje na njegov značaj u neurodegenerativnim bolestima (Sebastián-Serrano et al., 2015).

4.4. Uloga purinske signalizacija u fiziološkim i patološkim uslovima

Kao što je već pomenuto, glavna uloga mikroglije u fiziološkim uslovima je nadgledanje parenhima pomoću finih i veoma pokretnih nastavaka, u potrazi za mestima sa narušenom homeostazom (Kwon and Koh, 2020). Purinski receptori A3, $P2Y_{12}$, $P2Y_{13}$ i $P2X_4$ uključeni su u regulaciju pokretljivosti nastavaka i "nadgledanje" parenhima CNS (Haynes et al., 2006; Ohsawa et al., 2012; Kyrargyri et al., 2020). Posebno važnu ulogu u hemotaksičnom kretanju mikroglije imaju ADP-senzitivni receptori $P2Y_{12}R$ i $P2Y_{13}R$ (Haynes et al., 2006; Kyrargyri et al., 2020). U uslovima narušene homeostaze, visoka koncentracija vanćelijskog ATP deluje kao DAMP signal. Razgradnjom ATP, posredstvom NTPDaze 2, nastaje ADP koji se vezuje za $P2Y_{13}R$ na membranama mikroglijskih ćelija i deluje kao hemotaksički signal koji inicira migraciju mikroglije. Aktivacija $P2Y_{12}R$ pokreće signalnu kaskadu fosfatidilinzoitol 3'-kinaze (PI3K) i fosfolipaze C, što dalje aktivira protein kinazu B (Akt) (Irino et al., 2008). Konačan ishod ovakve signalizacije je interakcija nastavaka mikroglije sa integrinima vanćelijskog matriksa što omogućava migraciju (Ohsawa et al., 2010). Aktvacija $P2X_4R$ može pojačati migraciju i oslobađanje solubilnih faktora (Ohsawa et al., 2007). Uz pobrojane P2 receptora, važnu ulogu u regulaciji hemotaksije i inflamatornog statusa mikroglije imaju P1 receptori. Adenozinski A_1R i A_3R uključeni su u regulaciju hemotaksije mikroglije (Färber et al., 2008; Ohsawa et al., 2012), dok je $A_{2A}R$ uključen u proces retrakcije nastavaka (Orr et al., 2009). Izmenjena ekspresija P1 receptora u neurodegenerativnim bolestima ključno doprinosi promeni morfologije mikroglije ka reaktivnoj, utiče na proliferaciju (Gomes et al., 2013), kao i na njen inflamacijski kapacitet (Fiebich et al., 1996).

Aktivirana mikroglija ima sposobnost fagocitoze, odnosno, uklanjanja ćelijskog debrisa. U ovom procesu važnu ulogu imaju $P2Y_4R$ i $P2Y_6R$. Ova dva receptora najveći afinitet ispoljavaju prema uridinskim nukleotidima, UTP, odnosno, UDP (von Kügelgen and Harden, 2011), i ove receptora mikroglija pojačano eksprimira u patološkim uslovima, kada oštećeni neuroni, uz ATP, oslobađaju i znatne količine UDP (Koizumi et al., 2007). Aktivacija $P2Y_6R$ uključena je u prelazak mirujuće mikroglije u ameboidnu fagocitarnu formu (Bernier et al., 2013). S druge strane, $P2Y_4R$ učestvuje u procesu pinocitoze (Li et al., 2013). Purinska signalizacija uključena je i u inflamacijski odgovor mikroglije posredstvom $P2X_7R$. Iako se ovaj receptor eksprimira na gotovo svim tipovima ćelija u CNS, najveći nivo ekspresije je utvrđen upravo u ćelijama mikroglije (Illes et al., 2012). Aktivacija $P2X_7R$ pokreće kaskadu nastanka inflamazoma, koja rezultira oslobađanjem IL-1β, a u ovom procesu neophodna je ko-stimulacija $P2X_7R$ i TLR4 receptora (Shieh et al., 2014).

Astrociti eksprimiraju brojne komponente purinskog signalnog sistema, posebno $A_{2A}R$, $P2Y_1R$, eN/CD73 i NTPDazu 2 (Zhang et al., 2014, 2016; Li et al., 2019). Signalizacija posredovana $P2Y_1R$ učestvuje u održavanju homeostaze kalcijuma u astrocitima, koji je ključan za brojne aspekte funkcionisanja astrocita, poput modulacije sinaptičke aktivnosti i održavanja krvno-moždane barijere (Bazargani and Attwell, 2016). U uslovima narušene homeostaze, aktivirani astrociti obavljaju uloge poput održavanja KMB, uklanjanja neurotransmitera iz sinapsi, oslobađanje gliotransmitera itd. O značaju i uključenosti purinske transmisije u tim procesima govori promenjena ekspresija brojnih komponenti, među kojima se, na primer u modelu AD znatno pojačava ekspresija *P2ry2, Enpp2, Enpp5* i *Gja,* a smanjuje ekspresija *Adora2a, Adora2b, P2ry14, Entpd1, Entpd2 i Enpp4* (Orre et al., 2014; Kamphuis et al., 2015; Grubman et al., 2019; Habib et al., 2020; Lau et al., 2020; Zhou et al., 2020). $P2Y_1R$ značajno doprinosi izmenjenom statusu astrocita u patološkim uslovima

(Shinozaki et al., 2017), naročito u AD (Delekate et al., 2014; Reichenbach et al., 2018), gde se nivo $P2Y_1R$ u astrocitima povećava, kako u animalnim modelima AD, tako i na *post mortem* tkivu AD pacijenata, što je naročito uočljivo u blizini β-amiloidnih plaka (Delekate et al., 2014; Reichenbach et al., 2018).

Astrociti eksprimiraju CD73/eN koji reguliše lokalnu koncentraciju adenozina. Aktivacija astrocita je povezana sa povećanjem ekspresije ovog enzima kod pacijenata koji boluju od neurodegenerativnih bolesti (Orr et al., 2015) ali i u animalnim modelima (Orr et al., 2015, 2018). Uz CD73/eN obično se uočava povećanje ekspresije $A_{2A}R$, koji je uključen u regulaciju preuzimanja glutamata i γ-aminobuterne kiseline (GABA) iz sinapsi (Matos et al., 2012; Cristóvão-Ferreira et al., 2013), ali i kontroli neuroinflamacije u patofiziološkim stanjima (Nedeljkovic, 2019). Blokada $A_{2A}R$ i njegove signalizacije poboljšava kognitivne deficite u animalnim modelima neurodegeneracije povezane sa kognitivnim deficitom (Orr et al., 2015), Iako je mnogo literaturnih podataka koji jasno ukazuju na narušenu regulaciju komponentni purinskog signalnog sistema u astrocitima u patološkim stanjima, dalja istraživanja su neophodna kako bi se utvrdilo da li su ovakvi fenomeni i razlike koje se uočavaju posledica postojanja subpopulacije astrocita koje nose ove promene ili specifičnih mikroniša u kojima se ove promene dešavaju (Slika 4).

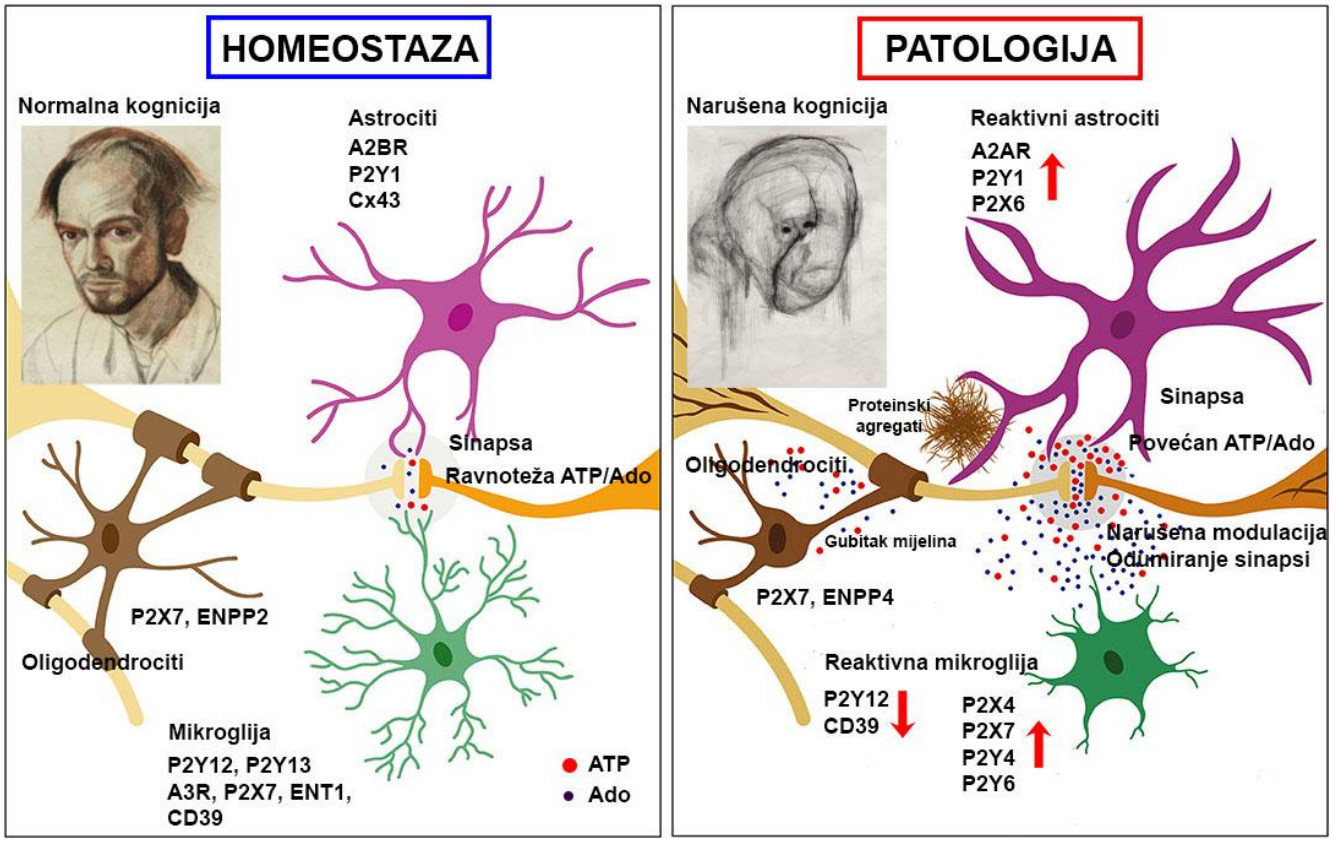

Slika 4. Kompente purinske signalizacije u uslovima homeostaze i patologije (*Modifikovani iz Pietrowski et al 2021*)

II CILJ ISTRAŽIVANJA

Purinski signalni sistem ima centralnu ulogu u etiopatogenezi mnogih neurodegenerativnih bolesti, a brojni sintetički agonisti/antagonisti purinskih receptora izučavaju se kao potencijalni terapeutici u neurodegenerativnim i neuroinflamacijskim bolestima. Pored receptora, veoma važnu ulogu u neuroinflamacijskim dešavanjima imaju i enzimi ektonukleotidaze koji regulišu dostupnost liganada purinskih receptore, a čija uloga u neurodegenerativnim bolestima nije najbolje proučena.

Stoga je glavni cilj ove doktorske disertacije ispitivanje uloge purinske transmisije u uspostavljanju morfološkog i funkcionalnog profila aktivacije glijskih ćelija, u modelu neurodegeneracije i neuroinflamacije izazvane trimetil-kalajem (TMK). S obzirom na to da se neurodegeneracija izazvana TMK progresivno razvija tokom tri nedelje, istraživanja su izvedena 2, 4, 7 i 21 dan od aplikacije TMK, sa posebnim fokusom na hipokampus i njegove podregije CA1, CA3, i hilus/DG.

U skladu sa opštim ciljem postavljeni su sledeći specifični ciljevi:

1) Utvrditi vremenski i regionalni profil neurodegeneracije u hipokampusu ženki pacova;
2) Ispitati vremenski profil neuroinflamacije i suptilne promene morfologije aktiviranih glijskih ćelija;
3) Utvrditi vremenski profil hidrolazne aktivnosti ektonukleotidaza *in situ*;
4) Ispitati promene ekspresije NTPDaza1/CD39 i eN/CD73 na genskom nivou;
5) Ispitati ćelijsku lokalizaciju NTPDaza1/CD39 i eN/CD73;
6) Ispitati promene genske ekspresije purinskih receptora na $P2X_4R$, $P2X_7R$, $P2Y_2R$, $P2Y_6R$, $P2Y_{12}R$, A_1R, $A_{2A}R$, $A_{2B}R$, A_3R;
7) Ispitati ćelijsku lokalizaciju purinskih receptora koji su od značaja za procese aktivacije glijskih ćelija $P2Y_{12}R$, $P2Y_1R$, $P2X_7$, A_1R i $A_{2A}R$;
8) Ispitati povezanost uočenih promena komponenti purinskog signalnog sistema sa funkcionalnim fenotipovima aktiviranih glijskih ćelija.

III RADOVI PROIZAŠLI IZ DOKTORSKE DISERTACIJE

NEUROSCIENCE
RESEARCH ARTICLE
M. Dragić et al. / Neuroscience 423 (2019) 38–54

Two Distinct Hippocampal Astrocyte Morphotypes Reveal Subfield-Different Fate during Neurodegeneration Induced by Trimethyltin Intoxication

Milorad Dragić,[a,b]* Marina Zarić,[b] Nataša Mitrović,[b] Nadežda Nedeljković[a] and Ivana Grković[b]

[a] Department for General Physiology and Biophysics, Faculty of Biology, University of Belgrade, Belgrade, Studentski trg 3, 11001 Belgrade, Serbia
[b] Department of Molecular Biology and Endocrinology, Vinča Institute of Nuclear Sciences, University of Belgrade, Mike Petrovića Alasa 12-14, 11001 Belgrade, Serbia

Abstract—Astrocytes comprise a heterogenic group of glial cells, which perform homeostatic functions in the central nervous system. These cells react to all kind of insults by changing the morphology and function that result in a transition from the quiescent to a reactive phenotype. Trimethyltin (TMT) intoxication, which reproduces pathological events in the hippocampus similar to those associated with seizures and cognitive decline, has been proven as a useful model for studying responses of the glial cells to neurodegeneration. In the present study, we have explored morphological varieties of astrocytes in the hippocampal subregions of ovariectomized female rats exposed to TMT. We have demonstrated an early loss of neurons in CA1 and DG subfields. Distinct morphotypes of protoplasmic astrocytes observed in CA1/CA3 and the hilus of control animals developed different responses to TMT intoxication, as assessed by GFAP-immunohistochemistry. In CA1 subregion, GFAP$^+$ astrocytes preserved their domain organization and responded with typical hypertrophy, while the hilar GFAP$^+$ astrocytes developed atrophy-like phenotype and increased expression of vimentin and nestin 7 days after the exposure. Both reactive and atrophied-like astrocytes expressed Kir4.1 in CA1/CA3 and the hilus of DG, respectively, indicating that these cells did not change their potential for normal activity at this time point of pathology. Together, the results demonstrate the persistence of two protoplasmic morphotypes of astrocytes, with distinct appearance, function, and fate after TMT-induced neurodegeneration, suggesting their pleiotropic roles in the hippocampal response to neurodegeneration.

Key words: astrocyte, morphotypes, regional difference, hippocampal neurodegeneration, morphology analysis.

INTRODUCTION

Astrocytes represent morphologically and functionally diverse cell type of the central nervous system (CNS), which perform essential roles in neural development, homeostasis, and plasticity (Sofroniew and Vinters, 2010; Khakh and Sofroniew, 2015). In respect to the morphological diversity, two main types of astrocytes are traditionally recognized based on immunolabeling against the well-known astrocyte marker, glial fibrillary acidic protein (GFAP). Protoplasmic astrocytes are the most abundant astrocyte subtype in the gray matter, usually displaying an ovoid cell body with several radially oriented and highly branched processes (Sofroniew and Vinters, 2010; Bayraktar et al., 2014). Fibrous astrocytes in the white matter are less complex, with a flattened cell body and longer, bilaterally oriented and less branched processes (Sofroniew and Vinters, 2010). It is supposed that the morphological heterogeneity of astrocytes reflects their functional diversity, similar to well-known heterogeneity of neuronal populations. Accordingly, several specialized and morphologically diverse astrocyte subtypes have been described in anatomically distinct brain regions, including Bergmann glia in the cerebellum, velate astrocytes, radial astrocyte in the dentate gyrus, Muller cells in the retina, marginal glia, etc. (Emsley and Macklis, 2006; Oberheim et al., 2012). In addition to the supportive and homeostatic functions, specialized astrocytes perform particular roles in defined brain regions, such as regulation of local neuronal activity, synaptic transmission and metabolism of local neurotransmitters, adjustment of blood flow or proliferation of stem cells in the neurogenic niches (Zhang and Barres, 2010; Bayraktar et al., 2014).

Astrocytes form a highly interconnected network *via* gap junctions, and closely monitor changes in neuroglial activity. Alterations in the environment induced by pathological insults are reflected as a profound changes

*Corresponding author. Address: Department for General Physiology and Biophysics, Faculty of Biology, University of Belgrade, Studentski trg 16, Belgrade, Serbia.
E-mail address: milorad.dragic@bio.bg.ac.rs (M. Dragić).

https://doi.org/10.1016/j.neuroscience.2019.10.022
0306-4522/

in the astrocytes morphology, characterized by hypertrophy, branching of stem processes (Wilhelmsson et al., 2006; Bardehle et al., 2013) and up-regulation of GFAP (Pekny and Pekna, 2014), accompanied by a significant alteration in gene expression (Sofroniew, 2009; Zamanian et al., 2012). However, even in the same brain area, distinct subtypes of astrocytes may respond differently to the same insult, leading to diverse reactive phenotype and differential expressions of transcription factors, chemokines and cytokines (Hamby et al., 2012), thus acquiring specific functional and morphological phenotypes to fulfill the requirements of the local pathological context. Quantitative analyses are necessary to distinguish the subtle changes of astrocytes that accompany mild injury of the brain regions or damages located at regions distant to severe injury.

Trimethyltin-chloride (TMT) is an organotin compound which induces selective neuronal loss and activation of glial cells in the limbic areas, leading to marked behavioral changes, such as hyperactivity, aggression, memory loss, learning impairment and seizures (Balaban et al., 1988; Trabucco et al., 2009; Geloso et al., 2011; Corvino et al., 2013; Lattanzi et al., 2013; Lee et al., 2016a). The intoxication induced by TMT in rodents has been proven as a model of progressive neurodegeneration of the hippocampus suitable to study the neuronal and glial cell responses (Geloso et al., 2011; Corvino et al., 2013; Lattanzi et al., 2013; Lee et al., 2016a). A neuronal damage shows a delayed onset (two to four days after intoxication), became clearly detectable at the end of the first week post-intoxication, and progressively worsens over three weeks (Haga et al., 2002; Trabucco et al., 2009; Geloso et al., 2011; Corvino et al., 2012; Little et al., 2012; Corvino et al., 2013; Lattanzi et al., 2013; Corvino et al., 2015). Although differences in the pattern of hippocampal degeneration have been described, depending on species, strain, age, dose, vehicle and route of administration, it has been suggested that the variety of neuropathological events observed in rodents are not related to species- or sex-related differences in the sensitivity to TMT toxicity, but rather to a different susceptibility to secondary effects produced by this neurotoxin (Haga et al., 2002; Trabucco et al., 2009; Geloso et al., 2011; Corvino et al., 2012; Little et al., 2012; Corvino et al., 2013; Lattanzi et al., 2013; Corvino et al., 2015). It was proposed that TMT directly affects granule cells of the dentate gyrus (DG), whereas CA pyramidal cells perish as a consequence of seizures produced by this neurotoxin (Ishida et al., 1997; Trabucco et al., 2009; Shin et al., 2011). Thus, the neuronal damage was demonstrated in the pyramidal and dentate granule cells of the hippocampus as early as 2 days post-dosing followed with glial cells activation (Balaban et al., 1988; Haga et al., 2002; Little et al., 2002; Little et al., 2012; Lattanzi et al., 2013). In the present study, we assumed that careful morphometric analysis of astrocytes in the days following intoxication might provide an insight into functional dynamics of their activation in the neurodegenerative and neurotoxic conditions. Such neurodegeneration and glial cells responses in the hippocampus of ovariectomized (OVX) rats are a good basis for studies on novel neuroprotective compounds, steroid hormones (Corvino et al., 2012; Corvino et al., 2013; Corvino et al., 2015; Lee et al., 2016b) and/or bioidentical hormones replacement regimes, currently ongoing in our laboratory. Furthermore, seizures and other behavioral patterns in distinct neuropathologies (Scharfman et al., 2005; Veliskova and Desantis, 2013), but also astrocyte morphology are affected by fluctuations of ovarian hormones during the estrus cycle (Luquin et al., 1993; Klintsova et al., 1995; Hajos et al., 2000; Arias et al., 2009). Thus, by intoxicating OVX females, we avoided fluctuating effects of ovarian hormones and studied the heterogeneity of astrocyte response in the hippocampus in an initial stable state. Additionally, the pattern of neuronal damage in the hippocampus of OVX females (Corvino et al., 2015) is comparable with events in intact rats of both gender (Haga et al., 2002; Trabucco et al., 2009; Geloso et al., 2011; Little et al., 2012; Corvino et al., 2013; Lattanzi et al., 2013; Corvino et al., 2015). Therefore, morpho-functional heterogeneity of astrocytes after TMT was characterized by using GFAP, vimentin and nestin immunolabeling, whereas their functional state was determined based on Kir4.1 expression. The results indicate that astrocytes in different hippocampal subfields have distinct morphology, and respond differently to TMT intoxication, which may give us a better understanding of the specific local homeostatic and protective role of the glial cells to the brain insult.

MATERIAL & METHODS

Ethics statement

All experimental procedures were approved by the Ethics Committee for the Use of Laboratory Animals of Vinca Institute of Nuclear Sciences, University of Belgrade; Republic of Serbia (Application No. 02/11; 323-07-02057/2017-05). Care was taken to minimize the pain and discomfort of the animals in accordance with the European Communities Council Directive (2010/63/EU).

Animals

This study was performed on two months old Wistar female rats (220–250 g) acquired from VINČA Institute's local colony. All animals (3 per cage) were housed in 12 h light/dark regime, constant humidity and temperature, food and water *ad libitum*.

Surgical procedure and treatment

Animals were bilaterally ovariectomized through a dorsal incision under ketamine (50 mg/kg) i.p. and xylazine (5 mg/kg) i.p. anesthesia and left for three weeks of postsurgical recovery. After recovery, animals received i.p. injection of TMT (8 mg/kg dissolved in 1 mL 0.9 % w/v saline) (Balaban et al., 1988; Latini et al., 2010; Little et al., 2012; Lattanzi et al., 2013; Corvino et al., 2015). Control animals received 0.9 % sterile saline injection of the same volume. TMT-injected animals were kept in separate cages due to aggressive behavior and sacri-

ficed by decapitation (Harvard apparatus, Holliston, MA, USA)

Assessment of behavior severity

TMT treated animals exhibited usual symptoms of TMT poisoning, such as hyper-excitability, tremors, and seizures (Trabucco et al., 2009; Geloso et al., 2011). Starting from day 1 after the exposure, animals were scored during a 5-min interval in brightly lit arenas (40 × 40 cm, 250 lux), for a hyperactivity/tremor, using the arbitrarily defined scale, as follows: (0) without symptoms, (1) hyperactivity and hyper-responsiveness (2) mild tremor with normal motor activity, and (3) systemic tremor (Trabucco et al., 2009). Behavioral severity score exhibited a bell-shaped curve which peaked at day 4 and decreases at day 7 (Fig. 1). Thus, three-time points have been chosen for the experiments – two, four and seven days after intoxication (2d TMT, 4d TMT, 7d TMT; Fig. 1; arrows, n = 5 rats/group, and appropriate controls were sacrificed at all three-time points). Animals also develop aggressive behavior after TMT poisoning, peaking at day 4: avoids hand by running and/or struggles when captured, or leaps, struggles, and bites when captured (Lee et al., 2016a).

Immunohistochemistry and light microscopy

Brains for immunohistochemistry and histology were carefully removed from the skull (n = 5 animals/group), fixed in 4 % PFA for 24 hours, cryoprotected in graded sucrose (10–30 % in 0.2 M phosphate buffer) and stored at 4 °C. Afterward, 20 µm thick coronal cryosections of the dorsal hippocampus were made, between 3.12 and 3.84 mm posterior to Bregma, air-dried for 2 hours and stored at – 20 °C until use. After washing steps in PBS, endogenous peroxidase was blocked in immersion of 0.3 % H_2O_2 in methanol for 20 min, followed by blocking in 5 % donkey serum at room temperature for 1 hour. Next, sections were probed with mouse anti-rat GFAP antibody (1:300 dilution, UC Davis/NIH NeuroMab Facility 73-240, ab10672298) overnight at 4 °C. After washing in PBS, sections were incubated with goat anti-mouse HRP-conjugated secondary antibody (1:200 dilutions, R&D Systems, HAF007). The signal was visualized with the use of 3,3′-S-diaminobenzidine-tetrahydrochloride kit (DAB, Abcam, UK) as a chromogen for HRP-conjugated secondary antibodies. After dehydration in graded ethanol (70 % – 100 %) and clearance in xylene, sections were mounted with the use of DPX-mounting medium (Sigma Aldrich, USA). Digital images (2088 × 1550 pixels) of DAB-stained astrocytes were acquired using LEITZ DM RB light microscope (Leica Mikroskopie & Systems GmbH, Wetzlar, Germany), a LEICA DFC320 CCD camera (Leica Microsystems Ltd., Heerbrugg, Switzerland) and LEICA DFC Twain Software (Leica, Germany).

For Fluoro-Jade C (FJC) staining, sections were air-dried at room temperature and immersed for 5 min in a 1 % NaOH dissolved in 80 % ethanol. Afterward, sections were rinsed in 70 % ethanol and distilled H2O. Then, incubation in 0.06 % potassium permanganate for 10 min was performed. After rinsing in water for 2 min, sections were incubated in FJC for 10 min. The working solution of FJC was made by adding 4 ml of 0.01 % stock solution into 0.1 % glacial acetic acid. After incubation in FJC, sections were rinsed in water and dried at 50 °C for 15–20 min. Finally, tissue was cleared in xylene for 3 min, and covered with DPX mounting medium. The FITC filter system was used for visualization of FJC staining at 20x magnification.

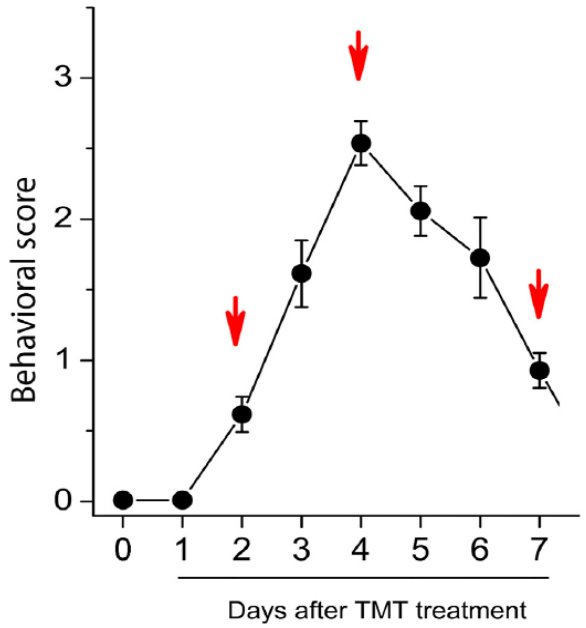

Fig. 1. Assessment of behavior severity. Behavioral signs were scored according to 0–3 scale (0, without symptoms; 1, hyperactivity and hyper-responsiveness, 2 mild tremor with normal motor activity; 3, systemic tremor). Animals (n = 5/group) were sacrificed at each time point (days 2, 4, 7 days after treatment; arrows). The data are reported as the mean ± SEM.

Cell count and mean surface area analysis

In order to evaluate neuronal degeneration, a semi-quantitative analysis of Nissl stained neurons was performed using *ImageJ* cell counter plugin (free download from https://imagej.net/Downloads). Images (40x objectives) of CA1, CA3, and DG were acquired for the analysis. Only neurons of *pyramidal cell layers* (*pcl*) and *granular cell layer* (*gcl*) showing unequivocally regularly shaped neuronal morphology with clearly visible nucleoli were included in the analysis. Between 4 and 6 sections were analyzed per brain (n = 5 brains/group). We captured 20 images of each subregion per group (60 images/experimental group) and counted cells in high-power field (2088 × 1550 pixels, HPF = 0.06 mm^2). Since Nissl staining detects fragmented nuclei and labels, small, intensely basophilic and cytoplasmic shrinkage, frequently seen outside the neurons and representing apoptotic bodies - the end products of apoptosis (Capurso et al., 1997), count of visible apoptotic bodies was performed. Apoptotic bodies were selected based on their location; only those clearly

distinguishable from glia, within the pyramidal layer were counted in *ImageJ* software and included in the study.

For density evaluation of GFAP$^+$ cells in the examined regions, we acquired 20 micrographs of each region (60 images/experimental group, 20x objective) and counted cells in high-power field (2088 × 1550 pixels, HPF = 0.25 mm^2). Only astrocytes with clearly immunolabeled bodies and processes were included in the total number of counted cells. Since there is no sharp demarcation between the polymorph layer of the dentate gyrus and proximal part of CA3 region, we addressed the cellular layer encompassed by blades of the granular layer as a hilar region.

Image acquisition and processing for morphological analysis

Images were acquired using 63 × 3.2 objectives and saved in .tiff format. We captured 320 images of single astrocyte from CA1, CA3 region and hilar region of the dorsal hippocampus (80 single astrocyte/experimental group) and all of them were taken blindly to treatment. Since we were assessing different morphological parameters, images of a single astrocyte were processed using NIH public software *ImageJ* (free download from https://imagej.net/Downloads). Original images were imported into *ImageJ* (Fig. 2A), converted to an 8-bit image (Fig. 2B), and then binarized (Fig. 2D), with a previously set up threshold (Fig. 2C). In order to acquire the image of a single astrocyte made of a continuous set of pixels, manual editing was performed if needed; some pixels where added to make processes continuous (Fernandez-Arjona et al., 2017), others that did not belong to astrocyte being edited were removed. The editing step was carefully done with a constant parable to the original image. Finally, the image was inverted (Fig. 2F) and ready for morphological analysis.

In the assessment of the mean surface area, we used 4 sections per animal and obtained 60 astrocytes per region (180 per experimental group). Micrographs were imported in NIH public software *ImageJ* converted to an 8-bit image and then binarized with a previously set up threshold. The threshold was carefully determined with constant comparison to the original image. Each astrocyte was selected and measured for its cell surface (pixel = 14.1025 μm) by investigators blinded to treatment groups. All image-capturing and threshold parameters were kept the same for each measurement between comparing groups.

Morphological analyses of astrocytes

In order to evaluate morphological changes of astrocytes after TMT exposure, seven morphological parameters were analyzed:

1) Fractal dimension (D_F) a unitless number that measures changes in detail (N) with alteration in scale (S), proved to be an excellent indicator of the object's complexity. D_F is calculated as the logarithmic ratio of N and S:

$$D_F = \frac{logN}{logS}$$

where N is the number of pixels in the image at a given scale (S). Higher values of fractal dimension point towards higher pattern complexity (Karperien et al., 2013). D_F was calculated using *ImageJ* plugin **FracLac.** The box-counting method was applied to count the number of a pixel containing boxes with successive changes in grid size. In order to avoid rotational variance, all astrocytes were positioned in a manner where its longest edge was parallel to the y-axis. Finally, the obtained average value of 12 measurements was included in the analysis, in accordance with validated protocol (Fernandez-Arjona et al., 2017).

2) Perimeter, a parameter also indicative of the complexity and branching pattern of astrocytes. It was measured by outlining each cell and then converting the number of pixels into μm using *ImageJ* (1 pixel = 14.1025 μm).

3) Circularity, a parameter, with values ranging from 0–1, measuring the deviation of the cell from a perfect circle.

4) The Length of GFAP stained processes was measured using *ImageJ* macro – *Measure skeleton length* (written by Volker Baecker, INSERM, 2010; http://mri.cnrs.fr/index.php?m = 67&c = 110). Binarized images were skeletonized and this macro was applied.

5) The number of primary branches manually assessed for each astrocyte, with two separate counts, obtaining an average value.

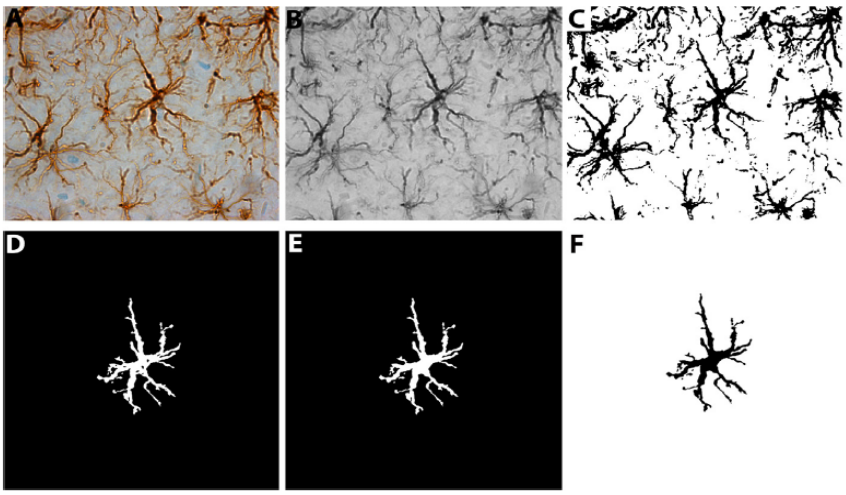

Fig. 2. Processing of astrocyte micrographs. Micrographs of single astrocytes were selected blind to treatment, and imported into *ImageJ* (A), converted to an 8-bit image (B). The threshold was set up (C) and the image was converted to a binary scale (D). In order to present an astrocyte that is made of a continuous set of pixels, function *fill holes* was applied (E), the image was inverted and ready for further analysis (F).

6) The number of secondary branches manually assessed for each astrocyte, with two separate counts, obtaining an average value.

7) Sholl analysis used to determine the branching complexity of astrocytes. Images were analyzed using *ImageJ* software, *Sholl analysis* plugin. Using multi-point tool, starting point was set to center of astrocyte's body, radius step was set to 2 μm, number of primary branches was manually added based on the previous counting, and Shoenon ramification index (RF) was calculated (maximum number of intersections/number of primary branches) (Morrison and Filosa, 2013).

Double immunofluorescence and confocal microscopy

After washing steps in PBS, followed by blocking in 5 % donkey serum at room temperature for 1 hour, incubations with rabbit anti-rat GFAP antibody (1:500 dilution, DAKO, abZ0034) antibody and secondary donkey anti-rabbit Alexa Fluor 555 (1:400 dilution, Invitrogen, ab162543) or mouse anti-rat GFAP antibody (1:300 dilution, UC Davis/NIH NeuroMab Facility 73–240, ab10672298) followed with secondary donkey anti-mouse Alexa Fluor 488 (1:400 dilution, Invitrogen, ab142672) were applied. After washing in PBS, sections were incubated in the primary antibodies: mouse anti-rat vimentin antibody (1:200 dilution, DAKO M0725, ab10013485), mouse anti-rat nestin antibody (1:10 dilution, Sigma N5413, ab1841032) and rabbit anti-rat Kir4.1 antibody (1:300 dilution, Alomone labs, APC-035). Secondary donkey anti-mouse Alexa Fluor 488 (1:400 dilution, Invitrogen, ab142672) was applied for 2 hr. All primary and secondary antibodies were separately applied. The sections were mounted in Mowiol (Calbiochem, La Jolla, CA). Confocal imaging was performed using confocal laser-scanning microscope (LSM 510, Carl Zeiss GmbH, Jena, Germany) using Ar Multi-line (457, 478, 488 and 514 nm) and HeNe (543 nm) lasers using 63x (x2 digital zoom) DIC oil, 40x (x2 digital zoom) and 20x objective and monochrome camera AxioCam ICm1 camera (Carl Zeiss GmbH, Germany). We captured representative $GFAP^+$ astrocytes seven days after exposure when most notable morphological changes were observed.

Statistical analysis

All results are presented as mean ± SEM. One-way analysis of variance (One-way ANOVA) was performed for statistical comparison between controls in each region. Two-way analysis of variance (two-way ANOVA) was performed to determine the effects of time (2, 4, 7 days after TMT injection), hippocampal subfield (CA1, CA3 region, and DG) and the interactions between them for morphological parameters. Tuckey's *posthoc* test was performed for multiple comparisons between experimental groups. Statistical analysis was done using GraphPad Prism 6 software package (San Diego, CA). Results were considered significant at $p < 0.05$.

RESULTS

Astrocyte heterogeneity in the control OVX hippocampus and dentate gyrus

Distribution and heterogeneity of hippocampal astrocytes in OVX animals were assessed with GFAP immunoreactivity (*ir*). Although the staining was detectable in the entire structure, regional differences were observed. Typical fibrous astrocytes were present in the alveus and fimbria, with flattened cell bodies and 2–4 branches extending parallel with the white matter fibers (Fig. 3A). The highest density of $GFAP^+$ astrocytes was observed in the *stratum lacunosum-moleculare* (*slm*), where the cells with long processes appeared to radiate away from the CA layer. In the *stratum oriens* (*so*) and *stratum radiatum* (*sr*) of CA1/CA3 regions typical stellate astrocytes with 5–7 primary branches (Fig. 3B) were found. Although few $GFAP^+$ cells were located between pyramidal neurons, the layer was generally devoid of astrocytes. However, perivascular astrocytes with their endfeet surrounding the blood vessels were observed in *so* and *sr* (Fig. 3C). The cells displayed stellate morphology, different in size, with one or more primary processes and the endfeet adhering to the vessel surface. All astrocytes occupied discrete domains with only marginal overlap between their thin secondary and tertiary $GFAP^+$ processes. The common feature of astrocytes in CA region is the absence of GFAP-*ir* at the astrocytic bodies (Fig. 3E). In the hilar region, astrocytes also displayed stellate morphology with 7–10 primary branches radiating in all directions (Fig. 3I). Their branches appear to be thicker and shorter than those in CA regions and bodies were clearly recognizable by GFAP-*ir* (Fig. 3F). Astrocytes were concentrated in the central part of the hilus, often surrounding neurons. Subgranular zone contained astrocytes with oval bodies and few long processes extending through *gcl* into the molecular layer (*ml*) (Fig. 3G). Although the cell's bodies were not always visible, many thin radial branches traversing between densely packed granular cells could be seen. In *ml*, besides typical stellate astrocytes, yet another type with radial and broomy shape was observed (Fig. 3H). Their long processes ran parallel to each other and perpendicular to *gcl*, sometimes reaching it and terminating superficially. Most of these processes terminated in *ml*, but some even reached out of the hippocampal fissure. Only a few stellate cells were scattered in *gcl*. Domain organization was also apparent in DG area. In the *ml* near the crest of DG, periventricular astrocytes (Fig. 3D) and marginal glia (Fig. 3J) were seen. The subtypes of astrocytes identified in the hippocampal subregions are summarized in Table 1.

Astrocytes complexity and morphology differ by subregion in the control hippocampus

Astrocytes diversity in the CA1, CA3 and DG subfields of Ctrl (OVX) animals were further analyzed by determining morphometric parameters from microscopic images

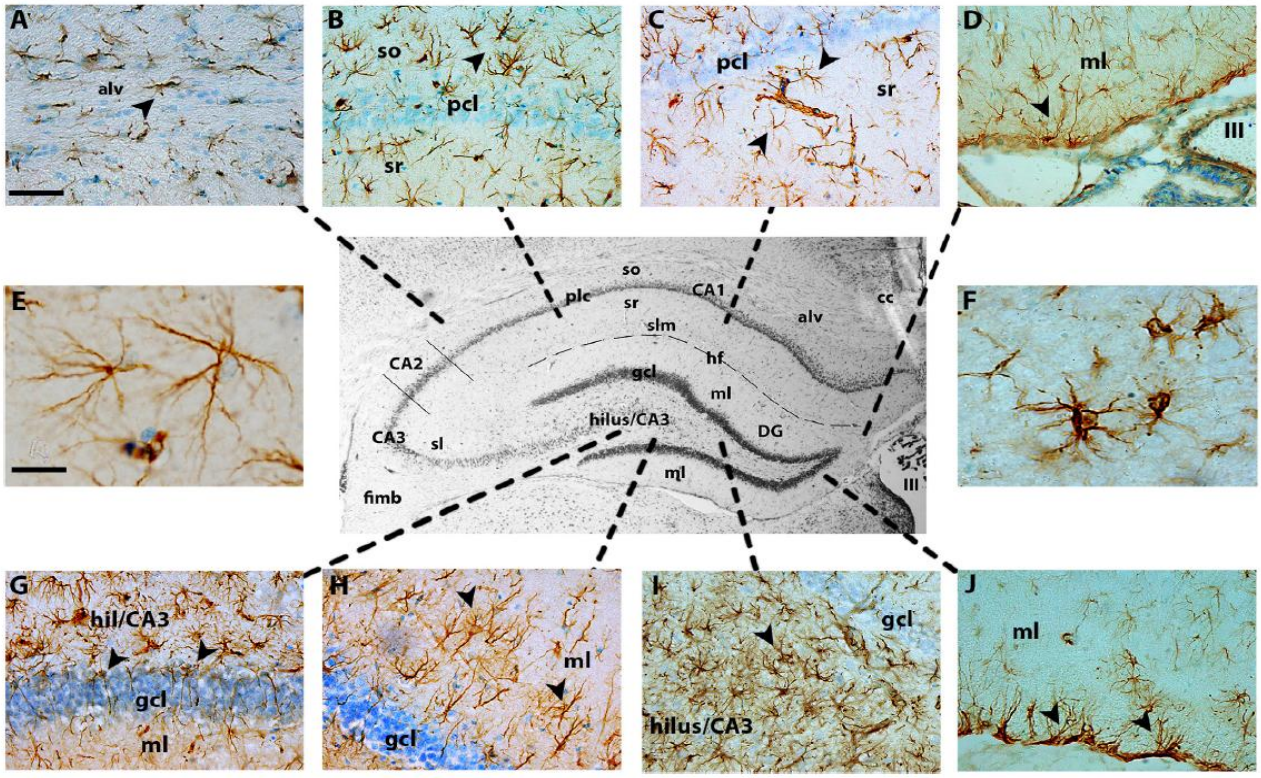

Fig. 3. Distribution of astrocyte morphological subtypes in the hippocampus of OVX female rats. Micrographs of fibrous astrocytes in the alveus (A) and protoplasmic astrocytes in CA1 region (B). Characteristic astrocyte morphotype of CA1 subregion (E). Vascular endfeet of astrocytes were seen throughout the hippocampus, e.g. CA1 (C) and the hilar region of DG (I). Periventricular astrocytes around the third ventricle were observed (D), while the line between DG and thalamus occupies pial glia (J). Another morphotype of protoplasmic astrocytes is observed in the hilar region of DG (I, F). The subgranular layer is occupied with radial glia, which processes traverse the granular cell layer, terminating superficially in the inner molecular layer (G). In the molecular layer, astrocytes have broomy-like morphology with branches parallel to each other (H). Scale bar in micrographs (A, B, C, D, G, H, I, J) = 50 μm; (E, F) = 20 μm. Abbreviations: *alv – alveus, so – stratum oriens, sr – stratum radiatum, pcl – pyramidal cell layer, ml – molecular layer, gcl – granular cell layer, hil – hilar region, III – third ventricle.*

Table 1. Astrocyte subtypes observed in subregions of hippocampus and dentate gyrus.

Astrocyte subtypes							
Hippocampus	Radial glia	Protoplasmic type 1	Protoplasmic type 2	Fibrous	Perivascular	Marginal	Periventricular
CA1							
Stratum oriens	–	+	–	–	+	–	+
Stratum radiatum	–	+	–	–	+	–	+
Stratum pyramidale	-	+/–	–	–	–	–	–
Stratum lacunosum-moleculare	–	+	–	–	+	–	–
CA3							
Stratum oriens	–	+	–	–	–	–	–
Stratum radiatum	–	+	–	–	+	–	–
Stratum lucidum	–	+	–	–	–	–	–
Stratum pyramidale	–	+/–	–	–	–	–	–
Alveus/Fimbria	–	–	–	+	–	–	–
Dentate gyrus							
Hilus	–	–	+	–	+	–	–
Molecular layer	+	–	+	–	–	+	+
Subgranular region	+	–	+	–	–	–	–
Granular cell layer	–	–	+/–	–	–	–	–

obtained by GFAP immunohistochemistry. We have determined the fractal dimension (D_f) which is a measure of cell complexity, wherein higher values correlate with more complex cell morphology (Di Ieva et al., 2014). Astrocytes in CA1 and CA3 showed lower D_f values compared to those in DG (Fig. 4A, Table 2), while similar D_f was determined for astrocytes in CA1/CA3 regions. The perimeter, which is the measure of general morphology, was significantly lower in CA1 and CA3 compared to DG astrocytes (Fig. 4B, Table 2). Parameter length of GFAP stained processes revealed a similar pattern, i.e. astrocytes in CA1 and CA3 showed lower values than DG astrocytes (Fig. 4C, Table 2). The number of primary and secondary branches in three examined regions was significantly higher in DG, in respect to CA1 and CA3 (Fig. 4D, Table 2). The cells in CA1 displayed less secondary branches in comparison to CA3 and DG (Fig. 4E, Table 2). The values of the Shoenon coefficient, which reflects branching complexity, were in the accordance with the observed morphology, corroborating that the glial cells in CA1 and CA3 displayed lesser morphological complexity than those in DG (Fig. 4F, Table 2). The results of one-way ANOVA analysis and Tuckey's *post hoc* test were summarized in Table 2.

TMT induces neuronal damage/death in CA1 and DG

Spatiotemporal features and extent of hippocampal lesions were assessed using Nissl staining (Fig. 5A). In Ctrl hippocampi, no changes in neuronal morphology were observed. At 2d TMT, only a few necrotic/damaged cells and slight disorganization of CA1 pyramidal cells were noticed (data not shown), without a change in the overall number of viable neurons in the subfields of interest. In *pcl* of CA1 and *gcl* of DG, damaged neurons, necrotic cells, and apoptotic bodies became apparent at 4d TMT, which resulted in a significant decrease in neuronal cell counts in CA1 subfield. At 7d TMT, a large number of degenerated neurons in CA1 subfield and numerous apoptotic bodies were visible. Nissl staining also revealed neuronal death in *gcl* of DG, where apoptotic bodies were scattered within the layer. At the same time-point, the hilar subfield was also populated with small, darkly-stained cells, suggesting gliosis. In the examined time frame, no pathological changes were observed in the distal and medial CA3 subregion.

Cell counting followed by two-way ANOVA revealed significant effect of time ($F_{(3,106)} = 34.97$, $p < 0.0001$),

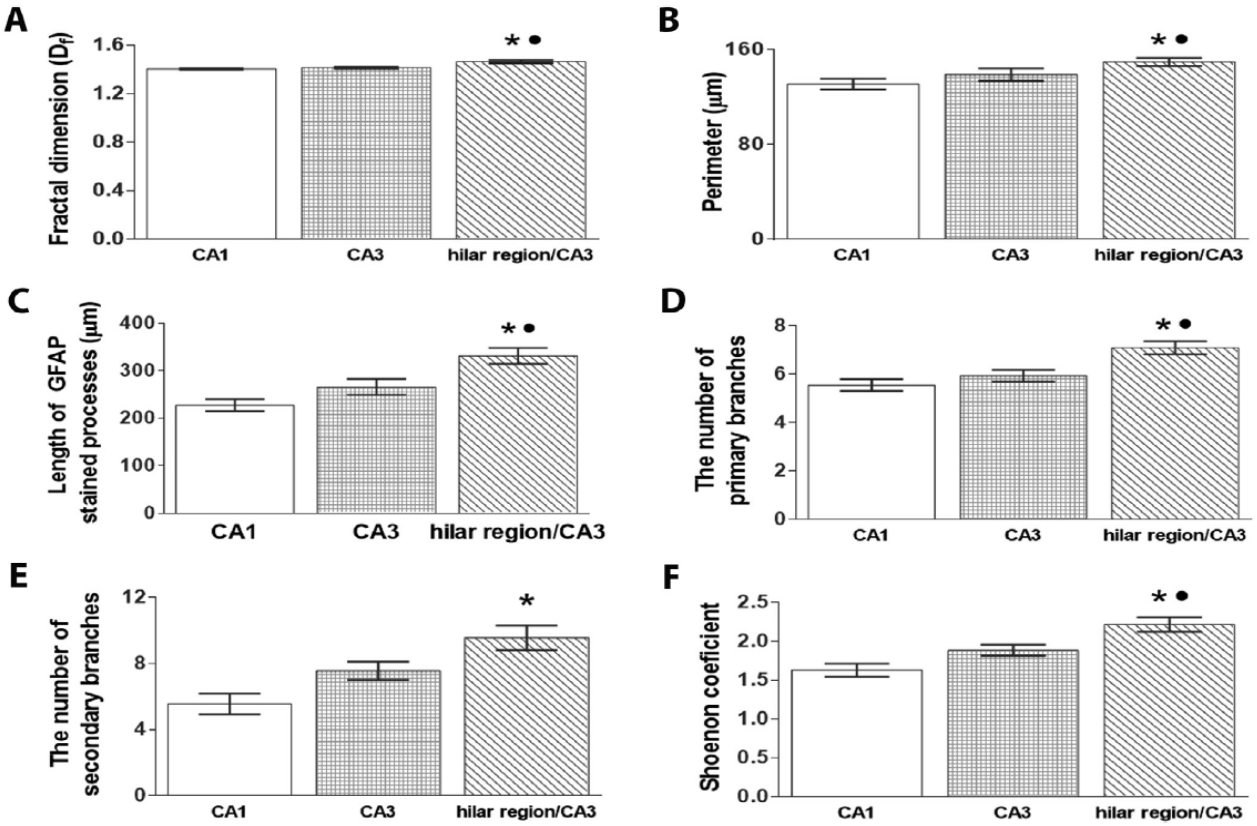

Fig. 4. Morphological parameters of astrocytes in control hippocampus. A fractal dimension (A), perimeter (B), length of GFAP stained processes (C), number of primary (D) and secondary branches (E) and Shoenon coefficient (F) of astrocytes in CA1, CA3 and DG of control (Ctrl) hippocampus. The values are given as means ± SEM. * $p < 0.05$ (or less) indicates differences between CA1 *vs* DG; •$p < 0.05$ (or less) indicates differences between CA3 and DG analyzed with one-way ANOVA followed by a Tukey's multiple comparison test.

Table 2. Results of one-way ANOVA analysis and *post-hoc test* of control astrocytes morphological parameters.

CA1*vs*CA3*vs*DG		Fractal dimension	Perimeter	Length of GFAP stained processes	No. of primary branches	No. of secondary branches	Shoenon ramification
ANOVA	F values	$F_{2, 53} = 12.58$	$F_{2, 56} = 5.36$	$F_{2, 57} = 11.57$	$F_{2, 55} = 10.19$	$F_{2, 55} = 7.49$	$F_{2, 55} = 12.13$
	p values	$p < 0.0001$	$p < 0.01$	$p < 0.0001$	$p < 0.001$	$p < 0.01$	$p < 0.0001$
Post hoc test							
CA1 *vs* CA3		*NSD*	*NSD*	*NSD*	*NSD*	*NSD*	*NSD*
CA1 *vs* DG		$p < 0.0001$	$p < 0.01$	$p < 0.0001$	$p < 0.001$	$p < 0.001$	$p < 0.0001$
CA3 *vs* DG		$p < 0.0001$	$p < 0.05$	$p < 0.05$	$p < 0.01$	*NSD*	$p < 0.05$

NSD – no statistical difference.

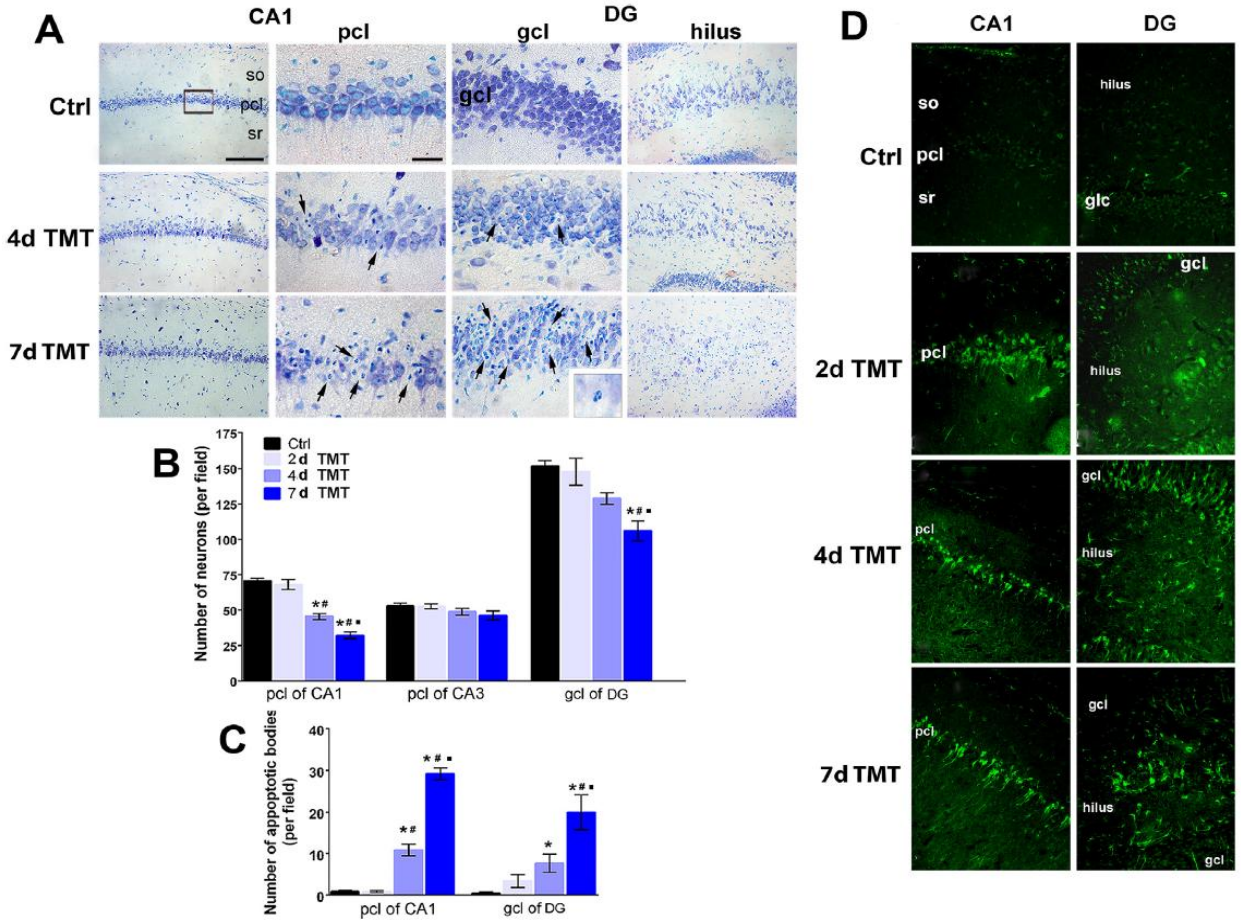

Fig. 5. Neuronal degeneration in the hippocampus following TMT intoxication. A) Micrographs of Nissl stained coronal sections from the dorsal hippocampus of Ctrl rats treated with saline or 4 and 7 days after TMT. Neuronal loss and apoptotic bodies are clearly detectable in both CA1 and DG (arrows), 4 and 7 days post-TMT. A progressive reduction in neuronal number is accompanied with small, darkly-stained cells, also suggesting gliosis. Scale bar 100 μm for low magnification and 25 μm for high magnification. B) Cell counts of Nissl stained surviving neurons in *pcl* of CA1 and CA3, and *gcl* of DG. C) Clearly visible apoptotic bodies in the pyramidal cell layer (*pcl*) of CA1 and the granular cell layer (*gcl*) of DG. The values are given as means ± SEM. Significance shown inside the graphs: $^{*}p < 0.05$ or less compared to Ctrl; $^{\#}p < 0.05$ or less compared to 2d TMT; $^{\bullet}p < 0.05$ or less compared to 4d TMT. D) Fluoro-Jade C representative images of Ctrl hippocampal CA1 and DG regions. After TMT, a marked neurodegeneration is observed 2d and 4d in both, *pcl* of CA1 and *gcl* of DG. On 7d TMT, degenerative neurons are still present in *pcl* of CA1, while hilar neurons are now labeled with FJC (H).

hippocampal subfields ($F_{(2,106)} = 500.5$, $p < 0.0001$) and their interaction ($F_{(6,106)} = 5.5$, $p < 0.0001$). *Post hoc* test showed a significantly lower number of surviving neurons at day 4 and 7 in CA1 ($p < 0.001$ and $p < 0.0001$, respectively) and 7 days post-TMT in the granular cell layer of DG ($p < 0.001$) compared with appropriate Ctrl

(Fig. 5B). In contrast, the number of surviving neurons localized in CA3 region was not altered by TMT. Accordingly, with the observed decline in the number of surviving neurons, a gradual increase of visible apoptotic bodies was detectable in CA1 and DG. A moderate to a large number of apoptotic bodies was found (individual differences were observed) in 4- and 7-days post-TMT intoxication (Fig. 5C). Taken together these data indicate that a significant amount of neurons of CA1 and DG underwent cell death during the first week after TMT intoxication.

TMT-induced neurodegeneration was further confirmed by FJC staining (Fig. 5D). Fluorescent microscopy analysis of FJC-stained sections showed no stained neurons in the hippocampi of Ctrl, as expected. At 2d TMT, many stained degenerating neurons were already evident in CA1, and at lover extent in DG, as have been reported (Balaban et al., 1988; Little et al., 2012). The FJC staining progressively increased at 4d TMT and completely overlapped with that obtained by Nissl staining, corroborating pronounced neuronal degeneration and cell loss in *pcl* of CA1 and *gcl* of DG. At 7d TMT, FJC staining was decreased in *gcl* of DG, but was increased in the hilar subfield of DG where neurodegeneration begins. Again, no pathological changes were observed in the distal and medial CA3 subregion during the examined timeframe (data not shown).

Changes of GFAP-*ir* astrocytes morphology after TMT intoxication

When TMT was applied, changes in the number and morphology of GFAP-*ir* astrocytes were noticeable with the marked difference between examined regions (Fig. 6A). At 2d TMT, astrocytes in *so* and *sr* moved their cell bodies closer to the *pcl* of CA1, creating dense glial fronts against the layer. Similar observations were obtained in CA3 and the hilar region of DG. At 4d TMT and 7d TMT, many hypertrophied astrocytes in CA1 subregion were seen. The intersections between $GFAP^+$ stained processes were not observed, but rather polarization towards the injury site, indicating preserved domain organization. The glia of the hilar subregion responded differently than those in CA1 region. Hypertrophy could be seen two days post-exposure, but from that time-point, their morphology was mostly atrophied. Interestingly, it seems that the domain organization remained in all three regions even seven days after intoxication.

In order to confirm descriptive observations after TMT intoxication, density and mean surface of GFAP-*ir* astrocytes were calculated. Cell counting followed by two-way ANOVA revealed significant differences in the cell counts/filed, time after TMT exposure and their interaction (hippocampal subfields: $F_{(2,92)} = 75.7$, $p < 0.0001$; time post-TMT: $F_{(3,92)} = 22.3$, $p < 0.0001$; interaction: $F_{(6,92)} = 14.7$, $p < 0.0001$). The response of astrocytes to TMT resulted in an increase of $GFAP^+$ cells in examined subfields, particularly in CA1, at 4d TMT (Fig. 6B). In CA3 and the hilar region, astrocyte numbers peaked 2d after TMT exposure and thereafter gradually returned to the baseline level. However, the most profound astrocytic response, both in terms of their number and response duration, was observed in CA1, where an increased number of astrocytes persisted even at 7d TMT.

Morphological hallmarks of reactive astrocytes are the cellular hypertrophy and process elongation, thus astrogliosis is expected to be associated with an increase in mean surface area (Verkhratsky et al., 2014). Analyses of mean surface of $GFAP^+$ astrocytes followed by two-way ANOVA confirmed significant difference in mean surface area according to subfield, time and its interaction (hippocampal subfield: $F_{(2,532)} = 70.8$, $p < 0.0001$; time: $F_{(3,532)} = 45.8$, $p < 0.0001$; interaction: $F_{(6,532)} = 16.9$, $p < 0.0001$). In CA1 subfield, the mean surface area increased from 2d TMT afterward and remained elevated at 7d TMT (Fig. 6C), while in CA3, the mean surface area increased only at 7d TMT in respect to Ctrl ($p < 0.01$). In the hilus of DG, the mean surface area peaked at 2d TMT and thereafter decreased, being at 7d TMT still higher than in Ctrl. Changes in $GFAP^+$ mean surface area in the hilus of DG were associated with a decrease in astroglial complexity and reduction in branching, which is indicative of cell atrophy (Verkhratsky et al., 2014; Lee and MacLean, 2015). In order to evaluate the dynamics of morphological changes in distinct subfields, a thorough analysis of relevant morphological parameters was performed.

Morphometric analysis of activated astrocytes followed by two-way ANOVA revealed that fractal dimension, perimeter, length of GFAP stained processes, number of primary and secondary branches as well as Shoenon ramification index showed a significant effect of the anatomical subregion, time, and their interaction (Table 3). Parameter circularity showed only the effect of time. The results of *posthoc* analysis are presented in Fig. 7. After intoxication, astrocytes of CA1 region increased their complexity that is reflected in the higher number of primary and secondary branches followed by an increase in perimeter and the Shoenon ramification coefficient. $GFAP^+$ astrocytes of CA3 region did not change morphology in the first 4 days, but subtle changes in the number of secondary branches were observable at 7d after intoxication. Although astrocytes in the hilar region initially responded with a more complex phenotype to TMT intoxication, simplified complexity and branching status of GFAP-*ir* astrocytes in the subfield at 7d TMT also indicated different fate than in CA1 (Fig. 7, Table 3).

Subregion-different vimentin/nestin expression after TMT intoxication

In order to examine the hippocampal subregional-different response of astrocytes, we investigated changes in two other markers known to be upregulated in pathology – vimentin, and nestin. Together with GFAP, intermediate filaments such as vimentin and nestin represent indicators of reactive gliosis in CNS (Pekny and Nilsson, 2005; Pekny et al., 2007; Sofroniew and Vinters, 2010). Vimentin is a marker of immature astrocytes and is not normally expressed at a high level in the adult brain. Further, the upregulation of vimentin is a hallmark in models

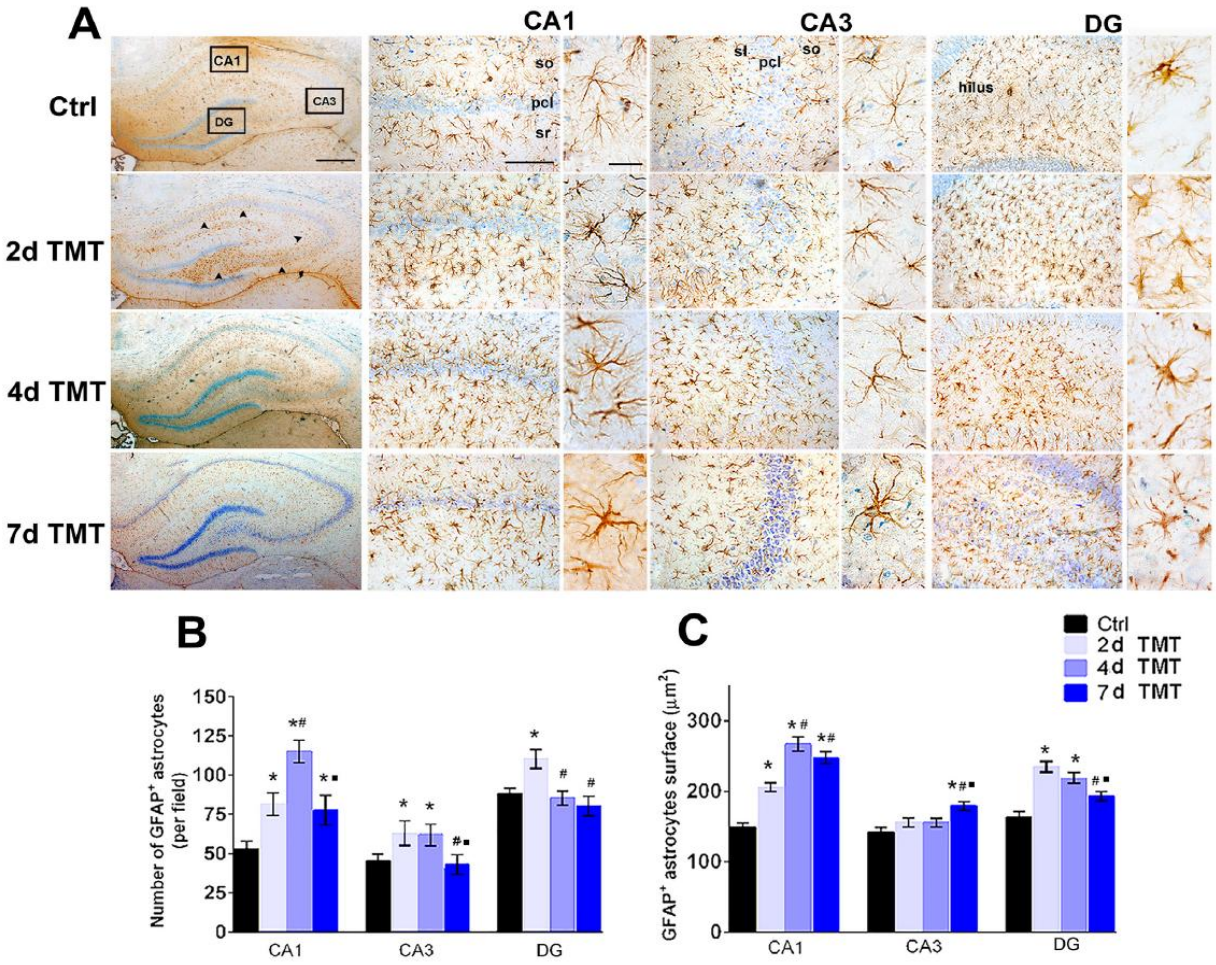

Fig. 6. Changes of astrocytes morphology after TMT intoxication in the hippocampus. A) Representative micrographs of GFAP staining from Ctrl hippocampi and from hippocampi collected at different time points after TMT exposure: 2, 4 and 7 days. Scale bar 500 μm for micrographs of whole hippocampi, and scale bar 100 μm for micrographs of subregions. The high magnification images represent a typical morphology of subregion/time-specific GFAP$^+$ astrocytes. A considerable proportion of GFAP$^+$ astrocytes exhibited hypertrophy. Astrocytes in the hilus of DG showed atrophy-like morphology. Scale bar 25 μm for high magnification of astrocytes. Cell counts (B) and the cellular surface of GFAP$^+$ astrocytes (C) in CA1, CA3 and DG area. Data represent mean ± SEM. Significance shown inside the graphs: $^*p < 0.05$ or less compared to Ctrl; $^{\#}p < 0.05$ or less compared to 2d TMT; $^{\bullet}p < 0.05$ or less compared to 4d TMT.

of brain damage, including neurotoxins (Andersson et al., 1994). In Ctrl animals, vimentin-*ir* cells were exclusively found in the alveus and fimbria (data not shown). In CA1 and CA3 regions, no vimentin-*ir* was observed on GFAP$^+$ astrocytes in Ctrl nor 7d after TMT (Fig. 8A). A few scattered vimentin-*ir* cells were first detectable in the hilus of DG 4-d post-TMT (data not shown), where the number of double GFAP$^+$/vimentin$^+$ astrocytes had dramatically increased 7d post TMT, specifically overlapping with atrophy-like astrocytes in this region.

Nestin is a type VI intermediate filament expressed in progenitor cells during the development of CNS (Sofroniew and Vinters, 2010). In the adult rat brain, nestin can be only found in subependymal stem cells of the subventricular zone and in endothelial cells. In some pathological conditions, nestin is expressed in reactive astrocytes (Duggal et al., 1997; Pekny and Pekna, 2014), also has been shown association of nestin with the site of TMT-induced damage (Geloso et al., 2004). Thus, no nestin-*ir* was detected in the hippocampal subregions of Ctrl animals (Fig. 8B), as well as in the first 4 days after intoxication (data not shown). At 7d TMT, activated hypertrophied astrocytes of CA1 and CA3 expressed only GFAP while double GFAP$^+$/nestin$^+$ cells were exclusively found within the hilar region of DG.

Expression of Kir4.1 after TMT exposure

The functional state of reactive astrocytes after TMT intoxication was examined by Kir4.1-*ir* (Fig. 8C, D). Kir4.1 is an inwardly rectifying K$^+$ channel exclusive for astrocytes and involved in maintaining resting

Table 3. Results of two-way ANOVA analysis and *post-hoc test* of astrocyte morphology parameters after TMT intoxication.

Effect of TMT on astrocyte morphology		Fractal dimension	Perimeter	Circularity	Length of GFAP stained processes	No. of primary branches	No. of secondary branches	Shoenon coefficient
Subregion	F values	$F_{2,\ 227} = 45.49$	$F_{2,\ 222} = 10.58$	$F_{2,\ 225} = 1.41$	$F_{2,\ 225} = 13.80$	$F_{2,\ 223} = 9.21$	$F_{2,\ 221} = 6.59$	$F_{2,\ 218} = 13.79$
	p values	$p < 0.0001$	$p < 0.0001$	$p = 0.075$	$p < 0.0001$	$p < 0.001$	$p < 0.01$	$p < 0.0001$
Time	F values	$F_{3,\ 227} = 14.78$	$F_{3,\ 222} = 9.31$	$F_{3,\ 225} = 4.15$	$F_{3,\ 225} = 18.43$	$F_{3,\ 223} = 7.09$	$F_{3,\ 221} = 25.82$	$F_{3,\ 218} = 3.11$
	p values	$p < 0.0001$	$p < 0.0001$	$p < 0.01$	$p < 0.0001$	$p < 0.001$	$p < 0.0001$	$p < 0.05$
Interaction Subregion * Time	F values	$F_{6,\ 227} = 3.11$	$F_{6,\ 222} = 4.46$	$F_{6,\ 225} = 1.94$	$F_{6,\ 225} = 9.36$	$F_{6,\ 223} = 2.99$	$F_{6,\ 221} = 7.10$	$F_{6,\ 218} = 12.57$
	p values	$p < 0.01$	$p < 0.001$	$p = 0.245$	$p < 0.0001$	$p < 0.01$	$p < 0.0001$	$p < 0.0001$
CA1	OVX	1.403 ± 0.007	130.9 ± 4.5	0.793 ± 0.018	227.7 ± 12.5	5.55 ± 0.25	6.16 ± 0.51	1.62 ± 0.08
	TMT 2d	1.466 ± 0.009*	172.3 ± 7.9*	0.825 ± 0.018	365.1 ± 18.6	6.30 ± 0.27	9.55 ± 0.56*	2.19 ± 0.08*
	TMT 4d	1.451 ± 0.007*	172.8 ± 7.3*	0.816 ± 0.010	356.5 ± 22.4	6.00 ± 0.26	8.55 ± 0.39	2.41 ± 0.11*
	TMT 7d	1.471 ± 0.009*	157.8 ± 4.3*	0.818 ± 0.011	352.0 ± 17.8	6.10 ± 0.28	7.55 ± 0.37	2.44 ± 0.12*
CA3	OVX	1.414 ± 0.007	134.6 ± 4.9	0.815 ± 0.015	266.1 ± 16.8	5.94 ± 0.25	7.55 ± 0.56	1.88 ± 0.07
	TMT 2d	1.438 ± 0.006	148.7 ± 4.3	0.821 ± 0.013	304.9 ± 14.9	6.35 ± 0.30	7.80 ± 0.53	1.76 ± 0.05
	TMT 4d	1.421 ± 0.006	150.4 ± 5.4	0.793 ± 0.016	280.3 ± 13.1	5.80 ± 0.24	7.25 ± 0.46	1.86 ± 0.05
	TMT 7d	1.428 ± 0.008	137.8 ± 5.0	0.808 ± 0.010	230.6 ± 14.3	5.33 ± 0.29	4.66 ± 0.46*	1.84 ± 0.04
DG	OVX	1.464 ± 0.012	149.6 ± 3.4	0.816 ± 0.015	331.5 ± 16.6	7.10 ± 0.27	9.55 ± 0.75	2.21 ± 0.09
	TMT 2d	1.512 ± 0.009*	148.2 ± 4.32	0.879 ± 0.007*	410.3 ± 22.8	7.55 ± 0.44	10.05 ± 0.67	2.41 ± 0.13
	TMT 4d	1.479 ± 0.006	146.1 ± 4.1	0.823 ± 0.015	318.0 ± 13.0	6.90 ± 0.40	8.25 ± 0.53	1.935 ± 0.09#
	TMT 7d	1.473 ± 0.008#	133.7 ± 5.9	0.796 ± 0.016#	233.4 ± 13.1	5.31 ± 0.32*,#,●	4.31 ± 0.41*,#,●	1.74 ± 0.08*,#,●

* $p < 0.05$ (or less), compared to OVX control.
\# $p < 0.05$ (or less), compared to TMT 2d.
● $p < 0.05$ (or less), compared to TMT 4d.

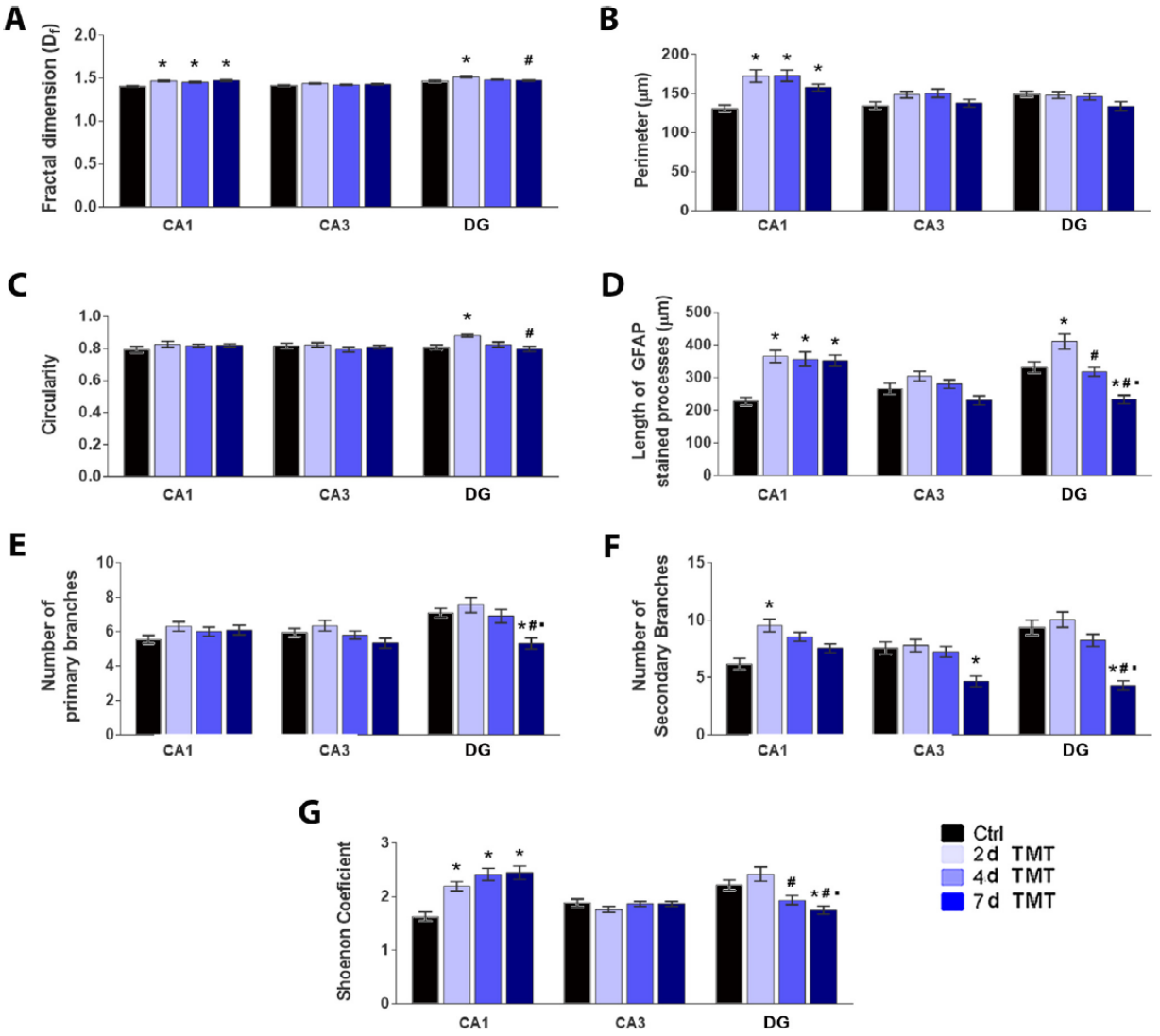

Fig. 7. Morphological parameters of astrocytes after TMT intoxication. A fractal dimension (A), perimeter (B), circularity (C), length of GFAP stained processes (D), number of primary (E) and secondary branches (F) and Shoenon coefficient (G) of astrocytes in CA1/CA3 and DG. The values are given as means ± SEM. Significance shown inside the graphs: *p < 0.05 or less compared to Ctrl; #p < 0.05 or less compared to 2d TMT; ●p < 0.05 or less compared to 4d TMT.

membrane potential of astrocytes, K^+ buffering, cell volume, maturation, and cell cycle and facilitating glutamate transport (Nwaobi et al., 2016). In Ctrl animals, Kir4.1 labeled the bodies and nicely depicted processes of astrocytes through the entire hippocampus, and co-localized with GFAP (Fig. 8C). At 7d TMT, in all three regions of the hippocampus higher Kir4.1-*ir* was observed, also corroborating hypertrophied morphology in CA1 and CA3, and less complex astrocytes in the hilar region of DG (Fig. 8C). Furthermore, in the hilus of DG 7d post-TMT, Kir4.1$^+$ less-complex astrocytes were also vimentin- and nestin-positive (Fig. 8D).

DISCUSSION

Glial fibrillary acid protein (GFAP) is an intermediate filament vastly expressed in astrocytes, particularly up-regulated during different CNS pathologies (Sofroniew and Vinters, 2010; Pekny and Pekna, 2014). Even though it does not reflect the full morphology of astrocytes, it is still used as a reliable and sensitive marker of both quiescent and reactive glia. In DAB-reacted immunohistochemistry GFAP labels primary, secondary and to some extent tertiary branches of astrocytes, but it is absent in the finely branched processes, therefore partially underestimating

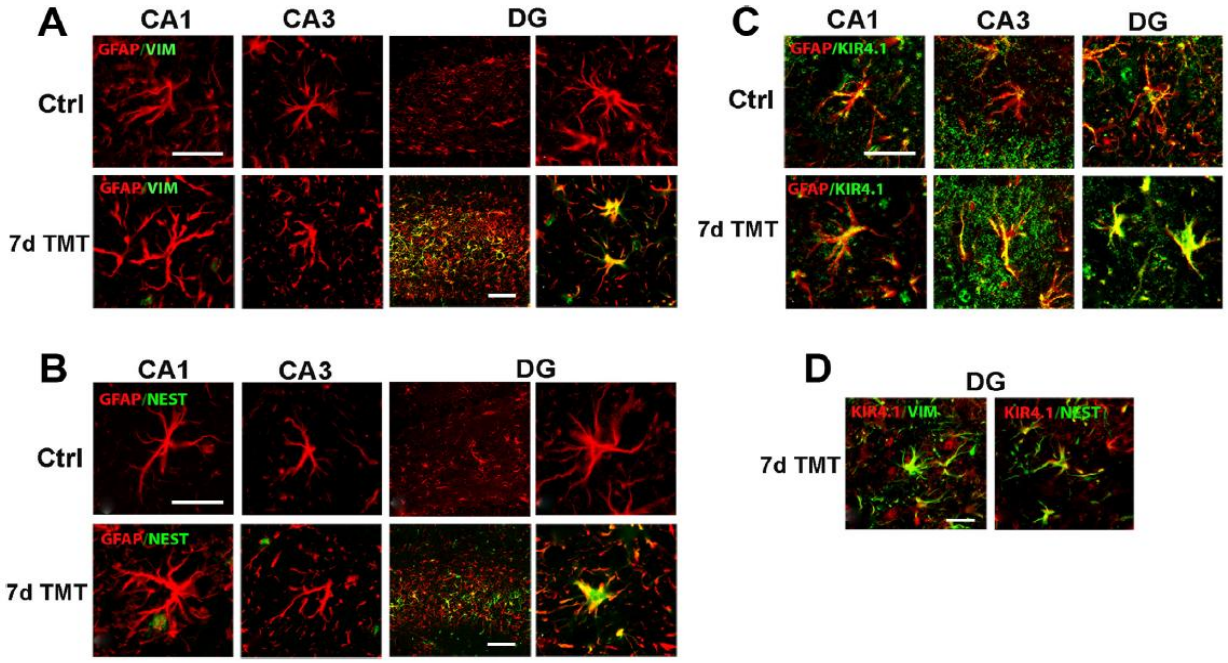

Fig. 8. Double immunofluorescent staining of GFAP with vimentin (VIM), nestin (NEST) and Kir4.1 in the hippocampus 7 days after TMT intoxication. A) In CA1, CA3 and DG regions of Ctrl sections, double GFAP$^+$/VIM$^+$ cells were not observed. In CA1 and CA3 regions 7 days post-TMT, only GFAP$^+$ hypertrophied astrocytes were detected. In the hilar region of DG, GFAP$^+$ astrocytes with altered morphology clearly overlap with vimentin. B) In CA1, CA3 and DG regions of Ctrl sections, double GFAP$^+$/NEST$^+$ cells were not seen. In CA1 and CA3 regions, only GFAP$^+$-hypertrophied astrocytes 7d after TMT were observed, while double GFAP$^+$/NEST$^+$ cells were scattered within the hilar region of DG. C) Double GFAP$^+$/Kir4.1$^+$ cells were clearly observed in the hippocampal CA1, CA3 and DG regions of Ctrl sections. Overlaid images revealed overlapping expression of GFAP and Kir4.1 in astrocytes of CA1 and CA3 as well as in GFAP$^+$ astrocytes in DG 7 days post-TMT. D) In the hilus of DG, Kir4.1$^+$ astrocytes are also VIM$^+$ and NEST$^+$. Scale bar 25 μm for high magnification and scale bar 100 μm for low magnification.

branching pattern of astrocytes and domain coverage. In this respect, there are potential limitations to our methodological approach, and confocal microscopy would provide a more informative results. Given that a present study utilizes morphometry in order to evaluate spatio-temporal response of astrocyte to neurodegeneration, usage of DAB staining method is quite acceptable for in-depth morphological analysis of astrocytes and other cells in CNS (Cashion et al., 2003; Pirici et al., 2009; Olude et al., 2015; Fernandez-Arjona et al., 2017; Morrison et al., 2017). Although regional differences in the expression of GFAP are noted, it has been shown that almost all astrocytes in a healthy hippocampus express a readily detectable GFAP (Middeldorp and Hol, 2011; Khakh and Sofroniew, 2015).

Based on GFAP-*ir,* we identified seven different astrocyte subtypes in the hippocampus of Ctrl female rats, which is mostly in agreement with existing literature described in intact animals (Kosaka and Hama, 1986; Kalman and Hajos, 1989). A single-cell fractal analysis is a measure of morphological complexity, and the indicator of a degree to which cell fills surrounding space (Montague and Friedlander, 1989, 1991). This analysis revealed substantial differences between astrocytes of CA1/CA3 and the hilus of DG, indicating more complex phenotype of the hilar astrocytes. Also, differences in other parameters between CA1/CA3- and the hilar-GFAP$^+$ protoplasmic astrocytes were observed. Such morphological heterogeneity may serve to fulfill regional-specific physiological requirements (Zhang and Barres, 2010; Bayraktar et al., 2014), leading to different functional profiles of these cells.

In the rat model of TMT-induced neurodegeneration, it is well established that the beginning of neuronal damage (2–4 days after intoxication) is accompanied by glial cells activation (Haga et al., 2002; Trabucco et al., 2009; Geloso et al., 2011; Corvino et al., 2012; Little et al., 2012; Corvino et al., 2013; Lattanzi et al., 2013; Corvino et al., 2015). The present study describes GFAP-*ir* astrocytes responses that accompany neuronal cell loss in the hippocampus induced by TMT. As expected, first behavioral signs manifested as hyper-excitability and hyper-responsiveness appeared 2d after TMT and coincided with neuronal damage in the hippocampal CA1 subfields. The wave of neuronal injury spread in the next two days, inducing neuronal cell loss of CA1 and DG subfields; thus our findings are in agreement with results reported by Balaban et al. (1988), Little et al. (2012), Corvino et al. (2015), Haga et al. (2002), etc. Based on available literature data, it is most likely that TMT disturbs excitatory/inhibitory synaptic balance critical for hippocampal information processing (Geloso et al., 2011; Corvino et al., 2013; Corvino et al., 2015; Lee et al., 2016b), causing behavioral signs typical for TMT intoxication. The ear-

liest occurrence of apoptotic bodies in CA1 field at 4d post-TMT implies that apoptosis itself began after 2 days and probably amplified at day 4, when mild tremor progressed into the systemic one. Furthermore, activation of astrocytes was an early event, triggered concomitantly with neuronal damage but before signs of cell death in the corresponding subfields.

In accordance with diverse morphology of astrocytes in the subregions of Ctrl hippocampus, TMT intoxication led to the subregion-different response of GFAP$^+$ astrocytes. Activation of astrocytes was most prominent in CA1, where firstly occurred and persisted for the investigated time frame. These astrocytes exhibited significantly larger mean surface area in comparison with the cells in all other subfields. At 2d TMT, astrocytes polarized towards the region of neurodegeneration, enclosed *pcl* and created a dense glial front against the layer in which the neuronal damage occurred. At 4d TMT, astrocytes invaded *pcl* of CA1, probably reflecting their ability to enclose the site of neuronal degeneration and to clear tissue debris, protecting other regions from damage (Tasdemir-Yilmaz and Freeman, 2014; Liddelow and Barres, 2017). The same frontal formation of astrocytes was observed throughout the hippocampus. Moreover, during whole post-exposure period astrocytes appear to retain their domain organization with minimal overlaps in the areas of high synaptic density. It should be noted that full domain organization could be more accurately evaluated using *state-of-art* techniques (Oberheim et al., 2008), but robust changes on a larger scale might be detected by GFAP-*ir*. However, organization of astrocytes that we observed implies that TMT-activated astrocytes probably continue to modulate healthy synapses and achieve other functions important for neuroprotection of undamaged cells (Heller and Rusakov, 2015; Kelly et al., 2018). Even though the main indicator of astrocyte complexity – fractal dimension remained nearly the same in all examined time points, changes of other parameters corroborate that TMT-induced activation of astrocytes is a dynamic process, which involves continuous remodeling (Sun and Jakobs, 2012). The general trend in CA1 is an overall increase in complexity of activated astrocytes particularly indicated by augmentation in fractal dimension, perimeter, and branching complexity. Since the increase in secondary branches of CA1-GFAP$^+$ astrocytes was detected prior to neuronal death, this could serve as an early alarmin of upcoming neuronal alterations and astrocyte activation (Yeh et al., 2011).

In the hilus of DG, astrocytes showed a different pattern of activation from that observed in CA1 hippocampal subfield. The initial increase in general complexity seen 2 days after intoxication corresponds to classical hypertrophy, and was followed by a steady decline towards less complex morphological phenotype. At 7d TMT, most of the hilar astrocytes had enlarged bodies with a significant reduction in branching complexity, which could be described as atrophy-like morphology. According to the existing literature, astroglial atrophy is defined as a reduction in surface area and morphological complexity, mainly reflected on branching pattern (Olabarria et al., 2010; Yeh et al., 2011; Kulijewicz-Nawrot et al., 2012; Plata et al., 2018). Besides morphometric parameters, there is no unanimous consensus or proposed marker for the evaluation of this phenomenon. Admittedly, changes in some functional markers were found, but they are pathology- rather than atrophy-specific (Rodriguez-Arellano et al., 2016). Atrophy-like morphology comprised a significant decrease in the number and length of primary and secondary branches. Also, Sholl analysis supported atrophy of branching pattern, pointing to a significant reduction in the size of the astrocytic domain (Plata et al., 2018). Namely, characteristic of an early stages of various neurodegenerative diseases such as epilepsy, Alzheimer's disease, and some psychiatric disorders are represented by a simultaneous presence of beneficial hypertrophy of astrocytes in CA subregions, and astroglial atrophy noticed in the hilus, with preserved total number of GFAP$^+$ astrocytes (Verkhratsky et al., 2014; Lee and MacLean, 2015; Rodriguez-Arellano et al., 2016). Such atrophy-like morphology is reflected as a loss of astrocytic domain organization in terms of their territorial coverage. Consequently, reduced support may largely influence the survival of neurons, and synaptic activity, thus ultimately decreasing neuronal connectivity and plasticity (Rodriguez-Arellano et al., 2016; Plata et al., 2018). Also, it might be a cause of neurodegeneration in the hilar region at 7d post-TMT that we detected. Since DG represents the main input of afferent projections from entorhinal cortex, which is also a target of TMT (Balaban et al., 1988), observed morphological atrophy could be a contributor to seizures but also cognitive impairment seen in TMT exposed animals (Trabucco et al., 2009; Geloso et al., 2011).

The disparity in morphological dynamics of reactive astrocytes was further confirmed by two other intermediate filaments, vimentin and nestin, known to be up-regulated in various pathologies (Andersson et al., 1994; Pekny and Nilsson, 2005, Gilyarov, 2008). We found that vimentin-*ir* is limited to the hilar region of DG, pointing to a reactive phenotype of astrocytes and ongoing neuronal degeneration (Pekny and Nilsson, 2005; Kelso et al., 2011). In contrast to vimentin$^+$ astrocytes, the hilar nestin$^+$ astrocytes were less in number and strictly located in the perilesional area. Co-localization of both vimentin and nestin with GFAP again pointed to atrophy-like morphology of the hilar astrocytes. Seven days after TMT intoxication, expression of Kir4.1 was present in all examined subregions and confined to reactive GFAP$^+$ astrocytes. Furthermore, Kir4.1 was co-expressed on both vimentin$^+$- and nestin$^+$-hilar astrocytes, indicating that atrophied phenotype successfully regulates its pattern of protein expression and therefore represents a unique glial signature. The expression of Kir4.1 was retained in both body and branches of astrocytes following the similar pattern observed in controls, suggesting that morphological atrophy precedes functional changes. In addition to being expressed in activated astrocytes, nestin re-expression usually points to a potential proliferative state of reactive glia (Gilyarov, 2008). It has been shown that precondition for a mature astrocyte

to re-enter a cell cycle is the downregulation of Kir4.1 or its shift from astrocyte processes to the cell body (Stewart et al., 2010). Namely, expression of Kir4.1 is essential for astrocyte maturation and its high expression has a negative impact on cellular division, since the resting membrane of astrocytes correlates with its proliferative potential (Cone, 1970; Higashimori and Sontheimer, 2007). Seven days post-TMT, immunoreactivity of Kir4.1 on astrocytic bodies and processes rather than its down-regulation or shift, points to mature phenotype rather than a proliferative one. However, further research is required for answering the question of whether early morphological atrophy is accompanied by functional imparity at later stages of TMT-induced neurodegeneration, and to fully understand the fate of glial atrophy.

Generally, three types of astrocyte changes in various neuropathologies were seen: changes in numbers of astrocytes, morphological remodeling, and reactive astrogliosis (Plata et al., 2018). The specific combination of such astrocytic pathologies could characterize particular neurodegeneration or a distinct stage of its progression (Verkhratsky and Parpura, 2016). It is known that in response to mild/moderate CNS insults, reactive astrocytes are non-proliferative resident cells, which do not migrate and exhibit varying degrees of cellular hypertrophy (Wilhelmsson et al., 2006; Khakh and Sofroniew, 2015). Based on our morphological analysis, all parameters pointed to reactive gliosis that could be described as mild to moderate with preserved domain organization in CA1 region. On the other hand, dynamic morphological remodeling of astrocytes in the hilus was seen. Thus, observed differences in astrocyte response between two hippocampal regions affected by TMT are, at least in part, the consequence of astrocyte heterogeneity and the existence of two distinct $GFAP^+$ astrocytes subpopulations. In general, the difference in response of protoplasmic astrocytes between CA1 and the dentate hilus could be put in the perspective of distinctive cytoarchitecture of these anatomical regions in terms of number of neurons, and synapse density, afferent and efferent inputs, thus creating a diverse three-dimensional microenvironment which could influence astrocyte morphology (Kosaka and Hama, 1986; West et al., 1991; Emsley and Macklis, 2006; Zhang and Barres, 2010). In such organization, selective vulnerability of hippocampal subregions has been demonstrated in several neuropathologies, including temporal lobe epilepsy, transient global ischemia and neurodegenerative disorders such as Alzheimer's disease (Morrison and Hof, 2002; Geddes et al., 2003; Ouyang et al., 2007; Levesque and Avoli, 2013). Furthermore, neurotoxins that selectively target hippocampus i.e. kainic acid and pilocarpine, produce the same pattern of CA injury as a consequence of neurotoxin-induced seizures (Levesque and Avoli, 2013). Careful observation of TMT-induced pattern of neurodegeneration yielded that the dentate gyrus is the primary target of TMT, while CA regions suffer as a consequence of secondary effects of intoxication i.e. seizures (Ishida et al., 1997; Trabucco et al., 2009; Shin et al., 2011). Therefore, TMT-induced model of hippocampal neurodegeneration shares numerous pathogenic mechanisms with other models of hippocampal injury, especially temporal lobe epilepsy (Trabucco et al., 2009; Geloso et al., 2011; Blumcke et al., 2013).

In summary, our results provide the anatomical and morphological description of $GFAP^+$ astrocytes in the hippocampus of Ctrl animals and after TMT intoxication. Morphometric analysis reveals the existence of two distinct $GFAP^+$ morphotypes of astrocytes, which respond differently to TMT-induced hippocampal neurodegeneration. The novelty of this study is in-depth analysis of astrocyte morphology in the time-dependent manner, which could contribute to understanding the dynamics of astrocyte activation. By combining morphometric parameters, we were able to determine baseline morphology of astrocyte and to categorize them accordingly. Considering all changes in the morphology of $GFAP^+$-astrocyte in specific anatomical regions, their activation could be characterized as mild to moderate. In addition, we showed that astrogliosis is a dynamic process; glial morphological remodeling and reactivity are obligatory components of hippocampal neurodegeneration induced by TMT. Furthermore, vimentin and nestin expression confirmed regional-specific astrocyte activation, supporting our hypothesis. Our findings shed light on involvement of astrocyte in the progression of TMT-induced hippocampal neurodegeneration. This quantitative methodology is sensitive, available and could contribute to understanding different pathologies progression, depict roles of specific cell types and their involvement.

AUTHOR CONTRIBUTION

All authors contributed sufficiently to being listed as authors of this paper. MD and IG designed the research. NM and NN contributed to design the research. MD, MZ, NM, IG performed experiments. MD and MZ processed the results. MD and IG analyzed and interpreted the data. MD and IG wrote the manuscript. NM and NN revised the manuscript. All authors approved the final version of the manuscript.

DECLARATION OF COMPETING INTEREST

The authors declare that they have no known competing financial interests or personal relationships that could have appeared to influence the work reported in this paper.

ACKNOWLEDGMENT

We would like to thank the Center for Laser Microscopy, Faculty of Biology, University of Belgrade, and dear colleague Marija Adžić for helping with confocal laser microscopy and imaging. The study was entirely supported by the Ministry of Education, Science and Technological Development of the Republic of Serbia, Grants No III41014 and OI173044.

REFERENCES

Andersson H, Luthman J, Olson L (1994) Trimethyltin-induced expression of GABA and vimentin immunoreactivities in astrocytes of the rat brain. Glia 11:378–382.

Arias C, Zepeda A, Hernandez-Ortega K, Leal-Galicia P, Lojero C, Camacho-Arroyo I (2009) Sex and estrous cycle-dependent differences in glial fibrillary acidic protein immunoreactivity in the adult rat hippocampus. Horm Behav 55:257–263.

Balaban CD, O'Callaghan JP, Billingsley ML (1988) Trimethyltin-induced neuronal damage in the rat brain: comparative studies using silver degeneration stains, immunocytochemistry and immunoassay for neuronotypic and gliotypic proteins. Neuroscience 26:337–361.

Bardehle S, Kruger M, Buggenthin F, Schwausch J, Ninkovic J, Clevers H, Snippert HJ, Theis FJ, Meyer-Luehmann M, Bechmann I, Dimou L, Gotz M (2013) Live imaging of astrocyte responses to acute injury reveals selective juxtavascular proliferation. Nat Neurosci 16:580–586.

Bayraktar OA, Fuentealba LC, Alvarez-Buylla A, Rowitch DH (2014) Astrocyte development and heterogeneity. Cold Spring Harbor Perspect Biol 7 a020362.

Blumcke I, Thom M, Aronica E, Armstrong DD, Bartolomei F, Bernasconi A, Bernasconi N, Bien CG, Cendes F, Coras R, Cross JH, Jacques TS, Kahane P, Mathern GW, Miyata H, Moshe SL, Oz B, Ozkara C, Perucca E, Sisodiya S, Wiebe S, Spreafico R (2013) International consensus classification of hippocampal sclerosis in temporal lobe epilepsy: a task force report from the ILAE commission on diagnostic methods. Epilepsia 54:1315–1329.

Capurso SA, Calhoun ME, Sukhov RR, Mouton PR, Price DL, Koliatsos VE (1997) Deafferentation causes apoptosis in cortical sensory neurons in the adult rat. J Neurosci: Off J Soc Neurosci 17:7372–7384.

Cashion AB, Smith MJ, Wise PM (2003) The morphometry of astrocytes in the rostral preoptic area exhibits a diurnal rhythm on proestrus: relationship to the luteinizing hormone surge and effects of age. Endocrinology 144:274–280.

Cone Jr CD (1970) Variation of the transmembrane potential level as a basic mechanism of mitosis control. Oncology 24:438–470.

Corvino V, Di Maria V, Marchese E, Lattanzi W, Biamonte F, Michetti F, Geloso MC (2015) Estrogen administration modulates hippocampal GABAergic subpopulations in the hippocampus of trimethyltin-treated rats. Front Cell Neurosci 9:433.

Corvino V, Marchese E, Giannetti S, Lattanzi W, Bonvissuto D, Biamonte F, Mongiovi AM, Michetti F, Geloso MC (2012) The neuroprotective and neurogenic effects of neuropeptide Y administration in an animal model of hippocampal neurodegeneration and temporal lobe epilepsy induced by trimethyltin. J Neurochem 122:415–426.

Corvino V, Marchese E, Michetti F, Geloso MC (2013) Neuroprotective strategies in hippocampal neurodegeneration induced by the neurotoxicant trimethyltin. Neurochem Res 38:240–253.

Di Ieva A, Grizzi F, Jelinek H, Pellionisz AJ, Losa GA (2014) Fractals in the neurosciences, Part I: general principles and basic neurosciences. Neuroscientist: Rev J Bringing Neurobiol Neurol Psychiatry 20:403–417.

Duggal N, Schmidt-Kastner R, Hakim AM (1997) Nestin expression in reactive astrocytes following focal cerebral ischemia in rats. Brain Res 768:1–9.

Emsley JG, Macklis JD (2006) Astroglial heterogeneity closely reflects the neuronal-defined anatomy of the adult murine CNS. Neuron Glia Biol 2:175–186.

Fernandez-Arjona MDM, Grondona JM, Granados-Duran P, Fernandez-Llebrez P, Lopez-Avalos MD (2017) Microglia morphological categorization in a rat model of neuroinflammation by hierarchical cluster and principal components analysis. Front Cell Neurosci 11:235.

Geddes DM, LaPlaca MC, Cargill RS (2003) Susceptibility of hippocampal neurons to mechanically induced injury. Exp Neurol 184:420–427.

Geloso MC, Corvino V, Cavallo V, Toesca A, Guadagni E, Passalacqua R, Michetti F (2004) Expression of astrocytic nestin in the rat hippocampus during trimethyltin-induced neurodegeneration. Neurosci Lett 357:103–106.

Geloso MC, Corvino V, Michetti F (2011) Trimethyltin-induced hippocampal degeneration as a tool to investigate neurodegenerative processes. Neurochem Int 58:729–738.

Gilyarov AV (2008) Nestin in central nervous system cells. Neurosci Behav Physiol 38:165–169.

Haga S, Haga C, Aizawa T, Ikeda K (2002) Neuronal degeneration and glial cell-responses following trimethyltin intoxication in the rat. Acta Neuropathol 103:575–582.

Hajos F, Halasy K, Gerics B, Szalay F, Michaloudi E, Papadopoulos GC (2000) Ovarian cycle-related changes of glial fibrillary acidic protein (GFAP) immunoreactivity in the rat interpeduncular nucleus. Brain Res 862:43–48.

Hamby ME, Coppola G, Ao Y, Geschwind DH, Khakh BS, Sofroniew MV (2012) Inflammatory mediators alter the astrocyte transcriptome and calcium signaling elicited by multiple G-protein-coupled receptors. J Neurosci: Off J Soc Neurosci 32:14489–14510.

Heller JP, Rusakov DA (2015) Morphological plasticity of astroglia: understanding synaptic microenvironment. Glia 63:2133–2151.

Higashimori H, Sontheimer H (2007) Role of Kir4.1 channels in growth control of glia. Glia 55:1668–1679.

Ishida N, Akaike M, Tsutsumi S, Kanai H, Masui A, Sadamatsu M, Kuroda Y, Watanabe Y, McEwen BS, Kato N (1997) Trimethyltin syndrome as a hippocampal degeneration model: temporal changes and neurochemical features of seizure susceptibility and learning impairment. Neuroscience 81:1183–1191.

Kalman M, Hajos F (1989) Distribution of glial fibrillary acidic protein (GFAP)-immunoreactive astrocytes in the rat brain I. Forebrain. Exp Brain Res 78:147–163.

Karperien A, Ahammer H, Jelinek HF (2013) Quantitating the subtleties of microglial morphology with fractal analysis. Front Cell Neurosci 7:3.

Kelly P, Hudry E, Hou SS, Bacskai BJ (2018) In Vivo Two Photon Imaging Of Astrocytic Structure And Function In Alzheimer's disease. Front Aging Neurosci 10:219.

Kelso ML, Liput DJ, Eaves DW, Nixon K (2011) Upregulated vimentin suggests new areas of neurodegeneration in a model of an alcohol use disorder. Neuroscience 197:381–393.

Khakh BS, Sofroniew MV (2015) Diversity of astrocyte functions and phenotypes in neural circuits. Nat Neurosci 18:942–952.

Klintsova A, Levy WB, Desmond NL (1995) Astrocytic volume fluctuates in the hippocampal CA1 region across the estrous cycle. Brain Res 690:269–274.

Kosaka T, Hama K (1986) Three-dimensional structure of astrocytes in the rat dentate gyrus. J Comp Neurol 249:242–260.

Kulijewicz-Nawrot M, Verkhratsky A, Chvatal A, Sykova E, Rodriguez JJ (2012) Astrocytic cytoskeletal atrophy in the medial prefrontal cortex of a triple transgenic mouse model of Alzheimer's disease. J Anat 221:252–262.

Latini L, Geloso MC, Corvino V, Giannetti S, Florenzano F, Viscomi MT, Michetti F, Molinari M (2010) Trimethyltin intoxication up-regulates nitric oxide synthase in neurons and purinergic ionotropic receptor 2 in astrocytes in the hippocampus. J Neurosci Res 88:500–509.

Lattanzi W, Corvino V, Di Maria V, Michetti F, Geloso MC (2013) Gene expression profiling as a tool to investigate the molecular machinery activated during hippocampal neurodegeneration induced by trimethyltin (TMT) administration. Int J Mol Sci 14:16817–16835.

Lee B, Sur B, Cho SG, Yeom M, Shim I, Lee H, Hahm DH (2016a) Wogonin attenuates hippocampal neuronal loss and cognitive dysfunction in trimethyltin-intoxicated rats. Biomol Ther 24:328–337.

Lee KM, MacLean AG (2015) New advances on glial activation in health and disease. World J Virol 4:42–55.
Lee S, Yang M, Kim J, Kang S, Kim J, Kim JC, Jung C, Shin T, Kim SH, Moon C (2016b) Trimethyltin-induced hippocampal neurodegeneration: a mechanism-based review. Brain Res Bull 125:187–199.
Levesque M, Avoli M (2013) The kainic acid model of temporal lobe epilepsy. Neurosci Biobehav Res 37:2887–2899.
Liddelow SA, Barres BA (2017) Reactive astrocytes: production, function, and therapeutic potential. Immunity 46:957–967.
Little AR, Benkovic SA, Miller DB, O'Callaghan JP (2002) Chemically induced neuronal damage and gliosis: enhanced expression of the proinflammatory chemokine, monocyte chemoattractant protein (MCP)-1, without a corresponding increase in proinflammatory cytokines. Neuroscience 115:307–320.
Little AR, Miller DB, Li S, Kashon ML, O'Callaghan JP (2012) Trimethyltin-induced neurotoxicity: gene expression pathway analysis, q-RT-PCR and immunoblotting reveal early effects associated with hippocampal damage and gliosis. Neurotoxicol Teratol 34:72–82.
Luquin S, Naftolin F, Garcia-Segura LM (1993) Natural fluctuation and gonadal hormone regulation of astrocyte immunoreactivity in dentate gyrus. J Neurobiol 24:913–924.
Middeldorp J, Hol EM (2011) GFAP in health and disease. Prog Neurobiol 93:421–443.
Montague PR, Friedlander MJ (1989) Expression of an intrinsic growth strategy by mammalian retinal neurons. PNAS 86:7223–7227.
Montague PR, Friedlander MJ (1991) Morphogenesis and territorial coverage by isolated mammalian retinal ganglion cells. J Neurosci: Off J Soc Neurosci 11:1440–1457.
Morrison H, Young K, Qureshi M, Rowe RK, Lifshitz J (2017) Quantitative microglia analyses reveal diverse morphologic responses in the rat cortex after diffuse brain injury. Sci Rep-Uk:7.
Morrison HW, Filosa JA (2013) A quantitative spatiotemporal analysis of microglia morphology during ischemic stroke and reperfusion. J Neuroinflamm 10:4.
Morrison JH, Hof PR (2002) Selective vulnerability of corticocortical and hippocampal circuits in aging and Alzheimer's disease. Prog Brain Res 136:467–486.
Nwaobi SE, Cuddapah VA, Patterson KC, Randolph AC, Olsen ML (2016) The role of glial-specific Kir4.1 in normal and pathological states of the CNS. Acta Neuropathol 132:1–21.
Oberheim NA, Goldman SA, Nedergaard M (2012) Heterogeneity of astrocytic form and function. Methods Mol Biol 814:23–45.
Oberheim NA, Tian GF, Han X, Peng W, Takano T, Ransom B, Nedergaard M (2008) Loss of astrocytic domain organization in the epileptic brain. J Neurosci: Off J Soc Neurosci 28:3264–3276.
Olabarria M, Noristani HN, Verkhratsky A, Rodriguez JJ (2010) Concomitant astroglial atrophy and astrogliosis in a triple transgenic animal model of Alzheimer's disease. Glia 58:831–838.
Olude MA, Mustapha OA, Aderounmu OA, Olopade JO, Ihunwo AO (2015) Astrocyte morphology, heterogeneity, and density in the developing African giant rat (Cricetomys gambianus). Front Neuroanat 9.
Ouyang YB, Voloboueva LA, Xu LJ, Giffard RG (2007) Selective dysfunction of hippocampal CA1 astrocytes contributes to delayed neuronal damage after transient forebrain ischemia. J Neurosci 27:4253–4260.
Pekny M, Nilsson M (2005) Astrocyte activation and reactive gliosis. Glia 50:427–434.
Pekny M, Pekna M (2014) Astrocyte reactivity and reactive astrogliosis: costs and benefits. Physiol Rev 94:1077–1098.
Pekny M, Wilhelmsson U, Bogestal YR, Pekna M (2007) The role of astrocytes and complement system in neural plasticity. Int Rev Neurobiol 82:95–111.
Pirici D, Mogoanta L, Margaritescu O, Pirici I, Tudorica V, Coconu M (2009) Fractal analysis of astrocytes in stroke and dementia. Rom J Morphol Embryo 50:381–390.
Plata A, Lebedeva A, Denisov P, Nosova O, Postnikova TY, Pimashkin A, Brazhe A, Zaitsev AV, Rusakov DA, Semyanov A (2018) Astrocytic Atrophy Following Status Epilepticus Parallels Reduced Ca(2+) Activity and Impaired Synaptic Plasticity in the Rat Hippocampus. Front Mol Neurosci 11:215.
Rodriguez-Arellano JJ, Parpura V, Zorec R, Verkhratsky A (2016) Astrocytes in physiological aging and Alzheimer's disease. Neuroscience 323:170–182.
Scharfman HE, Goodman JH, Rigoulot MA, Berger RE, Walling SG, Mercurio TC, Stormes K, Maclusky NJ (2005) Seizure susceptibility in intact and ovariectomized female rats treated with the convulsant pilocarpine. Exp Neurol 196:73–86.
Shin EJ, Jeong JH, Chung YH, Kim WK, Ko KH, Bach JH, Hong JS, Yoneda Y, Kim HC (2011) Role of oxidative stress in epileptic seizures. Neurochem Int 59:122–137.
Sofroniew MV (2009) Molecular dissection of reactive astrogliosis and glial scar formation. Trends Neurosci 32:638–647.
Sofroniew MV, Vinters HV (2010) Astrocytes: biology and pathology. Acta Neuropathol 119:7–35.
Stewart TH, Eastman CL, Groblewski PA, Fender JS, Verley DR, Cook DG, D'Ambrosio R (2010) Chronic dysfunction of astrocytic inwardly rectifying K+ channels specific to the neocortical epileptic focus after fluid percussion injury in the rat. J Neurophysiol 104:3345–3360.
Sun D, Jakobs TC (2012) Structural remodeling of astrocytes in the injured CNS. Neurosci: Rev J Bringing Neurobiol Neurol Psychiatry 18:567–588.
Tasdemir-Yilmaz OE, Freeman MR (2014) Astrocytes engage unique molecular programs to engulf pruned neuronal debris from distinct subsets of neurons. Genes Dev 28:20–33.
Trabucco A, Di Pietro P, Nori SL, Fulceri F, Fumagalli L, Paparelli A, Fornai F (2009) Methylated tin toxicity a reappraisal using rodents models. Arch Ital Biol 147:141–153.
Veliskova J, Desantis KA (2013) Sex and hormonal influences on seizures and epilepsy. Horm Behav 63:267–277.
Verkhratsky A, Parpura V (2016) Astrogliopathology in neurological, neurodevelopmental and psychiatric disorders. Neurobiol Dis 85:254–261.
Verkhratsky A, Parpura V, Pekna M, Pekny M, Sofroniew M (2014) Glia in the pathogenesis of neurodegenerative diseases. Biochem Soc Trans 42:1291–1301.
West MJ, Slomianka L, Gundersen HJ (1991) Unbiased stereological estimation of the total number of neurons in thesubdivisions of the rat hippocampus using the optical fractionator. Anatomical Rec 231:482–497.
Wilhelmsson U, Bushong EA, Price DL, Smarr BL, Phung V, Terada M, Ellisman MH, Pekny M (2006) Redefining the concept of reactive astrocytes as cells that remain within their unique domains upon reaction to injury. PNAS 103:17513–17518.
Yeh CY, Vadhwana B, Verkhratsky A, Rodriguez JJ (2011) Early astrocytic atrophy in the entorhinal cortex of a triple transgenic animal model of Alzheimer's disease. ASN neuro 3:271–279.
Zamanian JL, Xu L, Foo LC, Nouri N, Zhou L, Giffard RG, Barres BA (2012) Genomic analysis of reactive astrogliosis. J Neurosci: Off J Soc Neurosci 32:6391–6410.
Zhang Y, Barres BA (2010) Astrocyte heterogeneity: an underappreciated topic in neurobiology. Curr Opin Neurobiol 20:588–594.

(Received 23 July 2019, Accepted 14 October 2019)
(Available online 1 November 2019)

Microscopy and Microanalysis (2019), 1–9
doi:10.1017/S1431927618016306

Microscopy AND Microanalysis

Original Article

Application of Gray Level Co-Occurrence Matrix Analysis as a New Method for Enzyme Histochemistry Quantification

Milorad Dragić[1,2*], Marina Zarić[2], Nataša Mitrović[2], Nadežda Nedeljković[1] and Ivana Grković[2]

[1]Department for General Physiology and Biophysics, Faculty of Biology, University of Belgrade, Belgrade, Studentski trg 3, 11001 Belgrade, Serbia and [2]Department of Molecular Biology and Endocrinology, Vinča Institute of Nuclear Sciences, University of Belgrade, Mike Petrovića Alasa 12-14, 11001 Belgrade, Serbia

Abstract

Enzyme histochemistry is a valuable histological method which provides a connection between morphology, activity, and spatial localization of investigated enzymes. Even though the method relies purely on arbitrary evaluations performed by the human eye, it is still wildly accepted and used in histo(patho)logy. Texture analysis emerged as an excellent tool for image quantification of subtle differences reflected in both spatial discrepancies and gray level values of pixels. The current study of texture analysis utilizes the gray-level co-occurrence matrix as a method for quantification of differences between ecto-5′-nucleotidase activities in healthy hippocampal tissue and tissue with marked neurodegeneration. We used the angular second moment, contrast (CON), correlation, inverse difference moment (INV), and entropy for texture analysis and receiver operating characteristic analysis with immunoblot and qualitative assessment of enzyme histochemistry as a validation. Our results strongly argue that co-occurrence matrix analysis could be used for the determination of fine differences in the enzyme activities with the possibility to ascribe those differences to regions or specific cell types. In addition, it emerged that INV and CON are especially useful parameters for this type of enzyme histochemistry analysis. We concluded that texture analysis is a reliable method for quantification of this descriptive technique, thus removing biases and adding it a quantitative dimension.

Key words: ecto-5′-nucleotidase, enzyme histochemistry, gray-level co-occurrence matrix, pathology, texture analysis

(Received 7 November 2018; revised 20 December 2018; accepted 28 December 2018)

Introduction

Enzyme histochemistry is a widely used method in histology and histopathology providing a link between morphology and biochemistry. It is based on the catalytic activity of tissue enzymes, provided with a substrate, in its orthotropic localization (Patrick et al., 1980). Analysis of enzyme histochemistry gives important information on enzyme activity as well as its topographic localization (Meier-Ruge & Bruder, 2008). Visualization of the activity is accomplished using different reagents, which in reaction with the enzyme product forms an insoluble precipitate. One commonly used technique for visualization of different nucleotidase activities is lead-salt precipitation introduced by Wachstein and Meisel (1957). The reaction is based on adding lead(II) nitrate in reaction mix with substrates adenosine triphosphate, diphosphate and monophosphate (ATP, ADP and AMP, respectively) which in turn, upon hydrolysis of nucleotide phosphates, forms insoluble precipitate—lead(II) phosphate. Lead(II) phosphate is visualized with ammonia-sulfide, forming an insoluble black compound of lead(II) sulfide at the site of reaction (Wachstein & Meisel, 1957; Wagner et al., 1972). On the other hand, it has been shown that lead can form a significant amount of lead precipitate even when there are no nucleotides added in the reaction mix, making reactional artifact (Rosenthal et al., 1969) which negates the absolute quantification of this method. The original method has hence seen several modifications (Braun et al., 2003). Specificity testing in knock-out animals (Langer et al., 2008) and comparison of enzyme histochemistry with *in situ* fluorescence (Villamonte et al., 2018) confirmed its validity and specificity, despite reactional artifacts. Thus, enzyme histochemistry is still widely used and represents a valuable addition to classical histology, immunohistochemistry, and histopathology methods (Meier-Ruge & Bruder, 2008; Grkovic et al., 2014; Gampe et al., 2015; Grkovic et al., 2018; Villamonte et al., 2018).

Bearing all these in mind, no valid quantification of enzyme histochemistry has been performed yet, thus making it purely descriptive. On the other hand each image, i.e., micrograph, of enzyme histochemistry possesses unique textural features which could be extracted using statistical texture analysis. In texture analysis, various textural features are computed based on a distribution of different combinations of pixels, each having a specified position relative to each other in the analyzed image (Haralick et al., 1973; Lubner et al., 2015). Gray level co-occurrence matrix (GLCM) is a method which extracts second-order statistical textural features in a matrix where the number of rows and columns are equal to the number of gray levels, G, in certain image. Matrix $P(i, j|\Delta x, \Delta y)$ represents the relative frequency of separation of two pixels with distance $(\Delta x, \Delta y)$, both occurring in a given neighborhood, one having a values of intensity "i" and other with intensity

***Author for correspondence:** Milorad Dragić, E-mail: milorad.dragic@bio.bg.ac.rs

Cite this article: Dragić M, Zarić M, Mitrović N, Nedeljković N, Grković I (2019) Application of Gray Level Co-Occurrence Matrix Analysis as a New Method for Enzyme Histochemistry Quantification. *Microsc Microanal*. doi:10.1017/S1431927618016306

values of "*j*". Other matrix elements $P(i, j|d, \theta)$ contain information about probability values regarding changes between gray levels "*i*" and "*j*" in the context of distance (d) and angle (θ) (Haralick et al., 1973; Mohanaiah et al., 2013). Thus, by comparing the extracted features of two analyzed images, we can acquire information about differences in complexity, homogeneity, and uniformity. Textural analysis was initially used in technological sciences, but in the last two decades many studies applied and demonstrated usefulness of GLCM analysis in cytology, neuroscience, and medicine, especially in radiology (Losa & Castelli, 2005; Kassner & Thornhill, 2010; Kocinski et al., 2012; Pantic et al., 2012; Kim et al., 2015; Tesic et al., 2017). Although it found a wide usage in histology and histopathology (Mostaco-Guidolin et al., 2013; Fatima et al., 2014; Kather et al., 2016; Rajkovic et al., 2016), the applicability and potential of GLCM to enzyme histochemistry has yet to be determined.

Thus, the current study aims to utilize GLCM analysis in the quantification of differences in enzyme pattern activity obtained with enzyme histochemistry on healthy and tissue with pathology. For this purpose, we used a well-established model of hippocampal neurodegeneration, gliosis, and inflammation (Balaban et al., 1988; Geloso et al., 2011; Gasparova et al., 2012) and examined the histochemical activity of ecto-5′-nucleotidase (eN/CD73). Ecto-5′-nucleotidase is a glycosylphosphatidylinositol-anchored protein, with an active site facing the extracellular compartment. The eN is the rate-limiting enzyme for extracellular adenosine formation in the brain (Zimmermann et al., 2012), which in turn, exhibits strong tissue protective and anti-inflammatory actions (Antonioli et al., 2013*b*). It has been shown that the rate of eN activity does not necessarily correlate with the enzyme protein levels, but rather increases or decreases due to changes in kinetic properties and enzyme efficacy (Stanojevic et al., 2011; Mitrovic et al., 2016, 2017; Grkovic et al., 2018). CD73 also functions as a membrane receptor for extracellular matrix molecules and may participate in a control of cell adhesion and migration, in both normal and neoplastic cells (Sadej et al., 2008; Adzic & Nedeljkovic, 2018). The enzyme has a broad tissue distribution, being expressed in many cell types, including a number of tumor cells (Antonioli et al., 2013*a*). Thus, significant up-regulation of eN expression/activity by activated glial cells was demonstrated in several experimental models of human neuropathologies, including ischemia (Braun et al., 1998), temporal lobe epilepsy (Bonan et al., 2000; Bonan, 2012), traumatic brain injury (Nedeljkovic et al., 2006; Bjelobaba et al., 2011), amyotrophic lateral sclerosis (Ganderman et al., 2010), experimental autoimmune encephalomyelitis (Lavrnja et al., 2015), and glioma (Xu et al., 2013). Given that up-regulation of eN represents a common phenomenon in neurodegenerative disorders associated with neuroinflammation, we performed texture analysis as a method for quantification of differences between ecto-5′-nucleotidase activities in healthy hippocampal tissue and tissue with marked neurodegeneration.

Materials and Methods

Ethics Statement

All experimental procedures were approved by the Ethics Committee for the Use of Laboratory Animals of Vinca Institute of Nuclear Sciences, University of Belgrade; Republic of Serbia (Application No. 02/11; 323-07-02057/2017-05) according to the guidelines of the EU registered Serbian Laboratory Animal Science Association (SLASA), a member of the Federation of the European Laboratory Animal Science Associations (FELASA). Care was taken to minimize pain and discomfort of the animals as stated in NIH Guide for Care and Use of Laboratory Animals (1985) and the European Communities Council Directive (86/609/EEC).

Animals and Treatment

The study was performed on 2 month old Wistar female rats (220–250 g) obtained from a local colony of VINČA Institute. Rats were housed (two–three per cage) in 12 h light/dark cycle with free access to food and water. Rats were randomly divided into two experimental groups and injected with a single dose of saline (control, 1 ml/kg, $n = 8$) or TMT (treated group, 8 mg/kg, $n = 8$) i.p. and sacrificed by decapitation (Harvard Apparatus, Holliston, MA, USA) 7 days post-treatment.

Tissue Processing and Enzyme Histochemistry

Brains removed carefully from the skull ($n = 5$ brains/group) were fixed in 4% paraformaldehyde for 24 h and then cryoprotected in graded sucrose (10, 20, and 30% in 0.2 M phosphate buffer). Next, 20 μm thick coronal cryosections of the dorsal hippocampus were made, air-dried for 2 h, and stored at −20°C until use. Enzyme histochemistry for detection of AMPase activity was performed as previously described (Langer et al., 2008; Grkovic et al., 2014; Grkovic et al., 2018). Briefly, cryosections were pre-incubated for 30 min at room temperature in TRIS maleate buffer (50 mM TRIS-maleate, 2 mM levamisole, 2 mM $MgCl_2$, 0.25 M sucrose, pH 7.4). Reaction was then incubated at 37°C for 90 min for AMPase activity in TMS buffer solution [50 mM TRIS-maleate, 3% dextran T250, 0.25 M sucrose, 5 mM $MnCl_2$, 2 mM Pb $(NO_3)_2$, 2 mM $MgCl_2$] containing AMP (Sigma Aldrich, St. Louis, MO, USA) in 2 mM concentration. TMS buffer solution without substrate was used as a control. After color development in 1% (v/v) $(NH4)_2S$, sections were dehydrated in graded ethanol (70, 95, and 100%) washed in 100% xylol and mounted with DPX (Sigma Aldrich, St. Louis, MO, USA).

Relative intensity of histochemical reaction in CA1 field and hilus of dentate gyrus (DG) was assessed by using arbitrary scale which converts apparent histochemical intensity to grades, as follows: very strong (++++), strong (+++), medium (++), weak (+), and absence (−) of the reaction.

Image Processing and GLCM Analysis

High resolution digital images (2,088 × 1,550 pixels) were captured using a LEITZ DM RB light microscope (Leica Mikroskopie & Systems GmbH, Wetzlar, Germany), equipped with a LEICA DFC320 CCD camera (Leica Microsystems Ltd., Heerbrugg, Switzerland) and LEICA DFC Twain Software (Leica, Germany). All images were acquired at 400× magnification and saved in .tiff format. One hundred images (50 control + 50 TMT images) of the CA1 pyramidal region and 100 of the DG hilar region were taken. After conversion into 8-bit (Figs. 1, a1–d1) format, post image processing using the *ImageJ* plugin GLCM analyzer (https://imagej.nih.gov/ij/plugins/texture.html) was performed.

Two first order statistic parameters were calculated for all images [mean gray value (MGV) and integrated density (ID)].

GLCM analysis provides second-order statistics which reflect textural/spatial arrangements of pixels intensities present in the region of interest (ROI). Micrographs of dorsal hippocampus

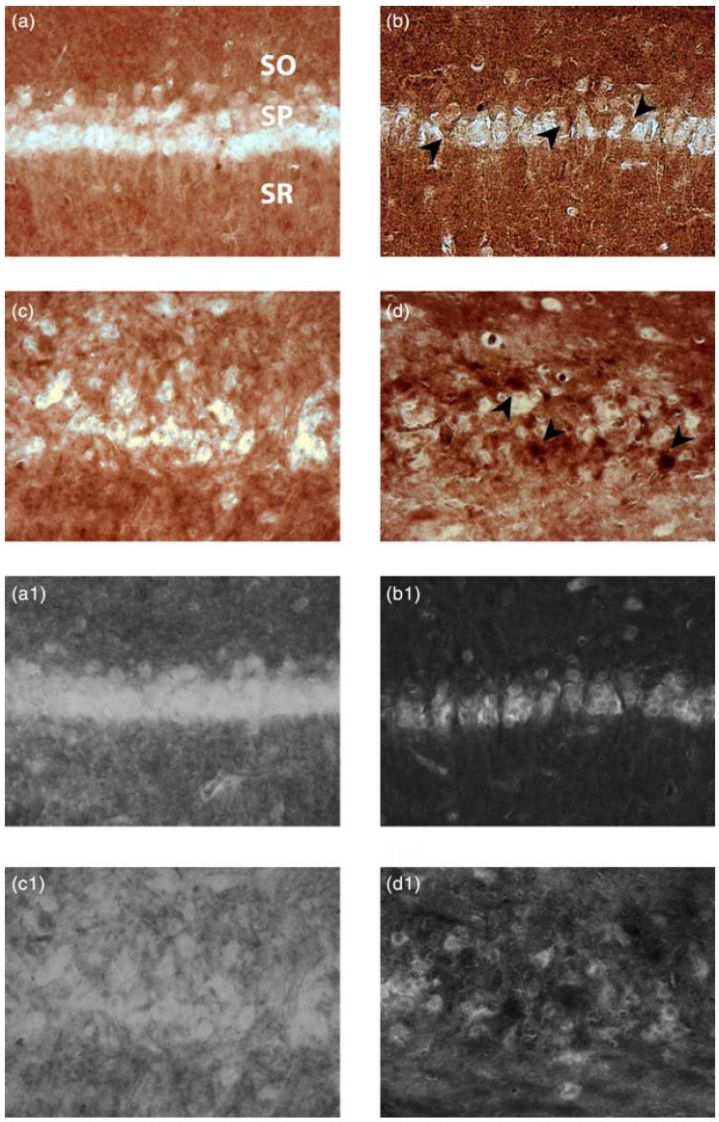

Fig. 1. Ectonucleotidase histochemistry in the presence of AMP in the hippocampal CA1 region (**a, b**) and hilus of DG (**c, d**) of control animals and the animals treated with TMT after 7 days (TMT 7d). Gray-scale images (a1, b1, c1, d1) represent micrographs from which GLCM parameters were extracted. Abbreviations stand for hippocampal layers—stratum oriens (SO), pyramidal cell layer (SP), and stratum radiatum (SR). Scale bar = 50 μm.

taken between 3.12 and 3.84 mm posterior to Bregma were processed and included in analysis. Furthermore, we positioned the camera in such way that pyramidal layer of CA1 region was in the middle of the image, capturing both stratum oriens (SO) and radiatum. Similarly, we have taken images of central region of DG where the hilar portion of CA3 ends and the polymorph layer begins. The hilar region of DG and CA1 region of hippocampus were chosen since those two subfields have different cytoarchitectonic organization, thus allowing us to examine usefulness of GLCM analysis in different patterns and brain regions.

Five parameters were extracted from GLCM. Angular second moment (ASM) measures homogeneity of the image. Using GLCM analyzer five parameters were obtained:

(1) ASM or uniformity measures homogeneity (Sharma et al., 2008) of the image and its calculated based on an equation:

$$\mathrm{ASM} = \sum_i \sum_j \{p(i,j)\}^2$$

where i and j are spatial coordinates of the function p (i, j);

(2) Contrast (CON) measures local variations present in the image (Baraldi & Parmiggiani, 1995) and its calculated based on an equation:

$$\mathrm{CON} = \sum_i \sum_j (i-j)^k p(i,j)^n$$

(3) Correlation (COR) measures gray-tone linear dependencies of adjacent pixels (Haralick et al., 1973) and it is calculated using the formula:

$$\mathrm{COR} = \frac{\sum_i \sum_j (i,j)p(i,j) - \mu_x \mu_y}{\sigma_x \sigma_y}$$

where σ and μ are means of standard deviation of function p (i, j);

(4) Inverse difference moment (INV) measures local homogeneity (Pantic et al., 2014) and its calculated with:

$$\mathrm{INV} = \sum_i \sum_j \frac{1}{1 + (i-j)^2} p(i,j)$$

(5) Entropy (ENT) measures structural disarrangement of image (Baraldi & Parmiggiani, 1995) and its calculated using equation:

$$\mathrm{ENT} = -\sum_i \sum_j p(i,j) \log(p(i,j))$$

The lowest value of ASM is attained when there are no dominant gray levels. CON measures local differences in the image. Highly contrasted regions will have high CON values, whereas more homogeneous regions will have low CON values. COR measures dependence of gray levels between two pixels separated by distance d. Low COR value means that the gray levels are generally independent from one another, or that there is no regular structure in the image. However, if COR is high, there is a high probability that one or several patterns repeat themselves inside the computational window. INV measures local similarities. It is expected to be higher for textures of organized and poorly contrasted features, with only a few gray levels at the same distance d from one another. This parameter quantifies the degree of homogeneity in the ROI. The ENT measures the lack of spatial organization inside the computational window. A high value of ENT corresponds to a rough texture, and a low one to the more homogeneous or smoother texture.

Receiver Operating Characteristic (ROC)

The performance of GLCM analysis used in the current study was evaluated using ROC curve analysis (Metz, 1978; Zweig & Campbell, 1993). The ROC analysis measures the ability of GLCM to quantify differences in a pattern of enzyme histochemical labeling caused by TMT, by discriminating textural information extracted from GLCM that is built upon inter-pixel COR of the original light microscopic image.

Immunoblot Analysis

Seven days after treatment, exposed ($n = 3$) and control ($n = 3$) animals were decapitated and brains were removed carefully from the skull. Entire hippocampus was isolated, homogenized in RIPA buffer (PB supplemented with 150 mM NaCl, 1% Triton X-1000, 0.1% SDS, 0.5% sodium deoxycholate, 10 μg/mL leupeptin, 2 μg/mL aprotinin, 5 mM EDTA, 1 mM EGTA, 5 mM NaF, and 1 mM PMSF) for 10 min at 4°C (3,000 rpm). The supernatant was collected and protein concentration was quantified using bovine serum albumin (BSA) as a standard (Markwell et al., 1978). Western blot analysis was performed as previously described (Grkovic et al., 2014; Grkovic et al., 2018). Briefly, equivalent amounts (30 μg of proteins) were resolved on 8% SDS-PAGE electrophoresis and transferred on polyvinylidene-difluoride membranes (0.45 μm, Millipore, Germany). After blocking in 5% BSA in PBST overnight at 4°C membranes were incubated with primary rabbit anti-rat eN antibody (1:2,000 dilution in 2.5% BSA in PBST, Cell Signaling, USA). The support membranes were re-probed with goat anti-rat β-actin antibody (1:500; Santa Cruz Biotechnology, CA, USA) used as a loading control. Visualization was performed on X-ray films (AGFA HealthCare NV, Mortsel, Belgium), using chemiluminescence (Immobilon Western Chemiluminescent HRP substrate, Millipore, Germany), after incubation in anti-rabbit or donkey anti-goat HRP conjugated IgG antibody (1:10,000 dilution; Santa Cruz Biotechnology, CA, USA). Scanned bands were transferred into a computer using a laser scanner and quantified by integrating band areas using ImageJ. The optical density of eN bands was normalized to the optical density of β-actin band from the same lane. Quantified data were expressed relative to the mean density obtained for the control. The results acquired from six separate measurements isolated from three animals are expressed as mean ± SEM.

Table 1. Enzyme Histochemistry of Ecto-5′-nucleotidase.

AMPase Activity		
Hippocampal Layer	Control	TMT 7d
CA1 region		
SO	++	++++
SP	–	++
SR	+	+++
Hilus of DG	+	+++

Data Analysis

All results are presented as mean ± SEM. For statistical comparison between experimental groups a Student's t test was performed and a value of $p < 0.05$ or less was considered significant. Statistical analysis and ROC curve analysis were performed using the GraphPad Prism 6 software package (San Diego, CA, USA).

Results

Enzyme Histochemistry

Ectonucleotidase histochemical analyses have been performed as previously described (Langer et al., 2008; Grkovic et al., 2014; Grkovic et al., 2018) in the presence of AMP as substrates and with the addition of lead nitrate, which resulted in a deposition of the reaction product (Fig. 1). Coronal sections obtained from control (Figs. 1a, 1c) and TMT-treated (Figs. b, d) animals have been processed, examined under the microscope, and photographed. Fifty digital images per each experimental group were collected and stored in .tiff format for further analyses. A predefined ROI within the CA1 hippocampal field (Figs. 1a, 1b) and the hilar region of DG (Figs. 1c, 1d) at each section was subjected to relative quantification analysis and image texture analyses, based on first-order (mean gray and ID) and second-order statistics (ASM, CON, COR, INV, and ENT).

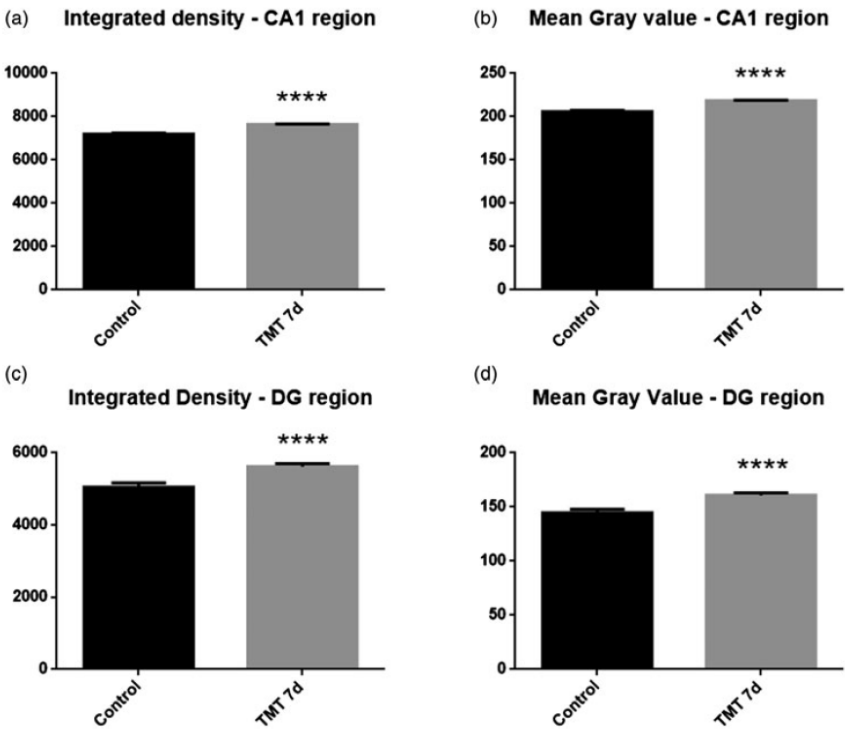

Fig. 2. ID (**a, c**) and MGV (**b, d**) for the CA1 region and hilus of DG. Significance shown inside the graphs: $^{*}p < 0.05$, $^{**}p < 0.01$, $^{***}p < 0.001$, $^{****}p < 0.0001$ or less and with respect to control.

Relative Intensity of Histochemical Reactions

Original images were carefully inspected and the intensities of histochemical reactions in CA1 layers were determined by an examiner unaware of the treatment, by using arbitrary scale as follows: very strong (++++), strong (+++), medium (++), weak (+), and absence (–) of the reaction (Table 1).

The overall intensity of histochemical reaction obtained with AMP was relatively high in control CA1, however for the most part it could not be assigned to individual cell types. Strong deposition of the reaction product has been obtained in the parenchyma of SO and stratum radiatum (SR), while stratum pyramidale (SP) was completely spared (Fig. 1a). On TMT sections, the overall intensity of histochemical reaction increased in SO and SR (Fig. 1b) and a certain level of staining was observed in SP, which could be assigned to glial cells (Fig. 1b, arrows). A similar pattern was noticed in DG. With regard to CA1 region of control sections, less intense staining was mostly limited to neuropil, clearly delineating neurons (Fig. 1c). Occasional glial cells could be detected as local deposition of reaction product. After TMT exposure, overall stronger intensity of labeling, especially depicting individual cells was observed (Fig. 1d).

Integrated Density and Mean Gray Value Measurements

The MGV quantifies the sum of all gray values of pixels selected in specific area divided by their number, while the ID is product of MGV and area (Fig. 2). ID of the CA1 region (Fig. 2a) is increased after TMT injection ($7{,}634 \pm 25.15$, $p < 0.0001$) compared to the control ($7{,}191 \pm 53.88$). MGV of the CA1 region (Fig. 2b) is also increased after intoxication (218.4 ± 0.72, $p < 0.0001$) compared to the control group (205.7 ± 1.542). In DG a similar trend was observed as ID (Fig. 2c) increased after treatment ($5{,}616 \pm 84.82$, $p < 0.001$) compared to the control ($5{,}053 \pm 114.9$) and MGV (Fig. 2d) showed an increase (160.7 ± 2.43, $p < 0.0001$) compared to the control (144.6 ± 3.28).

Gray Level Co-Occurrence Matrix Analysis

AMPase histochemistry in two examined regions of the hippocampus revealed marked differences in GLCM parameters between the control and TMT treated animals (Figs. 3 and 4). Parameters that represent tissue uniformity, ASM and INV, were significantly higher in TMT-exposed animals compared to control groups (Table 2) for both regions. Parameters measuring tissue heterogeneity, CON and ENT, decreased after TMT intoxication in both regions. Higher values for ASM and INV point to changes in tissue texture as a consequence of increased staining toward more homogeneous in the CA1 region as well as in DG, after TMT injection. On the other hand, decrease of ENT and CON values is expected, since increase in homogeneity will consequently lead toward decrease of image irregularity. COR increased only in the CA1 region after intoxication, while no changes are observed in DG.

ROC Curve Analysis of GLCM Parameters for CA1 Hippocampal Region

In order to access the discriminator ability of five GLCM parameters applied in this study, ROC curve analysis was performed.

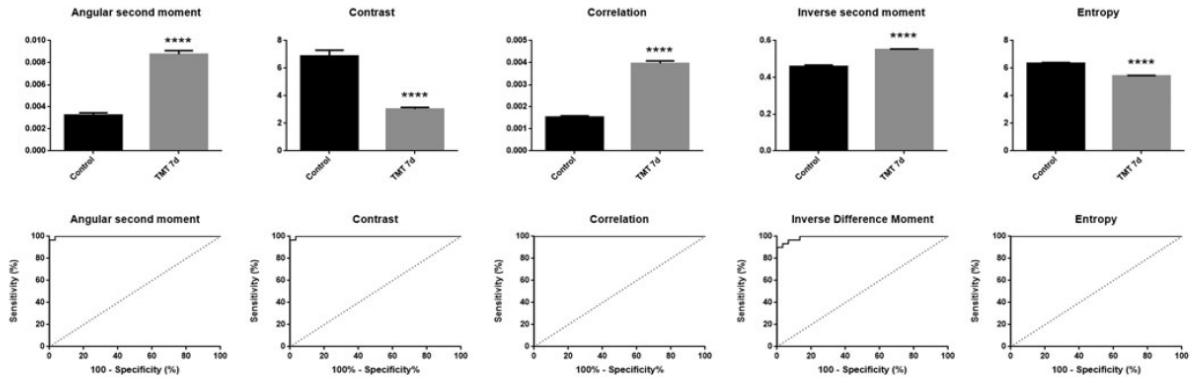

Fig. 3. Comparison of GLCM parameters and ROC analysis for the corresponding parameter for AMPase histochemistry of the CA1 hippocampal region. Significance shown inside the graphs: $*p < 0.05$, $**p < 0.01$, $***p < 0.001$, $****p < 0.0001$ or less and with respect to control.

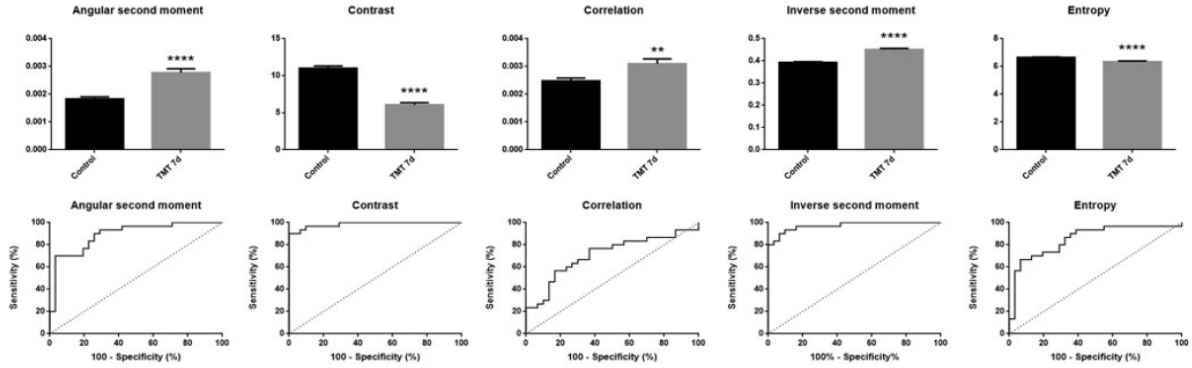

Fig. 4. Comparison of GLCM parameters and ROC analysis for the corresponding parameter for AMPase histochemistry of DG. Significance shown inside the graphs: $*p < 0.05$, $**p < 0.01$, $***p < 0.001$, $****p < 0.0001$ or less and with respect to control.

The area under the curve for ASM was 0.99 with sensitivity and specificity both being 100% for cut-off value ASM > 0.00547. Area of the ROC curve for CON was 0.99, while sensitivity and specificity were 100 and 96.67%, respectively. COR showed maximal values for area under the curve of 1.00, which reflected in sensitivity and specificity, both being 100% for criterion being COR > 0.00274. INV had area under the ROC curve of 0.99 while specificity was 100% and sensitivity 86.67% for the cut-off point being set at INV > 0.5188. Finally, ENT showed a maximal value under the ROC curve with also maximal values for both specificity and sensitivity of 100% for criterion ENT < 5.389 (Fig. 3).

ROC Curve Analysis of GLCM Parameters for Dentate Gyrus

The area under the curve for ASM was 0.89 with specificity and sensitivity being 90 and 74.19%, respectively, for criterion set at ASM > 0.00201. CON showed higher values and the curve of 0.98 with a specificity of 96.67% and a sensitivity of 90.32% for cut-off value set at CON < 9.286. COR revealed itself as poor discriminatory parameter as its value under the curve was 0.68 with a specificity and a sensitivity of only 76.67 and 61.29%, respectively, when the criterion was COR > 0.0025. On the other hand, INV showed an almost maximal value of 0.97 with a specificity of 90% and a sensitivity being 93.55% for cut-off value of INV > 0.419. Finally, the ENT had ROC curve area of 0.85, with a specificity and sensitivity being 90 and 64.52% for ENT < 6.625 (Fig. 4).

Results of Immunoblot Analysis

Since we observed an increase in AMPase product deposition after intoxication, we used western blot analysis for determining whether TMT caused changes in protein expression of ecto-5′-nucleotidase. Seven days post-exposure, immunoblot analysis showed an increase in protein abundance (165.92% ± 2.32%, $p < 0.01$) compared to the control (Fig. 5).

Discussion

Enzyme histochemistry is a valuable experimental and resourceful histopathological method, as it provides simultaneous information about function and spatial localization of the enzyme activity. However, without reliable quantification, the method relies on arbitrary evaluation of alterations induced by pathology that are apparent to the human eye. In recent years, texture analysis has been proved to be an excellent method for image analysis in number of imaging techniques, especially in medicine (Tixier et al.,

Table 2. Parameters of Image Texture Analysis of Hippocampus.

AMPase Activity		Image Texture Analysis				
Groups		ASM	CON	COR	INV	ENT
CA1	Control	0.00328 ± 0.0002	6.885 ± 0.4192	0.00152 ± 0.000058	0.4595 ± 0.007	6.357 ± 0.0503
	TMT 7d	0.00876 ± 0.0003	3.035 ± 0.1184	0.00396 ± 0.000117	0.5512 ± 0.003	5.444 ± 0.0318
	t	13.89	8.838	18.50	11.13	15.35
	p	<0.0001	<0.0001	<0.0001	<0.0001	<0.0001
DG	Control	0.00183 ± 0.00007	11.01 ± 0.3098	0.00248 ± 0.00099	0.3937 ± 0.002	6.653 ± 0.0312
	TMT 7d	0.00277 ± 0.00013	6.084 ± 0.2759	0.00309 ± 0.00017	0.4514 ± 0.005	6.345 ± 0.0465
	t	6.05	11.86	3.05	9.96	5.52
	p	<0.0001	<0.0001	<0.01	<0.0001	<0.0001

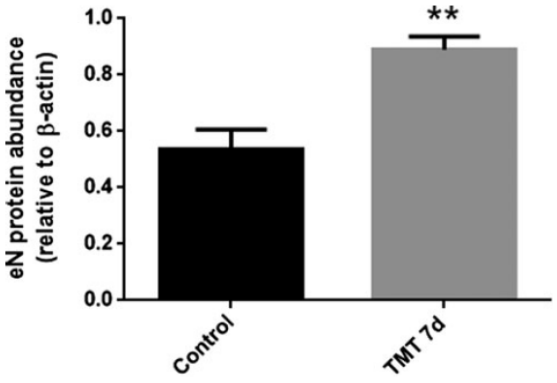

Fig. 5. Ecto-5′-nucleotidase relative protein expression. Bars represent mean protein abundance relative to β-actin ± SEM, from $n = 6$ separate determinations from three separate isolations (2–3 brains/group/isolation). Significance shown inside the graphs: $^{*}p < 0.05$, $^{**}p < 0.01$ or less and with respect to control.

2012; Kim et al., 2015; Lubner et al., 2015), as it offers both statistically valid quantification and describes image properties which are usually imperceptible to the human eye.

The current study demonstrates usage of GLCM analysis as a method for quantification of differences between activities of ecto-5′-nucleotidase in healthy hippocampal tissue and tissue with neurodegeneration. Validity of the applied method was evaluated, using ROC analysis and immunoblot analysis. Also, qualitative analysis of AMPase activity, using arbitrary intensity scale was performed independently. Since all images were captured under the same conditions, we calculated two first order statistic parameters—MGV and ID to establish that observed changes in staining intensity originate from increased deposition of lead at the site of reaction. Indeed, after TMT intoxication increase in MGV and ID points to increase in the number of dark pixels as a result of increased AMPase activity.

GLCM analysis could provide further analysis of specific changes in image texture which then could be interpreted in light of regional or cellular AMPase activity. Ecto-5′-nucleotidase is associated with astrocytes and synapse-rich hippocampal layers, especially SO and SR, thus resulting in relatively uniform staining of whole layers (Stanojevic et al., 2011; Mitrovic et al., 2016; Grkovic et al., 2018). After TMT intoxication, AMPase staining depicted fine processes and bodies of glial cells infiltrating the pyramidal CA1 layer and the hilar region of DG. TMT induces loss of pyramidal neurons and synapses (Balaban et al., 1988; Geloso et al., 2011; Gasparova et al., 2012) followed by reactive astrogliosis and microgliosis (Koczyk & Oderfeld-Nowak, 2000), which results in overall increase in AMPase staining observed in both regions. When considering GLCM parameters, all five indicated in that TMT-exposed tissue homogeneity of the staining is much pronounced. When adjacent pixels display high similarity, the high values of ASM are expected. Since glial cells with marked AMPase activity infiltrate the pyramidal layers and the hilar region of DG, difference between neighboring pixels is decreased, resulting in post-exposure augmentation of ASM. Similarly, when local gray values are uniform, INV values will be increased. Glial cells, by covering the pyramidal layer and increasing AMPase activity in neuropil of DG, balanced local gray values causing an increase of INV. On the other hand, CON measures the difference between highest and the lowest values of a contiguous set of pixels, i.e., amount of local variations present in the image (Haralick et al., 1973). Glia-infiltrated the pyramidal layer of the CA1 region and increased neuropil staining of DG, depicting individual cells which reduced differences between lowest and highest gray values, resulting in CON decrease. ENT measures structural disarrangement of the image or its complexity (Mohanaiah et al., 2013), hence high value of this parameter indicates textural heterogeneity. TMT decreases ENT values suggesting that overall increase in AMPase activity made tissue more homogeneous due to increase in expression and/or activity of eN in both glial cells and remaining synapses. Furthermore, post-intoxication increase in COR values corroborates image homogeneity due to increase in AMPase activity on synapses and glial cells, as COR measures gray-linear dependency of adjacent pixels (Stankovic et al., 2016). ROC analysis demonstrated high discriminatory power of GLCM parameters (Metz, 1978; Zweig & Campbell, 1993; Pantic et al., 2014), but since two analyzed regions have different patterns of AMPase activity we postulate that CON and INV are especially useful in analyzing this type of enzyme histochemistry. CON is a more globally oriented parameter, while inversion second moment gives information of local changes, especially useful when there are specific changes in enzyme activity on a specific cell type or part of a structure. Immunoblot analysis confirmed increase in protein expression of eN, but it should be noted that

besides changes in quantity, catalytic activity of enzyme could change, probably resulting in more AMP to adenosine conversion (Grkovic et al., 2014; Adzic & Nedeljkovic, 2018).

Conclusion

In summary, we demonstrated that GLCM analysis could be used as a tool for quantifying differences in enzyme histochemistry, with high sensitivity and discriminatory powers. Integration of this method, especially in assessment of enzyme activity in pathology could remove all biases from research and add a dimension of quantity to purely qualitative method.

Acknowledgment. The study was entirely supported by the Ministry of Education, Science and Technological Development of the Republic of Serbia Nos. III41014 and OI173044.

References

Adzic M & Nedeljkovic N (2018). Unveiling the role of ecto-5′-nucleotidase/CD73 in astrocyte migration by using pharmacological tools. *Front Pharmacol* **9**, 153.

Antonioli L, Blandizzi C, Pacher P & Hasko G (2013*a*). Immunity, inflammation and cancer: A leading role for adenosine. *Nat Rev Cancer* **13**, 842–857.

Antonioli L, Pacher P, Vizi ES & Hasko G (2013*b*). CD39 and CD73 in immunity and inflammation. *Trends Mol Med* **19**, 355–367.

Balaban CD, O'Callaghan JP & Billingsley ML (1988). Trimethyltin-induced neuronal damage in the rat brain: Comparative studies using silver degeneration stains, immunocytochemistry and immunoassay for neuronotypic and gliotypic proteins. *Neuroscience* **26**, 337–361.

Baraldi A & Parmiggiani F (1995). An investigation of the textural characteristics associated with gray level cooccurrence matrix statistical parameters. *IEEE Trans Geosci Remote Sens* **33**, 293–304.

Bjelobaba I, Parabucki A, Lavrnja I, Stojkov D, Dacic S, Pekovic S, Rakic L, Stojiljkovic M & Nedeljkovic N (2011). Dynamic changes in the expression pattern of ecto-5′-nucleotidase in the rat model of cortical stab injury. *J Neurosci Res* **89**, 862–873.

Bonan CD (2012). Ectonucleotidases and nucleotide/nucleoside transporters as pharmacological targets for neurological disorders. *CNS Neurol Disord Drug Targets* **11**, 739–750.

Bonan CD, Walz R, Pereira GS, Worm PV, Battastini AM, Cavalheiro EA, Izquierdo I & Sarkis JJ (2000). Changes in synaptosomal ectonucleotidase activities in two rat models of temporal lobe epilepsy. *Epilepsy Res* **39**, 229–238.

Braun N, Zhu Y, Krieglstein J, Culmsee C & Zimmermann H (1998). Upregulation of the Enzyme Chain Hydrolyzing Extracellular ATP after Transient Forebrain Ischemia in the Rat. *Journal of Neuroscience* **18**, 4891–4900.

Fatima K, Arooj A & Majeed H (2014). A new texture and shape based technique for improving meningioma classification. *Microsc Res Tech* **77**, 862–873.

Gampe K, Stefani J, Hammer K, Brendel P, Potzsch A, Enikolopov G, Enjyoji K, Acker-Palmer A, Robson SC & Zimmermann H (2015). NTPDase2 and purinergic signaling control progenitor cell proliferation in neurogenic niches of the adult mouse brain. *Stem Cells* **33**, 253–264.

Ganderman M, Peluffo H, Beckman JS, Cassina P & Barbeito L (2010). Extracellular ATP and the P2X7 receptor in astrocyte-mediated motor neuron death: Implications for amyotrophic lateral sclerosis. *J Neuroinflammation* **7**, 33.

Gasparova Z, Janega P, Stara V & Ujhazy E (2012). Early and late stage of neurodegeneration induced by trimethyltin in hippocampus and cortex of male Wistar rats. *Neuro Endocrinol Lett* **33**, 689–696.

Geloso MC, Corvino V & Michetti F (2011). Trimethyltin-induced hippocampal degeneration as a tool to investigate neurodegenerative processes. *Neurochem Int* **58**, 729–738.

Grkovic I, Bjelobaba I, Nedeljkovic N, Mitrovic N, Drakulic D, Stanojlovic M & Horvat A (2014). Developmental increase in ecto-5′-nucleotidase activity overlaps with appearance of two immunologically distinct enzyme isoforms in rat hippocampal synaptic plasma membranes. *J Mol Neurosci* **54**, 109–118.

Grkovic I, Mitrovic N, Dragic M, Adzic M, Drakulic D & Nedeljkovic N (2018). Spatial distribution and expression of ectonucleotidases in rat hippocampus after removal of ovaries and estradiol replacement. *Mol Neurobiol*. doi: 10.1007/s12035-018-1217-3.

Haralick R, Shanmugam K & Dinstein I (1973). Textural features for image classification. *IEEE Trans Syst Man Cybern* **SMC-3**, 610–621.

Kassner A & Thornhill RE (2010). Texture analysis: A review of neurologic MR imaging applications. *AJNR Am J Neuroradiol* **31**, 809–816.

Kather JN, Weis CA, Bianconi F, Melchers SM, Schad LR, Gaiser T, Marx A & Zollner FG (2016). Multi-class texture analysis in colorectal cancer histology. *Sci Rep* **6**, 27988.

Kim SY, Kim EK, Moon HJ, Yoon JH & Kwak JY (2015). Application of texture analysis in the differential diagnosis of benign and malignant thyroid nodules: Comparison with gray-scale ultrasound and elastography. *AJR Am J Roentgenol* **205**, W343–W351.

Kocinski M, Klepaczko A, Materka A, Chekenya M & Lundervold A (2012). 3D image texture analysis of simulated and real-world vascular trees. *Comput Methods Programs Biomed* **107**, 140–154.

Koczyk D & Oderfeld-Nowak B (2000). Long-term microglial and astroglial activation in the hippocampus of trimethyltin-intoxicated rat: Stimulation of NGF and TrkA immunoreactivities in astroglia but not in microglia. *Int J Dev Neurosci* **18**, 591–606.

Langer D, Hammer K, Koszalka P, Schrader J, Robson S & Zimmermann H (2008). Distribution of ectonucleotidases in the rodent brain revisited. *Cell Tissue Res* **334**, 199–217.

Lavrnja I, Laketa D, Savic D, Bozic I, Bjelobaba I, Pekovic S & Nedeljkovic N (2015). Expression of a second ecto-5′-nucleotidase variant besides the usual protein in symptomatic phase of experimental autoimmune encephalomyelitis. *J Mol Neurosci* **55**, 898–911.

Losa GA & Castelli C (2005). Nuclear patterns of human breast cancer cells during apoptosis: Characterisation by fractal dimension and co-occurrence matrix statistics. *Cell Tissue Res* **322**, 257–267.

Lubner MG, Stabo N, Lubner SJ, Del Rio AM, Song C, Halberg RB & Pickhardt PJ (2015). CT textural analysis of hepatic metastatic colorectal cancer: Pre-treatment tumor heterogeneity correlates with pathology and clinical outcomes. *Abdom Imaging* **40**, 2331–2337.

Markwell MA, Haas SM, Bieber LL & Tolbert NE (1978). A modification of the Lowry procedure to simplify protein determination in membrane and lipoprotein samples. *Anal Biochem* **87**, 206–210.

Meier-Ruge WA & Bruder E (2008). Current concepts of enzyme histochemistry in modern pathology. *Pathobiology* **75**, 233–243.

Metz CE (1978). Basic principles of ROC analysis. *Semin Nucl Med* **8**, 283–298.

Mitrovic N, Zaric M, Drakulic D, Martinovic J, Sevigny J, Stanojlovic M, Nedeljkovic N & Grkovic I (2017). 17beta-Estradiol-induced synaptic rearrangements are accompanied by altered ectonucleotidase activities in male rat hippocampal synaptosomes. *J Mol Neurosci MN* **61**(3), 412–422.

Mitrovic N, Zaric M, Drakulic D, Martinovic J, Stanojlovic M, Sevigny J, Horvat A, Nedeljkovic N & Grkovic I (2016). 17beta-Estradiol upregulates ecto-5′-nucleotidase (CD73) in hippocampal synaptosomes of female rats through action mediated by estrogen receptor-alpha and -beta. *Neuroscience* **324**, 286–296.

Mohanaiah P, Sathyanaravana P & Gurukumar L (2013). Image texture feature extraction using GLCM approach. *Int J Sci Res Publ* **3**.

Mostaco-Guidolin LB, Ko AC, Wang F, Xiang B, Hewko M, Tian G, Major A, Shiomi M & Sowa MG (2013). Collagen morphology and texture analysis: From statistics to classification. *Sci Rep* **3**, 2190.

Nedeljkovic N, Bjelobaba I, Subasic S, Lavrnja I, Pekovic S, Stojkov D, Vjestica A, Rakic L & Stojiljkovic M (2006). Up-regulation of ectonucleotidase activity after cortical stab injury in rats. *Cell Biol Int* **30**, 541–546.

Pantic I, Dacic S, Brkic P, Lavrnja I, Pantic S, Jovanovic T & Pekovic S (2014). Application of fractal and grey level co-occurrence matrix analysis in evaluation of brain corpus callosum and cingulum architecture. *Microsc Microanal* **20**, 1373–1381.

Pantic I, Pantic S & Basta-Jovanovic G (2012). Gray level co-occurrence matrix texture analysis of germinal center light zone lymphocyte nuclei: Physiology viewpoint with focus on apoptosis. *Microsc Microanal* **18**, 470–475.

Patrick WJ, Besley GT & Smith II (1980). Histochemical diagnosis of Hirschsprung's disease and a comparison of the histochemical and biochemical activity of acetylcholinesterase in rectal mucosal biopsies. *J Clin Pathol* **33**, 336–343.

Rajkovic N, Kolarevic D, Kanjer K, Milosevic NT, Nikolic-Vukosavljevic D & Radulovic M (2016). Comparison of monofractal, multifractal and gray level Co-occurrence matrix algorithms in analysis of breast tumor microscopic images for prognosis of distant metastasis risk. *Biomed Microdevices* **18**, 83.

Rosenthal AS, Moses HL, Ganote CE & Tice L (1969). The participation of nucleotide in the formation of phosphatase reaction product: A chemical and electron microscope autoradiographic study. *J Histochem Cytochem* **17**, 839–847.

Sadej R, Inai K, Rajfur Z, Ostapkowicz A, Kohler J, Skladanowski AC, Mitchell BS & Spychala J (2008). Tenascin C interacts with ecto-5′-nucleotidase (eN) and regulates adenosine generation in cancer cells. *Biochem Biophys Acta* **1782**, 35–40.

Sharma N, Ray AK, Sharma S, Shukla KK, Pradhan S & Aggarwal LM (2008). Segmentation and classification of medical images using texture-primitive features: Application of BAM-type artificial neural network. *J Med Phys* **33**, 119–126.

Stankovic M, Pantic I, DE Luka SR, Puskas N, Zaletel I, Milutinovic-Smiljanic S, Pantic S & Trbovich AM (2016). Quantification of structural changes in acute inflammation by fractal dimension, angular second moment and correlation. *J Microsc* **261**, 277–284.

Stanojevic I, Bjelobaba I, Nedeljkovic N, Drakulic D, Petrovic S, Stojiljkovic M & Horvat A (2011). Ontogenetic profile of ecto-5′-nucleotidase in rat brain synaptic plasma membranes. *Int J Dev Neurosci* **29**, 397–403.

Tesic V, Perovic M, Zaletel I, Jovanovic M, Puskas N, Ruzdijic S & Kanazir S (2017). A single high dose of dexamethasone increases GAP-43 and synaptophysin in the hippocampus of aged rats. *Exp Gerontol* **98**, 62–68.

Tixier F, Hatt M, Le Rest CC, Le Pogam A, Corcos L & Visvikis D (2012). Reproducibility of tumor uptake heterogeneity characterization through textural feature analysis in 18F-FDG PET. *J Nucl Med* **53**, 693–700.

Villamonte ML, Torrejon-Escribano B, Rodriguez-Martinez A, Trapero C, Vidal A, Gomez De Aranda I, Sevigny J, Matias-Guiu X & Martin-Satue M (2018). Characterization of ecto-nucleotidases in human oviducts with an improved approach simultaneously identifying protein expression and *in situ* enzyme activity. *Histochem Cell Biol* **149**, 269–276.

Wachstein M & Meisel E (1957). Histochemistry of hepatic phosphatases of a physiologic pH; with special reference to the demonstration of bile canaliculi. *Am J Clin Pathol* **27**, 13–23.

Wagner RC, Kreiner P, Barrnett RJ & Bitensky MW (1972). Biochemical characterization and cytochemical localization of a catecholamine-sensitive adenylate cyclase in isolated capillary endothelium. *Proc Natl Acad Sci USA* **69**, 3175–3179.

Xu S, Shao QQ, Sun JT, Yang N, Xie Q, Wang DH, Huang QB, Huang B, Wang XY, Li XG & Qu X (2013). Synergy between the ectoenzymes CD39 and CD73 contributes to adenosinergic immunosuppression in human malignant gliomas. *Neuro Oncol* **15**, 1160–1172.

Zimmermann H, Zebisch M & Strater N (2012). Cellular function and molecular structure of ecto-nucleotidases. *Purinergic Signal* **8**, 437–502.

Zweig MH & Campbell G (1993). Receiver-operating characteristic (ROC) plots: A fundamental evaluation tool in clinical medicine. *Clin Chem* **39**, 561–577.

ASN American Society for Neurochemistry

ASN Neuro
Volume 13: 1–18

DOI: 10.1177/17590914211044882
journals.sagepub.com/home/asn
SAGE

Microglial- and Astrocyte-Specific Expression of Purinergic Signaling Components and Inflammatory Mediators in the Rat Hippocampus During Trimethyltin-Induced Neurodegeneration

Milorad Dragić[1], Nataša Mitrović[2], Marija Adžić[1,3], Nadežda Nedeljković[1], and Ivana Grković[2]

Abstract

The present study examined the involvement of purinergic signaling components in the rat model of hippocampal degeneration induced by trimethyltin (TMT) intoxication (8 mg/kg, single intraperitoneal injection), which results in behavioral and neurological dysfunction similar to neurodegenerative disorders. We investigated spatial and temporal patterns of ecto-nucleoside triphosphate diphosphohydrolase 1 (NTPDase1/CD39) and ecto-5′ nucleotidase (eN/CD73) activity, their cell-specific localization, and analyzed gene expression pattern and/or cellular localization of purinoreceptors and proinflammatory mediators associated with reactive glial cells. Our study demonstrated that all Iba1+ cells at the injured area, irrespective of their morphology, upregulated NTPDase1/CD39, while induction of eN/CD73 has been observed at amoeboid Iba1+ cells localized within the hippocampal neuronal layers with pronounced cell death. Marked induction of $P2Y_{12}R$, $P2Y_6R$, and $P2X_4$-messenger RNA at the early stage of TMT-induced neurodegeneration might reflect the functional properties, migration, and chemotaxis of microglia, while induction of $P2X_7R$ at amoeboid cells probably modulates their phagocytic role. Reactive astrocytes expressed adenosine A_1, A_{2A}, and $P2Y_1$ receptors, revealed induction of complement component C3, inducible nitric oxide synthase, nuclear factor-kB, and proinflammatory cytokines at the late stage of TMT-induced neurodegeneration. An increased set of purinergic system components on activated microglia (NTPDase1/CD39, eN/CD73, and $P2X_7$) and astrocytes (A_1R, $A_{2A}R$, and $P2Y_1$), and loss of homeostatic glial and neuronal purinergic pathways ($P2Y_{12}$ and A_1R) may shift purinergic signaling balance toward excitotoxicity and inflammation, thus favoring progression of pathological events. These findings may contribute to a better understanding of the involvement of purinergic signaling components in the progression of neurodegenerative disorders that could be target molecules for the development of novel therapies.

Keywords

astrocyte-derived inflammation, eN/CD73, hippocampal neurodegeneration, microglial polarization, NTPDase1/CD39, purinergic receptors

Received May 19, 2021; Revised August 18, 2021; Accepted for publication August 20, 2021

Introduction

Neurotoxicants, such as trimethyltin (TMT)-chloride, have been reported as risk factors for the development of neurodegenerative disorders (Kotake, 2012; Pompili et al., 2020; Yegambaram et al., 2015). In rats, TMT selectively targets the limbic region, particularly the hippocampus, with a similar pattern as observed in humans and with comparable behavioral alterations (Corvino et al., 2013, 2015; Ferraz da Silva et al., 2017; Geloso et al., 2011; Haga et al., 2002; Lattanzi et al., 2013; Lee et al., 2016; Trabucco et al., 2009). TMT-induced neurodegeneration in rats is characterized by early astrocyte

[1]Department for General Physiology and Biophysics, Faculty of Biology, University of Belgrade, Belgrade, Serbia
[2]Department of Molecular Biology and Endocrinology, VINČA Institute of Nuclear Sciences-National Institute of the Republic of Serbia, University of Belgrade, Belgrade, Serbia
[3]Center for Laser Microscopy, Faculty of Biology, University of Belgrade, Belgrade, Serbia

Corresponding Author:
Ivana Grković, Department of Molecular Biology and Endocrinology, VINČA Institute of Nuclear Sciences - National Institute of the Republic of Serbia, University of Belgrade, Mike Petrovića Alasa 12-14, P.O.Box 522-090 11000 Belgrade, Serbia.
Email: istanojevic@vin.bg.ac.rs; istanojevic@gmail.com

activation followed by sustained astrogliosis, the response of resident microglial to hippocampal neuronal loss that progressively worsens over 3 weeks (Dragic et al., 2019b, 2021; Haga et al., 2002; Little et al., 2002, 2012), as well as a cognitive deficit in various tasks similar to human neurodegenerative disorders such as Alzheimer's disease and temporal lobe epilepsy (Chvojkova et al., 2021; Corvino et al., 2013; Geloso et al., 2011; Lattanzi et al., 2013; Lee et al., 2016; Pompili et al., 2020; Trabucco et al., 2009; Ye et al., 2020). Thus, TMT neurotoxicity is a valuable tool for studying changes in molecular signatures of glial cells during the progression of neurodegeneration that accompanies hippocampal dysfunction.

In general, glial cells, microglia, and astrocytes are crucial in monitoring, maintaining, and preserving the metabolic and structural integrity of the central nervous system (CNS), and respond to noxious stimuli and insults to the brain. Alterations in CNS homeostasis immediately lead to changes in microglial cells morphology and functional polarization toward one of the two complex phenotypes, detrimental that release proinflammatory cytokines and reactive oxygen species (ROS) and reactive nitrogen species or prorepair, an antiinflammatory phenotype that express molecular markers such as arginase-1 (Arg1) (Illes et al., 2020; Zabel & Kirsch, 2013), with a full repertoire of transitional states between them. In response to brain injury, astrocytes assume reactive states that may be discriminated based on the proliferation and induction of proinflammatory mediators and ROS (Verkhratsky et al., 2014). Furthermore, different polarized states of reactive astrocytes are characterized, determined as dominantly harmful, a proinflammatory type that might releases the neurotoxic complement C3 directly leading to neuron death, and the dominantly neuroprotective type (Liddelow & Barres, 2017), but also with the repertoire of transitional microenvironment-dependent states.

Communication between astrocytes, microglia, and degenerating neurons is mediated via different signaling molecules, and one of the strongest is adenosine triphosphate (ATP) (Sperlagh & Illes, 2007). A large amount of extracellular ATP, released from injured neurons and activated glial cells, acts as a "danger signal" and activates specific ligand-gated P2X channels and G-protein-coupled P2Y receptors (Burnstock, 2017; Di Virgilio et al., 2009; Sperlagh & Illes, 2007), promoting microglial chemotaxis and phagocytosis as well as the release of proinflammatory cytokines (Bernier et al., 2013; Franke et al., 2012; Haynes et al., 2006; Illes et al., 2020). Enzymes responsible for calibrating the duration, and degree of P2 receptor activation are functionally coupled membrane-bound ectonucleotidases named ecto-nucleoside triphosphate diphosphohydrolase 1 (NTPDase1/CD39) and ecto-5′ nucleotidase (eN/CD73) that rapidly hydrolyze ATP to adenosine (Grkovic et al., 2019a; Matyash et al., 2017; Zimmermann et al., 2012). NTPDase1/CD39 is dominantly expressed at microglia and endothelial cells and hydrolyzes ATP and adenosine diphosphate (ADP) to adenosine monophosphate (AMP) (Braun et al., 2000; Grkovic et al., 2019b; Matyash et al., 2017; Robson et al., 2006; Zimmermann et al., 2012). The resulting AMP is hydrolyzed to adenosine by eN/CD73, widely expressed in the hippocampus (Grkovic et al., 2019a, 2019b; Zimmermann et al., 2012). Adenosine G-protein-coupled receptors (A_1R, $A_{2A}R$, $A_{2B}R$, and A_3R) mediate modulatory effects of adenosine in an inflammatory environment (Hasko & Cronstein, 2013; Nedeljkovic, 2019). The two ectonucleotidases act together as an immune checkpoint since they determine the ATP/adenosine ratio and the inflammatory status of the tissue. Therefore, an altered function of NTPDase1/CD39 and eN/CD73 and dysregulation of the purinergic signaling are largely implicated in the pathophysiology of several neurological diseases, including Alzheimer's and Parkinson disease, multiple sclerosis, and astroglioma (Burnstock, 2017), but their cell-specific localization during neurodegeneration is rarely explored. Furthermore, NTPDase1/CD39 and eN/CD73 represent promising pharmacological targets in the treatment of neuroinflammatory processes (Antonioli et al., 2013).

It has been previously described an early change in astrocyte morphology that precedes neuronal loss, particular reactive astrocyte phenotypes, and their dynamic remodeling after TMT intoxication (Dragic et al., 2019b). It was also found that TMT-induced mitochondrial depolarization is independent of extracellular Ca^{2+} and disturbed antioxidative defense, but also upregulated main proinflammatory factors and components of signaling pathways responsible for astrocyte reactivity, and markers of proinflammatory subtype of astrocytes in vitro (Dragic et al., 2021). Induction of $P2X_2R$ in glial cells has been reported after TMT intoxication (Latini et al., 2010), but the involvement of other purinergic signaling components has not been explored. The main goal of the present study was to explore the cell-specific localization of NTPDase1/CD39 and eN/CD73 and the expression of purinergic receptors specific for microglia in the early and the late stage of hippocampal neurodegeneration induced by TMT. Furthermore, there is no information on whether TMT-induced inflammation in rats is caused by reactive microglia and/or astrocytes. Thus, in the present study, we analyzed NTPDase1/CD39 and eN/CD73, and purinergic receptors expression patterns in the context of activation of glial cells, inflammation, and its potential resolution after TMT intoxication. We also hypothesized that components of purinergic signaling may assign functional states of glial cells.

Material and Methods

Animals, Surgical Procedure, and Treatment

Two-month-old female rats of the Wistar strain (200–220 g) maintained in the local animal facility were used in the study. Appropriate actions were taken to alleviate the pain and discomfort of the animals following the compliance with the European Communities Council Directive (2010/

63/EU) for animal experiments, and the research procedures were approved by the Ethical Committee for the Use of Laboratory Animals. Animals were housed 3–4/cage, in a 12 h light/dark regime, constant humidity and temperature, and free access to food and water.

It was previously shown that TMT-induced hippocampal neurodegeneration and gliosis, the pattern of which was comparable in adult rats of both sexes (Corvino et al., 2015; Dragic et al., 2019b; Geloso et al., 2011; Haga et al., 2002; Little et al., 2012; Trabucco et al., 2009). However, given that the expression of ectonucleotidases in the brain is modulated/regulated by gonadal steroids and differs in two sexes (Grkovic et al., 2019b; Mitrovic et al., 2016, 2017), the study was performed in female rats, bilaterally ovariectomized 3 weeks before TMT injection as we described previously (Dragic et al., 2019b).

On day zero, animals of the TMT group received TMT (8 mg/kg dissolved in 1 mL 0.9% w/v saline) (in the form of a single intraperitoneal [i.p.] injection), whereas the control (Ctrl) group received an adequate volume of 0.9% saline solution. The animals were returned to their cages, and monitored for unusual signs of behavior until sacrifice, as reported previously (Dragic et al., 2019b). At 7 and 21 days post intoxication (dpi), animals of TMT and age-matched Ctrl groups (10 animals/group) were sacrificed by decapitation (Harvard apparatus, Holliston, MA, USA).

Histochemistry, Immunohistochemistry, and Immunofluorescence Microscopy

Brains ($n = 5$ per group) were carefully removed from the skull, fixed in 4% paraformaldehyde for 24 h, cryoprotected in graded sucrose (10%–30% in 0.2 M phosphate buffer), and stored at 4 °C, as described before (Dragic et al., 2019b; Grkovic et al., 2019b). The brains were cryosectioned in serial 25 µm thick coronal sections and the sections at 3.12–3.84 mm anteroposterior to Bregma were air-dried and stored at – 20 °C until use.

Nissl Staining. Alterations in hippocampal cytoarchitecture induced by TMT injection were evaluated by Nissl staining. Sections were kept in 0.5% thionine solution for 20 min, washed in tap water, dehydrated in graded ethanol (70%–100%), cleared in xylene for 2 × 5 min, and covered with DPX-mounting medium (Sigma Aldrich, USA).

Immunohistochemistry and Immunofluorescence. Slides were kept at room temperature (RT) for 30 min before staining. After washing in phosphate-buffered saline (PBS), slides were put in 0.3% H_2O_2 in methanol for 20 min, to block endogenous peroxidase, and then immersed in 5% donkey normal serum at RT for 1 h to block nonspecific binding. Sections were probed with primary antibodies, overnight at 4 °C in a humid chamber. After washing in PBS (3 × 5 min), sections were incubated with horseradish peroxidase (HRP)-conjugated secondary antibodies (2 h, RT in a humid chamber). The list of antibodies used for immunohistochemistry (IHC) and immunofluorescence (IF) is presented in Table 1. The immunoreaction was visualized with 3,3′S-diaminobenzidine-tetrahydrochloride (Abcam, UK), which is converted to the insoluble brown precipitate by HRP. Sections were washed in distilled water, dehydrated in graded ethanol solutions (70%–100%), cleared in xylene, and mounted with the use of DPX-mounting medium (Sigma Aldrich, USA). Sections were analyzed under a LEITZ DM RB light microscope (Leica Mikroskopie & Systems GmbH, Wetzlar, Germany), equipped with a LEICA DFC320 CCD camera (Leica Microsystems Ltd, Heerbrugg, Switzerland), and LEICA DFC Twain Software (Leica, Germany). All images were captured at 40× magnification.

The identical protocol has been applied for double and triple IF staining, with the omission of the methanol/H_2O_2 step. After incubation with primary antibodies (Table 1), sections were probed with fluorescence dye-labeled secondary antibodies and mounted with Mowiol (Calbiochem, La Jolla, CA). For double and triple IF staining, primary and secondary antibodies were separately applied for each labeling. Sections incubated without primary antibodies or with rat preimmune sera were used as negative Ctrls. Sections were analyzed by a confocal laser-scanning microscope (LSM 510, Carl Zeiss GmbH, Jena, Germany), using Ar multiline (457, 478, 488, and 514 nm), HeNe (543 nm), and HeNe (643 nm) lasers using 63× (2× digital zoom) DIC oil, 40× and monochrome camera AxioCam ICm1 camera (Carl Zeiss GmbH, Germany).

Enzyme Histochemistry. Ectonucleotidase enzyme histochemistry based on the ATP/ADP- and AMP-hydrolyzing activities of NTPDase1/CD39 and eN/CD73, respectively, have been applied (Dragic et al., 2019a; Grkovic et al., 2019b). Briefly, cryosections were preincubated for 30 min at RT in Tris-maleate sucrose (TMS) buffer, containing 0.25 M sucrose, 50 mM Tris-maleate, 2 mM $MgCl_2$ (pH 7.4), and 2 mM levamisole, to inhibit tissue nonspecific alkaline phosphatase. The enzyme reaction was carried out at 37 °C/60 min, in TMS buffer, containing 2 mM $Pb(NO3)_2$, 5 mM $MnCl_2$, 3% dextran T250, and 1 mM substrate (ATP, ADP, or AMP). After thorough washing, slides were immersed in 1% (v/v) $(NH_4)_2S$, and the product of enzyme reaction was visualized as an insoluble brown precipitate at a site of the enzyme activity. After dehydration in graded ethanol solutions (70%–100% EtOH, and 100% xylol), slides were mounted with a DPX-mounting medium (Sigma Aldrich, USA). The sections were examined under a LEITZ DM RB light microscope (Leica Mikroskopie & Systems GmbH, Wetzlar, Germany), equipped with a LEICA DFC320 CCD camera (Leica Microsystems Ltd, Heerbrugg, Switzerland)

Table 1. List of Antibodies.

Antibody	Source and type	Used dilution	Manufacturer
Iba1	Goat, polyclonal	1:400$^{IHC, IF}$	Abcam ab5076, RRID: AB_2224402
CD73, rNu-9L(14,15)	Rabbit, polyclonal	1:300$^{IHC, IF}$	Ectonucleotidases-ab.com
CD39, mN1-2C(14,15)	Guinea pig, polyclonal	1:200^{IF}	Ectonucleotidases-ab.com
Arg1	Rabbit, polyclonal	1:200^{IF}	Sigma AV45673, RRID: AB_1844986
iNOS	Rabbit, polyclonal	1:200^{IF}	Abcam ab15323, RRID: AB_301857
CD68	Rabbit, polyclonal	1:200^{IF}	Abcam ab125212, RRID: AB_10975465
$P2Y_{12}$	Rabbit, polyclonal	1:300^{IF}	Sigma P4817, RRID: AB_261954
GFAP	Mouse, monoclonal	1:100^{IF}	UC Davis/NIH NeuroMab Facility (73–240), RRID: AB_10672298
GFAP	Rabbit, polyclonal	1:500^{IF}	DAKO, Agilent Z0334, RRID: AB_10013382
C3	Goat, polyclonal	1:300^{IF}	Thermo Fisher Scientific PA1-29715 RRID: AB_AB_2066730
TNF-α	Goat, polyclonal	1:100^{IF}	Santa Cruz Biotechnology, sc-1350, RRID: AB_2204365
IL-10	Goat, polyclonal	1:100^{IF}	Santa Cruz Biotechnology, sc-1783, RRID: AB_2125115
NF-kB	Rabbit, polyclonal	1:100^{IF}	Santa Cruz Biotechnology, sc-109, RRID: AB_632039
IL-1β/IL-1F2	Goat, polyclonal	1:100^{IF}	R&D Systems, AF-501-NA, RRID: AB_ 354508
$P2Y_1$	Rabbit, polyclonal	1:300^{IF}	Alomone Labs; APR-0009, RRID: AB_2040070
A_{2A}	Rabbit, polyclonal	1:300 ^{IF}	Abcam, ab3461, RRID: AB_303823
$P2X_7$	Rabbit, polyclonal	1:400 ^{IF}	Alomone Labs, APR-004, RRID: AB_2040068
A_1R	Rabbit, polyclonal	1:200 ^{IF}	Novus Biologicals, NB300-549, RRID: AB_10002337
Anti-mouse IgG Alexa Fluor 488	Donkey, polyclonal	1:400^{IF}	Invitrogen A21202, RRID: AB_141607
Anti-goat IgG Alexa Fluor 488	Donkey, polyclonal	1:400^{IF}	Invitrogen A-11055, RRID: AB_142672
Anti-rabbit IgG Alexa Fluor 555	Donkey, polyclonal	1:400^{IF}	Invitrogen A-21428, RRID: AB_141784
Anti-mouse IgG Alexa Fluor 647	Donkey, polyclonal	1:400^{IF}	Thermo Fisher Scientific A-31571, RRID: AB_162542
Anti-goat HRP-conjugated IgG	Rabbit, polyclonal	1:200^{IHC}	R&D Systems, HAF017 RRID: AB_56258
Anti-rabbit IgG Alexa Fluor 488	Donkey, polyclonal	1:400^{IF}	Invitrogen A-21206, RRID: AB_141708
Anti-guinea pig IgG Alexa Fluor 555	Goat, polyclonal	1:200^{IF}	Invitrogen A-21435, RRID: AB_2535856
Anti-mouse HRP-conjugated IgG	Goat, polyclonal	1:200^{IHC}	R&D Systems, HAF007 RRID: AB_562588
Anti-goat HRP-conjugated IgG	Rabbit, polyclonal	1:200^{IHC}	R&D Systems, HAF017 RRID: AB_56258

Note. Arg1 = arginase-1; GFAP = glial fibrillary acidic protein; HRP = horseradish peroxide; IF = immunofluorescence; IgG = immunoglobulin G; IHC = immunohistochemistry; IL-10 = interleukin-10; IL-1F2 = interleukin-1F2; IL-1β = interleukin-1β; iNOS = inducible nitric oxide synthase; NF-kB = nuclear factor-kB; TNF-α = tumor necrosis factor-α.

and analyzed using LEICA DFC Twain Software (Leica, Germany).

IF Quantification. Raw multiimage IF micrographs were used to measure integrated fluorescence density expressed as arbitrary units (AUs) and the density confined within five predefined regions of interest (ROIs), with background fluorescence subtraction for at least three images per ROI and $n = 5$ sections per animal per group (JACoP ImageJ plugin). A degree of overlap and correlation between multiple channels was estimated by calculating Pearson's correlation coefficient (PCC) (Dunn et al., 2011). PCC is a statistical parameter that reflects both cooccurrence (degree at which intensities of two channels for each pixel are beyond or above the threshold), and correlation (pixel-for-pixel proportionality in the signal levels of the two channels). PCC values range from 1 (for two images whose fluorescence intensities are perfectly, linearly related) to -1 (for two images whose fluorescence intensities are perfectly, but inversely, related to one another). Values near zero reflect distributions of probes that are uncorrelated with one another. The results are expressed as mean PCC ± standard error of the mean (SEM).

Gene Expression Analysis by Quantitative Reverse Transcriptase-Polymerase Chain Reaction

Total RNA was extracted from the hippocampal formation (7 and 21 dpi and appropriate age-matched Ctrls, $n = 5$ animals per group) using TRIzol Reagent (Invitrogen, Carlsbad, CA, USA), according to the manufacturer's instructions. Purity and the concentration of isolated RNA were assessed by OD_{260}/OD_{280} and OD_{260}, respectively. Complementary DNA (cDNA) was synthesized using a High-Capacity cDNA Reverse Transcription Kit (ThermoFisher Scientific, MA, USA) and stored at −20 °C

Table 2. Primer Sequences Used for RT-qPCR.

Gene	Sequence (5′- −3′)	Length (bp)
NTPDase1 (*Entpd1*)	TCAAGGACCCGTGCTTTTAC TCTGGTGGCACTGTTCGTAG	150
eN (*Nt5e*)	CAAATCTGCCTCTGGAAAGC ACCTTCCAGAAGGACCCTGT	160
$P2X_4R$ (*P2rx4*)	ACCAGGAAACGGACTCTGTG TCACGGTGACGATCATGTTGG	168
$P2X_7R$ (*P2rx7*)	ATTGTTAGGCCAATGGCAAG AACACCTTCACCGTCTCCAC	190
$P2Y_2R$ (*P2ry2*)	TCACCCGCACCCTCTATTAC GCCAGGAAGTAGAGCACAGG	139
$P2Y_6R$ (*P2ry6*)	CAGTTATGGAGCGGGACAAT GTAAACTGGGGGTAGCAGCA	104
$P2Y_{12}R$ (*P2ry12*)	CGAAACCAAGTCACTGAGAGGA CCAGGAATGGAGGTGGTGTTG	162
$P2Y_1R$ (*P2ry1*)	CTGGATCTTCGGGGATGTTA CTGCCCAGAGACTTGAGAGG	138
A_1R (*Adora1*)	GTGATTTGGGCTGTGAAGGT GAGCTCTGGGTGAGGATGAG	194
$A_{2A}R$ (*Adora2a*)	TGCAGAACGTCACCAACTTC CAAAACAGGCGAAGAAGAGG	141
$A_{2B}R$ (*Adora2b*)	CGTCCCGCTCAGGTATAAAG CCAGGAAAGGAGTCAGTCCA	104
A_3R (*Adora3*)	TTCTTGTTTGCCTTGTGCTG AGGGTTCATCATGGAGTTCG	129
IL-1β (*Il1b*)	CACCTCTCAAGCAGAGCACAG GGGTTCCATGGTGAAGTCAAC	79
TNFα (*Tnf*)	CCCCCATTACTCTGACCCCT CCCAGAGCCACAATTCCCTT	88
IL-6 (*Il6*)	CCGGAGAGGAGACTTCACAG ACAGTGCATCATCGCTGTTC	160
IL-10 (*Il10*)	GCTCAGCACTGCTATGTTGC GTCTGGCTGACTGGGAAGTG	106
C3 (*C3*)	GCGGTACTACCAGACCATCG CTTCTGGCACGACCTTCAGT	166
iNOS (*Nos2*)	ACACAGTGTCGCTGGTTTGA AACTCTGCTGTTCTCCGTGG	125
Arg1 (*Arg1*)	CTGTGGTAGCAGAGACCCAGA GGTTGTCAGCGGAGTGTTGA	161
S100a10 (*S100a10*)	GTACCCACACCTTGATGCGT CGAAAGCTCCTCTGTCATTGG	130
CycA (*Ppia*)	CAAAGTTCCAAAGACAGCAGAAAA CCACCCTGGCACATGAAT	114
HPRT1 (*Hprt1*)	GGTCCATTCCTATGACTGTAGATTTT CAATCAAGACGTTCTTTCCAGTT	126
GAPDH (*Gapdh*)	CAACTCCCTCAAGATTGTCAGCAA GGCATGGACTGTGGTCATGA	118

Note. Arg1 = arginase-1; CycA = cyclophilin A; GAPDH = glyceraldehyde-3-phosphate dehydrogenase; HPRT1 = hypoxanthine phosphoribosyltransferase 1; IL-10 = interleukin-10; IL-1β = interleukin-1β; IL-6 = interleukin-6; iNOS = inducible nitric oxide synthase; RT-qPCR=quantitative reverse transcriptase-polymerase chain reaction; TNF-α = tumor necrosis factor-α.

until use. Quantitative real-time polymerase chain reaction (PCR) was performed using Power SYBR™ Green PCR Master Mix (Applied Biosystems, MA, USA) and ABI Prism 7000 Sequence Detection System (Applied Biosystems, MA, USA) under the following conditions: 10 min of enzyme activation at 95 °C, 40 cycles of 15 s denaturation at 95 °C, 30 s annealing at 60 °C, 30 s amplification at 72 °C, and 5 s fluorescence measurement at 72 °C. Primer sequences used for the amplification are given in Table 2. To compare the relative expression levels of the studied transcripts, we validated three *housekeeping genes*: glyceraldehyde-3-phosphate dehydrogenase (*Gapdh*), cyclophilin A (*CycA*), and hypoxanthine-

guanine phosphoribosyltransferase (*Hprt*). Cycle threshold (Ct) values in all examined animals for all *housekeeping genes* were within the same half of the same cycle making it all acceptable as a reference gene. The expression profiles of genes that we studied were comparable when normalized to *all housekeeping genes*. Thus, for relative quantification of target genes, we used the $2^{-\Delta\Delta Ct}$ method, using *CycA* as a reference gene. Samples obtained from five animals for each experimental group were run in duplicate. Amplification efficacy was assessed by the generation of internal standard curves by several-fold dilutions of generated cDNA while melting curve analysis at the end of each experiment was used to confirm the formation of a single PCR product. The results were expressed as the abundance of target messenger RNA (mRNA)/CycA-mRNA at 7 and 21 dpi relative to a corresponding Ctrl ± standard deviation (SD). Relative expressions of target genes normalized against CycA used as a housekeeping gene are shown in Supplementary Table 1.

Statistical Analysis

Data were analyzed for normality and appropriate parametric tests were used. All values are presented as mean ± SD or SEM. Between-group comparisons for 7 and 21 dpi were analyzed using an unpaired *t*-test. The values of $p < .05$ or less were considered statistically significant. For all statistical analyses, Graphpad Prism 5.04 (Graphpad) software was used.

Results

Spatiotemporal Patterns of Neurodegeneration and Gliosis After TMT Exposure

TMT-induced hippocampal degeneration was confirmed by Nissl staining (Figure 1a). As we have shown previously (Dragic et al., 2019b), cell injury was observed in the hilar/proximal CA3 (hilus/pCA3) at 7 dpi. This is followed by the almost complete disappearance of staining in neuronal somata in CA1 and the proximal and medial CA3 (p/mCA3) regions at 21 dpi (Figure 1a), as already reported (Geloso et al., 2011; Haga et al., 2002; Latini et al., 2010; Little et al., 2012). As reported previously (Dragic et al., 2019b), immunostaining of astrocyte marker glial fibrillary acidic protein (GFAP) showed the presence of pronounced astrogliosis at 7 dpi as well as 21 dpi (Figure 1b).

A great morphological diversity of reactive microglia was observed (Figure 1c and d). Specifically, highly ramified Iba1-immunoreactive (*ir*) cells, evenly distributed in the Ctrl hippocampal tissue (Figure 1c), were gradually transformed to rod Iba1-*ir* cells in synaptic layers of CA1 and the hilar/pCA3 at 4 dpi (data not shown). Besides rod shape, a range of other reactive Iba1-*ir* morphotypes was observed, from hyperramified to bushy/amoeboid. At 7 dpi, rod Iba1-*ir* cells populated the synaptic layers in the entire CA1 and the hilar/pCA3 sectors, while $Iba1^+$cells in the neuronal cell layers attained amoeboid morphology (Figure 1c and d). At 21 dpi, most of the heavily labeled $Iba1^+$ cells with pronounced amoeboid morphology were located in the pyramidal cell layer and especially in p/mCA3 region. Interestingly, rod Iba1-*ir* cells were not observed in the hilar/pCA3, whereas the hilar area and granular cell layer appeared completely without Iba1-*ir* at the latest time point (Figure 1c).

Expression of NTPDase1/CD39, eN/CD73, and Purinoreceptors Involved in Microglial Reactivity

The main goal of the present study was to explore the involvement of the purinergic signaling system in TMT-induced hippocampal neurodegeneration and gliosis. We first analyzed the expression of genes encoding NTPDase1/CD39 and eN/CD73. There was a significant increase in the relative expression of NTPDase1/CD39-mRNA in the hippocampal tissue at 7 and 21 dpi ($p < .01$ and $p < .0001$, respectively) when compared with age-match Ctrls. Although the relative expression of eN/CD73-mRNA in the hippocampal tissue at 7 dpi did not change, the enzyme mRNA levels significantly increased at 21 dpi when compared with age-match Ctrl ($p < .01$) (Figure 2a).

The pattern of the enzyme activity in the hippocampus and the localization of upregulated NTPDase1/CD39 in response to TMT were determined by enzyme histochemistry using ATP and ADP as a substrate (Braun et al., 2000; Grkovic et al., 2019b). In accordance with well-known data (Braun et al., 2000; Grkovic et al., 2019b; Robson et al., 2006), the typical patterns of histochemical reaction for ATPase/ADPase activities were observed in Ctrl hippocampi, labeling synaptic layers, ramified microglia, and endothelial cells typical for NTPDase1/CD39 (Figure 2b). In the first four days after intoxication (data not shown), reduction of staining in neuropil through hippocampus was noticed particularly when ADP was used as a substrate. This reduction was accompanied by a parallel increase of lead-phosphate deposition that nicely delineated cellular membranes of microglia. At 7 dpi lead-phosphate depositions delineated reactive microglia that covered the strata but also entered the neuronal layers (Figure 2b). At 21 dpi, activated microglia accounted for most of the enhanced ATPase/ADPase activities, revealing strong staining of CA strata, while dentate gyrus (DG) was mostly without reaction (Figure 2b). The obtained patterns of ATP/ADP enzyme activities closely corresponded to Iba1-*ir* (Figure 1c), suggesting that reactive microglial cells upregulated NTPDase1/CD39 after the exposure to TMT.

eN/CD73 activity and localization in response to TMT were determined using AMP-based enzyme histochemistry (Figure 2c) and eN/CD73-directed immunocytochemistry (Figure 2d). In intact hippocampal tissue, diffuse histochemical reaction and eN/CD73-*ir* were observed in synaptic layers,

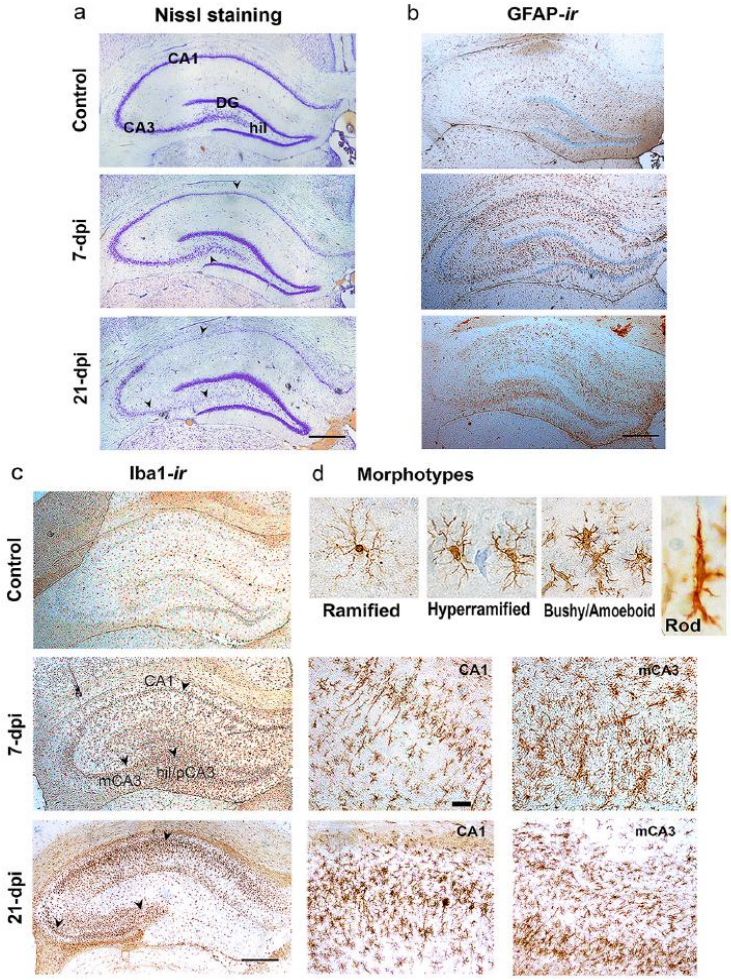

Figure 1. Spatiotemporal pattern of hippocampal neurodegeneration and gliosis after TMT exposure (a) thionine staining of coronal sections obtained from control animals and at 7 and 21 dpi. Arrowheads indicated injured neuronal cell layers in the hippocampus. Scale bar = 500 μm. (b) Immunohistochemical staining of GFAP in control animals and at 7 and 21 dpi. Scale bar = 500 μm. (c) Immunohistochemical staining of Iba1 in the whole hippocampal area and corresponding enlarged CA1 and mCA3 at 7 and 21 dpi. Scale bar = 500 μm (under 5× magnification), and 100 μm (under 20× magnification). (d) Representative images of different Iba1-*ir* morphological phenotypes are observed in control and after TMT exposure.
Note. dpi = days post intoxication; GFAP = glial fibrillary acidic protein; *ir* = immunoreactive; mCA3 = medial CA3; TMT = trimethyltin.

while neuronal cell layers remained unstained, as were shown previously (Dragic et al., 2019a; Grkovic et al., 2019b). From 7 dpi and afterward, products of AMPase activity were accumulated in the neuronal strata, infiltrating within neuronal cell layers (Figure 2c). eN/CD73-*ir* completely reflected patterns observed by AMPase, depicted individual round-shaped elements that covered neuronal layers and were most noticeable at the late stage of TMT-induced neurodegeneration (21 dpi, Figure 2d). Cellular localization of eN/CD73-*ir* was determined by triple IF directed to GFAP, Iba1, and eN/CD73 (Figure 3a). At 7 and 21 dpi, eN/CD73-*ir* overlapped with Iba1-*ir* at amoeboid cells infiltrated within neuronal cell layers, while colocalization with GFAP-*ir* was not observed. The colocalization of main microglial ectonucleotidase NTPDase1/CD39, and eN/CD73 was demonstrated by double-IF labeling, which showed colocalization of NTPDase1/CD39 and eN/CD73 at amoeboid cells, while ramified and rod NTPDase1/CD39-*ir* cells within synaptic layers did not show eN/CD73-*ir* (Figure 3b). The degree of colocalization was estimated by the Pearson correlation coefficient (PCC) (Figure 3c). The raising PCC values indicated increase in colocalization of Iba1/eN/CD73 ($p < .0001$) and

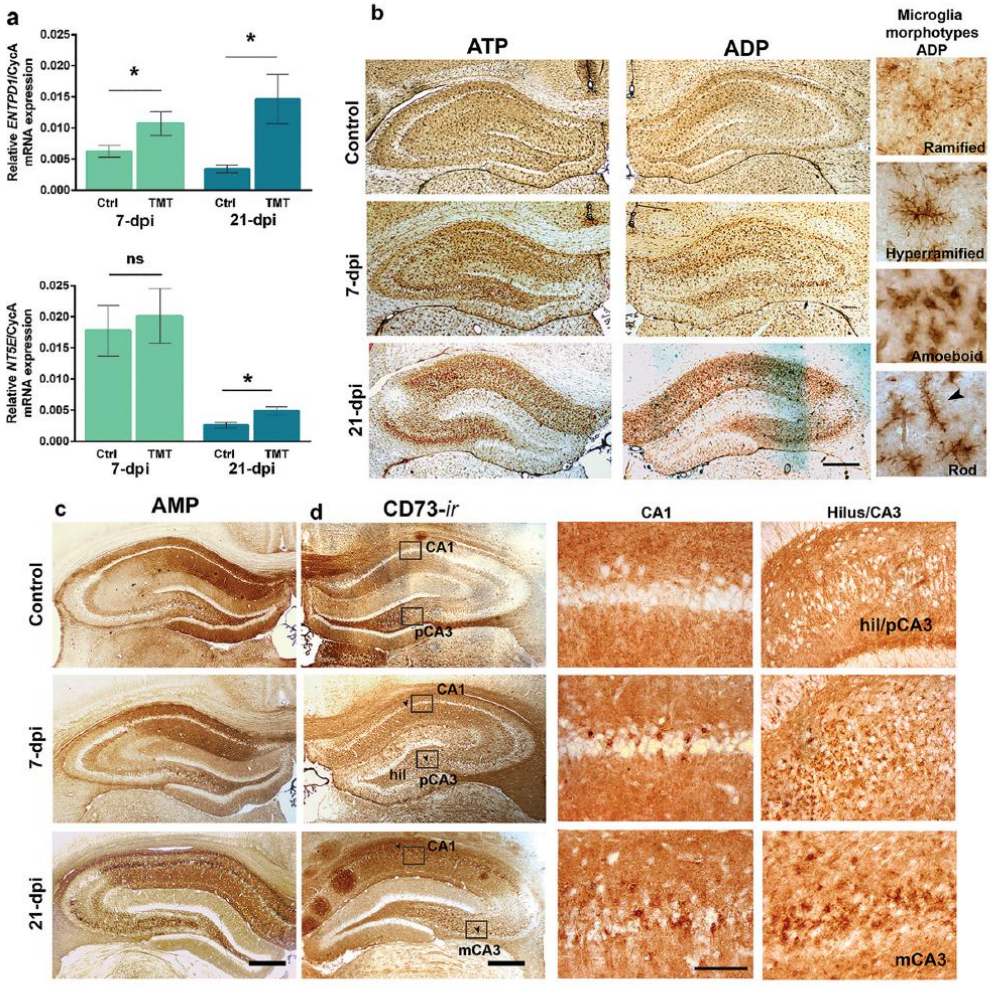

Figure 2. Expression and activity of NTPDase1/CD39 and eN/CD73 in the hippocampal region after TMT exposure (a) RT-qPCR analysis of genes encoding NTPDase1/CD39 and eN/CD73 in the Ctrl hippocampal tissue, 7 and 21 dpi, respectively. Bars represent mean mRNA expression of target gene relative to CycA ± SD. Significance shown inside the graphs: $*p < .05$ or less compared to age-match Ctrl. In the presence of ATP or ADP (b) and AMP (c) as substrate, enzyme histochemistry labeled cells and structures correspond to ectonucleotidase activities in the hippocampal region of Ctrl, 7 and 21 dpi. Microglial cells were clearly labeled by ATP and ADP enzyme histochemistry. High magnifications of microglial morphotypes observed by ADPase enzyme histochemistry were inserted. (d) eN/CD73-*ir* in the hippocampal region of Ctrl section, 7 and 21 dpi. Rectangles show eN/CD73-*ir* areas—CA1, hil/pCA3 and mCA3 captured under higher magnification. eN/CD73 depicted individual round-shaped elements in the neuronal layers and were most noticeable at 21 dpi. Scale bar = 500 µm (under 5× magnification), and 50 µm (under 40× magnification).

Note. ADP = adenosine diphosphate; AMP = adenosine monophosphate; ATP = adenosine triphosphate; Ctrl = control; CycA = cyclophilin A; dpi = days post intoxication; eN/CD73 = ecto-5′ nucleotidase; hil/pCA3 = hilar/proximal CA3; *ir* = immunoreactive; mCA3 = medial CA3; mRNA = messenger RNA; NTPDase1/CD39 = ectonucleoside triphosphate diphosphohydrolase 1; RT-qPCR = quantitative reverse transcriptase-polymerase chain reaction; SD = standard deviation; TMT = trimethyltin.

NTPDase1/CD39-eN/CD73 ($p < .0001$) signals at both time points after TMT exposure, whereas negative PCC values for GFAP-*ir* and eN/CD73-*ir* ($p = .32$) corroborated the lack of astrocytic expression of eN/CD73 after TMT. The results pointed to the marked induction of NTPDase1/CD39 by Iba1$^+$ cells, and the colocalization with eN/CD73 at amoeboid Iba1$^+$ cells after TMT exposure (Figure 3c).

Since the role of extracellular ATP is closely related to its breakdown products, changes in mRNA expression of ATP/ADP-sensitive P2 and adenosine P1 receptors in the

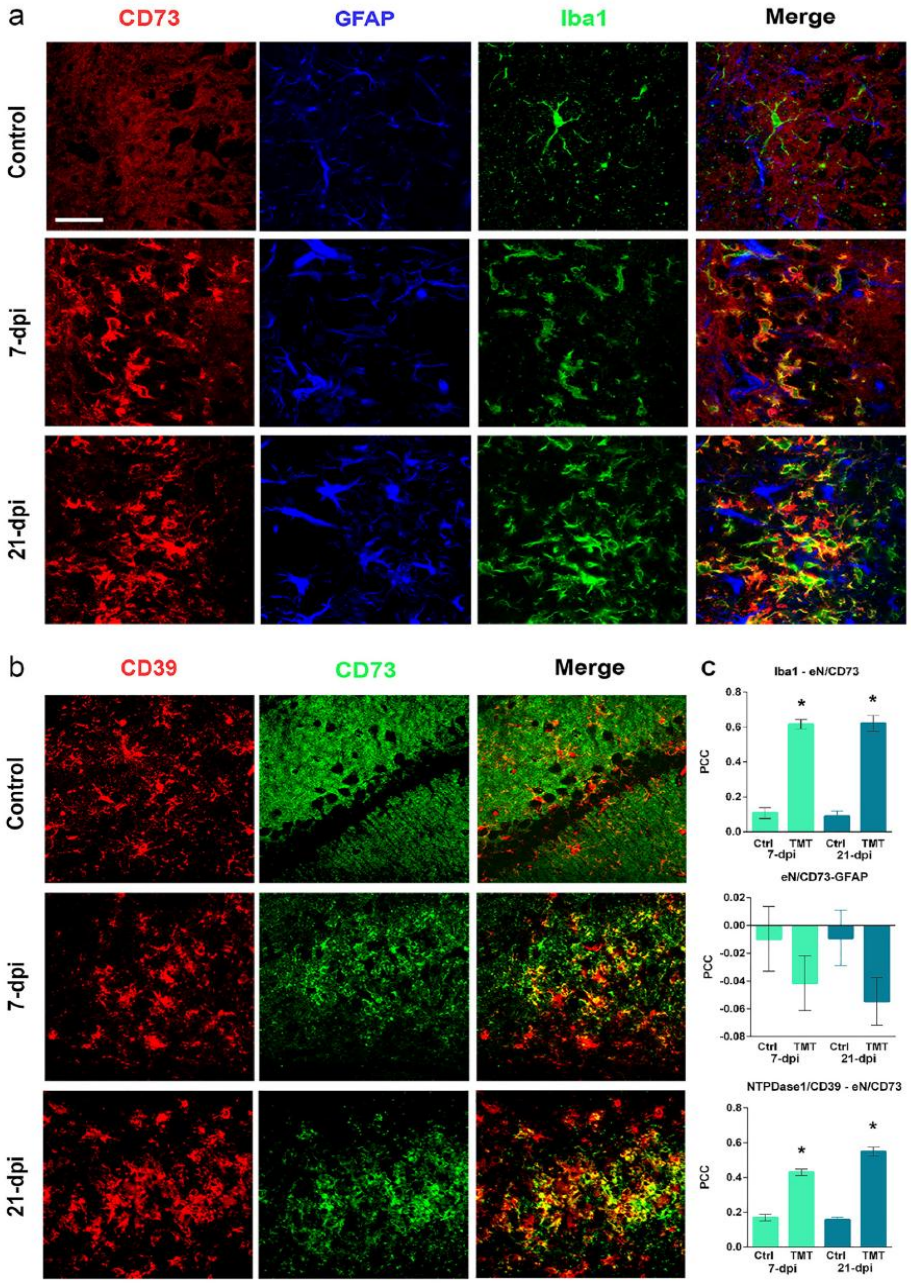

Figure 3. Identification of cells that upregulate eN/CD73 in the hippocampal region after TMT exposure (a) triple IF labeling directed to eN/CD73 (red), astrocyte marker GFAP (blue), and microglial marker Iba1 (green) in the Ctrl, 7 and 21 dpi hippocampi. Overlaid images (merge) reveal the overlapping signal corresponding to Iba1-*ir* and eN/CD73-*ir* at 7 and 21 dpi. (b) Double-IF labeling directed to NTPDase1/CD39 (red) and eN/CD73 (green), showing the overlapping signals (merge) at 7 and 21 dpi. Scale bar = 50 µm. (c) PCC indicates the level of signal overlap between Iba1-*ir* and eN/CD73-*ir*, eN/CD73-*ir* and GFAP-*ir* and NTPDase1/CD39-*ir* and eN/CD73-*ir*. Bars show mean PCC ± SEM, from 3 ROI selected from 5 sections. Significance shown inside the graphs: $^{*}p < .05$ or less compared to age-match Ctrl.
Note. Ctrl = control; dpi = days post intoxication; eN/CD73 = ecto-5′ nucleotidase; *ir* = immunoreactive; NTPDase1/CD39 = ecto-nucleoside triphosphate diphosphohydrolase 1; GFAP = glial fibrillary acidic protein; IF = immunofluorescence; PCC = Pearson correlation coefficient; SEM = standard error of the mean; ROI = region of interest; TMT = trimethyltin.

hippocampus during TMT-induced neurodegeneration were explored (Figure 4). Regarding ATP/ADP-sensitive P2 receptors mainly expressed by microglia (Illes et al., 2020), a significant increase in the relative abundance of $P2X_4R$-, $P2Y_2R$-, and $P2Y_6R$-mRNA levels were observed, at both 7 dpi ($p < .0001$, $p < .0001$, $p < .0001$, respectively) and 21 dpi ($p < .001$, $p < 0.0001$, $p < .001$, respectively) when compared to age-matched Ctrls (Figure 4). The $P2Y_{12}R$-mRNA level of the specific microglial receptor (Illes et al., 2020) was robustly increased at 7 dpi ($p < .0001$) while a slight increase was observed at 21 dpi ($p < .05$) (Figure 4). $P2X_7R$- and $P2Y_1R$-mRNA levels were significantly increased at both 7- ($p < .001$ and $p < .05$, respectively) and 21 dpi ($p < .01$ and $p < .001$, respectively), when compared to age-match Ctrl. Furthermore, analysis of adenosine P1 receptors showed an increase in A_3R-mRNA levels at both 7 and 21 dpi when compared to age-match Ctrl ($p < .001$ and $p < .01$, respectively), together with induction of A_1R-mRNA relative abundances at 21 dpi ($p < .01$, Figure 4). There are no changes in $A_{2B}R$-mRNA relative abundances at both 7 and 21 dpi. Relative expressions of target genes for all tested time points are shown in Supplemental Table 1.

The Inflammatory Status of the Hippocampal Tissue After TMT Exposure

It is known that activated glial cells develop functional phenotypes, which may be roughly categorized as proinflammatory or antiinflammatory. Therefore, we first assessed the inflammatory status of the hippocampal tissue at the early (7 dpi) and the late (21 dpi) stage of TMT-induced neurodegeneration by determining the expression of several inflammatory markers. As shown in Figure 5, only tumor necrosis factor-α (TNF-α)-mRNA level was significantly increased at 7 dpi when compared to Ctrl ($p < 0.0001$), while interleukin (IL)-1β-, IL-6-, IL-10-mRNA relative abundances were significantly increased at 21 dpi ($p < .01$, $p < .01$, and $p < .001$, respectively, Figure 5). We also examined the main markers of two extreme polarization states of microglia/macrophages (inducible nitric oxide synthase [iNOS] and Arg1), as well as C3 and S100a10 as markers that are often used to discriminate between functional states of astrocytes. iNOS-, C3- and S100a10-mRNA levels were significantly increased at both 7- ($p < .001$, $p < .0001$, $p < .001$, respectively) and 21 dpi ($p < .01$, $p < .0001$, $p < .05$, respectively) when compared to age-match Ctrl (Figure 5). Arg1-mRNA level was decreased at 7 dpi ($p < .0001$), while no changes were detected at 21 dpi when compared to age-match Ctrl (Figure 5). Relative expressions of target genes for all tested time points are shown in Supplementary Table 1.

Functional State of Reactive Microglia and Astrocytes

Next, we sought to determine the cellular source of inflammation and performed colocalization of Iba1 or GFAP against inflammatory markers. Neither of the tested proinflammatory cytokines (IL-1β, TNF-α, and IL-10) and C3 (data not shown) nor polarization marker iNOS (Figure 6) was found in association with Iba1-*ir*. However, Iba1-*ir* cells colocalized with Arg1-*ir* and phagocytic marker CD68-*ir* at 7 and 21 dpi (Figure 6). A signal cooccurrence was observed at rod and amoeboid cells at 7 and 21 dpi, while only amoeboid $Iba1^+$ cells were abundantly labeled with eN/CD73 (Figure 6). The induction of the chemotaxis microglial marker $P2Y_{12}R$ was also observed at Iba1-*ir* cells at 7 dpi (Figure 6). Although a slight increase in the relative gene expression of $P2Y_{12}R$ was observed, $Iba1^+$ cells of amoeboid morphology did not colocalize with $P2Y_{12}R^+$ at 21 dpi (Figure 6). It is important to emphasize that ramified morphology of $Iba1^+$ cells (Figure 6) corresponds to Ctrl microglia as well as to $Iba1^+$ cells with the same morphology in the hippocampal areas distant from the site of neurodegeneration at both 7 and 21 dpi. Moreover, $P2X_7$-*ir* clearly labeled neurons in Ctrl hippocampi as well as at 7 dpi (Figure 6), while $P2X_7$-*ir* signal clearly overlapped with amoeboid microglia at 21 dpi. On the other hand, colocalization of $P2X_7R$ with GFAP-*ir* astrocytes could not be observed in Ctrls and investigated time points.

The lack of expression of proinflammatory cytokines and markers by Iba1-*ir* microglial cells, and clearly labeled $iNOS^+$ and $C3^+$ cells around $Iba1^+$ cells, prompted us to explore their astroglial expression (Figure 7). Except for neuronal TNF-α-*ir* at the site of neurodegeneration at 7 dpi, the signals that correspond to IL-1β, TNF-α, and IL-10 almost completely overlapped with GFAP-*ir* at 7 dpi and/or 21 dpi (Figure 7). At 7 dpi, iNOS- and C3-*ir* were also observed at neurons, while almost all GFAP-*ir* cells at the injured area expressed iNOS, nuclear factor-kB (NF-kB), and C3, suggesting that astrocytes were the major source of the inflammatory factors at the late stage of TMT-induced neurodegeneration. The fluorescence intensity of all investigated inflammatory markers was significantly increased at both 7 and 21 dpi (Figure 7).

Since astrocytic $P2Y_1R$ is involved in the regulation of several cytokines/chemokines expression (e.g., IL-6, and TNF-α) (Kuboyama et al., 2011), and $A_{2A}R$ upregulation in activated glial cells facilitates the release of cytokines (Paiva et al., 2019), we explore their localization. In addition, prolonged adenosine A_1R signaling and its cross-talk with $A_{2A}R$ might enhance $A_{2A}R$-mediated neurotoxicity in neurodegenerative disorders (Stockwell et al., 2017). Thus, massive induction of $P2Y_1R$ and $A_{2A}R$ was found on GFAP-*ir* and C3-*ir* astrocytes at 7 and 21 dpi, while A_1R shifted from neurons to GFAP-*ir* astrocytes at 7 dpi and fully colocalize with GFAP-*ir* at 21 dpi at the sites of neurodegeneration (mCA3 or CA1) (Figure 8). Neither one of the investigated receptors was not observed at $Iba1^+$ cells, suggesting the involvement of the purinoreceptors in the proinflammatory astrocyte phenotype after TMT intoxication.

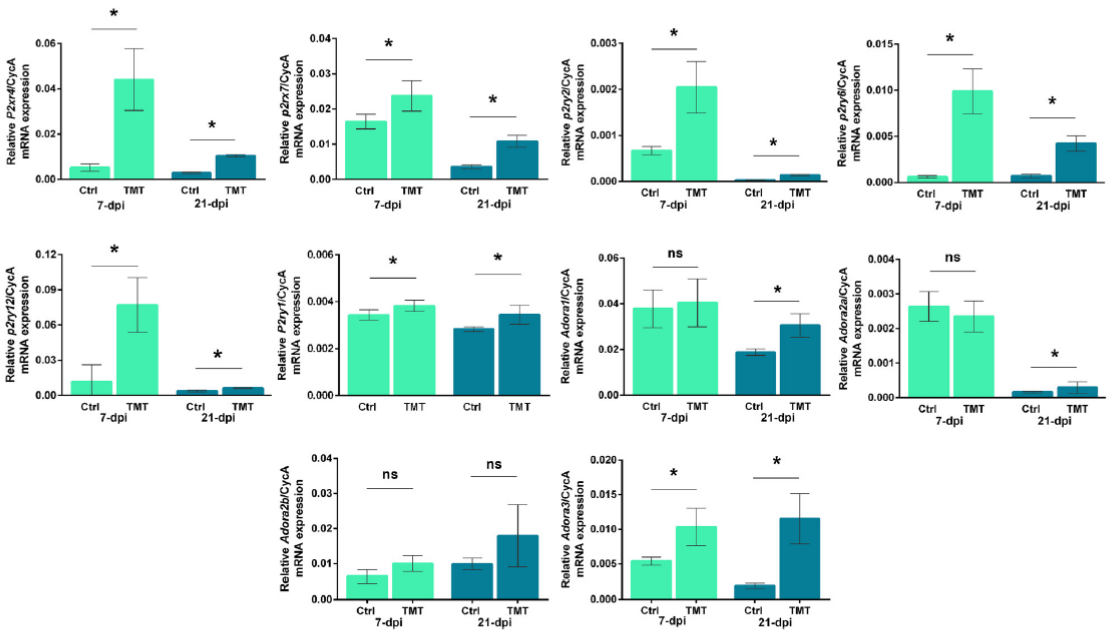

Figure 4. Purinoceptors gene expression in the hippocampal region after TMT exposure The abundances of transcripts coding for $P2X_4$, $P2X_7$, $P2Y_1R$, $P2Y_2R$, $P2Y_6R$, $P2Y_{12}R$, A_1R, $A_{2A}R$, $A_{2B}R$, and A_3R were assessed by RT-qPCR at 7 and 21 dpi. Bars represent mean mRNA expression of target gene relative to CycA ± SD. Significance shown inside the graphs: $^*p < .05$ or less compared to age-match Ctrl.
Note. Ctrl = control; CycA = cyclophilin A; SD = standard deviation; RT-qPCR = quantitative reverse transcriptase-polymerase chain reaction; dpi = days post intoxication; mRNA = messenger RNA.

Discussion

The results of the present study corroborate the existing data on the spatiotemporal pattern of neurodegeneration and gliosis in the rat TMT model (Corvino et al., 2013, 2015; Haga et al., 2002; Latini et al., 2010; Little et al., 2012; Trabucco et al., 2009). As described and analyzed previously (Dragic et al., 2019b), reactive astrocytes (from day 2 post-TMT) were polarized toward the jeopardized regions, enclosing it and probably creating a protective glial barrier, keeping other regions from damage at the early stage of TMT-induced neurotoxicity (Dragic et al., 2019b). Microglial activation induced by TMT slightly lagged behind astrocyte reactivation, as observed earlier (Haga et al., 2002), and is manifested as a robust increase in the number of $Iba1^+$ cells due to migration or proliferation of resident microglia (Little et al., 2002). However, we observed that synaptic layers in the affected sectors became largely populated with *rod* $Iba1^+$ cells, occasionally found in a train formation at the early stage of neurodegeneration. Rod microglia are usually found at the early stages of neurodegenerative disorders in association with undamaged neurons and axons, and not in aggregation with other glial cells (Au & Ma, 2017; Zabel & Kirsch, 2013), which could be an indicator of their protective and reparative role (Boche et al., 2013). Rod cells may provide new cells and transform into amoeboid microglia (Tam & Ma, 2014). We also observed that injured neuronal cell layers of the hippocampal CA areas became sequentially infiltrated with $Iba1^+$ cells of amoeboid shape, particularly at the late stage of neurodegeneration induced by TMT.

As a marker of microglia (Almolda et al., 2013; Braun et al., 2000), NTPDase1/CD39 activity and expression were markedly upregulated in all Iba1-*ir* cells after TMT intoxication, irrespective of their shape and position. On the other hand, as the final and the rate-limiting enzyme in the extracellular degradation of ATP, eN/CD73 showed a selective switch from neuropil to amoeboid Iba1-*ir* cells, implicating that the differential induction might be an adaption to specific hippocampal microenvironment, that is, site of injury or specific function. The transition between functional states of reactive microglia is accompanied by the morphological transformation of the cells, and among the critical factors that trigger the transition are ATP, adenosine, vitamin E, IL-34, and chemokine fractalkine (Boche et al., 2013; Wollmer et al., 2001). Furthermore, NTPDase1/CD39 and eN/CD73 upregulation may represent a defense mechanism against excess levels of extracellular ATP originating from damaged cells (Braun et al., 2000; Burnstock, 2017). Thus, enhanced activity of NTPDase1/CD39 may contribute to the prevention of receptor desensitization on prolonged exposure to elevated ATP and prevent activated microglia from overstimulation by

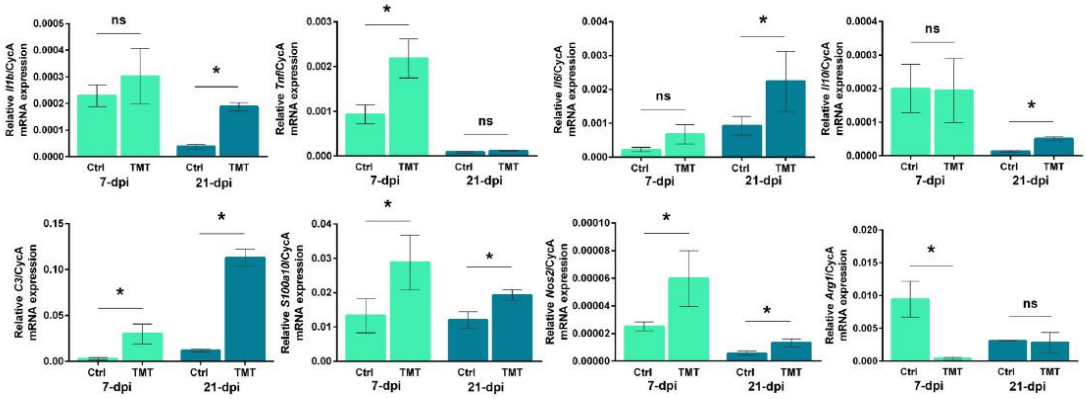

Figure 5. Proinflammatory status of the rat hippocampal region after TMT exposure The abundance of transcripts coding IL-1β, TNF-α, IL-6, IL-10, C3, S100a10, iNOS, and Arg1. Bars represent mean mRNA expression of target gene relative to CycA ± SD. Significance shown inside the graphs: *$p < .05$ or less compared to age-match Ctrl.
Note. Arg1 = arginase-1; CycA = cyclophilin A; IL-10 = interleukin-10; IL-1β = interleukin-1β; iNOS = inducible nitric oxide synthase; mRNA = messenger RNA; TMT = trimethyltin; TNF-α = tumor necrosis factor-α; SD = standard deviation.

ATP. The parallel eN/CD73 activity on amoeboid Iba1$^+$ cells probably facilitates the formation of adenosine that exerts neuro- and immunomodulatory actions (Di Virgilio et al., 2009; Illes et al., 2020). Furthermore, NTPDase1/CD39 and eN/CD73 not only catabolize extracellular ATP and provide adenosine but also function as clusters of differentiation and

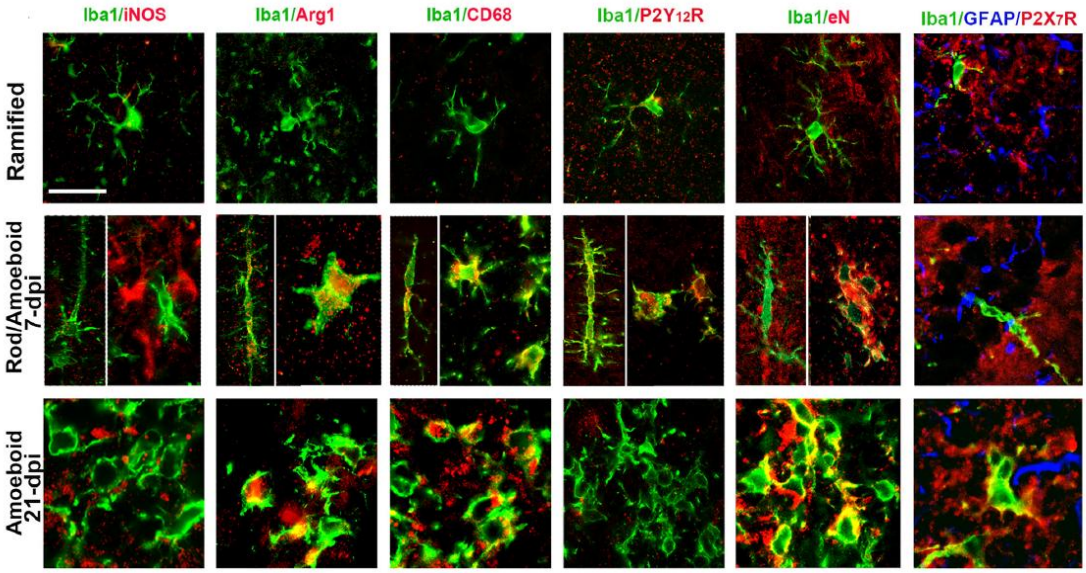

Figure 6. Assessment of the functional state of reactive microglia after TMT exposure. Ramified morphology of Iba1+cells corresponds to control microglia but also to ramified Iba1$^+$ cells in the hippocampal areas distant from the site of neurodegeneration at both 7 and 21 dpi. Double immunofluorescent staining of Iba1 and iNOS, Arg1, CD68, P2Y12 receptor (R), and eN/CD73, and triple immunofluorescent staining of Iba1, GFAP and P2X7R in the injured area 7 and 21 dpi, reveal Iba1-*ir* morphotypes that expressed Arg1-, CD68-, P2Y12-, P2X7- as well as eN-*ir*. Scale bar = 50 μm.
Note. Arg1 = arginase-1; dpi = days post intoxication; eN/CD73 = ecto-5′ nucleotidase; GFAP = glial fibrillary acidic protein; iNOS = inducible nitric oxide synthase; iNOS = inducible nitric oxide synthase; TMT = trimethyltin.

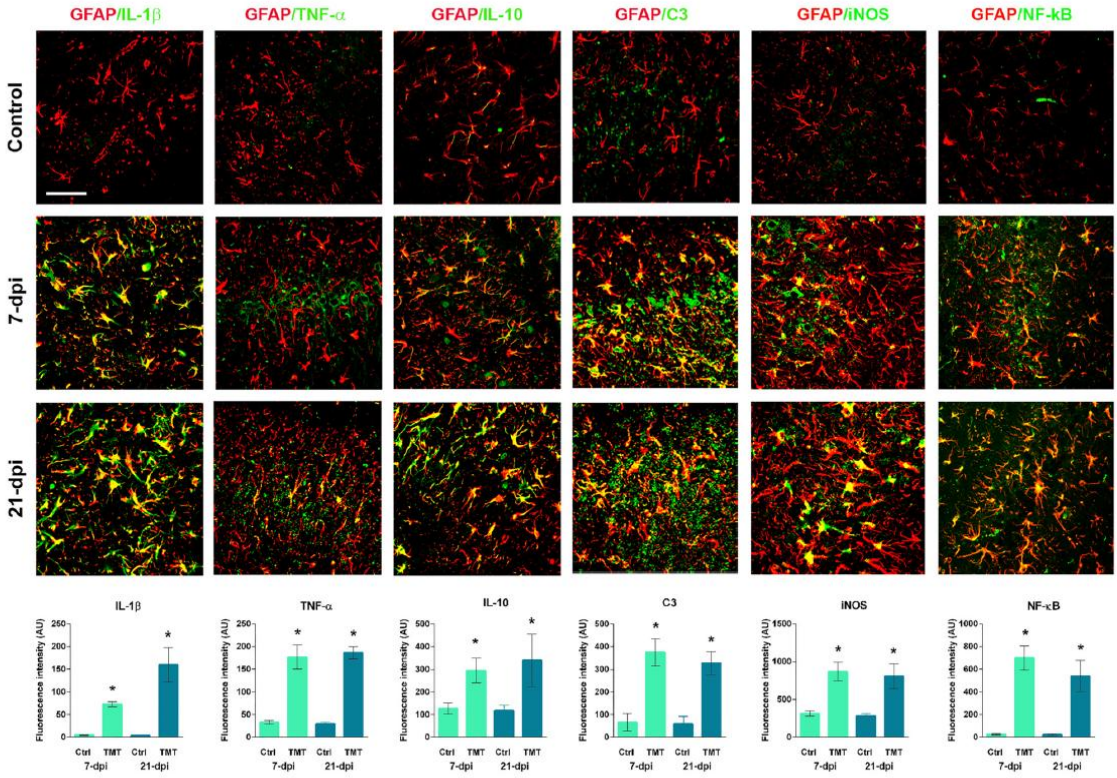

Figure 7. Assessment of the functional state of reactive astrocytes after TMT exposure. Double immunofluorescent staining of GFAP and IL-1β, TNF-α, IL-10, C3, iNOS and NF-kB and corresponding integrated fluorescence density expressed as AUs ± SEM in the injured CA area at 7 and 21 dpi. Significance shown inside the graphs: $^{*}p < .05$ or less compared to age-match Ctrl.
Note. AU = arbitrary unit; Ctrl = control; dpi = days post intoxication; GFAP = glial fibrillary acidic protein; IL-10 = interleukin-10; IL-1β = interleukin-1β; iNOS = inducible nitric oxide synthase; NF-kB = nuclear factor-kB; SEM = standard error of the mean; TMT = trimethyltin; TNF-α = tumor necrosis factor α.

cell adhesion molecules, which regulate the adhesion and glial cell migration through specific interactions with extracellular matrix components (Koizumi et al., 2007).

Microglial cell migration and chemotaxis depend on purinergic signaling via P2 receptors (Illes et al., 2020; Koizumi et al., 2007), which also triggers their shift to amoeboid phenotype (Illes et al., 2020). Thus, we found an increase in relative gene expression of $P2Y_{12}R$ specifically at the early stage (7 dpi) of TMT-induced neurodegeneration. This receptor is activated by extracellular ATP released from damaged cells that trigger microglial processes extension and migration to the site of injury (Illes et al., 2020). Further, we found an increase in $P2X_4$ relative gene expression that may contribute to both migratory as well as secretory properties of microglia, and interacts with the $P2Y_{12}R$ in the regulation of chemotaxis (Illes et al., 2020). At this stage, an increase of $P2Y_6$-mRNA level was observed, a receptor upregulated when neurons become damaged and send diffusible uridine 5′-diphosphate (UDP) signals to microglia (Illes et al., 2020). Adenosine also affects extension and chemotaxis to the site of active neurodegeneration via $P2Y_{12}R/A_3R$ coactivation (Haynes et al., 2006; Ohsawa et al., 2012). The ADP-driven process extension was reversed to process retraction during proinflammatory condition coincident with $P2Y_{12}R$ protein downregulation (Orr et al., 2009), which we observed at the late stage of TMT-induced neurodegeneration. Additionally, $P2Y_6R$ stimulation blocks ATP-dependent migration of microglia, most likely by shifting its migratory phenotype to an amoeboid/phagocytic one (Bernier et al., 2013; Koizumi et al., 2007), and which upregulation persist at the late stage (21 dpi) of neurodegeneration. The mRNA levels of $P2X_7R$, the ATP-sensitive receptor predominantly localized on microglial cells in the brain (Illes et al., 2020), were also increased at both the early and the late stage of neurodegeneration.

Concerning the polarization state of microglia, our data showed that Iba1-*ir* cells coexpressed specific marker Arg1, and did not colocalize with proinflammatory

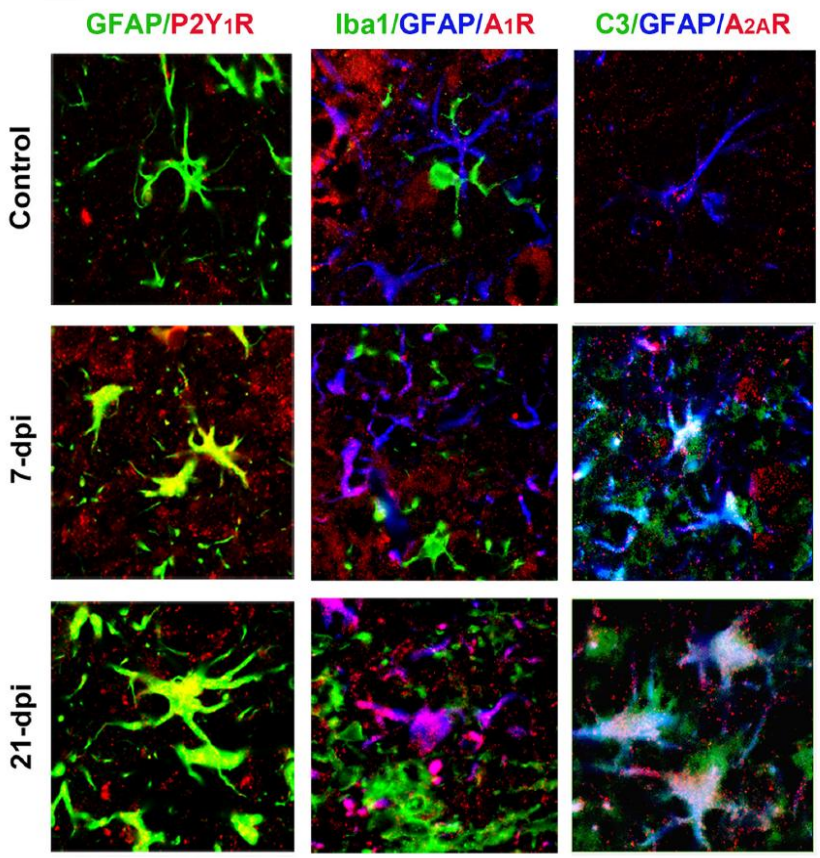

Figure 8. Association of P2Y1 and adenosine receptors with GFAP$^+$ astrocytes in the hippocampus after TMT exposure. Double IF reveals that GFAP-*ir* cells colocalized with $P2Y_1R$ in the injured hippocampal area at 7 and 21 dpi. Representative micrographs of triple IF staining of A_1R and markers of glial cells (Iba1 and GFAP) reveal neuronal A_1R staining in the Ctrl, colocalization with GFAP$^+$ cells at 7 dpi, and complete overlap of GFAP- and A_1R-*ir* at 21 dpi in the injured hippocampal area, without colocalization with Iba1-*ir* cells. Representative triple staining micrographs with C3, GFAP and $A_{2A}R$ reveal colocalization of all three signals in the injured hippocampal area at 7 and 21 dpi. Scale bar = 50 μm.

Note. GFAP = glial fibrillary acidic protein; TMT = trimethyltin; *ir* = immunoreactive; Ctrl = control; dpi = days post intoxication; IF = immunofluorescence.

markers iNOS, NF-kB, C3, and investigated proinflammatory cytokines, indicating that reactive microglial cells at the site of TMT-induced neurodegeneration were not a source of inflammatory molecules. The upregulation of NTPDase1/CD39 by reactive microglial cells was previously demonstrated in experimental autoimmune encephalomyelitis, where the induction of NTPDase1/CD39 tended to be associated with Arg1-*ir* and phagocytic marker CD68-*ir* microglial cells (Jakovljevic et al., 2019). Upregulation and specific localization of eN/CD73 on amoeboid Iba1$^+$ cells that were also associated with Arg1- and CD68-*ir* at the late stage of neurodegeneration induced by TMT support results that such eN/CD73 expression might promote macrophages/microglia to *phagocytic state* (Xu et al., 2018). In addition, $P2X_7$-*ir*, greatly localized on neurons at the early stage of neurodegeneration, colocalized with amoeboid Iba1-*ir* cells at the late stage of neurodegeneration. It is well known that $P2X_7R$ expression at amoeboid microglial cells modulates clearance of extracellular debris thus affecting their phagocytic role (Campagno & Mitchell, 2021). Given that CD39/CD73 tandem effectuate the whole cascade of extracellular ATP degradation, they might be taken as an "immunological switch" that leads to the antiinflammatory cell state (Antonioli et al., 2013), however, additional experiments are required to test this hypothesis.

According to the literature data (Little et al., 2002, 2012) early neurodegenerative response to TMT is not accompanied by increased gene expression of most proinflammatory cytokines. We found moderate induction of TNF-α in neurons at the early stage of TMT-induced neurodegeneration, while almost all $GFAP^+$ cells around damaged areas (CA1 and mCA3) were the source of IL-1β, TNF-α, and IL-10 particularly at the late stage of TMT-induced neurodegeneration, supporting in vitro results (Dragic et al., 2021) and studies that showed upregulation of other proinflammatory mediators at the later stages of TMT-induced neurodegeneration (Lattanzi et al., 2013; Liu et al., 2005; Morita et al., 2008). Furthermore, $P2X_7R$ is considered as a major driver of inflammation (Di Virgilio et al., 2017; Erb et al., 2019; Franke et al., 2012; Peterson et al., 2010), and we observed increased neuronal staining with $P2X_7R$ at both the early and the late stage of TMT-induced neurodegeneration. A wave of neurodegeneration induced by TMT might provide conditions for a sustained ATP release and prolonged $P2X_7R$ activation with the resulting postponed induction of IL-1β, together with TNF-α, and IL-6. Reactive astrocytes might initiate upregulation of $P2Y_2R$, as we observed after TMT intoxication, leading to a proinflammatory response (Peterson et al., 2010).

We have also observed that reactive astrocytes coexpressed iNOS, NF-kB, C3, and found increased expression of S100a10-mRNA. Taken together with the expression of main proinflammatory markers, it could be concluded that TMT-induced reactive astrogliosis exerts a complex molecular signature with the predominantly inflammatory phenotype (Escartin et al., 2021), mainly located around the sites of ongoing neurodegeneration. These proinflammatory astrocytes at the injured area also upregulate A_1R and $A_{2A}R$ receptors. In the hippocampus, adenosine exerts inhibitory function under physiological conditions due to the high expression of neuronal A_1R, modulating important processes such as learning and memory (Costenla et al., 2010; Stockwell et al., 2017). On the other hand, under pathological conditions, an increase of both mRNA and protein levels and aberrant signaling via hippocampal $A_{2A}R$ have been demonstrated to contribute to active neuroinflammation and cognitive deficits (Hu et al., 2016), both of which are seen in TMT-induced neurodegeneration (Geloso et al., 2011). Adenosine signaling via neuronal A_1R supports survival, exerts neuroprotective effects, and has anticonvulsive properties (Glass et al., 1996). Thus, the shift of A_1R immunoreactivity from neurons to astrocytes could render neurons vulnerable to secondary effects of TMT, such as seizures (Trabucco et al., 2009), while prolonged adenosine A_1R signaling and its cross-talk with $A_{2A}R$ might enhance $A_{2A}R$-mediated neurotoxicity in neurodegenerative disorders (Stockwell et al., 2017). Taken together with a concomitant increase of astrocytic $A_{2A}R$, these results could be put in perspective of potential formation of A_1R–$A_{2A}R$ heteromers, which are shown to contribute to dysregulation of glutamate homeostasis and favor excitotoxicity (Borroto-Escuela et al., 2018; Hou et al., 2020). A high amount of ATP released after TMT intoxication would be degraded by $Iba1^+/CD39^+/CD73^+$ cells thus producing high levels of adenosine around the sites of injury. Adenosine in such a microenvironment may activate astrocytic A_1R and $A_{2A}R$ supporting their proinflammatory phenotype (Nedeljkovic, 2019; Paiva et al., 2019; Popoli & Pepponi, 2012). Additional experiments are necessary to fully elucidate the role of adenosine in such a complex pathological environment. Induction of $P2Y_1R$ on reactive astrocytes further confirms their detrimental phenotype after TMT-induced neurotoxicity, since this receptor is also involved in the regulation of several cytokines/chemokines expression (Kuboyama et al., 2011), and causes astrocytic hyperactivity and dysfunction in an animal model of neurodegeneration (Delekate et al., 2014).

In summary, identification of expressional timeline of selected purinoreceptors and ectonucleotidases provides a framework for the reconstruction of their involvement in the initiation and progression of neurodegenerative events after TMT intoxication. This study suggests that proinflammatory astrocytes phenotype is possibly developed as a response to TMT intoxication. Increased availability of ligands such as ATP and adenosine coupled with a distinct set of activated glial purinergic repertoire ($P2X_7$, $A_{2A}R$, $P2Y_1$, and A_1R) and loss of homeostatic glial and neuronal purinergic pathways ($P2Y_{12}$ and A_1R) may shift purinergic signaling balance toward excitotoxicity and inflammation, thus ultimately favoring progression of pathological events. Targeting the upstream nucleotide metabolic pathway that controls adenosine production to modulate neural-immune interactions and neurodegeneration-related machinery represents a promising therapeutic strategy for intervening in disease progression.

Acknowledgments

The research was funded by the Ministry of Education, Science, and Technological Development of the Republic of Serbia Nos. 451-03-1/2021-16/14 –0902102 and 451-03-68/2020-14/200178. The authors thank Professor Jean Sevigny from the Faculté de Médecine, Université Laval, Quebec City, QC, Canada for a kind gift of rabbit anti-rat NTPDase1/CD39 (mN1-2C) and eN/CD73 (rNu-9L) antibodies used in this study. We would also like to thank our Dr. Ivana Bjelobaba, Institute for Biological Research "Siniša Stanković," National Institute of the Republic of Serbia, University of Belgrade, Belgrade, Serbia, for providing us with qPCR primers used in this study.

Author Contributions

All authors meet the International Committee of Medical Journal Editors (ICMJE) criteria for authorship for this article. I.G. conceived and directed the projects. M.D. and I.G. designed experiments and performed all histology, analyzed the data, and wrote the manuscript. N.M. performed qPCR experiments. M.A. was involved in confocal microscopy and image acquisition. N.N. was involved in data interpretation and wrote the manuscript. All authors had full access to all of the data in this study and take complete responsibility for the

integrity of the data and accuracy of the data analysis. All authors read, revised, and approved the final manuscript.

Data Availability Statement

The data that support the findings of this study are available from the corresponding author upon reasonable request.

Ethics Approval

The Ethical Committee approved all animal procedures for the Use of Laboratory Animals of "VINČA" Institute of Nuclear Sciences —National Institute of Republic of Serbia, University of Belgrade, Belgrade, Serbia, and animals were treated following the European Community Council Directive of 86/609/ EEC for animal experiment.

Declaration of Conflicting Interests

The authors declared no potential conflicts of interest with respect to the research, authorship, and/or publication of this article.

Funding

The authors disclosed receipt of the following financial support for the research, authorship, and/or publication of this article: This work was supported by the Ministarstvo Prosvete, Nauke i Tehnološkog Razvoja (grant numbers 451-03-68/2020-14/200178 and 451-03-1/2021-16/14 –0902102).

ORCID iD

Ivana Grković https://orcid.org/0000-0003-4476-7871

Supplemental Material

Supplemental material for this article is available online.

References

Almolda, B., Gonzalez, B., & Castellano, B. (2013). Microglia detection by enzymatic histochemistry. *Methods in Molecular Biology*, *1041*, 243–259. https://doi.org/10.1007/978-1-62703-520-0_22

Antonioli, L., Pacher, P., Vizi, E. S., & Haskó, G. (2013). CD39 and CD73 in immunity and inflammation. *Trends in Molecular Medicine*, *19*, 355–367. https://doi.org/10.1016/j.molmed.2013.03.005

Au, N. P. B., & Ma, C. H. E. (2017). Recent advances in the study of bipolar/rod-shaped microglia and their roles in neurodegeneration. *Frontiers in Aging Neuroscience*, *9*, 128. https://doi.org/10.3389/fnagi.2017.00128

Bernier, L. P., Ase, A. R., Boue-Grabot, E., & Séguéla, P. (2013). Inhibition of $P2X_4$ function by P2Y6 UDP receptors in microglia. *Glia*, *61*, 2038–2049. https://doi.org/10.1002/glia.22574

Boche, D., Perry, V. H., & Nicoll, J. A. (2013). Review: Activation patterns of microglia and their identification in the human brain. *Neuropathology and Applied Neurobiology*, *39*, 3–18. https://doi.org/10.1111/nan.12011

Borroto-Escuela, D. O., Hinz, S., Navarro, G., Rafael Franco, R., Müller, C.E., & Fuxe, K. (2018). Understanding the role of adenosine $A_{2A}R$ heteroreceptor complexes in neurodegeneration and neuroinflammation. *Frontiers in Neuroscience*, *12*, 43. https://doi.org/10.3389/fnins.2018.00043

Braun, N., Sevigny, J., Robson, S. C., Enjyoji, K., Guckelberger, O., Hammer, K., Di Virgilio, F., & Zimmermann, H. (2000). Assignment of ecto-nucleoside triphosphate diphosphohydrolase-1/cd39 expression to microglia and vasculature of the brain. *European Journal of Neuroscience*, *12*, 4357–4366.

Burnstock, G. (2017). Purinergic signalling: Therapeutic developments. *Frontiers in Pharmacology*, *8*, 661. https://doi.org/10.3389/fphar.2017.00661

Campagno, K. E., & Mitchell, C. H. (2021). The $P2X_7$ receptor in microglial cells modulates the endolysosomal axis, autophagy, and phagocytosis. *Frontiers in Cellular Neuroscience*, *15*, 645244. https://doi.org/10.3389/fncel.2021.645244

Chvojkova, M., Kubova, H., & Vales, K. (2021). Effects of dizocilpine, midazolam and their co-application on the trimethyltin (TMT)-induced rat model of cognitive deficit. *Brain Sciences*, *11*. https://doi.org/10.3390/brainsci11030400

Corvino, V., Di Maria, V., Marchese, E., Lattanzi, W., Biamonte, F., Michetti, F., & Geloso, M. C. (2015). Estrogen administration modulates hippocampal GABAergic subpopulations in the hippocampus of trimethyltin-treated rats. *Frontiers in Cellular Neuroscience*, *9*, 433. https://doi.org/10.3389/fncel.2015.00433

Corvino, V., Marchese, E., Michetti, F., & Geloso, M. C. (2013). Neuroprotective strategies in hippocampal neurodegeneration induced by the neurotoxicant trimethyltin. *Neurochemical Research*, *38*, 240–253. https://doi.org/10.1007/s11064-012-0932-9

Costenla, A. R., Cunha, R. A. de Mendonca, A. (2010). Caffeine, adenosine receptors, and synaptic plasticity. *Journal of Alzheimer's Disease*, *20*(Suppl 1), S25–S34. https://doi.org/10.3233/JAD-2010-091384

Delekate, A., Fuchtemeier, M., Schumacher, T., Ulbrich, C., Foddis, M., & Petzold, G.C. (2014). Metabotropic P2Y1 receptor signalling mediates astrocytic hyperactivity in vivo in an Alzheimer's Disease mouse model. *Nature Communications*, *5*, 5422. https://doi.org/10.1038/ncomms6422

Di Virgilio, F., Ceruti, S., Bramanti, P., & Abbracchio, M.P (2009). Purinergic signalling in inflammation of the central nervous system. *Trends in Neurosciences*, *32*, 79–87. https://doi.org/10.1016/j.tins.2008.11.003

Di Virgilio, F., Dal Ben, D., Sarti, A. C., Giuliani, A.L., & Falzoni, S. (2017). The $P2X_7$ receptor in infection and inflammation. *Immunity*, *47*, 15–31. https://doi.org/10.1016/j.immuni.2017.06.020

Dragic, M., Milicevic, K., Adzic, M., Stevanović, I., Ninković, M., Grković, I., Pavle Andjus, P., & Nedeljković, N. (2021). Trimethyltin increases intracellular Ca(2+) Via L-type voltage-gated calcium channels and promotes inflammatory phenotype in rat astrocytes in vitro. *Molecular Neurobiology*. 58(4):1792-1805 https://doi.org/10.1007/s12035-020-02273-x

Dragic, M., Zaric, M., Mitrovic, N., Nedeljković, N., & Grković, I. (2019a). Application of gray level Co-occurrence matrix analysis as a new method for enzyme histochemistry quantification. *Microscopy and Microanalysis*, *25*, 690–698. https://doi.org/10.1017/S1431927618016306

Dragic, M., Zaric, M., Mitrovic, N., Nedeljković. N., & Grković, I. (2019b). Two distinct hippocampal astrocyte morphotypes reveal subfield-different fate during neurodegeneration induced by trimethyltin intoxication. *Neuroscience*, *423*, 38–54. https://doi.org/10.1016/j.neuroscience.2019.10.022

Dunn, K. W., Kamocka, M. M., & McDonald, J. H. (2011). A practical guide to evaluating colocalization in biological microscopy. *American Journal of Physiology-Cell Physiology*, *300*, C723–C742. https://doi.org/10.1152/ajpcell.00462.2010

Erb, L., Woods, L. T., Khalafalla, M. G., & Weisman, G. A. (2019). Purinergic signaling in Alzheimer's disease. *Brain Research Bulletin*, *151*, 25–37. https://doi.org/10.1016/j.brainresbull.2018.10.014

Escartin, C., Galea, E. Lakatos, A., O'Callaghan, J. P., Petzold, G. C., Serrano-Pozo, A., Steinhäuser, C., Volterra, A., Carmignoto, G., Agarwal, A., Allen, N. J., Araque, A., Barbeito, L., Barzilai A., Bergles D. E., Bonvento G., Butt A. M., Chen W. T., Cohen-Salmon M., . . . Verkhratsky A. (2021). Reactive astrocyte nomenclature, definitions, and future directions. *Nature Neuroscience*, *24*, 312–325. https://doi.org/10.1038/s41593-020-00783-4

Ferraz da Silva, I., Freitas-Lima, L. C., Graceli, J. B., & Rodrigues, L. C. M. (2017). Organotins in neuronal damage, brain function, and behavior: A short review. *Frontiers in Endocrinology (Lausanne)*, *8*, 366. https://doi.org/10.3389/fendo.2017.00366

Franke, H., Verkhratsky, A., Burnstock, G., & Illes, P. (2012). Pathophysiology of astroglial purinergic signalling. *Purinergic Signalling*, *8*, 629–657. https://doi.org/10.1007/s11302-012-9300-0

Geloso, M. C., Corvino, V., & Michetti, F. (2011). Trimethyltin-induced hippocampal degeneration as a tool to investigate neurodegenerative processes. *Neurochemistry International*, *58*, 729–738. https://doi.org/10.1016/j.neuint.2011.03.009

Glass, M., Faull, R. L., Bullock, J. Y., Jansen, K., Mee, E. W., Walker, E. B., Synek, B. J., & Dragunow, M. (1996). Loss of A1 adenosine receptors in human temporal lobe epilepsy. *Brain Research*, *710*, 56–68. https://doi.org/10.1016/0006-8993(95)01313-X

Grkovic, I., Drakulic, D., Martinovic, J., & Mitrovic, N. (2019a). Role of ectonucleotidases in synapse formation during brain development: Physiological and pathological implications. *Current Neuropharmacology*, *17*, 84–98. https://doi.org/10.2174/1570159X15666170518151541

Grkovic, I., Mitrovic, N., Dragic, M., Adžić, M., Drakulić, D., & Nedeljković, N. (2019b). Spatial distribution and expression of ectonucleotidases in Rat hippocampus after removal of ovaries and estradiol replacement. *Molecular Neurobiology*, *56*, 1933–1945. https://doi.org/10.1007/s12035-018-1217-3

Haga, S., Haga, C., Aizawa, T., & Ikeda, K. (2002). Neuronal degeneration and glial cell-responses following trimethyltin intoxication in the rat. *Acta Neuropathologica*, *103*, 575–582. https://doi.org/10.1007/s00401-001-0505-5

Hasko, G., & Cronstein, B. (2013). Regulation of inflammation by adenosine. *Frontiers in Immunology*, *4*, 85. https://doi.org/10.3389/fimmu.2013.00085

Haynes, S. E., Hollopeter, G., Yang, G., Kurpius, D., Dailey, M. E., Gan, W. B., & Julius, D. (2006). The P2Y12 receptor regulates microglial activation by extracellular nucleotides. *Nature Neuroscience*, *9*, 1512–1519. https://doi.org/10.1038/nn1805

Hou, X., Li, Y., Huang, Y., Zhao, H., & Gui, L. (2020). Adenosine receptor A1–A2a heteromers regulate EAAT2 expression and glutamate uptake via YY1-induced repression of PPARgamma transcription. *PPAR Research*, *2020*, 2410264. https://doi.org/10.1155/2020/2410264

Hu, Q., Ren, X., Liu, Y., Li, Z., Zhang, L., Chen, X., He, C., & Chen, J. F. (2016). Aberrant adenosine A2A receptor signaling contributes to neurodegeneration and cognitive impairments in a mouse model of synucleinopathy. *Experimental Neurology*, *283*, 213–223. https://doi.org/10.1016/j.expneurol.2016.05.040

Illes, P., Rubini, P., Ulrich, H., Zhao, Y., & Tang, Y. (2020). Regulation of microglial functions by purinergic mechanisms in the healthy and diseased CNS. *Cells*, *9*:1108. https://doi.org/10.3390/cells9051108

Jakovljevic, M., Lavrnja, I., Bozic, I., Milosevic, A., Bjelobaba, I., Savic, D., Sévigny, J., Pekovic, S., Nedeljkovic, N., & Laketa, D. (2019). Induction of NTPDase1/CD39 by reactive microglia and macrophages is associated with the functional state during EAE. *Frontiers in Neuroscience*, *13*, 410. https://doi.org/10.3389/fnins.2019.00410

Koizumi, S., Shigemoto-Mogami, Y., Nasu-Tada, K., Shinozaki, Y., Ohsawa, K., Tsuda, M., Joshi, B. V., Jacobson, K. A., Kohsaka, S., & Inoue, K. (2007). UDP Acting at P2Y6 receptors is a mediator of microglial phagocytosis. *Nature*, *446*, 1091–1095. https://doi.org/10.1038/nature05704

Kotake, Y. (2012). Molecular mechanisms of environmental organotin toxicity in mammals. *Biological & Pharmaceutical Bulletin*, *35*, 1876–1880. https://doi.org/10.1248/bpb.b212017

Kuboyama, K., Harada, H., Tozaki-Saitoh, H., Tsuda, M., Ushijima, K., & Inoue, K. (2011). Astrocytic P2Y(1) receptor is involved in the regulation of cytokine/chemokine transcription and cerebral damage in a rat model of cerebral ischemia. *Journal of Cerebral Blood Flow & Metabolism*, *31*, 1930–1941. https://doi.org/10.1038/jcbfm.2011.49

Latini, L., Geloso, M. C., Corvino, V., Giannetti, S., Florenzano, F., Viscomi, M. T., Michetti, F., & Molinari, M. (2010). Trimethyltin intoxication up-regulates nitric oxide synthase in neurons and purinergic ionotropic receptor 2 in astrocytes in the hippocampus. *Journal of Neuroscience Research*, *88*, 500–509.

Lattanzi, W., Corvino, V., Di Maria, V., Michetti, F., & Geloso, M. C. (2013). Gene expression profiling as a tool to investigate the molecular machinery activated during hippocampal neurodegeneration induced by trimethyltin (TMT) administration. *International Journal of Molecular Sciences*, *14*, 16817–16835. https://doi.org/10.3390/ijms140816817

Lee, S., Yang, M., Kim, J., Kang, S., Kim, J., Kim, J. C., Jung, C., Shin, T., Kim, S. H., & Moon, C. (2016). Trimethyltin-induced hippocampal neurodegeneration: A mechanism-based review. *Brain Research Bulletin*, *125*, 187–199. https://doi.org/10.1016/j.brainresbull.2016.07.010

Liddelow, S. A.Barres, B. A. (2017). Reactive astrocytes: Production, function, and therapeutic potential. *Immunity*, *46*, 957–967. https://doi.org/10.1016/j.immuni.2017.06.006

Little, A. R., Benkovic, S. A., Miller, D. B., & O'Callaghan, J. P. (2002). Chemically induced neuronal damage and gliosis: Enhanced expression of the proinflammatory chemokine, monocyte chemoattractant protein (MCP)-1, without a corresponding increase in proinflammatory cytokines(1). *Neuroscience*, *115*, 307–320. https://doi.org/10.1016/S0306-4522(02)00359-7

Little, A. R., Miller, D. B., Li, S., Kashon, M. L., & O'Callaghan, J. P. (2012). Trimethyltin-induced neurotoxicity: Gene expression pathway analysis, q-RT-PCR and immunoblotting reveal early effects associated with hippocampal damage and gliosis. *Neurotoxicology and Teratology*, *34*, 72–82. https://doi.org/10.1016/j.ntt.2011.09.012

Liu, Y., Imai, H., Sadamatsu, M., Tsunashima, K., & Kato, N. (2005). Cytokines participate in neuronal death induced by trimethyltin in the rat hippocampus via type II glucocorticoid receptors. *Neuroscience Research*, *51*, 319–327. https://doi.org/10.1016/j.neures.2004.12.005

Matyash, M., Zabiegalov, O., Wendt, S., Matyash, V., & Kettenmann, H. (2017). The adenosine generating enzymes CD39/CD73 control microglial processes ramification in the mouse brain. *PLoS One*, *12*, e0175012. https://doi.org/10.1371/journal.pone.0175012

Mitrovic, N., Gusevac, I., Drakulic, D., Stanojlović, M., Zlatković, J., Sévigny, J., Horvat, A., Nedeljković, N., & Grković, I. (2016). Regional and sex-related differences in modulating effects of female sex steroids on ecto-5′-nucleotidase expression in the rat cerebral cortex and hippocampus. *General and Comparative Endocrinology*, *235*, 100–107. https://doi.org/10.1016/j.ygcen.2016.06.018

Mitrovic, N., Zaric, M., Drakulic, D., Martinović, J., Sévigny, J., Stanojlović, M., Nedeljković, N., & Grković, I. (2017). 17beta-estradiol-induced synaptic rearrangements are accompanied by altered ectonucleotidase activities in male rat hippocampal synaptosomes. *Journal of Molecular Neuroscience*, *61*, 412–422. https://doi.org/10.1007/s12031-016-0877-6

Morita, M., Imai, H., Liu, Y., Xu, X., Sadamatsu, M., Nakagami, R., Shirakawa, T., Nakano, K., Kita, Y., Yoshida, K., Tsunashima, K., & Kato, N. (2008). FK506-protective effects against trimethyltin neurotoxicity in rats: Hippocampal expression analyses reveal the involvement of periarterial osteopontin. *Neuroscience*, *153*, 1135–1145. https://doi.org/10.1016/j.neuroscience.2008.01.078

Nedeljkovic, N. (2019). Complex regulation of ecto-5′-nucleotidase/CD73 and A_{2A}R-mediated adenosine signaling at neurovascular unit: A link between acute and chronic neuroinflammation. *Pharmacological Research*, *144*, 99–115. https://doi.org/10.1016/j.phrs.2019.04.007

Ohsawa, K., Sanagi, T., Nakamura, Y., Suzuki, E., Inoue, K., & Kohsaka, S. A. (2012). Adenosine A3 receptor is involved in ADP-induced microglial process extension and migration. *Journal of Neurochemistry*, *121*, 217–227. https://doi.org/10.1111/j.1471-4159.2012.07693.x

Orr, A. G., Orr, A. L., Li, X. J., Gross, R. E., & Traynelis, S. F. (2009). Adenosine A(2A) receptor mediates microglial process retraction. *Nature Neuroscience*, *12*, 872–878. https://doi.org/10.1038/nn.2341

Paiva, I., Carvalho, K.Santos, P., Cellai, L., Pavlou, M. A. S., Jain, G., Gnad, T., Pfeifer, A., Vieau, D., Fischer, A., Buée, L., Outeiro, T. F., & Blum, D. (2019). A2a R-induced transcriptional deregulation in astrocytes: An in vitro study. *Glia*, *67*, 2329–2342. https://doi.org/10.1002/glia.23688

Peterson, T. S., Camden, J. M., Wang, Y., Seye, C. I., Wood, W. G., Sun, G. Y., Erb, L., Petris, M. J., & Weisman, G. A. (2010). P2y2 nucleotide receptor-mediated responses in brain cells. *Molecular Neurobiology*, *41*, 356–366. https://doi.org/10.1007/s12035-010-8115-7

Pompili, E., Fabrizi, C., Fumagalli, L., & Fornai, F. (2020). Autophagy in trimethyltin-induced neurodegeneration. *Journal of Neural Transmission (Vienna)*, *127*, 987–998. https://doi.org/10.1007/s00702-020-02210-1

Popoli, P., & Pepponi, R. (2012). Potential therapeutic relevance of adenosine A2B and A2A receptors in the central nervous system. *Cns & Neurological Disorders Drug Targets*, *11*, 664–674. https://doi.org/10.2174/187152712803581100

Robson, S. C., Sevigny, J.., & Zimmermann, H. (2006). The E-NTPDase family of ectonucleotidases: Structure function relationships and pathophysiological significance. *Purinergic Signalling*, *2*, 409–430. https://doi.org/10.1007/s11302-006-9003-5

Sperlagh, B., & Illes, P. (2007). Purinergic modulation of microglial cell activation. *Purinergic Signalling*, *3*, 117–127. https://doi.org/10.1007/s11302-006-9043-x

Stockwell, J., Jakova, E., & Cayabyab, F. S. (2017). Adenosine A1 and A2A receptors in the brain: Current research and their role in neurodegeneration. *Molecules*, *22*(4), 676. https://doi.org/10.3390/molecules22040676

Tam, W. Y.Ma, C. H. (2014). Bipolar/rod-shaped microglia are proliferating microglia with distinct M1/M2 phenotypes. *Scientific Reports*, *4*, 7279. https://doi.org/10.1038/srep07279

Trabucco, A., Di Pietro, P., Nori, S. L., Fulceri, F., Fumagalli, L., Paparelli, A., & Fornai, F. (2009). Methylated tin toxicity a reappraisal using rodents models. *Archives Italiennes de Biologie*, *147*, 141–153. PMID: 20162863.

Verkhratsky, A., Parpura, V., Pekna, M., Pekny, M., & Sofroniew, M. (2014). Glia in the pathogenesis of neurodegenerative diseases. *Biochemical Society Transactions*, *42*, 1291–1301. https://doi.org/10.1042/BST20140107

Wollmer, M. A., Lucius, R., Wilms, H., Held-Feindt, J., Sievers, J., & Mentlein, R. (2001). ATP And adenosine induce ramification of microglia in vitro. *Journal of Neuroimmunology*, *115*, 19–27. https://doi.org/10.1016/S0165-5728(01)00257-0

Xu, S., Zhu, W., Shao, M., Zhang, F., Guo, J., Xu, H., Jiang, J., Ma, X., Xia, X., Zhi, X., Zhou, P., & Lu, F. (2018). Ecto-5′-nucleotidase (CD73) attenuates inflammation after spinal cord injury by promoting macrophages/microglia M2 polarization in mice. *Journal of Neuroinflammation*, *15*, 155. https://doi.org/10.1186/s12974-018-1183-8

Ye, M., Han, B. H., Kim, J. S., Kim, K., & Shim, I. (2020). Neuroprotective effect of bean phosphatidylserine on TMT-induced memory deficits in a rat model. *International Journal of Molecular Sciences*, *21*(14), 4901. https://doi.org/10.3390/ijms21144901

Yegambaram, M., Manivannan, B., Beach, T. G., & Halden, R. U. (2015). Role of environmental contaminants in the etiology of Alzheimer's disease: A review. *Current Alzheimer Research*, *12*, 116–146. https://doi.org/10.2174/1567205012666150204121719

Zabel, M. K., & Kirsch, W. M. (2013). From development to dysfunction: Microglia and the complement cascade in CNS homeostasis. *Ageing Research Reviews*, *12*, 749–756. https://doi.org/10.1016/j.arr.2013.02.001

Zimmermann, H., Zebisch, M., & Strater, N. (2012). Cellular function and molecular structure of ecto-nucleotidases. *Purinergic Signalling*, *8*, 437–502. https://doi.org/10.1007/s11302-012-9309-4

IV DISKUSIJA

Neurodegenerativne bolesti su vodeći uzrok invaliditeta i različitih stepena nesposobnosti i hendikepa u svetu, a drugi uzročnik smrtnosti. Procenjuje se da ~90 miliona ljudi godišnje umire od neke od neurodegenerativnih bolesti (Wimo et al., 2010). Briga o osobama koje pate od različitih neurodegeneracija predstavlja ogromno ekonomsko i socijalno opterećenje pri čemu indirektni troškovi lečenja pacijenata prevazilaze direktne (Wimo et al., 2010). Iako je značajan broj neurodegenerativnih bolesti poznat već duže od jednog veka, preostaje značajan prostor za unapređivanje terapijskih mogućnosti, koje posedujemo danas..Većina lekova koji su odobreni i indikovani za ove bolesti je simptomatske prirode (Yiannopoulou and Papageorgiou, 2013). Sve neurodegenerativne bolesti su praćene aktivacijom glijskih ćelija, astrocita i mikroglije koje pokreću proces neuroinflamacije. Neuroinflamacija ima za cilj da ograniči povredu, infekciju i/ili uzrok umiranja neurona i ponovo uspostavi homeostazu CNS (Lyman et al., 2014). Neuropatološka stanja su najčešće praćena hroničnom inflamacijom koja doprinosi daljem razvoju i pogoršanju osnovne patologije i kao takva ima negativan uticaj na tok bolesti (DiSabato et al., 2016). Uzimajući u obzir da je celokupna dostupna terapija simptomatska, razumevanje mehanizama i mogućnost kontrole neuroinflamatornog procesa predstavljaju perspektivan pravac za razvijanje novih terapijskih strategija.

Purinska signalizacija kao vid međućelijske komunikacije predstavlja jedan od osnovnih načina komunikacije glijskih i nervnih ćelija, a poseban značaj ima i u iniciranju različitih faza neuroinflamacije. Stoga je regionalna i vremenska karakterizacija ekspresije komponentni purinske signalizacije, kao i utvrđivanje njihove ćelijske lokalizacije neophodno za rekonstrukciju događaja koji dovode/doprinose razvoju neurodegenerativnih bolesti i neuroinflamacije. Utvrđivanje vremenskog i regionalnog obrazca neurodegeneracije u eksperimentalnom modelu neurodegeneracije hipokampusa izazvane trimetil-kalajem, omogućava povezivanje ovih promena sa promenama u ekspresiji komponenti purinskog signalnog sistema, što može dovesti do identifikacije potencijalnih ciljnih mesta za terapijsko delovanje kako u pogledu konkretnog receptora/enzima tako i u pogledu vremenskog okvira kada bi potencijalno terapijsko sredstvo imalo najveći učinak.

1. Trimetil-kalaj izaziva promene ponašanja pacova koje su praćene progresivnim gubitkom piramidnih neurona CA1-CA3 regiona hipokapusa

U skladu sa opštim i specifičnim ciljevima ove doktorske disertacije, praćeno je ponašanje životinja u periodu od tri nedelje nakon intoksikacije, a potom su uočene promene u ponašanju korelisane sa vremenskim i regionalnim profilom neurodegeneracije hipokampusa kod ovarijektomisanih ženki *Wistar* pacova. Jedan od glavnih razloga zbog čega su korišćene ovarijektomisane ženke je taj što mnoge komponentne purinske signalizacije a naročito ektonukleotidaze značajno variraju u zavisnosti od faze estrusnog ciklusa (Mitrović et al., 2016, 2019; Grković et al., 2019b). Takođe, i drugi parametri variraju u zavisnosti od faze estrusnog ciklusa poput nivoa glijskog kiselog fibrilarnog proteina (GFAP) (Arias et al., 2009). S obzirom da su promene genske i proteinske ekspresije ektonukleotidaza u hipokampusu ovarijektomisanih ženki dobro okarakterisane kroz ranije publikovane radove naše grupe, prednost je data ovom model sistemu u odnosu na mužjake.

Iako brojni radovi nedvosmisleno ukazuju da TMK izaziva smrt piramidnih neurona hipokampusa sa odloženim početkom delovanja (2-4 dana nakon intoksikacije) (Haga et al., 2002; Trabucco et al., 2009; Geloso et al., 2011; Lattanzi et al., 2013; Corvino et al., 2015), ne postoji jasno utvrđen vremenski i regionalni profil za najčešće korišćenu dozu (8 mg/kg) kao ni profil ponašanja pacova u prvim nedeljama nakon intoksikacije. Takođe, na osnovu dostupne literature utvrđeno je da ne postoji razlika u profilu neurodegeneracije između ovarijektomisanih i intaktnih ženki, kao i da tretman 17β-estradiolom ne utiče na tok i profil neurodegenrativnih promena nakon intoksikacije TMK (Corvino et al., 2015). Stoga je prvi cilj ove doktorske disertacije bio da se utvrdi vremenski i regionalni profil neurodegeneracije izazvane TMK u hipokampusu ovarijektomisanih ženki pacova i da se prati ponašanje životinja tokom tri nedelje. Prve promene u ponašanju uočene kao pojačana osetljivost na dodir i zvukove i blagi tremor primećene su drugog dana od intoksikacije TMK. Iako tada nije primećena smrt neurona u CA regionima hipokampusa, gotovo svi neuroni su se obojili na fluorožad C (FJC) što ukazuje na aktivan proces neurodegeneracije već nakon dva dana od intoksikacije (Corvino et al., 2015). Četiri dana nakon intoksikacije TMK jasno se uočava gubitak neurona i prisustvo apoptotskih tela i na histološkom i na FJC bojenju u CA1 regionu i mCA3/DG regionu (Balaban et al., 1988; Haga et al., 2002; Little et al., 2012), dok blagi tremor prelazi u sistemski. S obzirom da TMK dovodi do selektivnog propadanja glutamatnih neurona, dok su inhibitorni zaštićeni (Geloso et al., 1997, 2011), uočene promene ponašanja su najverovatnije posledica narušavanja ekscitatorno-inhibitornih sinapsi koje su neophodne za normalno funkcionisanje neurona u hipokampusu (Geloso et al., 2011; Corvino et al., 2013; Lattanzi et al., 2013; Lee et al., 2016). U sedmom danu od intoksikacije, dolazi do oporavka ponašanja, životinje ispoljavaju samo pojačanu osetljivost na dodir i zvuk. Ovo je u skladu sa promenama na histološkom nivou kada se uočava još veći broj apoptotskih tela u CA1 i u mCA3/DG regionu i primetno smanjenje broja neurona te je ova faza označena i kao rana faza neurodegeneracije. S obzirom na to da nema novih aktivnih mesta neurodegeneracije, uočeni boljitak ponašanja je verovatno posledica uspostavljanja ravnoteže i kompenzatornih mehanizama ekscitatorno-inhibtornih sinapsi u hipokampusu (Earley et al., 1992; Geloso et al., 2011). Tri nedelje nakon intoksikacije, kao i u sedmom danu, ne postoje nova mesta neurodegenracije, već se u CA1 i mCA3/DG regionima uočava upečatljiv gubitak neurona, te je ovo označeno kao kasna faza neurodegeneracije, i prisustvo velikog broja tamno obojenih jedara koja su naselila ove regione, a koji ukazuju na intenzivu gliozu, što je i u skladu sa postojećom literaturom (Balaban et al., 1988; Haga et al., 2002; Trabucco et al., 2009; Latini et al., 2010; Little et al., 2012; Corvino et al., 2013, 2015).

2. Neurodegeneracija izazvana trimetil-kalajem praćena je aktivacijom glijskih ćelija

Tokom ispitivanja neurodegenerativnih promena primenom histološkog bojenja, uočeno je progresivno povećanje brojnosti tamno obojenih jedara u sinaptičkim slojevima CA1 i mCA3/DG regiona, što je, na osnovu njihove veličine i pozicije, ukazivalo na prisustvo reaktivne glioze. Reaktivna glioza je proces koji je karakterstičan za patološka stanja nervnog sistema, pri čemu glijske ćelije prolaze kroz promene u regulaciji ekspresije gena, ali i metaboličko, biohemijsko i morfološko remodelovanje. Ove promene za rezultat imaju da reaktivne glijske ćelije dobijaju nove ili da potpuno/delimično gube one funkcije koje imaju u homeostatskim uslovima (Escartin et al., 2021). Jedna od prvih promena koja je odraz aktivacije astrocita i mikroglije je promena njihove morfologije. Na osnovu imunoreaktivnosti

(*ir*) na GFAP u kontrolnim hipokampusima ovarijektomisanih ženki utvrđeno je prisustvo sedam različitih morfo-funkcionalnih podtipova astrocita, što je u skladu sa postojećom literaturom (Kosaka and Hama, 1986; Kálmán and Hajós, 1989), te se može zaključiti da ovarijektomija ne utiče na gubitak ili pojavu novih podtipova astrocita. Detaljna morfološka analiza praćenjem seta morfometrijskih parametara koji procenjuju kompleksnost astrocita ukazala je na jasne razlike u morfološkoj složenosti između astrocita koji se nalaze u CA1 i distalnom CA3 regionu (dCA3) u odnosu na astrocite koji su prisutni u mCA3/DG. Hipokampus u užem smislu (*hippocampus proper*) i zubata vijuga (*gyrus dentatus*), iako funkcionalno povezane predstavljaju dve anatomske strukture, te se postojanje ovakve morfološke heterogenosti može staviti u kontekst postojanja region-specifičnih fizioloških funkcija koje ove ćelije obavljaju a što se reflektuje, delom, i kroz morfološku dihotomiju astrocita u ovim regionima (Zhang and Barres, 2010; Bayraktar et al., 2014).

Shodno postojanju morfološke heterogenosti $GFAP^+$ ćelija u subregionima kontrolnog hipokampusa, intoksikacija TMK dovela je i do aktivacije astrocita specifične za subregione, koja se pre svega ogleda u jasnim razlikama u morfologiji. Aktivacija astrocita je već drugog dana uočena u CA1 regionu i bila je pristuna i u trećoj nedelji nakon intoksikacije. Nakon drugog dana primećena je polarizacija nastavaka reaktivnih astrocita prema piramidnim neuronima CA1 sloja, koji su tako formirali front prema regionu gde je proces neurodegeneracije već počeo. U četvrtom danu uočava se prisustvo astrocita u piramidnom sloju CA1 regiona, što potvrđuje sposobnost ovih ćelija da okruže mesto aktivne neurodegeneracije, izoluju ga od zdravog tkiva, uklanjaju ćelijski debris i tako štite druge regione od sekundarnih povreda (Tasdemir-Yilmaz and Freeman, 2014; Liddelow and Barres, 2017). Iako se domenska organizacija ne može sasvim pouzdano proceniti na osnovu GFAP-*ir* (Oberheim et al., 2008), raspored reaktivnih astrocita nakon intoksikacije ukazuje da oni zadržavaju svoju domensku organizaciju i nastavljaju da u određenoj meri obavljaju funkcije koje doprinose zaštiti neoštećenih ćelija i održavanju zdravih sinapsi (Heller and Rusakov, 2015; Kelly et al., 2018) . Detaljna morfometrijska analiza $GFAP^+$ ćelija CA1 regiona pokazala je da je fraktalna dimenzija, glavna mera kompleksnosti ćelijske morfologije (Montague and Friedlander, 1989, 1991), povećana od drugog dana nakon intoksikacije TMK i da se te vrednosti zadržavaju tokom prve nedelje. Iako ovaj parametar nije promenjen u prvih sedam dana, gotovo svi drugi morfometrijski parametri ukazuju na to da je aktivacija astrocita nakon izlaganja TMK dinamičan proces, koji podrazumeva kontinuirano remodelovanje (Sun and Jakobs, 2012). Sumarno, na osnovu svih parametara, astrociti CA1 regiona pokazuju povećanje kompleksnosti od drugog dana nakon intoksikacije koje se zadržava kroz sve posmatrane tačke. Interesantno je da je broj sekundarnih grana $GFAP^+$ ćelija CA1 regiona povećan već nakon drugog dana od intoksikacije kada nije primećena smrt neurona. Shodno tome, ovaj parametar bi mogao biti kandidat za morfološki *alarmin*, odnosno, promenu koja bi upućuvala na postojanje određenih patoloških dešavanja u tkivu (Yeh et al., 2011). Astrociti mCA3/DG regiona pokazali su drugačiji obrazac aktivacije. Inicijalni odgovor ovih astrocita, u drugom danu intoksikacije bio je kao i u CA1 regionu, klasična hipertrofija, praćena povećanjem površine i fraktalne dimenzije. Već od četvrtog dana uočava se postepen prelazak iz hipetrofije u morfološki stadijum koji se može opisati kao *atrofija*. U sedmom danu nakon intoksikacije gotovo svi astrociti u ovom regionu imaju krupna ćelijska tela značajno manje površine i manji broj primarnih i sekundarnih grana, što ukazuje na smanjenje ukupne morfološke složenosti (Olabarria et al., 2010; Yeh et al., 2011; Kulijewicz-Nawrot et al., 2012; Plata et al., 2018). Šolova analiza razgranatosti $GFAP^+$ ćelija potvrdila je atrofiju primarnih i

sekundarnih grana što jasno ukazuje na smanjenje domena koje ovakva ćelija zauzima (Plata et al., 2018). Jedna od karakteristika ranih stadijuma epilepsije, AD i nekih psihijatriskih bolesti jeste prisustvo hipetrofiranih astrocita u CA regionima i atrofiranih astrocita u hilarnom regionu (Verkhratsky et al., 2014; Lee and MacLean, 2015; Rodríguez-Arellano et al., 2016). Smanjenje prostornog domena, odnosno površine koju atrofičan astrocit pokriva ukazuje na smanjenu funkcionalnu podršku neuronima, što utiče na električnu i sinaptičku aktivnost, kao i preživljavanje neurona (Rodríguez-Arellano et al., 2016; Plata et al., 2018). Stoga i atrofija astrocita može biti kontributivni faktor neurodegeneracije, jer je naročito izražena u mCA3/DG regionu. Kako je ovaj region mesto glavnih aferentnih ulaza iz entorinalne kore, koja je takođe meta delovanja TMK (Balaban et al., 1988), atrofija astrocita i potencijalno smanjeno preuzimanje adenozina u ove ćelije može biti uzročni faktor epileptičnih napada, a može doprineti kognitivnom deficitu koji je karakterističan za životinje izložene TMK (Trabucco et al., 2009; Geloso et al., 2011).

Osim morfometrijskih parametara, ne postoji pouzdani funkcionalni marker koji bi se mogao pripisati isključivo atrofičnim astrocitima (Rodríguez-Arellano et al., 2016). Stoga je u cilju ispitivanja daljih razlika, osim promena u morfologiji astrocita, ispitana ekspresija vimentina (VIM) i nestina (NEST), čija se ekspresija naročito povećava u patološkim stanjima (Andersson et al., 1994; Pekny and Nilsson, 2005; Gilyarov, 2008). Imunobojenje je pokazalo da su VIM^+ ćelije ograničene na region mCA3/DG i prisutne samo u sedmom danu nakon intoksikacije, što je dodatni pokazatelj reaktivnog fenotipa astrocita i mesta aktivne neurodegeneracije (Pekny and Nilsson, 2005; Kelso et al., 2011). Za razliku od VIM^+ ćelija, $NEST^+$ ćelije su bile manje brojne i lokalizovane samo oko mesta lezija. Oba markera su kolokalizovala sa $GFAP^+$ astrocitima, a poglavito sa onima sa atrofičnom morfologijom. S obzirom na to da se ova dva proteina često eksprimiraju na prekursorskim i proliferativnim ćelija, ispitan je funkcionalni marker astrocita Kir4.1, koji je negativno korelisan sa ćelijskom deobom (Gilyarov, 2008; Stewart et al., 2010). Kir4.1 se eksprimira na svim $GFAP^+$ ćelijama, kao i na VIM^+ i $NEST^+$ ćelijama, a dominantna distribucija po granama i telu astrocita upućuje na to da ove ćelije nisu proliferativne, kao i da uspešno regulišu proteinsku ekspresiju te da morfološka atrofija astrocita u ovom regionu prethodi eventualnim funkcionalnim promenama (Cone, 1970; Higashimori and Sontheimer, 2007). Dosadašnja istraživanja definisala su određeni konsezus o tipovima promena astrocita u neuropatologijama koja se ogledaju u promeni broja reaktivnih astrocita, remodelovanju morfologije ili reaktivnoj astrogliozi (Plata et al., 2018). Specifična kombinacija ovih promena može biti svojstvena neuropatologiji ili karakterisati određeni stadijum u njenoj progresiji (Verkhratsky and Parpura, 2016). U stanjima koja se mogu okarakterisati kao blaže ili umerene povrede/patologije CNS, reaktivni astrociti najčešće imaju očuvanu domensku organizaciju, ne migriraju, pokazaju različit stepen hipertrofije i ne poseduju proliferativni potencijal (Rodríguez-Arellano et al., 2016; Verkhratsky and Parpura, 2016). Rezultati morfometrijske analize i drugih parametara upućuju na to da reaktivna astroglioza koja se razvija kao odgovor na neurodegeneraciju izazvanu TMK ima dihotomu prirodu u ranim fazama neurodegeneracije., Reaktivna glioza u CA1 regionu može se opisati kao umerena pri čemu astrociti iskazuju klasičnu hipertrofiju i zadržavaju domensku organizaciju. U mCA3/DG regionu uočeno je dinamično morfološko remodelovanje koje je vodilo ka atrofiji astrocita. Razlike u odgovoru astrocita ovih regiona, barem delom, verovatno potiču i od prvobitne razlike u njihovoh morfologiji koja se uočava u kontroli. Takođe, CA1 i mCA3/DG imaju različitu citoarhitekturu koja se ogleda u broju neurona, gustini sinapsi kao i aferentnih i eferentnih veza. Sve ove razlike doprinose

nastajanju specifičnog mikrookruženja, koje posredno može uticati i na morfologiju astrocita koji se u njima nalaze (Kosaka and Hama, 1986; Zhang and Barres, 2010). Selektivna osetljivost hipokampalnih regiona pokazana je u nekoliko neuropatologija koje uključuju epilepsiju slepoočnog režnja, ishemiju i AD (Morrison and Hof, 2002; Geddes et al., 2003; Ouyang et al., 2007; Lévesque and Avoli, 2013). Na osnovu obrasca neurodegeneracije koju izaziva TMK, kao i razlika koje su uočene u morfologiji astrocita, može se pretpostaviti da je primarno mesto delovanja toksina mCA3/DG region, dok CA1 region strada kao posledica sekundarnih efekata intoksikacije poput epileptičnih napada i ekscitotoksičnosti (Trabucco et al., 2009).

Pored reaktivne astroglioze, u modelu neurodegeneracije izazane TMK prisutna je veoma izražena aktivacija ćelija mikroglije (Geloso et al., 2011). Aktivacija mikroglije kasni u odnosu na aktivaciju astrocita, pa se tako u drugom danu uočava tek poneka aktivirana mikroglija u svom početnom stupnju aktivacije, sa blago uvećanim ćelijskim telom i zadebljalim nastavcima (Haga et al., 2002). Već u četvrtom danu nakon intoksikacije primećen je značajan porast broja $Iba1^+$ ćelija, usled migracije ili proliferacije rezidentnih ćelija (Little et al., 2002). Ove ćelije odlikuje dominanto žbunasta (*engl. bushy*) ili štapolika (*engl. rod*) morfologija. Najviše $Iba1^+$ ćelija primećeno je u sinaptičkim slojevima, gde su preovladavale ćelije štapolikog oblika, naročito u *stratum radiatum*. Neke od ovih ćelija, samo u CA1 regionu, bile su postavljene u nizu, što se uočava u drugim patologijama (engl. *train formation*). Ova pojava bila je uočljiva u četvrtom i naročito u sedmom danu nakon intoksikacije, da bi nakon tri nedelje dominantna forma bila okruglasta/ameboidna forma. Štapolika forma mikroglije je karakteristična za ranu fazu neurodegeneracije i obično je povezana sa neoštećenim neuronima i aksonima (Zabel and Kirsch, 2013; Au and Ma, 2017), što ukazuje na njenu protektivnu i reparativnu ulogu (Boche et al., 2013). Takođe, štapolika mikroglija može biti izvor novih ćelija ili se transformisati u ameboidnu mikrogliju (Tam and Ma, 2014). Tri nedelje nakon intoksikacije, gotovo čitav piramidni sloj CA1 i mCA3/DG regiona bio je prekriven ameboidnim $Iba1^+$ ćelijama. Na osnovu dobijenih rezultata može se izvesti zaključak da se mikroglija aktivira sa zakašnjenjem u odnosu na reaktivne astrocite i da pretežno zauzima neuroprotektivni funkcionalni status, sličan M2 tipu .

3. Neurodegeneracija izazvana trimetil-kalajem dovodi do promena aktivnosti i ekspresiji NTPDaze 1 i eN

Kao posledica smrti neurona, u vanćelijsku sredinu se oslobađaju velike količine ATP koji deluje kao DAMP molekul i ostvaruje efekte posredstvom P2 receptora (Pietrowski et al., 2021). Višak oslobođenih nukleotida iz spoljašnje sredine uklanjaju NTPDaze, koje hidrolizom ATP do ADP i ADP do AMP, stvaraju supstrat za eN, koja obavlja finalno razlaganje i oslobađa adenozin a koji svoje efekte ostvaruje preko P1 receptora (Borea et al., 2018). Iako za većinu ektonukleotidaza danas postoje antitela, mnoga od njih ne uspevaju da specifično prepoznaju sva mesta na kojima se ovi enzimi eksprimiraju i/ili pokazuju aktivnost (Langer et al., 2008). Stoga je jedna od pouzdanih tehnika koja omogućava da se utvrdi veza između prostorne distribucije i aktivnosti ovih enzima metoda enzimske histohemije (Langer et al., 2008; Grković et al., 2019b). Metodom enzimske histohemije ispitan je obrazac aktivnosti ATPaze, ADPaze i AMPaze nakon intoksikacije TMK. Primenom ATP i ADP kao supstrata uočeno je jasno bojenje ćelija koje po svojoj morfologiji odgovaraju mikrogliji i potvrđuju dominantnu lokalizaciju NTPDaze1 na ovim ćelijama (Braun et al., 2000; Almolda et al.,

2013). U prva četiri dana nakon intoksikacije, kroz čitav hipokampus uočeno je bojenje ćelijskih elemenata koje po svojoj morfologiji odgovaraju poziciji i obliku Iba1$^+$ ćelija a dominanto u regionima aktivne neurodegeneracije. U kasnijim vremenskim tačkama, intenzivno bojenje uočeno je na svim ćelijskim elementima koje po svojoj morfologiji odgovaraju Iba1$^+$ ćelijama, nezavisno od njihove morfologije, što upućuje da je pojačana aktivnost NTPDaze1 nezavisna od morfologije ćelija. Za razliku od NTPDaze1, aktivnost eN uočena je tek od četvrtog dana, sporadično, intenzitet bojenja progresivno raste, i dostiže svoj maksimum tri nedelje nakon intoksikacije, jasno bojeći okruglaste ćelijske elemente koji su zašli u CA1 i mCA3/DG neuronski sloj. Razlika u lokalizaciji i aktivnosti NTPDaze 1 i eN može biti indikator adaptacije ovih ćelijskih elemenata na specifične uslove mikrosredine, kao i na različiti stepen neurodegeneracije u subregionima hipokampusa (Wollmer et al., 2001; Boche et al., 2013). Enzimska histohemija je, iako pouzdana i reproducibilna, kvalitativna metoda jer olovo-fosfat koji se akumulira na mestu hidrolitičke aktivnosti enzima nije direktno proporcionalan količini supstrata koju je enzim razložio (Wachstein and Meisel, 1957; Wagner et al., 1972). Stoga nije moguće izvući pouzdane zaključke o finim i diskretnim promenama u aktivnosti, kakve su uočene za aktivnost eN. U ovakvim situacijiama *in vitro* enzimski eseji takođe mogu prikriti *smer* promene aktivnosti, pogotovo ukoliko se eN gubi zajedno sa umiranjem sinapsi a pojavljuje na drugim ćelijskim elementima, što je slučaj u neurodegeneraciji izazvanoj TMK. Zato je u cilju pouzdane kvantifikacije enzimske histohemije primenjena teksturalna analiza kao napredna tehnika analize slike koja ima široku primenu u medicini i biologiji (Tixier et al., 2012; Kim et al., 2015; Tesic et al., 2017). Primena teksturalne analize omogućava kvantifikaciju i opisivanje određenih svojstava mikrografija, kao što su stepen homogenosti ili neuređenosti, koje nisu vidljive ljudskom oku, a istovremeno nudi mogućnost kvantifikacije tih parametara i njihovu statističku validaciju (Pantic et al., 2014). Parametri koje teksturalna analiza uzima u obzir dobijaju se primenom statistike drugog reda koja računa vrednosti osnovnih elemenata digitalne slike – *piksela* u digitalnim mikrografijama (Park et al., 2011). Aktivnost eN je prevashodno lokalizovana na sinapsama u kontrolnom hipokampusu, te je uočeno bojenje *stratum oriens* i *stratum radiatum*, dok se sloj piramidnih neurona ne boji (Grković et al., 2019b). Sedam dana nakon intoksikacije TMK dolazi do neznatnog slabljenja bojenja u neuropilu, dok piramidni sloj CA1 regiona kao i mCA3/DG biva naseljen tamnim depozitima AMPazne aktivnosti. Ove depozicije bojenja smanjuju površinu neobojenog piramidnog regiona, te su parametri teksturalne analize ukazali da su ovi regioni kvantitativno više homogeni od onih u kontroli (Park et al., 2011; Pantic et al., 2014; Tesic et al., 2017). Homogenost dalje ukazuje na to da je sličnost susdenih piksela na mikrografiji statistički značajno veća, odnosno da je došlo do pojačanog bojenja koje je sada uniformnije, što odgovara velikom broju okruglastih depozita koji se nalaze u CA1 i mCA3/DG regionu (Park et al., 2011; Tixier et al., 2012). Na osnovu primene teksturalne analize i vrednosti njenih parametara možemo zaključiti da je došlo do povećane aktivnosti eN, naročito u regionima aktivne neurodegeneracije.

U cilju identifikacije bojenih depozita koji su uočeni na enzimskoj histohemiji, primenjena je metoda imunohistohemije. Imunohistohemijsko bojenje na NTPDazu 1 i eN potvrdilo je uočene promene na enzimskoj histohemiji. NTPDaza1 kolokalizovala je praktično sa svim Iba1$^+$ ćelijama, dok je eN kolokalizovala isključivo sa Iba1$^+$ ćelijama ameboidne morfologije, čiji broj je bio najveći u kasnoj fazi neurodegeneracije. Analiza genske ekspresije je pokazala statistički značajan porast aktivnosti NTPDaze 1 u prvoj i trećoj nedelji, dok je eN bila povećana tek nakon tri nedelje od davanja TMK. Na osnovu dobijenih rezultata može se

zaključiti da postoji porast aktivnosti NTPDaze 1 i eN, a da je porast NTPDaze 1 region- i ćelijski-nespecifični fenomen, dok je eN specifično lokalizovana na $Iba1^+$ ćelijama okruglastog oblika. Povećana aktivnost NTPDaze1 i eN može predstavljati svojevrstan kompenzatorni mehanizam uklanjanja velike količine ATP koji se oslobađa iz oštećenih ćelija (Braun et al., 2000; Burnstock, 2017). Takođe, povećana aktivnost NTPDaze 1 može sprečiti desenzitizaciju receptora, koja se dešava usled produženog izlaganja visokim koncentracijama ATP, što bi posledično zaustavilo i preteranu aktivaciju P2 receptora na mikroglijskim ćelijama (Di Virgilio et al., 2009). Sa druge strane, ekspresija eN na ameboidnim $Iba1^+$ ćelijama verovatno doprinosi lokalnom povećanju koncentracije adenozina koji ostvaruje neuro- i imunomodulatorna svojstva (Di Virgilio et al., 2009; Illes et al., 2020), a čiji će ukupni efekat zavisiti od ekspresije P1 receptora (Nedeljkovic, 2019). Ova dva proteina osim svojih katalitičkih funkcija, ostvaruju i druge ne-enzimske uloge, kao adhezivni molekuli, regulišući adheziju i ćelijsku migraciju kroz interakciju sa različtim komponentama vanćelijskog matriksa (Wu et al., 2006). Stoga je moguće da specifična ekspresija NTPDaze1/eN na ameboidnoj mikrogliji pored katalitičke uloge ostvaruje i ulogu u migraciji te omogućava njeno ukotvljavanje na mestima aktivne neurodegeneracije, gde su ove ćelije i uočene.

4. Neurodegeneracija izazvana trimetil-kalajem uzrokuje promene ekspresije P2 i P1 receptora

ATP i adenozin svoje efekte ostvaruju delujući na različite purinske P2 i P1 receptore, čiji se repertoar značajno menja u patološkim stanjima (Pietrowski et al., 2021). Među ispitanim receptorima, $P2X_7R$, $P2Y_1R$, $P2Y_{12}R$ i svi P1 receptori, pokazuju bifazni odgovor nakon intoksikacije TMK, a to se ne uočava kod $P2X_4$, $P2Y_2$, $P2Y_6$. U drugom i četvrtom danu uočava se statistički značajan pad u genskoj ekspresiji, koji se potom u sedmom danu ili vraća na kontrolne vrednosti ili ih prevazilazi da bi tri nedelje nakon intoksikacije, nivoi iRNK gotovo svih receptora bili povišeni u odnosu na odgovarajuću kontrolu. Pretpostavlja se da je ovo prolazno smanjenje u prvim danima nakon intoksikacije posledica ćelijskog stresa usled delovanja toksina kao i povećanog nivoa kortikosterona koji su detektovani nakon TMK (Tsutsumi et al., 2002). S obzirom na to da se neurodegeneracija i smrt neurona uočavaju od četvrtog dana a intenzivno u prvoj i trećoj nedelji, povećana genska ekspresija $P2X_4$, $P2Y_2$ i $P2Y_6$, koji su uključeni u regulaciju fagocitoze, ukazuju na to da se ovaj proces aktivno odvija već u ranoj fazi neurodegeneracije (Illes et al., 2020). Uočeno je i kašnjenje aktivacije mikroglije u odnosu na astrocite, koje postaje vidljivo tek oko četvrtog dana od intoksikacije. Migracija mikroglije, kao glavnih fagocitirajućih ćelija u CNS, i njena hemotaksija je regulisana purinskom signalizacijom posredstvom P2 receptora (Koizumi et al., 2007; Illes et al., 2020). Takođe i sama tranzicija iz migratorne u ameboidnu formu posredovana je aktivacijom različtih P2 receptora (Illes et al., 2020). Jedan od glavnih receptora uključenih u migraciju i hemotaksiju mikroglije je $P2Y_{12}$ receptor, čija je relativna genska ekspresija povećana sedam dana nakon intoksikacije. S obzirom da je neurodegeneracija u ovoj vremenskoj tački izražena, verovatno je da oslobođeni ATP iz umirućih neurona deluje kao hemoatraktant i podstiče migraciju mikroglijskih ćelija na mesta povrede, što je i u saglasnosti sa enzimskom histohemijom i imunobojenjem (Illes et al., 2020). Uočeno povećanje genske ekspresije $P2X_4$ receptora takođe može ukazati na migratorna i sekretorna svojstva reaktivne mikroglije, a u interakciji sa $P2Y_{12}$ receptorom učestvuje u regulisanju procesa hemotaksije (Illes et al., 2020). Pored migratorne, jedna od glavnih funkcija reaktivne mikroglije je fagocitoza, te je

ispitana i ekspresija jednog od glavnih regulatora ovog procesa – $P2Y_6$ receptora (Xu et al., 2016). Uočeno je povećanje genske ekspresije $P2Y_6$ receptora koje koincidira sa početkom umiranja/degeneracije neurona, kada se pored ATP oslobađa i UDP koji deluje na ovaj receptor i podstiče fagocitozu (Illes et al., 2020). Pored P2 receptora, i adenozinski receptori učestvuju u regulisanju pokretljivosti mikroglije, od kojih se posebno izdvaja A_3 receptor (Ohsawa et al., 2012). Porast genske ekspresije ovog receptora nakon intoksikacije, a naročito koaktivacija $P2Y_{12}/A_3$ receptora aktivno doprinosi migraciji prema mestima aktivne neurodegeneracije (Haynes et al., 2006; Ohsawa et al., 2012). Primećen je i porast u genskoj ekspresiji $P2X_7$ receptora, koji najverovatnije doprinosi aktivaciji i inflamatornom statusu glijskih ćelija u ranoj i kasnoj fazi neurodegeneracije izazvane TMK (Illes et al., 2020). Kako je većina odabranih P2 receptora prevashodno svojestvena mikroglijskim ćelijama, ispitana je i ekspresija glavnog P2 receptora astrocita, $P2Y_1$, koji reguliše inflamacijski status kao i astrocit-astrocit signalizaciju putem jona Ca^{2+} (Kuboyama et al., 2011; Delekate et al., 2014). I u prvoj i u trećoj nedelji nakon intoksikacije uočeno je značajno povećanje genske ekspresije $P2Y_1$ što dodatno potvrđuje rezultate o statusu reaktivnih astrocita. Na osnovu dobijenih rezultata, jasno se uočava vremenski-zavisna promena u genskoj ekspresiji purinskih receptora i to onih koji su uključeni u procese migracije, fagocitoze i regulacije imunomodulatornog i inflamatornog odgovora.

5. Neurodegeneracija izazvana trimetil-kalajem uzrokuje inflamatornu aktivaciju glijskih ćelija

U literaturi nema mnogo podataka o inflamatornom statusu nakon intoksikacije TMK kod *Wistar* pacova, ili su studije rađene u prvim danima od davanja toksina kada nije pronađeno povećanje ekspresije molekula inflamacije (Little et al., 2002) ili su rađene na drugim sojevima (Little et al., 2012). Ispitani pro- i antiinflamacijski faktori (TNF-α, IL-1β, IL-6, iNOS, IL-10, Arg-1, C3, S100a10) pokazuju identičan trend u prva četiri dana kao i purinski receptori, smanjenje genske ekspresije (podaci nisu prikazani) koje je praćeno porastom prve nedelje nakon intoksikacije koji dostiže kontrolne vrednosti (IL-1β, IL-6, IL-10), ili ih prevazilazi (TNF-α, iNOS, C3, S100a10), dok je genska ekspresija Arg-1 značajno niža. Tri nedelje nakon davanja TMK, genska ekspresija TNF-α i Arg-1 se vraća na kontrolne vrednosti, dok su svi ostali ispitani geni pokazali porast u odnosu na odgovarajuću kontrolu. Ćelije odgovorne zaoslobađanje inflamacijskih faktora identifikovane su imunofluorescentnim bojenjem i kolokalizacijom ispitivanih faktora inflamacije sa markerima astrocita i mikroglije. Na osnovu takve analize utvđeno je da samo $GFAP^+$ ćelije eksprimiraju iNOS, C3, TNF-α, IL-1β i IL-10, NF-κB, naročito u kasnoj fazi neurodegeneracije. Ovaj rezultat zajedno sa rezultatima genske ekspresije jasno ukazuje da reatkivna astroglioza u modelu neurodegeneracije izazvane TMK poseduje složen i jedinstven molekulski potpis sa predominatno inflamacijskim fenotipom (Escartin et al., 2021). Astrociti su prve ćelije koje su reagovale na intoksikaciju *in vivo* promenom morfologije već posle dva dana, te je pretpostavljeno da TMK direktno ostvaruje efekat na ove ćelije (Dragić et al., 2021a). Jedna od *in vitro* studija ukazala je da TMK narušava Ca^{2+} signalizaciju astrocita, što je jedna od glavnih karakteristika koja se viđa i u drugim neurodegenerativnim poremećajima (Lim et al., 2014; Dragić et al., 2021a). Ovaj poremećaj je posledica aktivacije L-tipa voltažno-zavisnih kanala za Ca^{2+}, čija je aktivna uloga u inicijaciji reaktivne astroglioze potvrđena u nekoliko različitih eksprimentalnih *in vitro* i *in vivo* modela (Cheli et al., 2016). Tretman astrocita u kulturi TMK u trajanju od 24h pokrenuo je inflamacijski odgovor na gotovo svim genima koji su ispitani u *in vivo* modelu i značajno

povećao parametre oksidativnog stresa, što zajedno ukazuje da TMK ima sposobnost da direktno utiče na astrocite i izazove nastanak inflamacijskog fenotipa. Ranija *in vitro* istraživanja takođe su ukazala da TMK može da aktivira astrocite, ali ne i ćelije mikroglije, već da se one mogu aktivirati samo u ko-kulturi sa astrocitima (Röhl and Sievers, 2005). Kako su astrocitni nastavci glavni činioci KMB, moguće je da TMK koji se postepeno prelazi iz krvi u parenhim mozga (Geloso et al., 2011), prvo aktivira astrocita što se manifestuje kao reaktivna glioza uočena u drugom danu, što ili prethodi ili se dešava istovremeno sa procesom neurodegeneracije.

Sa druge strane, ćelije mikroglije nisu kolokalizovane ni sa jednim ispitivanim markerom inflamacije, ali su u ranoj fazi neurodegeneracije gotovo sve ćelije bile pozitivne na CD68 i Arg-1. Tri nedelje nakon davanja toksina, broj $CD68^+$/$Arg\text{-}1^+$/$Iba1^+$ ćelija je opao i mogao se uočiti samo oko mesta aktivne neurodegeneracije. Povećana ekspresija NTDPaze 1 na reaktivnoj mikrogliji je pokazana i u drugim patologijama CNS poput eksperimentalnog autoimunskog encefalomijelitisa, gde je utvrđeno da je ova NTPDaza predominantno poveazana sa $Arg\text{-}1^+$ i $CD68^+$ Iba1 ćelijama (Jakovljevic et al., 2019). Povećana ekspresija i specifična lokalizacija eN na ameobidnoj mikrogliji koja je takođe asocirana sa Arg-1 i CD68 tokom neurodegeneracije izazvane TMK ukazuju na mogućnost da ove ćelije vrše fagocitozu i da učestvuju u reparaciji tkiva (Xu et al., 2018), dok su astrociti glavni izvor faktora inflamacije.

6. Neurodegeneracija izazvana trimetil-kalajem dovodi do ekspresije specifičnog repertoara purinskih receptora na glijskim ćelijama

Purinska signalizacija je bitan regulatorni sistem koji doprinosi normalnom funkcionisanju neurona i glijskih ćelija u uslovima homeostaze. Patološka stanja dovode do narušavanja purinskog signalnog sistema što za posledicu ima promenu repertoara purinskih receptora na glijskim ćelija koji je najčešće specifičan za patologiju ili stadijum u njenoj progresiji (Pietrowski et al., 2021). Na osnovu rezultata genske ekspresije i značaja za razvoj patoloških stanja, izabran je set purinskih receptora čija je lokalizacija ispitana ($P2X_7R$, $P2Y_1R$, $P2Y_{12}R$, A_1R, $A_{2A}R$) u prvoj i trećoj nedelji nakon intoksikacije TMK (Lassmann et al., 2007; Pietrowski et al., 2021). Ove dve vremenske tačke su izdvojene od ostalih na osnovu histološkog profila neurodegeneracije kao i na osnovu promena u genskoj ekspresiji. U prvoj nedelji od intoksikacije veliki broj neurona je bio $P2X_7R$ imunoreaktivan, dok je u trećoj nedelji ameboidna mikroglija pokazala imunoreaktivnost na $P2X_7R$. S obzirom da je pokazano da $P2X_7R$ učestvuje u regulaciji fagocitoze, verovatno je da je u neurodegeneraciji izazvanoj TMK ameboidna mikroglija ima ulogu u procesu fagocitoze i uklanjanja ćelijskog debrisa (Campagno and Mitchell, 2021). Neophodni preduslov da se proces fagocitoze pokrene je da su ćelije mikroglije migrirale na mesto povrede. U ranim fazama neurodegeneracije $Iba1^+$ ćelije pokazuju visok nivo ekspresije $P2Y_{12}R$ receptora, nezavisno od morfologije, što upućuje na migratorno stanje, odnosno da se ove ćelije kreću prema mestu povrede (Haynes et al., 2006), verovatno prateći ATP/UTP signal koji se oslobađa iz umirućih neurona. Kako ova mikroglija eksprimira i NTPDazu 1 i eN, enzimski tandem koji efikasno razgrađuje ATP do adenozina, moguće je da ovaj specifični repertoar purinskih receptora i enzima predstavlja ‘’imunološki prekidač’’ koji doprinosi stvaranju anti-inflamacijske mikrosredine (Antonioli et al., 2013), uklanjajući visok nivo ATP na putu migracije.

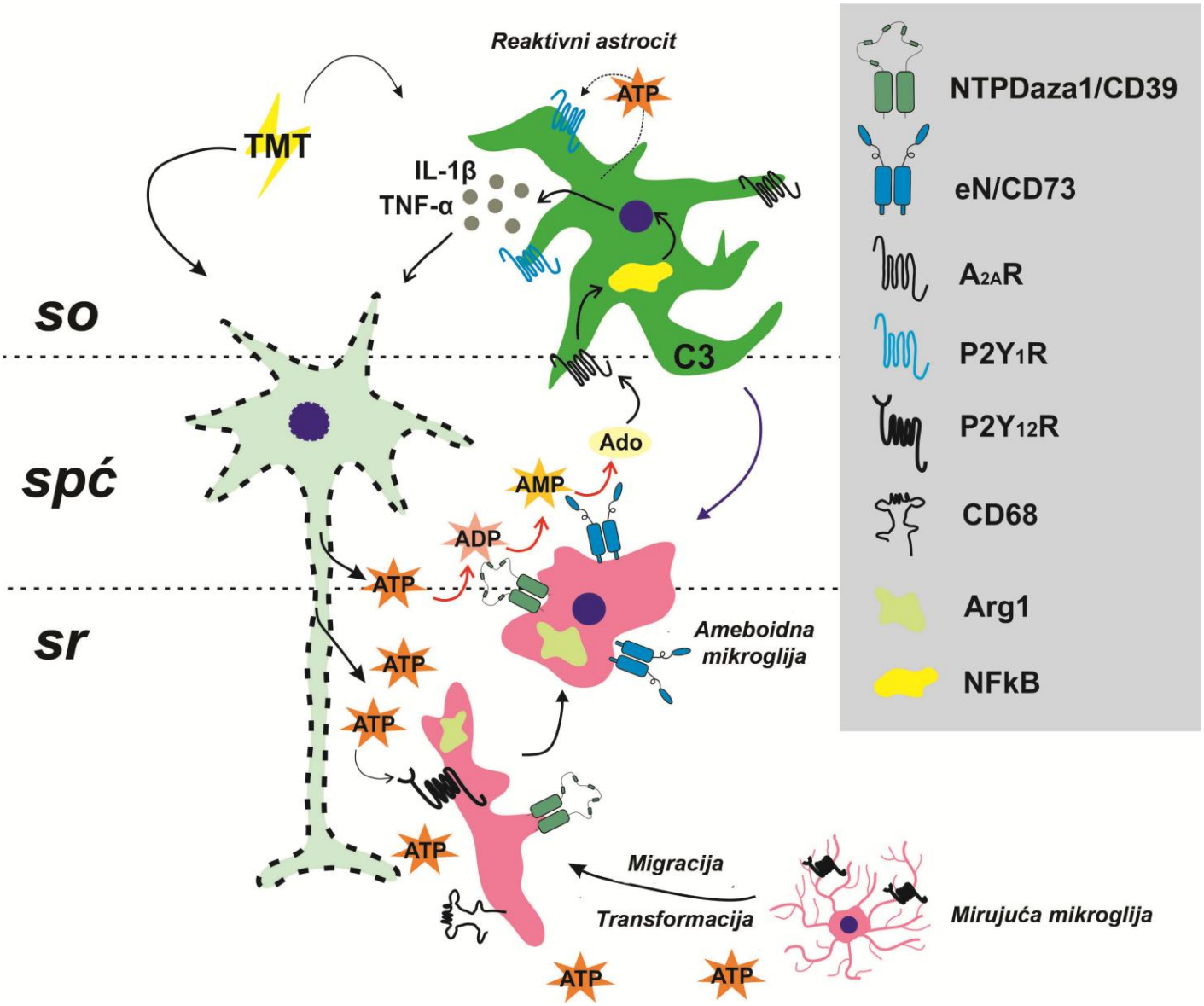

Slika 5. Uloga purinskog signalnog sistema u modelu neurodegeneracije izazvane trimetil-kalajem – *pretpostavljeni mehanizam* (opis u tekstu)

Sa druge strane, proinflamacijski astrociti u regionima neurodegeneracije pokazuju povećanu ekspresiju $P2Y_1R$ receptora, kao i adenozinskih A_1R i $A_{2A}R$ receptora. U fiziološkim uslovima u hipokampusu, adenozin ostvaruje svoje efekte prevashodno preko A_1 receptora, koji je dominantno eksprimiran na neuronima, i moduliše važne procese poput učenja i pamćenja (Costenla et al., 2010). Nakon intoksikacije TMK, u obe vremenske tačke uočava se gubitak neuronskog A_1R receptora, koji je verovatno uzrokovan gubitkom neurona, ali i njegovo eksprimiranje na reaktivnim astrocitima. Ovaj gubitak A_1R receptora može dodatno da učini neurone podložnim sekundarnim efektima TMK kakvi su epileptični napadi, s obzirom da adenozin ispoljava neuroprotektivno i antikonvulzivno dejstvo (Glass et al., 1996). Takođe,

neurodegenerativne promene praćene neuroinflamacijom dovode do povećanja genske i proteinske ekspresije $A_{2A}R$ receptora u hipokampusu, a signalizacija posredovana ovim receptorom doprinosi daljem razvoju neuroinflamacije i kognitivnom deficitu (Hu et al., 2016) koje se viđaju i u neurodegeneraciji izazvanoj TMK (Geloso et al., 2011). Produžena stimulacija astrocitnog A_1R receptora u njegovom sadejstvu sa $A_{2A}R$ receptorom mogu pojačati neurotoksičnost koja je posredovana $A_{2A}R$ receptorom u neurodegenerativnim bolestima (Stockwell et al., 2017). Pokazano je postojanje heteromernog kompleksa A_1R-$A_{2A}R$ receptora u neurodegenreracijama, za koje je utvrđeno da doprinose poremećaju homeostaze glutamata i time podstiču ekscitotoksičnost (Borroto-Escuela et al., 2018; Hou et al., 2020). S obzirom da se nakon intoksikacije TMK oslobađaju velike količine ATP koji se degraduje od strane $Iba1^+$/$NTPDaza1^+$/eN^+ ćelija do adenozina, moguće je da ovako lokalno produkovani adenozin aktivira A_1R i $A_{2A}R$ receptor na astrocitima čime doprinosi njihovom inflamatornom fenotipu (Popoli and Pepponi, 2012; Nedeljkovic, 2019; Paiva et al., 2019). Na kraju, pojačana ekspresija $P2Y_1R$ receptora na reaktivnim astrocitima dodatno potvrđuje njihov inflamacijski karakter s obzirom da je ovaj receptor uključen u regulaciju ekspresije različtih citokina/hemokina, kao i to da dovodi do narušene kalcijumske signalizacije u modelima neurodegenerativnih boleti (Delekate et al., 2014). Na osnovu dobijenih rezultata pretpostavljena je uloga purinske signalizacije u neurodegeneraciji izazvanoj TMK na slici 5. TMK dovodi do oštećenja neurona i utiče na aktivaciju astrocita. Neuroni koji umiru oslobađaju veće količine ATP koji deluje kao DAMP molekul. Mikroglija preko $P2Y_{12}R$ prati gradijent ATP i migrira ka mestima aktivne neurodegeneracija, razgrađujući na svom putu ATP posredstvom NTPDaze1/CD39. Akumulirani ATP i različiti faktori, uključujući i TMK deluju na astrocite koji zadobijaju inflamacijski fenotip. Ameboidna mikroglija pojačano eksprimira eN/CD73 čija aktivnost povećava lokalnu produkciju adenozina. Ovako nastali adenozin vezuje se za $A_{2A}R$ eksprimiran na astrocitima i dodatno doprinosi inflamaciji, što utiče na progresiju neurodegeneracije (Slika 5).

V ZAKLJUČCI

U skladu sa postavljenim ciljevima ove doktorske disertacije, a na osnovu dobijenih rezultata izvedeni su sledeći zaključci:

Jednokratna aplikacija TMK, u dozi od 8 mg/kg telesne težine izaziva :

1. **promene u ponašanju u vidu pojačane osetljivosti na dodir i zvuk, agresivnosti i sistemskog tremora koje počinju 2. dana od aplikacije toksina, dostižu vrhunac 4. dana, od kada dolazi do postepenog oporavka ponašanja;**

2. **progresivnu ćelijsku smrt neurona u CA1 i mCA3/DG regionima hipokampusa, koja se uočava počev od 2. dana nakon intoksikacije;**

3. **ranu dihotomu, prostorno-specifičnu morfološku transformaciju astrocita počev od 2. dana nakon intoksikacije, koja se ogleda se u hipetrofriji astrocita u CA1 regionu i atrofiji astrocita u mCA3/DG regionu**;

4. **povećanje genske ekspresije $P2Y_1R$, $A_{2A}R$ i A_1R receptora i neuroinflamatornu aktivaciju astrocita, koji su glavni izvor proinflamacijskih medijatora C3, TNF-α, IL-1β i iNOS**;

5. **vremenski-specifičnu odloženu aktivaciju mikroglije u zonama neurodegeneracije, koja ispoljava štapoliki i žbunasti oblik 4. dana nakon intoksikacije, i dominantno ameboidnu formu 21. dana nakon intoksikacije;**

6. **transformaciju mirujuće mikroglije u pretežno neuroprotektivni tip, koji pokazuje povećanu ekspresiju NTPDaze 1 u svim mikroglijskim ćelijama hipokampusa, i ekspresiju eN samo u amebodnim ćelijama na mestu neurodegeneracije, kao i porast ekspresije purinoreceptora uključenih u hemotaksu ($P2Y_{12}R$, $P2X_4R$, A_3R, $A_{2A}R$) i fagocitoznu ulogu kod mikroglije ($P2X_7R$, $P2Y_2R$, $P2Y_6R$);**

Uzevši u obzir sve rezultate i zaključke može se izvesti opšti zaključak:

Neurodegeneracija hipokampusa izazvana trimetil-kalajem pokazuje specifičan vremenski i prostorni obrazac koji odgovara promenama opaženim u oboljenjima kod kojih je oštećen hipokampus kod ljudi, poput Alchajmerove bolesti i epilepsije. Predstavljeni model je veoma pogodan za izučavanje aktivacije glijskih ćelija kroz vreme i za razliku od drugih modela, glavni inflamacijski akteri u razvoju patologije su astrociti. Sa druge strane, utvrđivanje vremenskog profila ekspresije odabranih purinskih receptora i ektonukleotidaza pruža potku za rekonstrukciju događaja tokom patologije, kao i njihovog doprinosa inicijaciji i progresiji neurodegeneracije koja je izazvana ovim toksinom. Rezultati ove doktorske disertacije ukazuju na povećanje vanćelijske koncentracije ATP i adenozina koje su spregnute sa ekspresijom specifičnog repertoara komponenti purinske signalizacije na reaktivnim glijskim ćelijama. Pojava ovakvog repertoara receptora ($P2X_7R$, $A_{2A}R$, $P2Y_1R$, A_1R) i enzima karakterističnog za patologiju na glijskim ćelijama zajedno sa gubitkom

homeostatskih receptora na mikrogliji i neuronima ($P2Y_{12}R$, A_1R) ukazuje na učešće purinske signalizacije u ekscitotoksičnosti i inflamaciji, što barem delom, rezultuje progresijom neurodegeneracije.

VI LITERATURA

Abbracchio MP, Burnstock G, Verkhratsky A, Zimmermann H (2009) Purinergic signalling in the nervous system: an overview. Trends in neurosciences 32:19–29.

Adzic M, Nedeljkovic N (2018) Unveiling the Role of Ecto-5'-Nucleotidase/CD73 in Astrocyte Migration by Using Pharmacological Tools. Frontiers in pharmacology 9:153.

Agostinho P, Madeira D, Dias L, Simões AP, Cunha RA, Canas PM (2020) Purinergic signaling orchestrating neuron-glia communication. Pharmacological research 162:105253.

Almolda B, González B, Castellano B (2013) Microglia detection by enzymatic histochemistry. Methods in molecular biology (Clifton, NJ) 1041:243–259.

Andersson H, Luthman J, Olson L (1994) Trimethyltin-induced expression of GABA and vimentin immunoreactivities in astrocytes of the rat brain. Glia 11:378–382.

Andersson H, Wetmore C, Lindqvist E, Luthman J, Olson L (1997) Trimethyltin exposure in the rat induces delayed changes in brain-derived neurotrophic factor, fos and heat shock protein 70. Neurotoxicology 18:147–159.

Antonioli L, Pacher P, Vizi ES, Haskó G (2013) CD39 and CD73 in immunity and inflammation. Trends in molecular medicine 19:355–367.

Arias C, Zepeda A, Hernández-Ortega K, Leal-Galicia P, Lojero C, Camacho-Arroyo I (2009) Sex and estrous cycle-dependent differences in glial fibrillary acidic protein immunoreactivity in the adult rat hippocampus. Hormones and behavior 55:257–263.

Arnò B, Grassivaro F, Rossi C, Bergamaschi A, Castiglioni V, Furlan R, Greter M, Favaro R, Comi G, Becher B, Martino G, Muzio L (2014) Neural progenitor cells orchestrate microglia migration and positioning into the developing cortex. Nature communications 5:5611.

Arvanitakis Z, Shah RC, Bennett DA (2019) Diagnosis and Management of Dementia: Review. JAMA 322:1589–1599.

Aschner M, Aschner JL (1992) Cellular and molecular effects of trimethyltin and triethyltin: relevance to organotin neurotoxicity. Neuroscience and biobehavioral reviews 16:427–435.

Au NPB, Ma CHE (2017) Recent Advances in the Study of Bipolar/Rod-Shaped Microglia and their Roles in Neurodegeneration. Frontiers in aging neuroscience 9:128.

Badimon A et al. (2020) Negative feedback control of neuronal activity by microglia. Nature 586:417–423.

Balaban CD, O'Callaghan JP, Billingsley ML (1988) Trimethyltin-induced neuronal damage in the rat brain: comparative studies using silver degeneration stains, immunocytochemistry and immunoassay for neuronotypic and gliotypic proteins. Neuroscience 26:337–361.

Bayraktar OA, Fuentealba LC, Alvarez-Buylla A, Rowitch DH (2014) Astrocyte development and heterogeneity. Cold Spring Harbor perspectives in biology 7:a020362.

Bazargani N, Attwell D (2016) Astrocyte calcium signaling: the third wave. Nature neuroscience 19:182–189.

Belcher SM, Zsarnovszky A, Crawford PA, Hemani H, Spurling L, Kirley TL (2006) Immunolocalization of ecto-nucleoside triphosphate diphosphohydrolase 3 in rat brain: implications for modulation of multiple homeostatic systems including feeding and sleep-wake behaviors. Neuroscience 137:1331–1346.

Bernier L-P, Ase AR, Boué-Grabot É, Séguéla P (2013) Inhibition of P2X4 function by P2Y6 UDP receptors in microglia. Glia 61:2038–2049.
Billingsley ML, Yun J, Reese BE, Davidson CE, Buck-Koehntop BA, Veglia G (2006) Functional and structural properties of stannin: roles in cellular growth, selective toxicity, and mitochondrial responses to injury. Journal of cellular biochemistry 98:243–250.
Bjelobaba I, Nedeljkovic N, Subasic S, Lavrnja I, Pekovic S, Stojkov D, Rakic L, Stojiljkovic M (2006) Immunolocaliyation of ecto-nucleotide pyrophosphatase/phosphodiesterase 1 (NPP1) in the rat forebrain. Brain research 1120:54-63.
Bjelobaba I, Stojiljkovic M, Lavrnja I, Stojkov D, Pekovic S, Dacic S, Laketa D, Rakic L, Nedeljkovic N (2009) Regional changes in ectonucleotidase activity after cortical stab injury in rat. General physiology and biophysics 28 Spec No:62–68.
Bjelobaba I, Stojiljkovic M, Pekovic S, Dacic S, Lavrnja I, Stojkov D, Rakic L, Nedeljkovic N (2007) Immunohistological determination of ecto-nucleoside triphosphate diphosphohydrolase1 (NTPDase1) and 5'-nucleotidase in rat hippocampus reveals overlapping distribution. Cellular and molecular neurobiology 27:731–743.
Bjelobaba I, Lavrnja I, Parabucki A, Stojkov D, Stojiljkovic M, Pekovic S, Nedeljkovic N (2010) The cortical stab injury induces beading of fibers expressing ecto-nucleoside triphosphate diphosphohydrolase 3. Neuroscience 170:107–116.
Blass-Kampmann S, Kindler-Röhrborn A, Deissler H, D'Urso D, Rajewsky MF (1997) In vitro differentiation of neural progenitor cells from prenatal rat brain: common cell surface glycoprotein on three glial cell subsets. Journal of neuroscience research 48:95–111.
Boche D, Perry VH, Nicoll JAR (2013) Review: activation patterns of microglia and their identification in the human brain. Neuropathology and applied neurobiology 39:3–18.
Boison D, Chen J-F, Fredholm BB (2010) Adenosine signaling and function in glial cells. Cell death and differentiation 17:1071–1082.
Bonan CD, Walz R, Pereira GS, Worm P V, Battastini AM, Cavalheiro EA, Izquierdo I, Sarkis JJ (2000) Changes in synaptosomal ectonucleotidase activities in two rat models of temporal lobe epilepsy. Epilepsy research 39:229–238.
Borea PA, Gessi S, Merighi S, Vincenzi F, Varani K (2018) Pharmacology of Adenosine Receptors: The State of the Art. Physiological reviews 98:1591–1625.
Borroto-Escuela DO, Hinz S, Navarro G, Franco R, Müller CE, Fuxe K (2018) Understanding the Role of Adenosine A2AR Heteroreceptor Complexes in Neurodegeneration and Neuroinflammation. Frontiers in neuroscience 12:43.
Braun N, Zhu Y, Krieglstein J, Culmsee C, Zimmermann H (1998) Upregulation of the enzyme chain hydrolyzing extracellular ATP after transient forebrain ischemia in the rat. The Journal of neuroscience : the official journal of the Society for Neuroscience 18:4891–4900.
Braun N, Sévigny J, Robson SC, Enjyoji K, Guckelberger O, Hammer K, Di Virgilio F, Zimmermann H (2000) Assignment of ecto-nucleoside triphosphate diphosphohydrolase-1/cd39 expression to microglia and vasculature of the brain. The European journal of neuroscience 12:4357–4366.
Braun N, Sévigny J, Mishra SK, Robson SC, Barth SW, Gerstberger R, Hammer K, Zimmermann H (2003) Expression of the ecto-ATPase NTPDase2 in the germinal zones of the developing and adult rat brain. The European journal of neuroscience 17:1355–1364.
Brock TO, O'Callaghan JP (1987) Quantitative changes in the synaptic vesicle proteins

synapsin I and p38 and the astrocyte-specific protein glial fibrillary acidic protein are associated with chemical-induced injury to the rat central nervous system. The Journal of neuroscience : the official journal of the Society for Neuroscience 7:931–942.
Burnstock G (1972) Purinergic nerves. Pharmacological reviews 24:509–581.
Burnstock G (2014) Purinergic signalling: from discovery to current developments. Experimental physiology 99:16–34.
Burnstock G (2017) Purinergic Signalling: Therapeutic Developments. Frontiers in pharmacology 8:661.
Burnstock G (2018) Purine and purinergic receptors. Brain and neuroscience advances 2:2398212818817494.
Burnstock G (2020) Introduction to Purinergic Signalling in the Brain. Advances in experimental medicine and biology 1202:1–12.
Buchet R, Millán JL, Magne D (2013) Multisystemic functions of alkaline phosphatases. Methods in molecular biology (Clifton, NJ) 1053:27–51.
Bushong EA, Martone ME, Jones YZ, Ellisman MH (2002) Protoplasmic astrocytes in CA1 stratum radiatum occupy separate anatomical domains. The Journal of neuroscience : the official journal of the Society for Neuroscience 22:183–192.
Campagno KE, Mitchell CH (2021) The P2X(7) Receptor in Microglial Cells Modulates the Endolysosomal Axis, Autophagy, and Phagocytosis. Frontiers in cellular neuroscience 15:645244.
Cannon JR, Greenamyre JT (2011) The role of environmental exposures in neurodegeneration and neurodegenerative diseases. Toxicological sciences : an official journal of the Society of Toxicology 124:225–250.
Chang LW, Wenger GR, McMillan DE, Dyer RS (1983) Species and strain comparison of acute neurotoxic effects of trimethyltin in mice and rats. Neurobehavioral toxicology and teratology 5:337–350.
Cheli VT, Santiago González DA, Smith J, Spreuer V, Murphy GG, Paez PM (2016) L-type voltage-operated calcium channels contribute to astrocyte activation In vitro. Glia 64:1396–1415.
Chen J, Tan Z, Zeng L, Zhang X, He Y, Gao W, Wu X, Li Y, Bu B, Wang W, Duan S (2013) Heterosynaptic long-term depression mediated by ATP released from astrocytes. Glia 61:178–191.
Colombo E, Farina C (2016) Astrocytes: Key Regulators of Neuroinflammation. Trends in immunology 37:608–620.
Colonna M, Butovsky O (2017) Microglia Function in the Central Nervous System During Health and Neurodegeneration. Annual review of immunology 35:441–468.
Cone CDJ (1970) Variation of the transmembrane potential level as a basic mechanism of mitosis control. Oncology 24:438–470.
Cook LL, Stine KE, Reiter LW (1984) Tin distribution in adult rat tissues after exposure to trimethyltin and triethyltin. Toxicology and applied pharmacology 76:344–348.
Corvino V, Di Maria V, Marchese E, Lattanzi W, Biamonte F, Michetti F, Geloso MC (2015) Estrogen administration modulates hippocampal GABAergic subpopulations in the hippocampus of trimethyltin-treated rats. Frontiers in cellular neuroscience 9:433.
Corvino V, Marchese E, Michetti F, Geloso MC (2013) Neuroprotective strategies in hippocampal neurodegeneration induced by the neurotoxicant trimethyltin. Neurochemical research 38:240–253.

Costa MA, Pellerito L, Izzo V, Fiore T, Pellerito C, Melis M, Musmeci MT, Barbieri G (2006) Diorganotin(IV) and triorganotin(IV) complexes of meso-tetra(4-sulfonatophenyl)porphine induce apoptosis in A375 human melanoma cells. Cancer letters 238:284–294.

Costenla AR, Cunha RA, de Mendonça A (2010) Caffeine, adenosine receptors, and synaptic plasticity. Journal of Alzheimer's disease : JAD 20 Suppl 1:S25-34.

Crain JM, Nikodemova M, Watters JJ (2009) Expression of P2 nucleotide receptors varies with age and sex in murine brain microglia. Journal of neuroinflammation 6:24.

Cristóvão-Ferreira S, Navarro G, Brugarolas M, Pérez-Capote K, Vaz SH, Fattorini G, Conti F, Lluis C, Ribeiro JA, McCormick PJ, Casadó V, Franco R, Sebastião AM (2013) A1R-A2AR heteromers coupled to Gs and G i/0 proteins modulate GABA transport into astrocytes. Purinergic signalling 9:433–449.

Cunha RA (2008) Different cellular sources and different roles of adenosine: A1 receptor-mediated inhibition through astrocytic-driven volume transmission and synapse-restricted A2A receptor-mediated facilitation of plasticity. Neurochemistry international 52:65–72.

Dejneka NS, Patanow CM, Polavarapu R, Toggas SM, Krady JK, Billingsley ML (1997) Localization and characterization of stannin: relationship to cellular sensitivity to organotin compounds. Neurochemistry international 31:801–815.

Delekate A, Füchtemeier M, Schumacher T, Ulbrich C, Foddis M, Petzold GC (2014) Metabotropic P2Y1 receptor signalling mediates astrocytic hyperactivity in vivo in an Alzheimer's disease mouse model. Nature communications 5:5422.

DePierre JW, Karnovsky ML (1974) Ecto-enzyme of granulocytes: 5'-nucleotidase. Science (New York, NY) 183:1096–1098.

Di Virgilio F, Ceruti S, Bramanti P, Abbracchio MP (2009) Purinergic signalling in inflammation of the central nervous system. Trends in neurosciences 32:79–87.

Diaz-Aparicio I et al. (2020) Microglia Actively Remodel Adult Hippocampal Neurogenesis through the Phagocytosis Secretome. The Journal of neuroscience : the official journal of the Society for Neuroscience 40:1453–1482.

DiSabato DJ, Quan N, Godbout JP (2016) Neuroinflammation: the devil is in the details. Journal of neurochemistry 139 Suppl:136–153.

Dragić M, Milićević K, Adžić M, Stevanović I, Ninković M, Grković I, Andjus P, Nedeljković N (2021a) Trimethyltin Increases Intracellular Ca(2+) Via L-Type Voltage-Gated Calcium Channels and Promotes Inflammatory Phenotype in Rat Astrocytes In Vitro. Molecular neurobiology 58:1792–1805.

Dragić M, Zeljković M, Stevanović I, Adžić M, Stekić A, Mihajlović K, Grković I, Ilić N, Ilić T V, Nedeljković N, Ninković M (2021b) Downregulation of CD73/A(2A)R-Mediated Adenosine Signaling as a Potential Mechanism of Neuroprotective Effects of Theta-Burst Transcranial Magnetic Stimulation in Acute Experimental Autoimmune Encephalomyelitis. Brain sciences 11.

Dugger BN, Dickson DW (2017) Pathology of Neurodegenerative Diseases. Cold Spring Harbor perspectives in biology 9.

Earley B, Burke M, Leonard BE (1992) Behavioural, biochemical and histological effects of trimethyltin (TMT) induced brain damage in the rat. Neurochemistry international 21:351–366.

Erkkinen MG, Kim M-O, Geschwind MD (2018) Clinical Neurology and Epidemiology of the Major Neurodegenerative Diseases. Cold Spring Harbor perspectives in biology 10.

Escartin C et al. (2021) Reactive astrocyte nomenclature, definitions, and future directions. Nature neuroscience 24:312–325.
Fam SR, Gallagher CJ, Salter MW (2000) P2Y(1) purinoceptor-mediated Ca(2+) signaling and Ca(2+) wave propagation in dorsal spinal cord astrocytes. The Journal of neuroscience : the official journal of the Society for Neuroscience 20:2800–2808.
Färber K, Markworth S, Pannasch U, Nolte C, Prinz V, Kronenberg G, Gertz K, Endres M, Bechmann I, Enjyoji K, Robson SC, Kettenmann H (2008) The ectonucleotidase cd39/ENTPDase1 modulates purinergic-mediated microglial migration. Glia 56:331–341.
Feldman RG, White RF, Eriator II (1993) Trimethyltin encephalopathy. Archives of neurology 50:1320–1324.
Fiebich BL, Akter S, Akundi RS (2014) The two-hit hypothesis for neuroinflammation: role of exogenous ATP in modulating inflammation in the brain. Frontiers in cellular neuroscience 8:260.
Fiebich BL, Biber K, Lieb K, van Calker D, Berger M, Bauer J, Gebicke-Haerter PJ (1996) Cyclooxygenase-2 expression in rat microglia is induced by adenosine A2a-receptors. Glia 18:152–160.
Florea A-M, Büsselberg D (2006) Occurrence, use and potential toxic effects of metals and metal compounds. Biometals : an international journal on the role of metal ions in biology, biochemistry, and medicine 19:419–427.
Florea A-M, Dopp E, Büsselberg D (2005a) Elevated Ca2+(i) transients induced by trimethyltin chloride in HeLa cells: types and levels of response. Cell calcium 37:251–258.
Florea A-M, Splettstoesser F, Dopp E, Rettenmeier AW, Büsselberg D (2005b) Modulation of intracellular calcium homeostasis by trimethyltin chloride in human tumour cells: neuroblastoma SY5Y and cervix adenocarcinoma HeLa S3. Toxicology 216:1–8.
Franke H, Illes P (2006) Involvement of P2 receptors in the growth and survival of neurons in the CNS. Pharmacology & therapeutics 109:297–324.
Frenguelli BG (2019) The Purine Salvage Pathway and the Restoration of Cerebral ATP: Implications for Brain Slice Physiology and Brain Injury. Neurochemical research 44:661–675.
Geddes DM, LaPlaca MC, Cargill RS 2nd (2003) Susceptibility of hippocampal neurons to mechanically induced injury. Experimental neurology 184:420–427.
Geloso MC, Corvino V, Cavallo V, Toesca A, Guadagni E, Passalacqua R, Michetti F (2004) Expression of astrocytic nestin in the rat hippocampus during trimethyltin-induced neurodegeneration. Neuroscience letters 357:103–106.
Geloso MC, Corvino V, Michetti F (2011) Trimethyltin-induced hippocampal degeneration as a tool to investigate neurodegenerative processes. Neurochemistry international 58:729–738.
Geloso MC, Vinesi P, Michetti F (1996) Parvalbumin-immunoreactive neurons are not affected by trimethyltin-induced neurodegeneration in the rat hippocampus. Experimental neurology 139:269–277.
Geloso MC, Vinesi P, Michetti F (1997) Calretinin-containing neurons in trimethyltin-induced neurodegeneration in the rat hippocampus: an immunocytochemical study. Experimental neurology 146:67–73.
Gessi S, Merighi S, Fazzi D, Stefanelli A, Varani K, Borea PA (2011) Adenosine receptor targeting in health and disease. Expert opinion on investigational drugs 20:1591–1609.

Gijsbers R, Ceulemans H, Stalmans W, Bollen M (2001) Structural and catalytic similarities between nucleotide pyrophosphatases/phosphodiesterases and alkaline phosphatases. The Journal of biological chemistry 276:1361–1368.
Gilyarov A V (2008) Nestin in central nervous system cells. Neuroscience and behavioral physiology 38:165–169.
Glass CK, Saijo K, Winner B, Marchetto MC, Gage FH (2010) Mechanisms underlying inflammation in neurodegeneration. Cell 140:918–934.
Glass M, Faull RL, Bullock JY, Jansen K, Mee EW, Walker EB, Synek BJ, Dragunow M (1996) Loss of A1 adenosine receptors in human temporal lobe epilepsy. Brain research 710:56–68.
Godeau D, Petit A, Richard I, Roquelaure Y, Descatha A (2021) Return-to-work, disabilities and occupational health in the age of COVID-19. Scandinavian journal of work, environment & health 47:408–409.
Goding JW, Grobben B, Slegers H (2003) Physiological and pathophysiological functions of the ecto-nucleotide pyrophosphatase/phosphodiesterase family. Biochimica et biophysica acta 1638:1–19.
Gomes C, Ferreira R, George J, Sanches R, Rodrigues DI, Gonçalves N, Cunha RA (2013) Activation of microglial cells triggers a release of brain-derived neurotrophic factor (BDNF) inducing their proliferation in an adenosine A2A receptor-dependent manner: A2A receptor blockade prevents BDNF release and proliferation of microglia. Journal of neuroinflammation 10:16.
Gourine A V, Dale N, Llaudet E, Poputnikov DM, Spyer KM, Gourine VN (2007) Release of ATP in the central nervous system during systemic inflammation: real-time measurement in the hypothalamus of conscious rabbits. The Journal of physiology 585:305–316.
Grković I, Bjelobaba I, Mitrović N, Lavrnja I, Drakulić D, Martinović J, Stanojlović M, Horvat A, Nedeljković N (2016) Expression of ecto-nucleoside triphosphate diphosphohydrolase3 (NTPDase3) in the female rat brain during postnatal development. Journal of chemical neuroanatomy 77:10–18.
Grkovic I, Bjelobaba I, Nedeljkovic N, Mitrovic N, Drakulic D, Stanojlovic M, Horvat A (2014) Developmental increase in ecto-5'-nucleotidase activity overlaps with appearance of two immunologically distinct enzyme isoforms in rat hippocampal synaptic plasma membranes. Journal of molecular neuroscience : MN 54:109–118.
Grković I, Drakulić D, Martinović J, Mitrović N (2019a) Role of Ectonucleotidases in Synapse Formation During Brain Development: Physiological and Pathological Implications. Current neuropharmacology 17:84–98.
Grković I, Mitrović N, Dragić M, Adžić M, Drakulić D, Nedeljković N (2019b) Spatial Distribution and Expression of Ectonucleotidases in Rat Hippocampus After Removal of Ovaries and Estradiol Replacement. Molecular neurobiology 56:1933–1945.
Grubman A, Chew G, Ouyang JF, Sun G, Choo XY, McLean C, Simmons RK, Buckberry S, Vargas-Landin DB, Poppe D, Pflueger J, Lister R, Rackham OJL, Petretto E, Polo JM (2019) A single-cell atlas of entorhinal cortex from individuals with Alzheimer's disease reveals cell-type-specific gene expression regulation. Nature neuroscience 22:2087–2097.
Habib N, McCabe C, Medina S, Varshavsky M, Kitsberg D, Dvir-Szternfeld R, Green G, Dionne D, Nguyen L, Marshall JL, Chen F, Zhang F, Kaplan T, Regev A, Schwartz M (2020) Disease-associated astrocytes in Alzheimer's disease and aging. Nature

neuroscience 23:701–706.
Haga S, Haga C, Aizawa T, Ikeda K (2002) Neuronal degeneration and glial cell-responses following trimethyltin intoxication in the rat. Acta neuropathologica 103:575–582.
Handa M, Guidotti G (1996) Purification and cloning of a soluble ATP-diphosphohydrolase (apyrase) from potato tubers (Solanum tuberosum). Biochemical and biophysical research communications 218:916–923.
Harry GJ, Lefebvre d'Hellencourt C (2003) Dentate gyrus: alterations that occur with hippocampal injury. Neurotoxicology 24:343–356.
Hashioka S, Wang YF, Little JP, Choi HB, Klegeris A, McGeer PL, McLarnon JG (2014) Purinergic responses of calcium-dependent signaling pathways in cultured adult human astrocytes. BMC neuroscience 15:18.
Haynes SE, Hollopeter G, Yang G, Kurpius D, Dailey ME, Gan W-B, Julius D (2006) The P2Y12 receptor regulates microglial activation by extracellular nucleotides. Nature neuroscience 9:1512–1519.
Heller JP, Rusakov DA (2015) Morphological plasticity of astroglia: Understanding synaptic microenvironment. Glia 63:2133–2151.
Hickman S, Izzy S, Sen P, Morsett L, El Khoury J (2018) Microglia in neurodegeneration. Nature neuroscience 21:1359–1369.
Hickman SE, Kingery ND, Ohsumi TK, Borowsky ML, Wang L, Means TK, El Khoury J (2013) The microglial sensome revealed by direct RNA sequencing. Nature neuroscience 16:1896–1905.
Higashimori H, Sontheimer H (2007) Role of Kir4.1 channels in growth control of glia. Glia 55:1668–1679.
Hou X, Li Y, Huang Y, Zhao H, Gui L (2020) Adenosine Receptor A1-A2a Heteromers Regulate EAAT2 Expression and Glutamate Uptake via YY1-Induced Repression of PPARγ Transcription. PPAR research 2020:2410264.
Howcroft TK, Campisi J, Louis GB, Smith MT, Wise B, Wyss-Coray T, Augustine AD, McElhaney JE, Kohanski R, Sierra F (2013) The role of inflammation in age-related disease. Aging 5:84–93.
Hu Q, Ren X, Liu Y, Li Z, Zhang L, Chen X, He C, Chen J-F (2016) Aberrant adenosine A2A receptor signaling contributes to neurodegeneration and cognitive impairments in a mouse model of synucleinopathy. Experimental neurology 283:213–223.
Illes P, Rubini P, Ulrich H, Zhao Y, Tang Y (2020) Regulation of Microglial Functions by Purinergic Mechanisms in the Healthy and Diseased CNS. Cells 9.
Illes P, Verkhratsky A, Burnstock G, Franke H (2012) P2X receptors and their roles in astroglia in the central and peripheral nervous system. The Neuroscientist : a review journal bringing neurobiology, neurology and psychiatry 18:422–438.
Irino Y, Nakamura Y, Inoue K, Kohsaka S, Ohsawa K (2008) Akt activation is involved in P2Y12 receptor-mediated chemotaxis of microglia. Journal of neuroscience research 86:1511–1519.
Jakovljevic M, Lavrnja I, Bozic I, Savic D, Bjelobaba I, Pekovic S, Sévigny J, Nedeljkovic N, Laketa D (2017) Down-regulation of NTPDase2 and ADP-sensitive P2 Purinoceptors Correlate with Severity of Symptoms during Experimental Autoimmune Encephalomyelitis. Frontiers in cellular neuroscience 11:333.
Jakovljevic M, Lavrnja I, Bozic I, Milosevic A, Bjelobaba I, Savic D, Sévigny J, Pekovic S, Nedeljkovic N, Laketa D (2019) Induction of NTPDase1/CD39 by Reactive Microglia and

Macrophages Is Associated With the Functional State During EAE. Frontiers in neuroscience 13:410.
Jarvis MF, Khakh BS (2009) ATP-gated P2X cation-channels. Neuropharmacology 56:208–215.
Jenkins SM, Barone S (2004) The neurotoxicant trimethyltin induces apoptosis via caspase activation, p38 protein kinase, and oxidative stress in PC12 cells. Toxicology letters 147:63–72.
Ji K, Akgul G, Wollmuth LP, Tsirka SE (2013) Microglia actively regulate the number of functional synapses. PloS one 8:e56293.
John Lin C-C, Yu K, Hatcher A, Huang T-W, Lee HK, Carlson J, Weston MC, Chen F, Zhang Y, Zhu W, Mohila CA, Ahmed N, Patel AJ, Arenkiel BR, Noebels JL, Creighton CJ, Deneen B (2017) Identification of diverse astrocyte populations and their malignant analogs. Nature neuroscience 20:396–405.
Kálmán M, Hajós F (1989) Distribution of glial fibrillary acidic protein (GFAP)-immunoreactive astrocytes in the rat brain. I. Forebrain. Experimental brain research 78:147–163.
Kamphuis W, Kooijman L, Orre M, Stassen O, Pekny M, Hol EM (2015) GFAP and vimentin deficiency alters gene expression in astrocytes and microglia in wild-type mice and changes the transcriptional response of reactive glia in mouse model for Alzheimer's disease. Glia 63:1036–1056.
Kane MD, Yang CW, Gunasekar PG, Isom GE (1998) Trimethyltin stimulates protein kinase C translocation through receptor-mediated phospholipase C activation in PC12 cells. Journal of neurochemistry 70:509–514.
Kang JY, Park SK, Guo TJ, Ha JS, Lee DS, Kim JM, Lee U, Kim DO, Heo HJ (2016) Reversal of Trimethyltin-Induced Learning and Memory Deficits by 3,5-Dicaffeoylquinic Acid. Oxidative medicine and cellular longevity 2016:6981595.
Kassed CA, Butler TL, Patton GW, Demesquita DD, Navidomskis MT, Mémet S, Israël A, Pennypacker KR (2004) Injury-induced NF-kappaB activation in the hippocampus: implications for neuronal survival. FASEB journal : official publication of the Federation of American Societies for Experimental Biology 18:723–724.
Kassed CA, Willing AE, Garbuzova-Davis S, Sanberg PR, Pennypacker KR (2002) Lack of NF-kappaB p50 exacerbates degeneration of hippocampal neurons after chemical exposure and impairs learning. Experimental neurology 176:277–288.
Kelly P, Hudry E, Hou SS, Bacskai BJ (2018) In Vivo Two Photon Imaging of Astrocytic Structure and Function in Alzheimer's Disease. Frontiers in aging neuroscience 10:219.
Kelso ML, Liput DJ, Eaves DW, Nixon K (2011) Upregulated vimentin suggests new areas of neurodegeneration in a model of an alcohol use disorder. Neuroscience 197:381–393.
Kim S-Y, Kim E-K, Moon HJ, Yoon JH, Kwak JY (2015) Application of Texture Analysis in the Differential Diagnosis of Benign and Malignant Thyroid Nodules: Comparison With Gray-Scale Ultrasound and Elastography. AJR American journal of roentgenology 205:W343-51.
Kiss DS, Zsarnovszky A, Horvath K, Gyorffy A, Bartha T, Hazai D, Sotonyi P, Somogyi V, Frenyo L V, Diano S (2009) Ecto-nucleoside triphosphate diphosphohydrolase 3 in the ventral and lateral hypothalamic area of female rats: morphological characterization and functional implications. Reproductive biology and endocrinology : RB&E 7:31.
Knowles AF (2011) The GDA1_CD39 superfamily: NTPDases with diverse functions. Purinergic signalling 7:21–45.

Koczyk D, Oderfeld-Nowak B (2000) Long-term microglial and astroglial activation in the hippocampus of trimethyltin-intoxicated rat: stimulation of NGF and TrkA immunoreactivities in astroglia but not in microglia. International journal of developmental neuroscience : the official journal of the International Society for Developmental Neuroscience 18:591–606.

Koizumi S, Shigemoto-Mogami Y, Nasu-Tada K, Shinozaki Y, Ohsawa K, Tsuda M, Joshi B V, Jacobson KA, Kohsaka S, Inoue K (2007) UDP acting at P2Y6 receptors is a mediator of microglial phagocytosis. Nature 446:1091–1095.

Kosaka T, Hama K (1986) Three-dimensional structure of astrocytes in the rat dentate gyrus. The Journal of comparative neurology 249:242–260.

Kovács Z, Dobolyi A, Kékesi KA, Juhász G (2013) 5'-nucleotidases, nucleosides and their distribution in the brain: pathological and therapeutic implications. Current medicinal chemistry 20:4217–4240.

Krady JK, Oyler GA, Balaban CD, Billingsley ML (1990) Use of avidin-biotin subtractive hybridization to characterize mRNA common to neurons destroyed by the selective neurotoxicant trimethyltin. Brain research Molecular brain research 7:287–297.

Kuboyama K, Harada H, Tozaki-Saitoh H, Tsuda M, Ushijima K, Inoue K (2011) Astrocytic P2Y(1) receptor is involved in the regulation of cytokine/chemokine transcription and cerebral damage in a rat model of cerebral ischemia. Journal of cerebral blood flow and metabolism : official journal of the International Society of Cerebral Blood Flow and Metabolism 31:1930–1941.

Kukulski F, Lévesque SA, Lavoie EG, Lecka J, Bigonnesse F, Knowles AF, Robson SC, Kirley TL, Sévigny J (2005) Comparative hydrolysis of P2 receptor agonists by NTPDases 1, 2, 3 and 8. Purinergic signalling 1:193–204.

Kukulski F, Lévesque SA, Sévigny J (2011) Impact of ectoenzymes on p2 and p1 receptor signaling. Advances in pharmacology (San Diego, Calif) 61:263–299.

Kulijewicz-Nawrot M, Verkhratsky A, Chvátal A, Syková E, Rodríguez JJ (2012) Astrocytic cytoskeletal atrophy in the medial prefrontal cortex of a triple transgenic mouse model of Alzheimer's disease. Journal of anatomy 221:252–262.

Kwon HS, Koh S-H (2020) Neuroinflammation in neurodegenerative disorders: the roles of microglia and astrocytes. Translational neurodegeneration 9:42.

Kyrargyri V, Madry C, Rifat A, Arancibia-Carcamo IL, Jones SP, Chan VTT, Xu Y, Robaye B, Attwell D (2020) P2Y(13) receptors regulate microglial morphology, surveillance, and resting levels of interleukin 1β release. Glia 68:328–344.

Lavrnja I, Laketa D, Savic D, Bozic I, Bjelobaba I, Pekovic S, Nedeljkovic N (2015) Expression of a second ecto-5'-nucleotidase variant besides the usual protein in symptomatic phase of experimental autoimmune encephalomyelitis. Journal of molecular neuroscience : MN 55:898–911.

Langer D, Hammer K, Koszalka P, Schrader J, Robson S, Zimmermann H (2008) Distribution of ectonucleotidases in the rodent brain revisited. Cell and tissue research 334:199–217.

Lassmann H, Brück W, Lucchinetti CF (2007) The immunopathology of multiple sclerosis: an overview. Brain pathology (Zurich, Switzerland) 17:210–218.

Latini L, Geloso MC, Corvino V, Giannetti S, Florenzano F, Viscomi MT, Michetti F, Molinari M (2010) Trimethyltin intoxication up-regulates nitric oxide synthase in neurons and purinergic ionotropic receptor 2 in astrocytes in the hippocampus. Journal of neuroscience research 88:500–509.

Lattanzi W, Corvino V, Di Maria V, Michetti F, Geloso MC (2013) Gene expression profiling as a tool to investigate the molecular machinery activated during hippocampal neurodegeneration induced by trimethyltin (TMT) administration. International journal of molecular sciences 14:16817–16835.
Lau S-F, Cao H, Fu AKY, Ip NY (2020) Single-nucleus transcriptome analysis reveals dysregulation of angiogenic endothelial cells and neuroprotective glia in Alzheimer's disease. Proceedings of the National Academy of Sciences of the United States of America 117:25800–25809.
Lawson LJ, Perry VH, Dri P, Gordon S (1990) Heterogeneity in the distribution and morphology of microglia in the normal adult mouse brain. Neuroscience 39:151–170.
Lazarowski ER, Boucher RC, Harden TK (2003) Mechanisms of release of nucleotides and integration of their action as P2X- and P2Y-receptor activating molecules. Molecular pharmacology 64:785–795.
Lee HY, Murata J, Clair T, Polymeropoulos MH, Torres R, Manrow RE, Liotta LA, Stracke ML (1996) Cloning, chromosomal localization, and tissue expression of autotaxin from human teratocarcinoma cells. Biochemical and biophysical research communications 218:714–719.
Lee KM, MacLean AG (2015) New advances on glial activation in health and disease. World journal of virology 4:42–55.
Lee S, Yang M, Kim J, Kang S, Kim J, Kim J-C, Jung C, Shin T, Kim S-H, Moon C (2016) Trimethyltin-induced hippocampal neurodegeneration: A mechanism-based review. Brain research bulletin 125:187–199.
Lévesque M, Avoli M (2013) The kainic acid model of temporal lobe epilepsy. Neuroscience and biobehavioral reviews 37:2887–2899.
Li H, Chen C, Dou Y, Wu H, Liu Y, Lou H-F, Zhang J, Li X, Wang H, Duan S (2013) P2Y4 receptor-mediated pinocytosis contributes to amyloid beta-induced self-uptake by microglia. Molecular and cellular biology 33:4282–4293.
Li Q, Cheng Z, Zhou L, Darmanis S, Neff NF, Okamoto J, Gulati G, Bennett ML, Sun LO, Clarke LE, Marschallinger J, Yu G, Quake SR, Wyss-Coray T, Barres BA (2019) Developmental Heterogeneity of Microglia and Brain Myeloid Cells Revealed by Deep Single-Cell RNA Sequencing. Neuron 101:207-223.e10.
Liddelow SA, Barres BA (2017) Reactive Astrocytes: Production, Function, and Therapeutic Potential. Immunity 46:957–967.
Lim D, Ronco V, Grolla AA, Verkhratsky A, Genazzani AA (2014) Glial calcium signalling in Alzheimer's disease. Reviews of physiology, biochemistry and pharmacology 167:45–65.
Little AR, Benkovic SA, Miller DB, O'Callaghan JP (2002) Chemically induced neuronal damage and gliosis: enhanced expression of the proinflammatory chemokine, monocyte chemoattractant protein (MCP)-1, without a corresponding increase in proinflammatory cytokines(1). Neuroscience 115:307–320.
Little AR, Miller DB, Li S, Kashon ML, O'Callaghan JP (2012) Trimethyltin-induced neurotoxicity: gene expression pathway analysis, q-RT-PCR and immunoblotting reveal early effects associated with hippocampal damage and gliosis. Neurotoxicology and teratology 34:72–82.
Lyman M, Lloyd DG, Ji X, Vizcaychipi MP, Ma D (2014) Neuroinflammation: the role and consequences. Neuroscience research 79:1–12.
Matias I, Morgado J, Gomes FCA (2019) Astrocyte Heterogeneity: Impact to Brain Aging and

Disease. Frontiers in aging neuroscience 11:59.
Matos M, Augusto E, Machado NJ, dos Santos-Rodrigues A, Cunha RA, Agostinho P (2012) Astrocytic adenosine A2A receptors control the amyloid-β peptide-induced decrease of glutamate uptake. Journal of Alzheimer's disease : JAD 31:555–567.
Matyash M, Zabiegalov O, Wendt S, Matyash V, Kettenmann H (2017) The adenosine generating enzymes CD39/CD73 control microglial processes ramification in the mouse brain. PloS one 12:e0175012.
Maynard CJ, Bush AI, Masters CL, Cappai R, Li Q-X (2005) Metals and amyloid-beta in Alzheimer's disease. International journal of experimental pathology 86:147–159.
Millán JL (2006) Alkaline Phosphatases : Structure, substrate specificity and functional relatedness to other members of a large superfamily of enzymes. Purinergic signalling 2:335–341.
Mills CD, Kincaid K, Alt JM, Heilman MJ, Hill AM (2000) M-1/M-2 macrophages and the Th1/Th2 paradigm. Journal of immunology (Baltimore, Md : 1950) 164:6166–6173.
Mitra J, Guerrero EN, Hegde PM, Wang H, Boldogh I, Rao KS, Mitra S, Hegde ML (2014a) New perspectives on oxidized genome damage and repair inhibition by pro-oxidant metals in neurological diseases. Biomolecules 4:678–703.
Mitra J, Vasquez V, Hegde PM, Boldogh I, Mitra S, Kent TA, Rao KS, Hegde ML (2014b) Revisiting Metal Toxicity in Neurodegenerative Diseases and Stroke: Therapeutic Potential. Neurological research and therapy 1.
Mitrović N, Dragić M, Zarić M, Drakulić D, Nedeljković N, Grković I (2019) Estrogen receptors modulate ectonucleotidases activity in hippocampal synaptosomes of male rats. Neuroscience Letters 712.
Mitrović N, Guševac I, Drakulić D, Stanojlović M, Zlatković J, Sévigny J, Horvat A, Nedeljković N, Grković I (2016) Regional and sex-related differences in modulating effects of female sex steroids on ecto-5'-nucleotidase expression in the rat cerebral cortex and hippocampus. General and comparative endocrinology 235:100–107.
Montague PR, Friedlander MJ (1989) Expression of an intrinsic growth strategy by mammalian retinal neurons. Proceedings of the National Academy of Sciences of the United States of America 86:7223–7227.
Montague PR, Friedlander MJ (1991) Morphogenesis and territorial coverage by isolated mammalian retinal ganglion cells. The Journal of neuroscience : the official journal of the Society for Neuroscience 11:1440–1457.
Morrison JH, Hof PR (2002) Selective vulnerability of corticocortical and hippocampal circuits in aging and Alzheimer's disease. Progress in brain research 136:467–486.
Nedeljkovic N (2019) Complex regulation of ecto-5'-nucleotidase/CD73 and A(2A)R-mediated adenosine signaling at neurovascular unit: A link between acute and chronic neuroinflammation. Pharmacological research 144:99–115.
Nedeljkovic N, Bjelobaba I, Subasic S, Lavrnja I, Pekovic S, Stojkov D, Vjestica A, Rakic L, Stojiljkovic M (2006) Up-regulation of ectonucleotidase activity after cortical stab injury in rats. Cell biology international 30:541–546.
Nguyen PT, Dorman LC, Pan S, Vainchtein ID, Han RT, Nakao-Inoue H, Taloma SE, Barron JJ, Molofsky AB, Kheirbek MA, Molofsky A V (2020) Microglial Remodeling of the Extracellular Matrix Promotes Synapse Plasticity. Cell 182:388-403.e15.
Nilsberth C, Kostyszyn B, Luthman J (2002) Changes in APP, PS1 and other factors related to Alzheimer's disease pathophysiology after trimethyltin-induced brain lesion in the rat.

Neurotoxicity research 4:625–636.
Norden DM, Trojanowski PJ, Villanueva E, Navarro E, Godbout JP (2016) Sequential activation of microglia and astrocyte cytokine expression precedes increased Iba-1 or GFAP immunoreactivity following systemic immune challenge. Glia 64:300–316.
Nosi D, Lana D, Giovannini MG, Delfino G, Zecchi-Orlandini S (2021) Neuroinflammation: Integrated Nervous Tissue Response through Intercellular Interactions at the “Whole System” Scale. Cells 10.
O’Callaghan JP, Niedzwiecki DM, Means JC (1989) Variations in the neurotoxic potency of trimethyltin. Brain research bulletin 22:637–642.
Oberheim NA, Tian G-F, Han X, Peng W, Takano T, Ransom B, Nedergaard M (2008) Loss of astrocytic domain organization in the epileptic brain. The Journal of neuroscience : the official journal of the Society for Neuroscience 28:3264–3276.
Ogata K, Kosaka T (2002) Structural and quantitative analysis of astrocytes in the mouse hippocampus. Neuroscience 113:221–233.
Ogata S, Hayashi Y, Misumi Y, Ikehara Y (1990) Membrane-anchoring domain of rat liver 5’-nucleotidase: identification of the COOH-terminal serine-523 covalently attached with a glycolipid. Biochemistry 29:7923–7927.
Ohsawa K, Irino Y, Nakamura Y, Akazawa C, Inoue K, Kohsaka S (2007) Involvement of P2X4 and P2Y12 receptors in ATP-induced microglial chemotaxis. Glia 55:604–616.
Ohsawa K, Irino Y, Sanagi T, Nakamura Y, Suzuki E, Inoue K, Kohsaka S (2010) P2Y12 receptor-mediated integrin-beta1 activation regulates microglial process extension induced by ATP. Glia 58:790–801.
Ohsawa K, Sanagi T, Nakamura Y, Suzuki E, Inoue K, Kohsaka S (2012) Adenosine A3 receptor is involved in ADP-induced microglial process extension and migration. Journal of neurochemistry 121:217–227.
Oksanen M, Lehtonen S, Jaronen M, Goldsteins G, Hämäläinen RH, Koistinaho J (2019) Astrocyte alterations in neurodegenerative pathologies and their modeling in human induced pluripotent stem cell platforms. Cellular and molecular life sciences : CMLS 76:2739–2760.
Olabarria M, Noristani HN, Verkhratsky A, Rodríguez JJ (2010) Concomitant astroglial atrophy and astrogliosis in a triple transgenic animal model of Alzheimer’s disease. Glia 58:831–838.
Oliveira-Giacomelli Á, Naaldijk Y, Sardá-Arroyo L, Gonçalves MCB, Corrêa-Velloso J, Pillat MM, de Souza HDN, Ulrich H (2018) Purinergic Receptors in Neurological Diseases With Motor Symptoms: Targets for Therapy. Frontiers in pharmacology 9:325.
Orr AG, Hsiao EC, Wang MM, Ho K, Kim DH, Wang X, Guo W, Kang J, Yu G-Q, Adame A, Devidze N, Dubal DB, Masliah E, Conklin BR, Mucke L (2015) Astrocytic adenosine receptor A2A and Gs-coupled signaling regulate memory. Nature neuroscience 18:423–434.
Orr AG, Lo I, Schumacher H, Ho K, Gill M, Guo W, Kim DH, Knox A, Saito T, Saido TC, Simms J, Toddes C, Wang X, Yu G-Q, Mucke L (2018) Istradefylline reduces memory deficits in aging mice with amyloid pathology. Neurobiology of disease 110:29–36.
Orr AG, Orr AL, Li X-J, Gross RE, Traynelis SF (2009) Adenosine A(2A) receptor mediates microglial process retraction. Nature neuroscience 12:872–878.
Orre M, Kamphuis W, Osborn LM, Melief J, Kooijman L, Huitinga I, Klooster J, Bossers K, Hol EM (2014) Acute isolation and transcriptome characterization of cortical astrocytes and

microglia from young and aged mice. Neurobiology of aging 35:1–14.
Othman T, Yan H, Rivkees SA (2003) Oligodendrocytes express functional A1 adenosine receptors that stimulate cellular migration. Glia 44:166–172.
Ouyang Y-B, Voloboueva LA, Xu L-J, Giffard RG (2007) Selective dysfunction of hippocampal CA1 astrocytes contributes to delayed neuronal damage after transient forebrain ischemia. The Journal of neuroscience : the official journal of the Society for Neuroscience 27:4253–4260.
Paiva I, Carvalho K, Santos P, Cellai L, Pavlou MAS, Jain G, Gnad T, Pfeifer A, Vieau D, Fischer A, Buée L, Outeiro TF, Blum D (2019) A(2A) R-induced transcriptional deregulation in astrocytes: An in vitro study. Glia 67:2329–2342.
Pantic I, Dacic S, Brkic P, Lavrnja I, Pantic S, Jovanovic T, Pekovic S (2014) Application of fractal and grey level co-occurrence matrix analysis in evaluation of brain corpus callosum and cingulum architecture. Microscopy and microanalysis : the official journal of Microscopy Society of America, Microbeam Analysis Society, Microscopical Society of Canada 20:1373–1381.
Park S, Kim B, Lee J, Goo JM, Shin Y-G (2011) GGO nodule volume-preserving nonrigid lung registration using GLCM texture analysis. IEEE transactions on bio-medical engineering 58:2885–2894.
Park SK, Kang JY, Kim JM, Yoo SK, Han HJ, Chung DH, Kim D-O, Kim G-H, Heo HJ (2019) Fucoidan-Rich Substances from Ecklonia cava Improve Trimethyltin-Induced Cognitive Dysfunction via Down-Regulation of Amyloid β Production/Tau Hyperphosphorylation. Marine drugs 17.
Pekny M, Nilsson M (2005) Astrocyte activation and reactive gliosis. Glia 50:427–434.
Piacentini R, Gangitano C, Ceccariglia S, Del Fà A, Azzena GB, Michetti F, Grassi C (2008) Dysregulation of intracellular calcium homeostasis is responsible for neuronal death in an experimental model of selective hippocampal degeneration induced by trimethyltin. Journal of neurochemistry 105:2109–2121.
Pietrowski MJ, Gabr AA, Kozlov S, Blum D, Halle A, Carvalho K (2021) Glial Purinergic Signaling in Neurodegeneration. Frontiers in neurology 12:654850.
Pilz RB, Willis RC, Seegmiller JE (1982) Regulation of human lymphoblast plasma membrane 5'-nucleotidase by zinc. The Journal of biological chemistry 257:13544–13549.
Piver WT (1973) Organotin compounds: industrial applications and biological investigation. Environmental health perspectives 4:61–79.
Plata A, Lebedeva A, Denisov P, Nosova O, Postnikova TY, Pimashkin A, Brazhe A, Zaitsev A V, Rusakov DA, Semyanov A (2018) Astrocytic Atrophy Following Status Epilepticus Parallels Reduced Ca(2+) Activity and Impaired Synaptic Plasticity in the Rat Hippocampus. Frontiers in molecular neuroscience 11:215.
Popoli P, Pepponi R (2012) Potential therapeutic relevance of adenosine A2B and A2A receptors in the central nervous system. CNS & neurological disorders drug targets 11:664–674.
Ransohoff RM (2016) A polarizing question: do M1 and M2 microglia exist? Nature neuroscience 19:987–991.
Reichenbach N, Delekate A, Breithausen B, Keppler K, Poll S, Schulte T, Peter J, Plescher M, Hansen JN, Blank N, Keller A, Fuhrmann M, Henneberger C, Halle A, Petzold GC (2018) P2Y1 receptor blockade normalizes network dysfunction and cognition in an Alzheimer's disease model. The Journal of experimental medicine 215:1649–1663.

Robson SC, Sévigny J, Zimmermann H (2006) The E-NTPDase family of ectonucleotidases: Structure function relationships and pathophysiological significance. Purinergic signalling 2:409–430.
Rodríguez-Arellano JJ, Parpura V, Zorec R, Verkhratsky A (2016) Astrocytes in physiological aging and Alzheimer's disease. Neuroscience 323:170–182.
Röhl C, Grell M, Maser E (2009) The organotin compounds trimethyltin (TMT) and triethyltin (TET) but not tributyltin (TBT) induce activation of microglia co-cultivated with astrocytes. Toxicology in vitro : an international journal published in association with BIBRA 23:1541–1547.
Röhl C, Sievers J (2005) Microglia is activated by astrocytes in trimethyltin intoxication. Toxicology and applied pharmacology 204:36–45.
Saul A, Hausmann R, Kless A, Nicke A (2013) Heteromeric assembly of P2X subunits. Frontiers in cellular neuroscience 7:250.
Schoen SW, Kreutzberg GW (1994) Synaptic 5'-nucleotidase activity reflects lesion-induced sprouting within the adult rat dentate gyrus. Experimental neurology 127:106–118.
Schulte am Esch J 2nd, Sévigny J, Kaczmarek E, Siegel JB, Imai M, Koziak K, Beaudoin AR, Robson SC (1999) Structural elements and limited proteolysis of CD39 influence ATP diphosphohydrolase activity. Biochemistry 38:2248–2258.
Sebastián-Serrano Á, de Diego-García L, Martínez-Frailes C, Ávila J, Zimmermann H, Millán JL, Miras-Portugal MT, Díaz-Hernández M (2015) Tissue-nonspecific Alkaline Phosphatase Regulates Purinergic Transmission in the Central Nervous System During Development and Disease. Computational and structural biotechnology journal 13:95–100.
Sévigny J, Sundberg C, Braun N, Guckelberger O, Csizmadia E, Qawi I, Imai M, Zimmermann H, Robson SC (2002) Differential catalytic properties and vascular topography of murine nucleoside triphosphate diphosphohydrolase 1 (NTPDase1) and NTPDase2 have implications for thromboregulation. Blood 99:2801–2809.
Shieh C-H, Heinrich A, Serchov T, van Calker D, Biber K (2014) P2X7-dependent, but differentially regulated release of IL-6, CCL2, and TNF-α in cultured mouse microglia. Glia 62:592–607.
Shinozaki Y, Shibata K, Yoshida K, Shigetomi E, Gachet C, Ikenaka K, Tanaka KF, Koizumi S (2017) Transformation of Astrocytes to a Neuroprotective Phenotype by Microglia via P2Y(1) Receptor Downregulation. Cell reports 19:1151–1164.
Shuto M, Higuchi K, Sugiyama C, Yoneyama M, Kuramoto N, Nagashima R, Kawada K, Ogita K (2009a) Endogenous and exogenous glucocorticoids prevent trimethyltin from causing neuronal degeneration of the mouse brain in vivo: involvement of oxidative stress pathways. Journal of pharmacological sciences 110:424–436.
Shuto M, Seko K, Kuramoto N, Sugiyama C, Kawada K, Yoneyama M, Nagashima R, Ogita K (2009b) Activation of c-Jun N-terminal kinase cascades is involved in part of the neuronal degeneration induced by trimethyltin in cortical neurons of mice. Journal of pharmacological sciences 109:60–70.
Smith TM, Kirley TL (1999) Site-directed mutagenesis of a human brain ecto-apyrase: evidence that the E-type ATPases are related to the actin/heat shock 70/sugar kinase superfamily. Biochemistry 38:321–328.
Sofroniew M V (2009) Molecular dissection of reactive astrogliosis and glial scar formation. Trends in neurosciences 32:638–647.

Sofroniew M V (2020) Astrocyte Reactivity: Subtypes, States, and Functions in CNS Innate Immunity. Trends in immunology 41:758–770.
Sofroniew M V, Vinters H V (2010) Astrocytes: biology and pathology. Acta neuropathologica 119:7–35.
Sträter N (2006) Ecto-5'-nucleotidase: Structure function relationships. Purinergic signalling 2:343–350.
Stewart TH, Eastman CL, Groblewski PA, Fender JS, Verley DR, Cook DG, D'Ambrosio R (2010) Chronic dysfunction of astrocytic inwardly rectifying K+ channels specific to the neocortical epileptic focus after fluid percussion injury in the rat. Journal of neurophysiology 104:3345–3360.
Stockwell J, Jakova E, Cayabyab FS (2017) Adenosine A1 and A2A Receptors in the Brain: Current Research and Their Role in Neurodegeneration. Molecules (Basel, Switzerland) 22.
Suadicani SO, Brosnan CF, Scemes E (2006) P2X7 receptors mediate ATP release and amplification of astrocytic intercellular Ca2+ signaling. The Journal of neuroscience : the official journal of the Society for Neuroscience 26:1378–1385.
Sun D, Jakobs TC (2012) Structural remodeling of astrocytes in the injured CNS. The Neuroscientist : a review journal bringing neurobiology, neurology and psychiatry 18:567–588.
Takenaka MC, Robson S, Quintana FJ (2016) Regulation of the T Cell Response by CD39. Trends in immunology 37:427–439.
Tam WY, Ma CHE (2014) Bipolar/rod-shaped microglia are proliferating microglia with distinct M1/M2 phenotypes. Scientific reports 4:7279.
Tang X, Yang X, Lai G, Guo J, Xia L, Wu B, Xie Y, Huang M, Chen J, Ruan X, Sui G, Ge Y, Zuo W, Zhao N, Zhu G, Zhang J, Li L, Zhou W (2010) Mechanism underlying hypokalemia induced by trimethyltin chloride: Inhibition of H+/K+-ATPase in renal intercalated cells. Toxicology 271:45–50.
Tang Y, Le W (2016) Differential Roles of M1 and M2 Microglia in Neurodegenerative Diseases. Molecular neurobiology 53:1181–1194.
Tasdemir-Yilmaz OE, Freeman MR (2014) Astrocytes engage unique molecular programs to engulf pruned neuronal debris from distinct subsets of neurons. Genes & development 28:20–33.
Tesic V, Perovic M, Zaletel I, Jovanovic M, Puskas N, Ruzdijic S, Kanazir S (2017) A single high dose of dexamethasone increases GAP-43 and synaptophysin in the hippocampus of aged rats. Experimental gerontology 98:62–69.
Tixier F, Hatt M, Le Rest CC, Le Pogam A, Corcos L, Visvikis D (2012) Reproducibility of tumor uptake heterogeneity characterization through textural feature analysis in 18F-FDG PET. Journal of nuclear medicine : official publication, Society of Nuclear Medicine 53:693–700.
Toggas SM, Krady JK, Billingsley ML (1992) Molecular neurotoxicology of trimethyltin: identification of stannin, a novel protein expressed in trimethyltin-sensitive cells. Molecular pharmacology 42:44–56.
Trabucco A, Di Pietro P, Nori SL, Fulceri F, Fumagalli L, Paparelli A, Fornai F (2009) Methylated tin toxicity a reappraisal using rodents models. Archives italiennes de biologie 147:141–153.
Tsutsumi S, Akaike M, Arimitsu H, Imai H, Kato N (2002) Circulating corticosterone alters the

rate of neuropathological and behavioral changes induced by trimethyltin in rats. Experimental neurology 173:86–94.
Verkhratsky A, Parpura V (2016) Astrogliopathology in neurological, neurodevelopmental and psychiatric disorders. Neurobiology of disease 85:254–261.
Verkhratsky A, Rodríguez JJ, Parpura V (2014) Neuroglia in ageing and disease. Cell and tissue research 357:493–503.
Vorhoff T, Zimmermann H, Pelletier J, Sévigny J, Braun N (2005) Cloning and characterization of the ecto-nucleotidase NTPDase3 from rat brain: Predicted secondary structure and relation to other members of the E-NTPDase family and actin. Purinergic signalling 1:259–270.
von Kügelgen I, Harden TK (2011) Molecular pharmacology, physiology, and structure of the P2Y receptors. Advances in pharmacology (San Diego, Calif) 61:373–415.
WACHSTEIN M, MEISEL E (1957) Histochemistry of hepatic phosphatases of a physiologic pH; with special reference to the demonstration of bile canaliculi. American journal of clinical pathology 27:13–23.
Wagner RC, Kreiner P, Barrnett RJ, Bitensky MW (1972) Biochemical characterization and cytochemical localization of a catecholamine-sensitive adenylate cyclase in isolated capillary endothelium. Proceedings of the National Academy of Sciences of the United States of America 69:3175–3179.
Wang X, Cai J, Zhang J, Wang C, Yu A, Chen Y, Zuo Z (2008) Acute trimethyltin exposure induces oxidative stress response and neuronal apoptosis in Sebastiscus marmoratus. Aquatic toxicology (Amsterdam, Netherlands) 90:58–64.
Wanner IB, Anderson MA, Song B, Levine J, Fernandez A, Gray-Thompson Z, Ao Y, Sofroniew M V (2013) Glial scar borders are formed by newly proliferated, elongated astrocytes that interact to corral inflammatory and fibrotic cells via STAT3-dependent mechanisms after spinal cord injury. The Journal of neuroscience : the official journal of the Society for Neuroscience 33:12870–12886.
Whittington DL, Woodruff ML, Baisden RH (1989) The time-course of trimethyltin-induced fiber and terminal degeneration in hippocampus. Neurotoxicology and teratology 11:21–33.
Wimo A, Winblad B, Jönsson L (2010) The worldwide societal costs of dementia: Estimates for 2009. Alzheimer's & dementia : the journal of the Alzheimer's Association 6:98–103.
Wink MR, Braganhol E, Tamajusuku ASK, Lenz G, Zerbini LF, Libermann TA, Sévigny J, Battastini AMO, Robson SC (2006) Nucleoside triphosphate diphosphohydrolase-2 (NTPDase2/CD39L1) is the dominant ectonucleotidase expressed by rat astrocytes. Neuroscience 138:421–432.
Wollmer MA, Lucius R, Wilms H, Held-Feindt J, Sievers J, Mentlein R (2001) ATP and adenosine induce ramification of microglia in vitro. Journal of neuroimmunology 115:19–27.
Wu Y, Sun X, Kaczmarek E, Dwyer KM, Bianchi E, Usheva A, Robson SC (2006) RanBPM associates with CD39 and modulates ecto-nucleotidase activity. The Biochemical journal 396:23–30.
Xu S, Zhu W, Shao M, Zhang F, Guo J, Xu H, Jiang J, Ma X, Xia X, Zhi X, Zhou P, Lu F (2018) Ecto-5'-nucleotidase (CD73) attenuates inflammation after spinal cord injury by promoting macrophages/microglia M2 polarization in mice. Journal of neuroinflammation 15:155.

Xu Y, Hu W, Liu Y, Xu P, Li Z, Wu R, Shi X, Tang Y (2016) P2Y6 Receptor-Mediated Microglial Phagocytosis in Radiation-Induced Brain Injury. Molecular neurobiology 53:3552–3564.
Xu S, Shao Q-Q, Sun J-T, Yang N, Xie Q, Wang D-H, Huang Q-B, Huang B, Wang X-Y, Li X-G, Qu X (2013) Synergy between the ectoenzymes CD39 and CD73 contributes to adenosinergic immunosuppression in human malignant gliomas. Neuro-oncology 15:1160–1172.
Yegutkin GG (2008) Nucleotide- and nucleoside-converting ectoenzymes: Important modulators of purinergic signalling cascade. Biochimica et biophysica acta 1783:673–694.
Yeh C-Y, Vadhwana B, Verkhratsky A, Rodríguez JJ (2011) Early astrocytic atrophy in the entorhinal cortex of a triple transgenic animal model of Alzheimer's disease. ASN neuro 3:271–279.
Yiannopoulou KG, Papageorgiou SG (2013) Current and future treatments for Alzheimer's disease. Therapeutic advances in neurological disorders 6:19–33.
Zabel MK, Kirsch WM (2013) From development to dysfunction: microglia and the complement cascade in CNS homeostasis. Ageing research reviews 12:749–756.
Zamanian JL, Xu L, Foo LC, Nouri N, Zhou L, Giffard RG, Barres BA (2012) Genomic analysis of reactive astrogliosis. The Journal of neuroscience : the official journal of the Society for Neuroscience 32:6391–6410.
Zatta P, Lucchini R, van Rensburg SJ, Taylor A (2003) The role of metals in neurodegenerative processes: aluminum, manganese, and zinc. Brain research bulletin 62:15–28.
Zhan Y, Paolicelli RC, Sforazzini F, Weinhard L, Bolasco G, Pagani F, Vyssotski AL, Bifone A, Gozzi A, Ragozzino D, Gross CT (2014) Deficient neuron-microglia signaling results in impaired functional brain connectivity and social behavior. Nature neuroscience 17:400–406.
Zhang L, Li L, Prabhakaran K, Borowitz JL, Isom GE (2006) Trimethyltin-induced apoptosis is associated with upregulation of inducible nitric oxide synthase and Bax in a hippocampal cell line. Toxicology and applied pharmacology 216:34–43.
Zhang Y, Barres BA (2010) Astrocyte heterogeneity: an underappreciated topic in neurobiology. Current opinion in neurobiology 20:588–594.
Zhang Y, Chen K, Sloan SA, Bennett ML, Scholze AR, O'Keeffe S, Phatnani HP, Guarnieri P, Caneda C, Ruderisch N, Deng S, Liddelow SA, Zhang C, Daneman R, Maniatis T, Barres BA, Wu JQ (2014) An RNA-sequencing transcriptome and splicing database of glia, neurons, and vascular cells of the cerebral cortex. The Journal of neuroscience : the official journal of the Society for Neuroscience 34:11929–11947.
Zhang Y, Sloan SA, Clarke LE, Caneda C, Plaza CA, Blumenthal PD, Vogel H, Steinberg GK, Edwards MSB, Li G, Duncan JA 3rd, Cheshier SH, Shuer LM, Chang EF, Grant GA, Gephart MGH, Barres BA (2016) Purification and Characterization of Progenitor and Mature Human Astrocytes Reveals Transcriptional and Functional Differences with Mouse. Neuron 89:37–53.
Zhou Y et al. (2020) Human and mouse single-nucleus transcriptomics reveal TREM2-dependent and TREM2-independent cellular responses in Alzheimer's disease. Nature medicine 26:131–142.
Zimmermann H (2008) ATP and acetylcholine, equal brethren. Neurochemistry international

52:634–648.
Zimmermann H, Zebisch M, Sträter N (2012) Cellular function and molecular structure of ecto-nucleotidases. Purinergic signalling 8:437–502.

VII PRILOZI

BIOGRAFIJA AUTORA

Milorad M. Dragić je rođen 27.05.1993. godine u Beogradu. Osnovnu i XIII beogradsku gimnaziju završio je sa odličnim uspehom. Biološki fakultet Univerziteta u Beogradu, studijska grupa Molekularna biologija i fiziologija upisao je 2012. godine, a diplomirao je 2016. godine sa prosečnom ocenom 9.78. Iste godine nastavlja master akademske studije Molekularna biologija i fiziologije na Biološkom fakultetu, modul Neurobiologija koji završava sa prosečnom ocenom 10 i odbranom master rada "Estradiol moduliše ekspresiju ektonukleotidaza u astrocitima hipokampusa ženki pacova". Nakon završenih master studija, 2017. godine upisuje doktorske studije na Biološkom fakultetu, studijski prograom Biologija, modul Eksperimentalna neurobiologija.

Od marta 2018. godine Milorad Dragić je zaposlen na Katedri za opštu fiziologiju i biofiziku, Biološki fakultet Univerzitet u Beogradu kao istraživač pripravnik na projektu "Ćelijska i molekulska osnova neuroinflamacije: potencijalna ciljna mesta za translacionu medicinu i terapiju" koji je finansiran od strane Ministarstva prosvete, nauke i tehnološkog razvoja R Srbije (III41014). Od aprila 2021. godine Milorad Dragić je zaposlen kao asistent na Katedri za opštu fiziologiju i biofiziku na kursevima Opšta fiziologija, Neurobiologija i Kvantitativne metode u neurobiologiji. Milorad Dragić je dobitnik nekoliko inostranih i domaćih granotva za organizovanje različitih studentskih radionica i radionica za učenike srednjih škola sa ciljem popularizacije neuronauka i povećanjem profesionalnih kompetencija studenata.

Milorad Dragić je član Srpskog biološkog društva, Društva za neuronauke Srbije i Evropske federacije društava za neuronauke (FENS). Autor je ili koautor 9 naučnih radova u međunarodnim vodećim časopisima iz M20 kategorije (jedan M21a, tri M21, četiri M22 i jedan M23). Autor je brojnih saopštenja na međunarodnim skupovima iz kategorije M34.

Образац изјаве о ауторству

Изјава о ауторству

Име и презиме аутора **Милорад М. Драгић**

Број индекса **Б3009/2017**

Изјављујем

да је докторска дисертација под насловом

Улога пуринског сигналног система у процесима неуродегенерације и неуроинфламације изазваних триметил-калајем у хипокампусу женки пацова

- резултат сопственог истраживачког рада;
- да дисертација у целини ни у деловима није била предложена за стицање друге дипломе према студијским програмима других високошколских установа;
- да су резултати коректно наведени и
- да нисам кршио/ла ауторска права и користио/ла интелектуалну својину других лица.

Потпис аутора

У Београду, _____

_____

Изјава о истоветности штампане и електронске верзије докторског рада

Име и презиме аутора **Милорад М. Драгић**

Број индекса **Б3009/2017**

Студијски програм **Биологија**

Наслов рада **Улога пуринског сигналног система у процесима неуродегенерације и неуроинфламације изазваних триметил-калајем у хипокампусу женки пацова**

Ментори **др Ивана Грковић и проф. др Надежда Нељекови**

Изјављујем да је штампана верзија мог докторског рада истоветна електронској верзији коју сам предао/ла ради похрањивања у **Дигиталном репозиторијуму Универзитета у Београду.**

Дозвољавам да се објаве моји лични подаци везани за добијање академског назива доктора наука, као што су име и презиме, година и место рођења и датум одбране рада.

Ови лични подаци могу се објавити на мрежним страницама дигиталне библиотеке, у електронском каталогу и у публикацијама Универзитета у Београду.

Потпис аутора

У Београду, _____

_____

Образац изјаве о коришћењу

Изјава о коришћењу

Овлашћујем Универзитетску библиотеку „Светозар Марковић“ да у Дигитални репозиторијум Универзитета у Београду унесе моју докторску дисертацију под насловом:

Улога пуринског сигналног система у процесима неуродегенерације и неуроинфламације изазваних триметил-калајем у хипокампусу женки пацова

која је моје ауторско дело.

Дисертацију са свим прилозима предао/ла сам у електронском формату погодном за трајно архивирање.

Моју докторску дисертацију похрањену у Дигиталном репозиторијуму Универзитета у Београду и доступну у отвореном приступу могу да користе сви који поштују одредбе садржане у одабраном типу лиценце Креативне заједнице (Creative Commons) за коју сам се одлучио/ла.

1. Ауторство (CC BY)
2. Ауторство – некомерцијално (CC BY-NC)
3. Ауторство – некомерцијално – без прерада (CC BY-NC-ND)
4. **Ауторство – некомерцијално – делити под истим условима (CC BY-NC-SA)**
5. Ауторство – без прерада (CC BY-ND)
6. Ауторство – делити под истим условима (CC BY-SA)

(Молимо да заокружите само једну од шест понуђених лиценци. Кратак опис лиценци је саставни део ове изјаве).

Потпис аутора

У Београду,_____

_____